Advances in Polymer Science 256

Martin Müller *Editor*

Polyelectrolyte Complexes in the Dispersed and Solid State II

Application Aspects

Springer

256
Advances in Polymer Science

For further volumes:
http://www.springer.com/series/12

Aims and Scope

The series Advances in Polymer Science presents critical reviews of the present and future trends in polymer and biopolymer science. It covers all areas of research in polymer and biopolymer science including chemistry, physical chemistry, physics, material science.

The thematic volumes are addressed to scientists, whether at universities or in industry, who wish to keep abreast of the important advances in the covered topics.

Advances in Polymer Science enjoys a longstanding tradition and good reputation in its community. Each volume is dedicated to a current topic, and each review critically surveys one aspect of that topic, to place it within the context of the volume. The volumes typically summarize the significant developments of the last 5 to 10 years and discuss them critically, presenting selected examples, explaining and illustrating the important principles, and bringing together many important references of primary literature. On that basis, future research directions in the area can be discussed. Advances in Polymer Science volumes thus are important references for every polymer scientist, as well as for other scientists interested in polymer science - as an introduction to a neighboring field, or as a compilation of detailed information for the specialist.

Review articles for the individual volumes are invited by the volume editors. Single contributions can be specially commissioned.

Readership: Polymer scientists, or scientists in related fields interested in polymer and biopolymer science, at universities or in industry, graduate students.

Special offer:
For all clients with a standing order we offer the electronic form of Advances in Polymer Science free of charge.

Martin Müller
Editor

Polyelectrolyte Complexes in the Dispersed and Solid State II

Application Aspects

With contributions by

C. Ankerfors · A. Bertin · S. Bouhallab · T. Croguennec · M. Müller · G. Petzold · S. Schwarz · L. Wågberg

Springer

Editor
Martin Müller
Leibniz Institute of Polymer Research Dresden
Department of Polyelectrolytes and Dispersions
Hohe Straße 6
D-01069 Dresden
Germany

ISSN 0065-3195 ISSN 1436-5030 (electronic)
ISBN 978-3-642-40745-1 ISBN 978-3-642-40746-8 (eBook)
DOI 10.1007/978-3-642-40746-8
Springer Heidelberg New York Dordrecht London

Preface

Nearly one decade ago a two volume edition on "Polyelectrolytes with Defined Molecular Architecture" edited by M. Schmidt appeared in the Advances in Polymer Science, which summarized progress in the field at that date. Within the total 11 chapters one was dedicated to "Polyelectrolyte Complexes," in which its authors addressed interpolyelectrolyte and polyelectrolyte/surfactant complexes as well as theoretical aspects of polyelectrolyte (PEL) complexation.

This new two-volume edition on "Polyelectrolyte Complexes in the Dispersed and Solid State: Principles and Applications" is intended to extend the content of this former chapter by bringing together selected state of the art contributions on principles and theory (Volume I) as well as on actual application aspects (Volume II) of polyelectrolyte complex (PEC) based particles and soft matter. In the Volume I progress and new knowledge on theoretical aspects of electrosorption phenomena between PEL and oppositely charged surfaces (A.G. Cherstvy and R.G. Winkler) and of the practically always apparent aggregation and clustering tendency of PEC particles (N.I. Lebovka) are reviewed. Recently identified important dynamic aspects of ion conductivity (C. Cramer and M. Schönhoff) within PEC soft matter and relaxation phenomena within PEL/protein PEC particles (S. Lindhoud and M.A. Cohen-Stuart) as well as structural aspects of interpolyelectrolyte complexes of novel synthetic polyionic species with nonlinear topology and polymer–inorganic hybrids (D.V. Pergushov, A.A. Zezin, A.B. Zezin, A.H.E. Müller) are reviewed. In Volume II, prominent recent applications of PEC particles are reviewed together with an outline of relevant key properties concerning colloidal stability, size, shape, compactness, surface, and biointeraction. The use and tailoring of PEC particle-modified relevant surfaces for paper making (C. Ankerfors and L. Wagberg), solid–liquid separation and water treatment (G. Petzold and S. Schwarz) are addressed. The last three contributions review PEC applications in the life sciences, including the role of PEL/protein complex assemblies in food

(S. Bouhallab and T. Croguennec), the use of DNA/polycation complexes for gene delivery and protection (A. Bertin), and the potential of sizable and shapable nanosized PEC particles in pharmaceutical applications such as controlled drug release (M. Müller).

Dresden, Germany Martin Müller

Contents

Adv Polym Sci (2014) 256: 1–24
DOI: 10.1007/12_2012_206

Published online: 15 June 2013

Polyelectrolyte Complexes for Tailoring of Wood Fibre Surfaces

Caroline Ankerfors and Lars Wågberg

Abstract The use of polyelectrolyte complexes (PECs) provides new opportunities for surface engineering of solid particles in aqueous environments to functionalize the solids either for use in interactive products or to tailor their adhesive interactions in the dry and/or wet state. This chapter describes the use of PECs in paper-making applications where the PECs are used for tailoring the surfaces of wood-based fibres. Initially a detailed description of the adsorption process is given, in more general terms, and in this respect both in situ formed and pre-formed complexes are considered. When using in situ formed complexes, which were intentionally formed by the addition of oppositely charged polymers, it was established that the order of addition of the two polyelectrolytes was important, and by adding the polycation first a more extensive fibre flocculation was found. PECs can also form in situ by the interaction between polyelectrolytes added and polyelectrolytes already present in the fibre suspension originating from the wood material, e.g. lignosulphonates or hemicelluloses. In this respect the complexation can be detrimental for process efficiency and/or product quality depending on the charge balance between the components, and when using the PECs for fibre engineering it is not recommended to rely on in situ PEC formation. Instead the PECs should be pre-formed before addition to the fibres. The use of pre-formed PECs in the paper-making process is described as three sub-processes: PEC formation, adsorption onto surfaces, and the effect on the adhesion between surfaces. The addition of PECs, and adsorption to the fibres, prior to formation of the paper network structure has shown to result in a significant increase in joint strength between the fibres and to an increased strength

C. Ankerfors
Swerea KIMAB, Box 7047, 164 07 Kista, Sweden

L. Wågberg (✉)
Department of Fibre and Polymer Technology, KTH Royal Institute of Technology, Teknikringen 56, 100 44 Stockholm, Sweden

The Wallenberg Wood Science Centre (WWSC), KTH Royal Institute of Technology, Teknikringen 56, 100 44 Stockholm, Sweden
e-mail: wagberg@kth.se

of the paper made from the fibres. The increased joint strength between the fibres is due to both an increased molecular contact area between the fibres and an increased molecular adhesion. The increased paper strength is also a result of an increased number of fibre/fibre contacts/unit volume of the paper network.

Contents

1 Setting the Scene: Polyelectrolytes in Papermaking

Briefly, paper is made from a very dilute aqueous suspension of anionically charged cellulosic fibres which, after water removal, form a fibrous network, i.e., a paper sheet. In many cases, filler particles such as ground or precipitated calcium carbonate or clay are added to the fibre suspension to enhance the optical performance or printability of the paper. Also, a variety of other components are added to improve specific properties of the paper sheet (e.g., wet and dry strength agents) or to facilitate the paper production process (e.g., retention aids to minimize the loss of fines and filler material to the process water, dewatering aids or defoaming chemicals). The majority of these chemical additives are polymers.

The strength of a paper sheet is determined by the strength of the individual constituent fibres, the strength of the joints bonding the fibres together, the number of such joints per volume and the sheet formation (a measure of how evenly the fibres are distributed in the sheet). The fact that the strength of the sheet is generally significantly lower than the strength of a fibre leads to the conclusion that the joints between fibres are of utmost importance [1, 2]. The strength of a fibre–fibre joint is due to mechanical interlocking, van der Waals interactions, ionic bonds, hydrogen bonds, polymer inter-diffusion between fibre surfaces and hydrophobic interactions [3]. For most of these factors, the actual molecular contact area in the fibre–fibre joint is crucial [4].

Thus, it is of interest to modify the fibre–fibre joint in order to improve the various parameters of the paper sheet. One example is the addition of a polyelectrolyte in the papermaking process to increase the strength of the fibre–fibre joints and thus increase the paper strength. A large variety of polyelectrolytes, natural and synthetic, are used to modify fibre surfaces in papermaking, some of which (e.g., starch) have been used for more than 50 years [3]. Instead of single polymers, alternating layers of cationic and anionic polyelectrolytes can be adsorbed, forming a polyelectrolyte multilayer (PEM) [5] on the fibre surface [6]. This procedure leads to a significant increase in paper strength.

The classic approach to increasing the strength is mechanical beating of the pulp. This strengthens the resulting paper by straightening and flexibilizing the fibres, leading to stronger fibre–fibre joints and a more uniform stress distribution in the sheet with beaten fibres [7]. The side effect, the production of fine material, leads to more difficult dewatering, which results in a wetter sheet and thereby higher production costs. Beating also generally leads to the formation of denser sheets, which in turn may lead to lower bending stiffness or lower light scattering, and greater shrinkage upon drying, which are undesirable effects for some paper grades. The problem of densification has to some extent been overcome by (partial) replacement of the beating with chemical treatment with polyelectrolytes.

Recently, it has been shown that it can be of both technical and economic interest to pre-form polyelectrolyte complexes (PECs) before letting the polyelectrolytes interact with the fibres [8, 9]. This procedure offers an industrially interesting method for exploiting the advantages of the separate polyelectrolytes and for creating a new, nanostructured unit (which in itself has a further advantage in enhancing paper properties). It is also very interesting from an industrial point of view because PECs with new properties can be formed from polyelectrolytes that already have the necessary application permission from the authorities. It is usually very expensive to introduce totally new chemicals.

In more general terms, the addition of PECs can be seen as a surface treatment that, in combination with all the polymers available today with exciting functionalities, such as antibacterial, conductive, UV- or thermoresponsive properties, offers very interesting possibilities for adding new functionality to a large variety of fibre-based materials.

2 Adsorption of PECs to Cellulose Fibres

In order to correctly describe the adsorption of PECs at the solid–liquid interface, it is important to decide how to define the interaction between a PEC and a solid surface, i.e., should it be considered an adsorption of a polyelectrolyte or an adsorption of nanosized colloids with a net charge? This naturally depends on a number of factors, but it is vital to establish what type of complex is being studied since a soluble complex will differ from a coacervate, which in turn will differ from a colloidal complex [10, 11]. In the present discussion, only colloidal complexes will be discussed and, as shown in Fig. 1, this type of complex can be represented by a nanosized colloid with a neutral core and a charged corona. The size of these colloids depends on their composition and on how they are prepared but, according to Dautzenberg [11], they are roughly in the size range between 10 and 100 nm. The charge of the complexes naturally depends on the preparation conditions and on the properties of the constituting polyelectrolytes. The corona naturally also has a cloud of counter-ions to balance the non-neutralized charges in the external layer(s) of the complex.

The adsorption of polyelectrolytes and charged colloids at the solid–liquid interface has attracted considerable interest over the years [12–14]. Since the early 1980s,

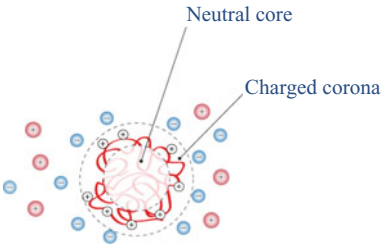

Fig. 1 Structure of the nanosized colloidal complex formed from mixing of oppositely charged polyelectrolytes

there has been a rapid development of our theoretical understanding of the adsorption processes and the mean-field theories have in general been very successful in describing polyelectrolyte adsorption at the solid–liquid interface [12, 15]. Good agreement has also been found between Monte Carlo simulations and thermodynamic models describing the adsorption of colloids at interfaces [16]. In mean-field models, it has been clearly demonstrated that the adsorption can be driven by an increase in entropy of the system due to the release of counter-ions from the polyelectrolyte/colloid and the solid surface and/or by a positive sign of the surface interaction parameter χ_s [12, 15], which is linked to an enthalpy change associated with the interaction between the polymer/polyelectrolyte/colloid and the surface. The adsorption of a highly charged polyelectrolyte to an oppositely charged surface is most commonly driven by the release of counter-ions (i.e., it is entropy driven), but in the case of a low charge density polyelectrolyte there may be a substantial contribution from nonionic interactions [12].

It is difficult to categorize colloidal complexes as either high-charged or low-charged systems because the charge of these materials is dependent on the composition of the complex, i.e., the constituting polyelectrolytes and the surrounding medium. Another complicating factor is the influence of the excess polyelectrolyte in the solution because this polyelectrolyte disturbs the adsorption process to an extent that depends on the charge and size of the polyelectrolyte in solution.

It has been shown [17] that the removal of the excess cationic polyelectrolyte led to a somewhat greater adsorption of complexes of polyallylamine hydrochloride (PAH) and polyacrylic acid (PAA) onto SiO_2 surfaces in water, with a net cationic charge and a degree of neutralization of 0.8, since the excess PAH diffused more rapidly to the surface and was adsorbed before the larger colloidal complexes could be adsorbed. When the PAH was removed, the complex adsorption dominated and the adsorbed amount thus increased. Similar results were found for the adsorption of cationic lattices onto cellulose fibres with an excess of cationic polyelectrolyte in solution [18], where it was found that a large excess of the cationic polyelectrolyte severely affected the amount adsorbed. Both these results show that the amount of free cationic polyelectrolyte in solution must be controlled in order to safely elucidate the mechanisms behind the adsorption of PEC onto any surface.

Using a simple filtration procedure on an anionic PEC formed between a cationic polyamideamine epichlorohydrin condensate (PAE) and carboxymethylcellulose

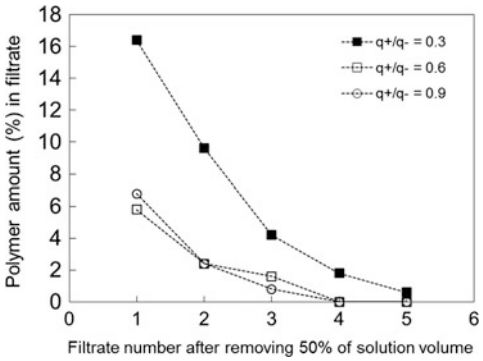

Fig. 2 The amount of polyelectrolyte remaining free in solution as a function of filtration cycle when 50% of the volume was between each filtration cycle for an anionic PEC formed between PAE and CMC. The $q+/q-$ is the ratio of cationic to anionic charges added in the formation of the complexes. Reprinted from Gärdlund et al. [19] Copyright (2003), with permission from Elsevier

(CMC), Gärdlund et al. [19] established that when the charge ratio was higher than 0.6 only a limited amount of free polymer (i.e., CMC) existed in solution. This is shown in Fig. 2, where the amount of free polymer in solution is shown as a function of washing cycle number when 50% of the volume of the PEC dispersion was removed in each cycle. From this, it can be concluded that when the degree of neutralization is higher than about 0.6 there will only be a limited amount of polyelectrolyte free in solution that might disturb the adsorption process. This amount is probably dependent on the properties of the polyelectrolyte used, but this has not yet been clarified.

Another important factor when studying the adsorption of a colloidal PEC to an oppositely charged surface is the dimension or geometry of the PEC and the amount of adsorbed charges associated with adsorption of a single complex at the solid–liquid interface. As shown in Fig. 1, the structure of the colloidal complex resembles a charged diblock copolymer micelle [20–22] with a neutral interior and a charged corona, with associated counter-ions. This will significantly affect the adsorption process because (i) the complex will not at re-conform with time to a flat conformation to the same extent as linear polyelectrolytes [23] and (ii) the amount of charges associated with one complex is more than enough to recharge the surface in an area corresponding to the size of the PEC. In other terms, this means that the amount of counter-ions released from the complexes will not be the same as the amount released from the surface, and this will lead to a recharging of the surface and a build-up of an osmotic pressure that will prevent further adsorption of PECs. This can also be viewed as a significant repulsion between the adsorbed complexes that will prevent the adsorption of further complexes. If this hypothesis is true, the addition of electrolyte will increase the adsorption of further PECs because the added electrolyte will decrease the osmotic pressure build-up upon PEC adsorption. As shown in Fig. 3 [19], this was indeed found for the adsorption of anionic PECs of PAE/CMC onto cellulose fibres pre-saturated with PAE as the NaCl concentration was increased. This figure clearly shows that the addition of NaCl significantly increased the adsorption.

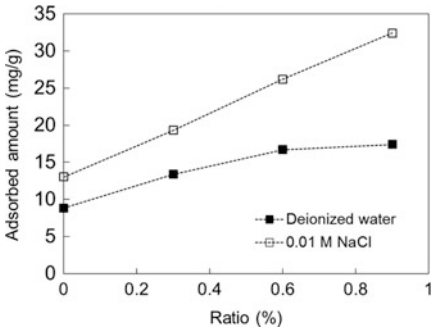

Fig. 3 Adsorption of PAE from PECs of PAE/CMC onto cellulose fibres as a function of the degree of neutralization of the colloidal complexes. The fibres were presaturated with PAE 10 mg/g at different NaCl concentrations. The value at a ratio of 0 corresponds to the presaturation treatment. Reprinted from Gärdlund et al. [19] Copyright (2003), with permission from Elsevier

This is not in accordance with a pure electrosorption according to mean-field theory [12] but it is in accordance with the build-up of an osmotic pressure due to non-neutralized charges of the adsorbed PEC on the solid, in combination with the dimensions and the composition of the PEC, as described above.

In an early work by Petzold and Lunkwitz [9], this efficiency of recharging of the fibres using cationic complexes of poly(diallyldimethylammonium chloride), PDADMAC, and poly(maleic acid-*co*-α-methylstyrene), MS-α-MeSty, was used to flocculate cellulose fibres, but the actual adsorption of the complexes was not measured. The adsorption of anionic complexes of polyethyleneimine (PEI) and CMC on fibres pretreated with a cationic PDMDAAC has also been studied by Hubbe et al. [24]. These authors found that when the charge of the complexes was decreased there was an increase in adsorption, indicative of an electrosorption process, but the authors also detected signs of nonionic interaction although they were not able to establish the molecular reason for this behaviour.

The adsorption of PECs onto different model surfaces has also been studied in order to establish the factors controlling the adsorption to cellulose surfaces. Gärdlund et al. [19] studied the adsorption of anionic PAE/CMC complexes onto SiO_2 model surfaces pre-saturated with PAE and, as shown in Fig. 4, there was an increase in the adsorbed amount as the charge of the complexes was decreased, showing the importance of the electrosorption process.

In another study [25], model surfaces of cellulose and SiO_2 were used to study the adsorption of PECs of cationic and anionic polyacrylamide (CPAM/APAM) and polyethylenesulfonate (PESNa) andPDADMAC in 1 and 100 mM NaCl. These results show several interesting features. Firstly, they all show that the adsorbed amount increased as the charge of the complexes decreased, indicating that the release of counter-ions is very important for the adsorption in all these systems. They also show that the adsorption of the low-charged CPAM/APAM system decreased as the salt concentration increased, whereas the adsorption increased for the high-charged PESNa/PDADMAC system. This is in agreement with the

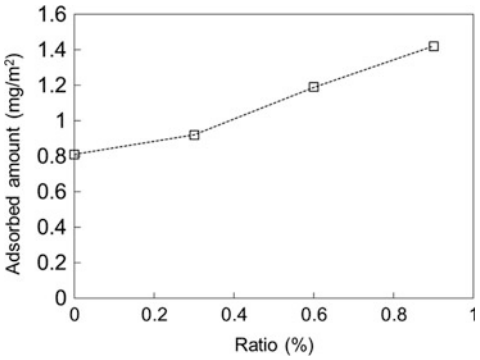

Fig. 4 Adsorption of PAE from anionic PAE/CMC complexes onto model SiO_2 surfaces presaturated with PAE. The NaCl concentration was 0.01 M and the value at a ratio of 0 corresponds to the presaturation treatment with PAE. Reprinted from Gärdlund et al. [19] , Copyright (2003), with permission from Elsevier

earlier discussion in which it was suggested that the build-up of an osmotic pressure was the cause of the limited adsorption for the more highly charged systems. For the low-charged system, this is not so important and there is a more typical electrosorption process in these systems. Saarinen et al. [25] also reported that SiO_2 and cellulose basically gave similar trends in adsorption but that the level of adsorption was different, probably due to a difference in charge, but also because different systems show different types of interaction with these two model surfaces.

Many types of cellulose fibres have a considerable amount of lignin and hemicelluloses left on the fibre surfaces, and model experiments using model surfaces of these compounds are very relevant for understanding the adsorption. Norgren et al. [26] used model lignin surfaces to study the adsorption of anionic complexes of PAH/PAA on net negative model surfaces of lignin at pH 7 and a NaCl concentration of 10 mM. Their results showed a significant adsorption of the anionic complexes under these conditions, which indicated that for lignin model surfaces there is a significant contribution from nonionic interactions to the adsorbed amount, although this was not observed for the cellulose surfaces. This shows both a complexity and the possibility of modifying the properties of cellulose fibres with PECs.

3 PEC for Controlling Adhesive Properties of Fibres

One PEC application with a potential for the pulp and paper industry is to improve the wet and dry strength of paper by increasing the adhesion between the fibres. For this purpose, PECs can be produced in two fundamentally different ways: in situ or by pre-formation (i.e., mixing the polycation and polyanion before addition to the pulp fibres). Both methods make it possible to improve the contact between fibres by creating a ductile joint between them. Examples of studies aiming at evaluating the performance of PECs as a strength agent will be presented, divided into these two categories.

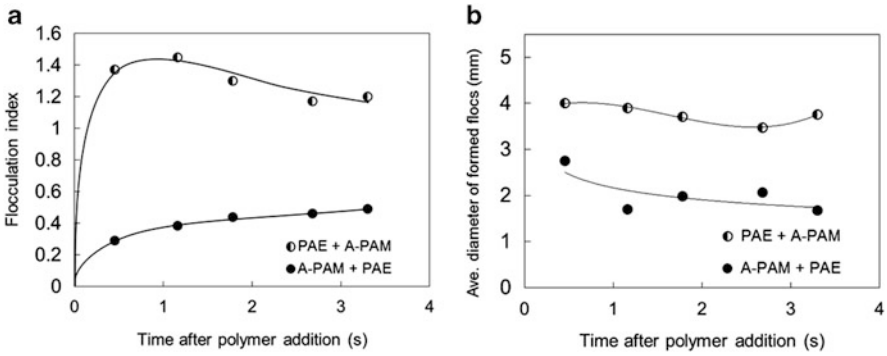

Fig. 5 Flocculation index (**a**) and average diameter of formed flocs (**b**) as a function of time after polymer addition for the APAM/PAE system for different orders of polymer addition. Addition levels: 1.5 mg/g fibre (PAE) and 0.6 mg/g fibre (APAM) [27]

3.1 PECs Produced In Situ

First, the in situ PECs will be considered. In this method, two polyelectrolyte components are added sequentially to the pulp suspension (e.g., by adding one polyelectrolyte and then the other component after a pre-selected time delay), forming PECs in situ. This method leads either to the formation of PECs directly on the fibre surfaces or to the formation of soluble complexes, colloidally stable PECs or macroscopic precipitates that can be deposited on the fibre surfaces.

The choice of pulp can affect the efficiency of the PEC treatment. Briefly, chemical pulping (e.g., Kraft pulping or the sulfite process) is a process aiming at a delignification of the wood fibre walls and thereby a liberation of the wood fibres in such a way that the shape and structure of the fibres are preserved. In the mechanical pulping processes (e.g., thermomechanical pulping or chemothermomechanical pulping), the most characteristic feature is the production of finer fibre material (referred to as fines) and also stiffer fibres with more charges compared to the chemical pulps, since the chemical composition of the fibres is more or less unchanged from that in the wood. The fines material has a very large surface area and thus also a large proportion of the surface charges.

The importance of the order of addition of the polyelectrolytes to a fully bleached softwood Kraft pulp has been studied by Wågberg et al. [27] by analysing, among other things, the flocculating ability of the polyelectrolytes and the size of the fibre flocs formed (see Fig. 5). It was found that adding the cationic polyelectrolyte (polyamideamine epichlorohydrin, PAE) first had the greatest effect on the flocculation, and also resulted in the formation of the largest fibre flocs. It was concluded that, at the right dosages, cationic patches could be formed on the fibre surfaces and that, after the subsequent addition of polyanion (anionic polyacrylamide, APAM), they were bridged together more efficiently than could be achieved with the cationic component alone.

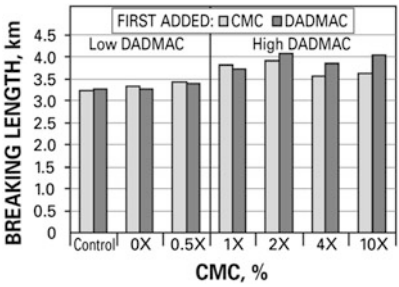

Fig. 6 Effect of amount and order of addition of PDADMAC and CMC on tensile strength development [28]. Reprinted with permission from TAPPI

The same influence of the order of polyelectrolyte addition was seen on the tensile strength (expressed as breaking length) using sequential addition of PDADMAC and CMC to pulp made from recycled copy paper; the highest paper strength being measured after addition of PDADMAC followed by CMC [28]. At a high level of addition of PDADMAC (supposedly enough to oversaturate the fibre surfaces), an increase in the amount of CMC added resulted in higher strength. It was hypothesized that this procedure led to the formation of a PEC, which was deposited on the fibres (Fig. 6).

In another study, PECs were made from combinations of crosslinked CPAM or cationic starch (CS) using either CMC or APAM as polyanion by sequential addition of the polyelectrolytes (adding the polycation first) to a similar 50/50 mixture of chemical and mechanical pulp, forming PECs in situ. The Scott bond strength, as a measure of the interfibre bonding, indicated that the amount of polyanion added after the polycation must not be too high or the complexes could have a negative influence on the paper strength. However, with larger amounts of polycation added before the CMC addition, fibre–fibre bonding and sheet strength were improved. It was also seen that the effect of the polyelectrolyte treatment on this pulp mixture was less than the effect on a pure chemical pulp and it was suggested that the stiffness of the mechanical pulp might be a limiting factor [29]. The same research group also evaluated the effect of in situ PECs on strength properties, together with different applied stress during the drying of the paper sheet. Generally, a higher stress during drying increases the tensile stiffness of the sheets, but not the tensile strength, since this parameter also depends on the fibre–fibre bonding within the sheet, which can deteriorate with a higher drying stress. With a sequential addition of CPAM and CMC to a fibre suspension with 50% bleached Kraft pulp and 50% bleached thermomechanical pulp [30], however, these relations were somewhat changed. With the CPAM/CMC addition, the tensile strength was increased without the higher drying stress having any negative effect on the bonding. Increased bonding between fibres with the PEC addition was suggested as a possible explanation for this. Adding CPAM alone did not stop the bonding from being impaired under a higher drying stress.

In a series of studies made by Hubbe and coworkers, PDADMAC was added in excess to different kinds of pulps, followed by the addition of CMC. This procedure led to an in situ formation of PECs, which were thereafter deposited onto the cellulose fibres, leading to a substantial increase in tensile strength in sheets formed

from the fibres [31]. With high polymer addition levels (as much as 40% of the dry fibre), the tensile strength was increased up to three times, but other problems such as stickiness, lowered dewatering rates, flocculation and translucence arose [31]. Another study showed that in-situ formed complexes (from PDADMAC and CMC) yielded a higher tensile strength of sheets formed from glass fibres than pre-formed PECs of the same polyelectrolytes [32], emphasising the great influence of the chemical addition strategy used. The glass fibres were used as a simplified model of cellulosic fibres in order to have a more defined system with, e.g. no fines, no swelling and no intrafibre porosity. Also, sheets formed from glass fibres without any polyelectrolytes have almost no cohesive strength, so that any increase in tensile strength with added polymer can be easily ascribed to the polymer addition.

The sequential addition of two oppositely charged polyelectrolytes is a commonly used industrial method for increasing the retention of filler and fine material, using so-called dual (component) retention aids [33]. The polyanions can also be replaced by anionically charged micro- or nanoparticles, as in the microparticulate retention aids [34]. Addition of the polycation first, followed by the polyanion, is an analogue to building the first two layers of a PEM structure [5], which was first introduced in the paper field by Wågberg et al. [6], and later studied extensively by several research teams [35–37].

3.2 In Situ PEC Formation with Wood Components

A special case of in situ PEC formation is to utilize a cationic polyelectrolyte together with the anionic material already present in the pulp suspension (i.e., in different wood components). Besides pulp fibres, fines and filler material, the paper furnish can also contain a considerable amount of molecules originating from the wood material. Native wood fibres are composed of cellulose, hemicellulose and lignin as major constituents, roughly one third of each, and, as previously mentioned, the main purpose of the pulping process is to liberate the wood fibres from each other to form a suspension of free fibres. Although the two principal pulping techniques (chemical and mechanical) are very different from each other, the wood compounds released to the process waters are basically the same, i.e., originating from lignin or hemicellulose, although the types and relative concentrations may differ. Other processes, such as bleaching and beating, may result in a further dissolution of chemical compounds from the fibre material into the aqueous phase. These dissolved and colloidal substances (DCS) are often polymeric substances with negative charges and, due to their ability to intervene with the papermaking process, they are often condescendingly referred to by papermakers as anionic trash. When cationic polymers (e.g., retention additives) are added to the fibre suspension, PECs can form spontaneously between the added polycations and these anionic wood components.

With today's striving towards more environmentally sound production processes and low water usage (especially in countries with water shortage), increased system

closure is used, i.e., circulation of the process water is employed. This leads to increasing concentrations of the mentioned substances in the circulating water [38]. With large amounts of DCS in the process water, aggregates may form. Deposits of aggregates of substances on machine parts may cause severe disturbances to paper machine runnability [39] and, in this respect, the addition of cationic polyelectrolyte can be detrimental to process efficiency. Although this is sometimes viewed as a problem leading to a high consumption of cationic additives, the process can have several advantages. The viscosity of the aqueous phase is lowered by the removal of unwanted dissolved or colloidal material and this facilitates drainage and dewatering [40, 41], which is an economic advantage because it reduces the energy needed for drying the paper sheet. Also, the PEC structures formed can be deposited onto the fibre surfaces, thus increasing the adhesive contact between the fibres.

In the papermaking process, lignin is generally considered to be a more difficult substance than hemicelluloses such as xylan, which can even act as a strength agent. The positive effect of released hemicelluloses on paper strength is well established in the literature [38]. Lignin, on the other hand (retained by the addition of CPAM, forming PECs in situ) acts only as a filler, i.e., a non-bonding spacer in the fibre crossings [38]. Extensive investigations of the interaction between different common retention chemicals and wood components were carried out by Ström et al. during the 1980s [42–46]. When a high-charge-density polycation (here, polyethyleneimine, PEI) was added to a pulp suspension, any lignosulfonates were consumed first and hemicelluloses such as xylan later [43, 47]. The effect of the lignosulfonate complexes depended on the relative amounts of the two oppositely charged polymers, forming complexes with different net charges. If the added polycation was in deficiency, the negatively charged PECs formed merely acted as a larger amount of fines material in the water phase. With increasing polycation dosage, cationic PECs were eventually formed, which could be deposited on the negative fibre surfaces and thereby remove them from the water phase.

The interactions between different polysaccharide additives (such as guar gum or starch) and the components in a variety of pulp suspensions (including whole pulp and washed pulp) have been described as a four-step process (Fig. 7): mixing of polysaccharides into the pulp suspension; complexation with DCS; adsorption of polysaccharides (free or complexed) onto fibres and fines material; and, finally, association of fines to the adsorbed polysaccharides on the fibres [48]. According to the authors, this agrees with the maximum fines retention, drainage and paper strength observed in industrial applications,

In a study with a similar purpose, i.e., the better understanding of the mechanisms by which cationic retention aids operate in the presence of DCS, the formation of colloidal and coacervate complexes from CPAM and sulfonated Kraft lignin was studied [49]. Using a CPAM with lower molecular weight, the formation of colloidal complexes was promoted over coacervate formation. With CPAM of higher molecular weight, the re-conformation (into colloidal PECs) was too slow, and coacervate complexes were formed.

Other reports concerning in-situ-prepared PEC focus on the formation of PECs and their effect on drainage and dewatering or as an aid for washing pulp [40, 41].

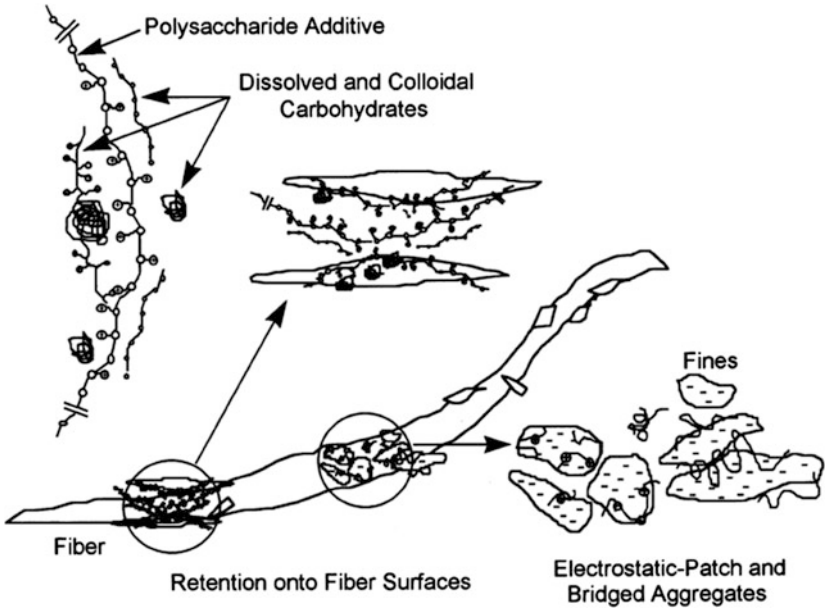

Fig. 7 Interaction between DCS and polysaccharide additives and retention on fibre surfaces. Reprinted from Rojas and Neuman [48] Copyright (1999), with permission from Elsevier. Please note that the components are not drawn to scale. The fibres are hollow cylinders with a fibre wall thickness around 4 μm, a cross-section of around 20 μm and a length of around 2 mm. The polysaccharides and the additives are charged macromolecules and the fines have a size between 1 and 100 μm

When PDADMAC was added, 80–90% of the lignin could be precipitated from aqueous solution if the pH was high, when most of the carboxyl groups in the lignin are dissociated, making the lignin water soluble. In the washing of pulp, it is desirable to have macroscopic complexes that precipitate.

In summary, PECs prepared in situ are able to increase not only retention but also paper strength. However, this latter advantage has not been extensively studied and, especially, not well controlled and exploited. The problem of controlling in situ PEC formation is to a large extent related to the chemical environment in which the in situ PEC formation occurs. The properties of the fibre material (e.g., surface charge, flexibility and swelling behaviour) depend on the pulping and bleaching processes used to produce the product grade. Although one paper machine (or even one entire paper production site) usually runs on the same pulp grade, which is seldom subject to change, different pulp qualities have different requirements with regard to the PECs, so that a future product would have to be specifically adapted to the given situation [42]. The concentrations of DCS may also differ over time as a result of variations in the incoming wood raw material. The paper furnish can also have considerable concentrations of various ions, and the concentrations can vary with time due to variations in, e.g., the fibre raw material. The presence of

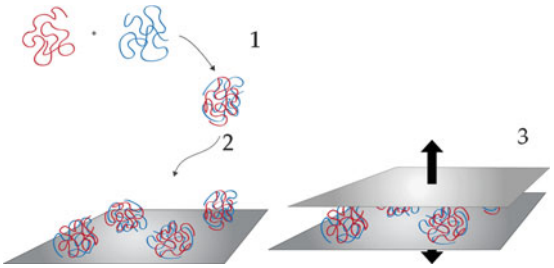

Fig. 8 Diagram of the three sub-processes in the use of pre-formed PECs as a strength agent: (*1*) PEC formation , (*2*) PEC adsorption onto a surface and (*3*) effect on adhesion between surfaces

ions (i.e., at higher conductivities) decreases the Debye length. At distances longer than the Debye length, the interactions between charged molecules are significantly weakened. The entropical driving forces that might promote adsorption (see Sect. 2) are weaker than at lower ionic strengths. In more practical terms, this means that interactions between fibres and polyelectrolyte or between polyelectrolyte and polyelectrolyte will not be as strong or as long-range at higher salt concentrations. The pH is another important factor because many of the chemicals involved are weak polyelectrolytes, changing their charge density with changing pH.

Together, these factors make in situ PEC formation an unreliable method. Besides in situ PEC formation, there is another possibility: to pre-form the complexes before addition to the pulp fibres.

3.3 Pre-formed PECs

In contrast to the formation of PEC structures in situ, PECs can also be formed before addition to the fibre suspension. We refer to these as pre-formed PECs. They are prepared by mixing two oppositely charged polyelectrolytes together in some way before further use as a paper chemical. The PEC preparation method that is predominantly used in the literature is polyelectrolyte titration, i.e., the slow addition of a solution of one polyelectrolyte to a solution of an oppositely charged one [11]. However, another PEC preparation method has recently been used, the so-called jet mixing method [50, 51].

One unique advantage of pre-formed PECs over in situ PECs is the possibility of controlling their formation and of analysing their structures and colloidal properties before addition to the pulp fibres. Since complex formation occurs in a separate environment, which is more controllable than the paper stock that can vary substantially with time, the PEC formation can also be made more reliable and robust than if it occurs in the fibre suspension.

The technique of using pre-formed PECs to enhance the adhesive interactions between fibres can be divided into three sub-processes (schematically illustrated in Fig. 8): formation of the complexes; adsorption of the complexes onto the fibre surfaces; and the performance of the PECs as a part of the fibre–fibre joint. The first

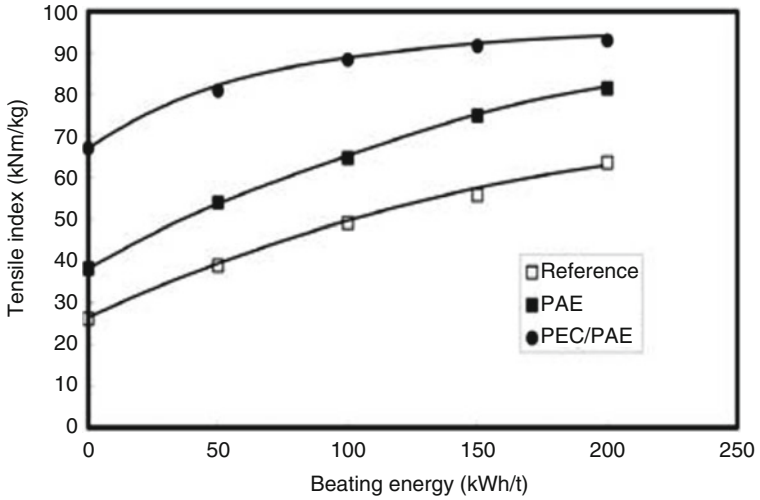

Fig. 9 Tensile index, i.e. the stress at break of paper sheets from HBK fibres subjected to chemical treatment (PAE or PAE/PEC), mechanical beating or a combination of both. From Gärdlund et al. [54]

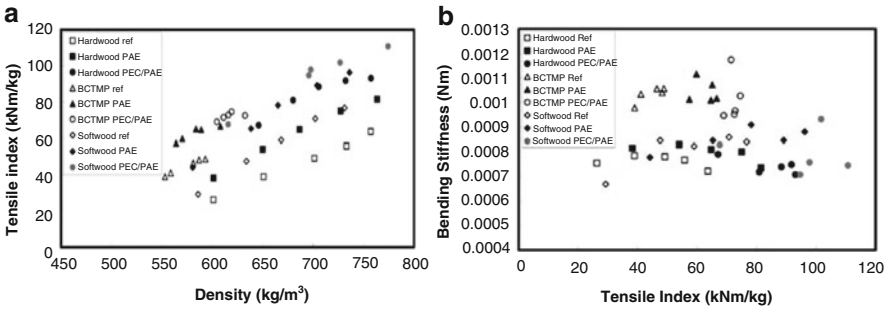

Fig. 10 The relationship between (**a**) tensile index, i.e. the stress at break, and sheet density and (**b**) bending stiffness and tensile index for all the pulps studied in Gärdlund et al. [54]

two sub-processes have already been discussed (formation by Petzold and Schwartz [52] and adsorption in Sect. 2) and will hence not be further discussed here.

The interaction between pre-formed PECs and pulp fibres has been systematically studied by several research teams, and the use of pre-formed PECs in papermaking has been demonstrated to significantly enhance the physical properties of paper. The PECs tested were combinations of PAA and PAH or of PAE and CMC [19, 53, 54]. An undesired densification occurred when the PECs were added to the various tested pulps, but this effect was not as pronounced as that achieved by mechanical beating, indicating the great potential for using PECs to enhance paper strength while maintaining a significant part of the paper bulk, as can be seen in Figs. 9 and 10 [54]. In another study, paper strength was reported to

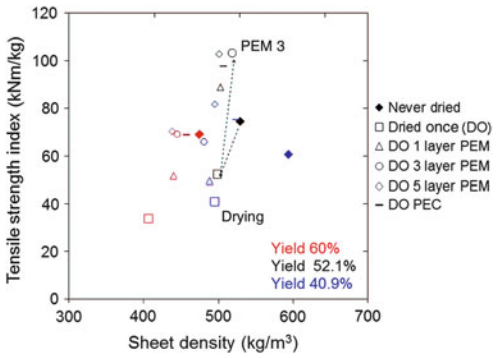

Fig. 11 Tensile strength index versus sheet density for different Kraft pulps. The arrows are guides to show the effect of the different operations on the 52.1% yield pulp. Redrawn from Torgnysdotter and Wågberg [4]

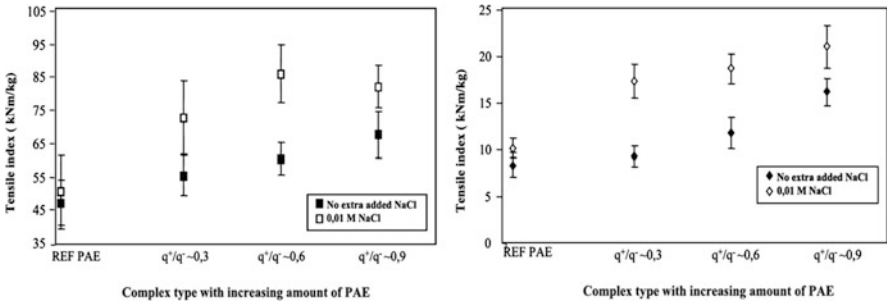

Fig. 12 The dry strength (*left*) and wet strength (*right*) of hand-sheets after treatment with PAE and anionic PECs of different ratios at two different salt concentrations. The general trend, with some variations, seems to be that the closer to charge neutrality the PEC is the higher is the strength. Reprinted from Gärdlund et al. [19] Copyright (2003), with permission from Elsevier

increase by up to 100% without any significant densification [4], as shown in Fig. 11. The strength increase was explained by stronger fibre contact zones. This will be further discussed in Sect. 3.3.

As previously discussed in Sect. 2, salt plays an important role in the performance of a PEC. Figure 12 shows the increase in wet and dry tensile index after the adsorption of one layer of PAE and thereafter the adsorption of anionic PECs with different charge ratios prepared from PAE and CMC. From these results, it is obvious that, although there was a clear effect of the PEC addition in deionized water, the effect was much greater in the presence of 0.01 M NaCl. PAE is a commonly used wet-strength additive in the paper industry, with the ability to bond covalently to the cellulose in the pulp fibres [55]. CMC is also commonly used in papermaking.

A new method for producing PECs by jet mixing [51, 56] was thoroughly investigated by Ankerfors et al. [17, 50] using the two polyelectrolytes PAA and PAH. The same two polyelectrolytes have previously been shown to increase paper

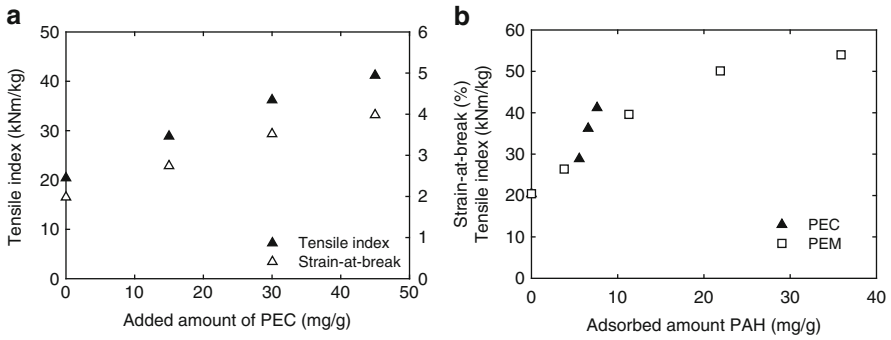

Fig. 13 (**a**) Tensile index and strain-at-break of sheets made of fibres treated with PECs prepared from PAA of molecular weight 5000 and PAH of molecular weight 15,000 at a charge ratio (anion/cation) of 0.8 as a function of PEC dose. (**b**) Tensile index of PEC-treated sheets (*filled triangles*) as a function of adsorbed amount of PAH [59] in comparison with the tensile index data for sheets made of fibres treated with PEMs after adsorption of layers 1, 3, 5 and 7 (*open squares*) [57]

strength, using the layer-by-layer technique [5] to build up a polyelectrolyte multilayer (PEM) on the fibre surfaces [6, 57, 58]. As previously mentioned, making an in situ PEC in the presence of pulp fibres is similar to adsorbing the first two layers of a PEM. To study and compare their effects on the strength of paper sheets formed under the same conditions, pre-formed PECs from PAA and PAH were compared with PEMs of the same components [59].

The effects of using PECs and PEMs as strength-enhancing chemicals can be compared in two ways: with reference to either the adsorbed amount or the number of treatments. For adsorbed amounts of PAH below 10 mg/g (Fig. 13b), the sheets made of PEC-treated fibres have a higher tensile index than those made of PEM-treated fibres. At higher dosage levels, the PEM treatment is superior to PEC treatment because it is possible to increase the amount of PAH adsorbed simply by adding more layers. This comparison also indicated that four or five PEMs would be needed to achieve the same tensile index level as achieved with the highest PEC dose. It should also be noted that, in this study, the density of the sheets, which is crucial for many paper properties, was unaffected by PEC treatment, in contrast to the effect of most traditional paper strength agents.

Using a peel force test, the adhesion force of PEC from polyvinylamine (PVAm)/CMC adsorbed onto wet membranes of regenerated cellulose was studied by Feng et al. [60]. Their study indicated that the cohesion of the complexes is very strong and that the failure eventually occurs at the cellulose complex interface and not within the complex itself, i.e., as an adhesive rather than a cohesive failure. After oxidizing the cellulosic surfaces (TEMPO/NaBr/NaClO), a higher delamination strength was achieved (Fig. 14). This was ascribed to the formation of imine and aminal linkages with hemiacetals on the oxidized cellulose. The highest wet adhesion was achieved with PVAm-rich complexes, which was opposite to their previous findings for dry or almost-dry adhesion [61]. Again, the importance of adapting the PECs for the purpose of each application and situation was emphasized.

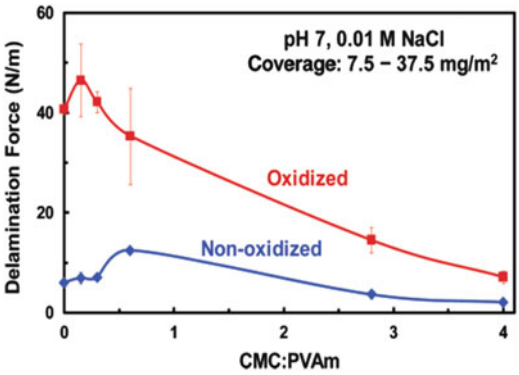

Fig. 14 Influence of cellulose film oxidation on the adhesion to PVAm/CMC complexes [60]. Reprinted with permission from Biomacromolecules. Copyright (2007) American Chemical Society

Pre-formed complexes of APAM and CPAM with different charge ratios and their effect on dewatering were studied [62]. The most important finding was a broader optimum concentration than for single CPAM. Although this paper focused on the use of PECs for enhancing dewatering, the authors also emphasized the importance of choosing the right complex type for each purpose and the possibility of finely tuning the dewatering effect by changing, e.g., the ratio of polycation to polyanion in the pre-formed complexes.

4 What Controls the Adhesion?

Having seen all the positive effects on paper strength of the addition of PECs, it is of course interesting to try to elucidate the molecular mechanism behind the positive effects of the PECs in increasing the adhesion between cellulose surfaces. What controls the adhesion between surfaces is a more general question that has been widely debated in recent decades, a discussion that to a great extent originates from the fascinating adhesive behaviour of the gecko's feet, allowing the lizards to climb up a wall or even to hang from the ceiling – and at different humidities.

It has been pointed out that the geometry of the adhering surfaces is of great importance for the adhesion. By studying the size of the attachment pads of animals (such as insects, spiders and geckos), it has been shown that animals with a large body mass increase their adhesion by increasing the number of filaments (setae) at a given radius of curvature (Fig. 15). An even larger body mass requires a smaller seta diameter and a smaller radius of curvature. A patterned surface has the advantage of establishing contact with different surface profiles, and is less sensitive (has an increased tolerance) to defects in individual contacts [63]. For a flat punch geometry it was found that the maximum force to separation scaled as $n^{1/4}$, where n is the number of contact points, and when the posts are finished with a half sphere the maximum force scales as $n^{1/2}$. The same conclusion was drawn by Lamblet et al. [64] from a study of PDMS–acrylic adhesive interfaces having pillars with different height-to-radius ratios and different surface flexibilities. The ordering of the surface

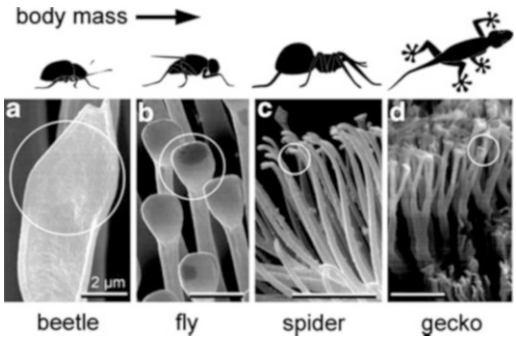

Fig. 15 Terminal elements (*circles*) in animals with hairy design of attachment pads. Note that heavier animals exhibit finer adhesion structures [63]. Copyright (2003) National Academy of Sciences, USA

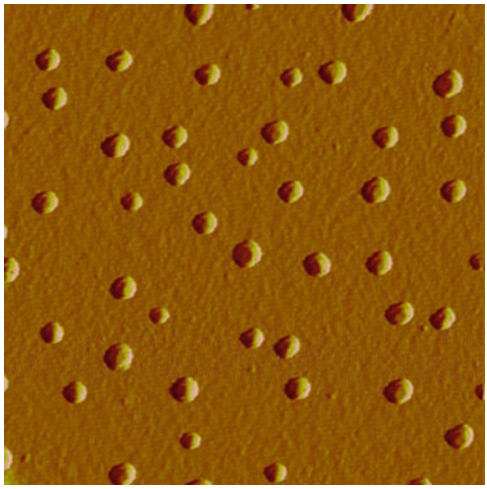

Fig. 16 AFM image of a PEC-covered surface with the possibility of several contact points [59]. The size of the image is 1×1 µm

pattern has also been shown to be important. Ordered arrays of micron-sized PDMS pillars were shown to have significantly higher adhesion than disordered arrays [65]. In both experimental studies and a developed model, the high sensitivity to geometrical effects was pointed out. In model studies using PAH/PAA complexes [59] it was also found that the complexes formed a random array of contact points at the solid liquid interface that could be efficient for the creation of efficient joints between two treated surfaces (Fig. 16).

Later studies of real gecko feet have shown that the true contact area and the minimized compliance in the loading direction are more important factors, especially for reversible adhesive design, than, e.g., the presence of fibrillar shapes alone. By adapting a theoretical model to the adhesive behaviour of many different materials over a wide range of loads (14 orders of magnitude in adhesive force), it was found that the adhesive materials must be sufficiently soft (i.e., compliant) to increase the true contact, but stiff enough to achieve high loads [65].

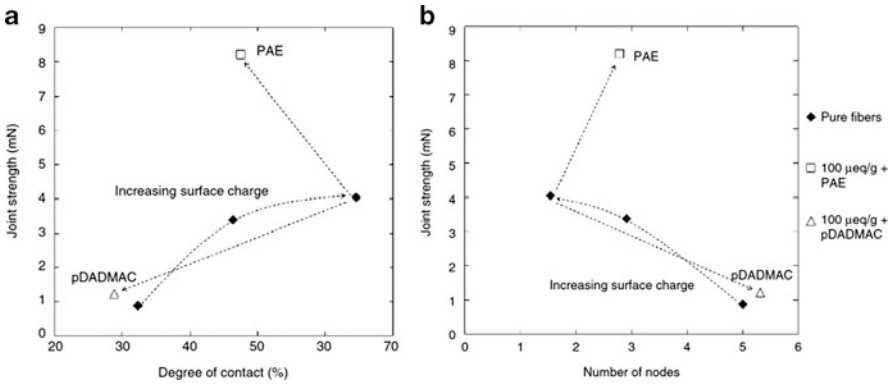

Fig. 17 (**a**) Fibre-fibre joint strength versus the degree of contact in the contact zones for surface-charged rayon fibres with charges of 35, 76 and 100 eq/g (*filled diamonds*), and of 100 eq/g with the addition of the wet-strength agent PAE (*open square*) or cationic fixing agent PDADMAC (*open triangle*). (**b**) Fibre–fibre joint strength versus the number of nodes of the contact zones for surface-charged rayon fibres with charges of 35, 76 and 100 eq/g, and of 100 eq/g with the addition of the wet-strength agent PAE or the cationic fixing agent PDADMAC (*symbols* as for **a**). From [66]

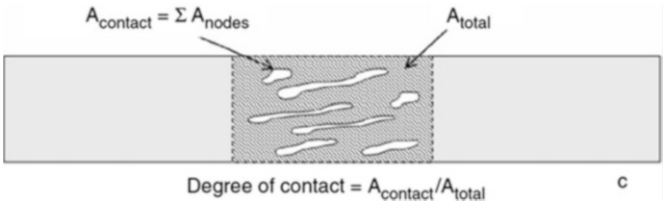

Fig. 18 How the degree of contact can be calculated, as a value describing the relative contact area of the single-fibre joint. From Torgnysdotter et al. [66]

In a more applied work, Kraft pulp fibres were treated with PEM or PEC (built by both PAA and PAH, where the cationic complexes were prepared by titration) [4]. It was pointed out that when designing a strong adhesive joint with a favourable stress distribution, it is important to have a contact zone of high quality, i.e., high work of adhesion and large molecular contact area (Fig. 16). Adding PEC or PEM significantly increased the tensile and compression strength by increasing the fibre–fibre joint strength [4]. In a continuation of this work, Rayon fibres were used as a model system and three different surface treatments were used on these fibres: (i) carboxymethylation to increase the surface charge of the fibres; (ii) PAE addition; and (iii) PDADMAC addition [66].

Whereas an increase in the fibre surface charge resulted in a greater degree of contact and a decrease in the number of contact points (due to a greater conformability of the surface, as a result of the increased swelling potential with increasing surface charge), the addition of PAE or PDADMAC had the reverse effect, i.e., the degree of contact decreased, but the number of contact points increased (Fig. 17). The PAE

treatment resulted in by far the highest joint strength for a given degree of contact or for a given number of nodes (Fig. 18). Cohesive failure of the paper sheets was seen to some extent (fibre fragments were pulled out), showing the great adhesive strength of the surface treatment. With increasing surface charge of the fibres and with PAE added, the tensile index of the paper increased significantly. With PDADMAC addition, however, the tensile index decreased. This was ascribed to a lower conformability of the fibres with adsorbed PDADMAC than with PAE.

The conclusion that a large number of just sufficiently compliant contact points between the fibres would be the most advantageous suggests that surface treatment with a PEC should offer great possibilities. Although only a few studies have been performed on this specific topic, current research suggests the potential of PECs to increase both the number of contact points between two surfaces and, of course, to offer a way to steer the mechanical properties of the joint by appropriate choice of polymer components and/or preparation conditions.

5 Future Outlook

The advantages of PECs lie in their three-dimensional structure and the relatively low polyelectrolyte concentration needed to reach this structure as compared with, for example, polymer lattices. Another major advantage is the possibility to vary the structure and properties of the complexes simply by changing their composition. This is more important than ever considering the large efforts that are needed to acquire necessary permits for the introduction of new chemicals, since the PECs can be prepared by already accepted polymers/polyelectrolytes and/or nanoparticles. The structural integrity of the PECs also allows them to retain a three-dimensional structure when adsorbed at a solid–liquid interface, which is essential, e.g., for flocculation efficiency. Flocculation is interesting in many industrial applications, not only for the paper industry but also in, e.g., waste water treatment.

Despite the rich literature on PECs, only a limited number of polymers (and nanoparticles) have been used to prepare PECs so far. Therefore, it would be interesting to test a more extensive range of other types of polymers, including block-copolymers, since the properties of the polymers and thereby the PECs can be tailored to reach a wider property space of the PECs. An additional possibility with block-copolymers would be to investigate other complexing interactions when forming PECs, apart from the pure electrostatic interactions that are the most commonly used today. Another interesting development is the combination of nanoparticles and polyelectrolytes for adhesive surface engineering. Recent results show that both adhesive pull-off forces and the work of adhesion can be tailored with this concept [67]. It has recently also been identified [68] that in order to form strong interfacial joints it is necessary to have a a) high interfacial adhesion b) a large molecular contact area and c) a low compliance of the material in the contact zone. By selecting the right starting materials for the PECs and by selecting the right preparation and adsorption conditions for the complexes these materials could be ideal for tailoring adhesion.

From a more practical point of view, a few open questions remain before PECs can be fully introduced as a common chemical to the pulp and paper industry. The most important remaining technical challenge is to increase the concentration of the produced PECs. Today, they are generally produced as dilute water suspensions that are difficult to add directly into different processes due to the large volumes needed for the required amount of PEC.

References

1. Davison RW (1972) Weak link in paper dry strength. Tappi 55:567–573
2. Page DH (1969) Theory for the tensile strength of paper. Tappi 52:674–681
3. Lindström T, Wågberg L, Larsson T (2005) On the nature of joint strength in paper - A review of dry and wet strength resins used in paper manufacturing. In: I'Anson SJ (ed) Advances in paper science and technology: transactions of the13th fundamental research symposium, Cambridge, UK, Sept 2005. Pulp and Paper Fundamental Research Society, Bury, UK, pp 457-562
4. Torgnysdotter A, Wågberg L (2006) Tailoring of fibre/fibre joints in order to avoid the negative impacts of drying on paper properties. Nord Pulp Pap Res J 21:411–418
5. Decher G, Hong JD, Schmitt J (1992) Buildup of ultrathin multilayer films by a self-assembly process: III. Consecutively alternating adsorption of anionic and cationic polyelectrolytes on charged surfaces. Thin Solid Films 210/211:831–835
6. Wågberg L, Forsberg S, Johansson A et al (2002) Engineering of fibre surface properties by application of the polyelectrolyte multilayer concept. Part I: modification of paper strength. J Pulp Pap Sci 28:222–227
7. Page DH (1985) The mechanism of strength development of dried pulps by beating. Svensk Papperstid 88:R30–R35
8. Ankerfors C (2012) Polyelectrolyte complexes: preparation, characterization, and use for control of wet and dry adhesion between surfaces. KTH Royal Institute of Technology, Stockholm
9. Petzold G, Lunkwitz K (1995) The interaction between polyelectrolyte complexes made from poly(dimethyldiallylammonium chloride) (PDMDAAC) and poly(maleic acid-co-α-methylstyrene) (P(MS-α-MeSty)) and cellulosic materials. Colloids Surf A 98:225–233
10. Bungenberg de Jong HG, Kryut HR (1929) Coacervation (partial miscibility in colloid systems). Proc Acad Sci Amsterdam 32:849
11. Dautzenberg H (2001) Polyelectrolyte complex formation in highly aggregating systems: methodical aspects and general tendencies. In: Radeva T (ed) Physical chemistry of polyelectrolytes. Dekker, New York
12. Fleer GJ, Cohen Stuart MA, Scheutjens JMHM et al (1993) Electrostatic effects: charged surfaces and polyelectrolyte adsorption. In: Polymers at interfaces. Chapman & Hall, London
13. Norde W (2003) Colloids and interfaces in life science. Marcel Dekker, New York
14. Van de Ven TGM (1989) Colloidal hydrodynamics. Academic, San Diego
15. Shubin V, Linse P (1995) Effect of electrolytes on adsorption of cationic polyacrylamide on silica: ellipsometric study and theoretical modeling. J Phys Chem 99:1285–1291
16. Linse P, Wennerström H (2012) Adsorption versus aggregation. Particles and surface of the same material. Soft Matter 8:2486–2493
17. Ondaral S, Ankerfors C, Ödberg L et al (2010) Surface-induced rearrangement of polyelectrolyte complexes: influence of complex composition on adsorbed layer properties. Langmuir 26:14606–14614
18. Alince B, Kinkal J, Bednar F et al (2002) The role of "free charge" in the deposition of latex particles onto pulp fibers. In: Daniels ES, Sudol ED, El-Aasser MS (eds) ACS Symp Ser. American Chemical Society, Washington, DC

19. Gärdlund L, Wågberg L, Gernandt R (2003) Polyelectrolyte complexes for surface modification of wood fibres II. Influence of complexes on wet and dry strength of paper. Colloids Surf A 218:137–149
20. Biggs S, Sakai K, Addison T et al (2007) Layer-by-layer formation of smart particle coatings using oppositely charged block copolymer micelles. Adv Mater 19:247–250
21. Toomey R, Mays J, Holley DW et al (2005) Adsorption mechanisms of charged, amphiphilic diblock copolymers: the role of micellization and surface affinity. Macromolecules 38:5137–5143
22. Wittmer J, Joanny J-F (1993) Charged diblock copolymers at interfaces. Macromolecules 26:2691–2697
23. Kramer G, Somasundaran P (2004) Fluorescence and ESR studies of the conformational behavior of oppositely charged polyelectrolytes at solid/liquid interfaces. J Colloid Interface Sci 273:115–120
24. Hubbe MA, Moore SM, Lee SY (2005) Effects of charge ratios and cationic polymer nature on polyelectrolyte complex deposition onto cellulose. Ind Eng Chem Res 44:3068–3074
25. Saarinen T, Österberg M, Laine J (2008) Adsorption of polyelectrolyte multilayers and complexes on silica and cellulose surfaces studied by QCM-D. Colloids Surf A 330:134–142
26. Norgren M, Gärdlund L, Notley SM et al (2007) Smooth model surfaces from lignin derivatives. II. Adsorption of polyelectrolytes and PECs monitored by QCM-D. Langmuir 23:3737–3743
27. Wågberg L, Lindström T (1987) Some fundamental aspects on dual component retention aid systems. Nord Pulp Pap Res J 2:49–55
28. Lofton MC, Moore SM, Hubbe MA et al (2005) Deposition of polyelectrolyte complexes as a mechanism for developing paper dry strength. Tappi J 4:3–8
29. Koljonen K, Vainio A, Hiltunen E et al (2003) The effect of polyelectrolyte adsorption on the strength properties of paper made from mixtures of mechanical and chemical pulps. In: Proceedings 5th International Paper and Coating Chemistry Symposium, Montreal, Canada, June 2003. Pulp and Paper Research Institute of Canada
30. Vainio A, Paulapuro H, Koljonen K et al (2006) The effect of drying stress and polyelectrolyte complexes on the strength properties of paper. J Pulp Pap Sci 32:9–13
31. Heermann ML, Welter SR, Hubbe MA (2006) Effects of high treatment levels in a dry-strength additive program based on deposition of polyelectrolyte complexes: how much glue is too much? Tappi J 5:9–14
32. Hubbe MA (2005) Dry-strength development by polyelectrolyte complex deposition onto non-bonding glass fibres. J Pulp Pap Sci 31:159–166
33. Lindström T (1989) Some fundamental chemical aspects on paper forming. In: Punton V and Baker CF (eds) Fundamentals of papermaking: transactions 9th fundamental research symposium, Cambridge, Sept 1989. Mechanical Engineering Publications, London
34. Andersson K, Lindgren E (1996) Important properties of colloidal silica in microparticulate systems. Nord Pulp Pap Res J 11:15–21
35. Agarwal M, Lvov Y, Varahramyan K (2006) Conductive wood microfibres for smart paper through layer-by-layer nanocoating. Nanotechnology 17:5319–5325
36. Agarwal M, Xing Q, Shim BS et al (2009) Conductive paper from lignocellulose wood microfibers coated with a nanocomposite of carbon nanotubes and conductive polymers. Nanotechnology 20: 215602
37. Renneckar S, Zhou Y (2009) Nanoscale coatings on wood: polyelectrolyte adsorption and layer-by-layer assembled film formation. ACS Appl Mater Interfaces 1:559–566
38. Lindström T, Söremark C, Westman L (1977) The influence on paper strength of dissolved and colloidal substances in the white water. Svensk Papperstid 80:341–345
39. Nylund J, Byman-Fagerholm H, Rosenholm JB (1993) Physico-chemical characterization of colloidal material in mechanical pulp. Nord Pulp Pap Res J 8:280–283
40. Li P, Pelton R (1992) Wood pulp washing. 1. Complex formation between kraft lignin and cationic polymers. Colloids Surf 64:217–222

41. Li P, Pelton R (1992) Wood pulp washing. 2. Displacement washing of aqueous lignin from model beds with cationic polymer solutions. Colloids Surf 64:223–234
42. Ström G (1984) For better or for worse: polyelectrolyte complexes in the stock. Svensk Papperstid 87:14–16, 19–20
43. Ström G, Barla P, Stenius P (1979) The formation of lignin sulphonate-polyethyleneimine complexes and its influence on pulp drainage. Svensk Papperstid 82:408–413
44. Ström G, Barla P, Stenius P (1982) The effect on pine xylan on the use of some polycations as retention and drainage aids. Svensk Papperstid 85:R100–R106
45. Ström G, Barla P, Stenius P (1985) The formation of polyelectrolyte complexes between pine xylan and cationic polymers. Colloids Surf 13:193–207
46. Ström G, Stenius P (1981) Formation of complexes, colloids and precipitates in aqueous mixtures of lignin sulfonate and some cationic polymers. Colloids Surf 2:357–371
47. Ödberg L, Ström G (1983) ESCA studies of retention and dewatering aids. The adsorption of polymin SN and polymin SN-lignosulfonate complexes on cellulose. Svensk Papperstid 86:R141–R145
48. Rojas OJ, Neuman RD (1999) Adsorption of polysaccharide wet-end additives in papermaking systems. Colloids Surf A 155:419–432
49. Vanerek A, van de Ven TGM (2006) Coacervate complex formation between cationic polyacrylamide and anionic sulfonated kraft lignin. Colloids Surf A 273:55–62
50. Ankerfors C, Ondaral S, Wågberg L et al (2010) Using jet mixing to prepare polyelectrolyte complexes: complex properties and their interaction with silicon oxide surfaces. J Colloid Interface Sci 351:88–95
51. Johnson BK, Prud'homme RK (2003) Mechanism for rapid self-assembly of block copolymer nanoparticles. Phys Rev Lett 91:118302
52. Petzold G, Schwartz S (2013) Polyelectrolyte complexes in flocculation applications. Adv Polym Sci. doi:10.1007/12_2012_205
53. Gärdlund L, Forsström J, Andreasson B et al (2005) Influence of polyelectrolyte complexes on the strength properties of papers from unbleached kraft pulps with different yields. Nord Pulp Pap Res J 20:36–42
54. Gärdlund L, Norgren M, Wågberg L et al (2007) The use of polyelectrolyte complexes (PECs) as strength additives for different pulps used for production of fine paper. Nord Pulp Pap Res J 22:210–216
55. Espy HH (1995) The mechanism of wet-strength development in paper: a review. Tappi J 78:90–99
56. Johnson BK, Prud'homme RK (2003) Chemical processing and micromixing in confined impinging jets. AIChE J 49:2264–2282
57. Eriksson M, Notley SM, Wågberg L (2005) The influence on paper strength properties when building multilayers of weak polyelectrolytes onto wood fibers. J Colloid Interface Sci 292:38–45
58. Lingström R, Wågberg L (2008) Polyelectrolyte multilayers on wood fibers: influence of molecular weight on layer properties and mechanical properties of papers from treated fibers. J Colloid Interface Sci 328:233–242
59. Ankerfors C, Lingström R, Wågberg L et al (2009) A comparison of polyelectrolyte complexes and multilayers: their adsorption behaviour and use for enhancing tensile strength of paper. Nord Pulp Pap Res J 24:77–86
60. Feng X, Pouw K, Leung V et al (2007) Adhesion of colloidal polyelectrolyte complexes to wet cellulose. Biomacromolecules 8:2161–2166
61. Feng X, Pelton R, Leduc M (2006) Mechanical properties of polyelectrolyte complex films based on polyvinylamine and carboxymethyl cellulose. Ind Eng Chem Res 45:6665–6671
62. Xiao L, Salmi J, Laine J et al (2009) The effects of polyelectrolyte complexes on dewatering of cellulose suspension. Nord Pulp Pap Res J 24:148–157
63. Arzt E, Gorb S, Spolenak R (2003) From micro to nano contacts in biological attachment devices. Proc Natl Acad Sci USA 100:10603–10606

64. Lamblet M, Verneuil E, Vilmin T et al (2007) Adhesion enhancement through micropatterning at polydimethylsiloxane-acrylic adhesive interfaces. Langmuir 23:6966–6974
65. Bakker HE, Lindström SB, Sprakel J (2012) Geometry- and rate-dependent adhesive failure of micropatterned surfaces. J Phys Condens Matter 24:065103
66. Torgnysdotter A, Kulachenko A, Gradin P et al (2007) The link between the fiber contact zone and the physical properties of paper: a way to control paper properties. J Compos Mater 41:1619–1633
67. Ankerfors C, Johansson E, Pettersson T et al (2013) Use of polyelectrolyte complexes and multilayers from polymers and nanoparticles to create sacrificial bonds between surfaces. J Colloid Interface Sci 391:28–35
68. Bartlett MD, Croll AB, King DR et al (2012) Looking beyond fibrillar features to scale gecko-like adhesion. Adv Mater 24:1078–1083

Adv Polym Sci (2014) 256: 25–66
DOI: 10.1007/12_2012_205

Published online: 24 August 2013

Polyelectrolyte Complexes in Flocculation Applications

Gudrun Petzold and Simona Schwarz

Abstract This review concentrates on the interactions between oppositely charged polyelectrolytes and on the formation of complexes, which can be used for different applications such as paper retention or water treatment. Three different possibilities for the appearance of polyelectrolyte complexes (PECs) in flocculation applications are described. Starting with the "classical" dual system (step-by-step addition of polycation and polyanion to a negatively charged suspension of fibers or particles), the interaction between a "soluble polyanion" (such as anionic trash) with polycation is described as well as the formation of well-defined pre-mixed PECs and their application as flocculants.

The influence of several parameters related to the characteristics of the solid materials (e.g., charge, particle size), the polyelectrolyte (e.g., type of charge, charge density, molar mass, hydrophobicity) and the flocculation regime (e.g., order of addition, pH, ionic strength) are discussed.

Research in this area shows great potential. Over the past 30 years, dual systems have been applied mainly in the paper industry. The application of PECs, described as particle-forming flocculants, provides new possibilities in solid–liquid separation processes. For an effective system, the application parameters have to be optimized (e.g. polymer type, concentration, charge, molecular weight). Therefore, direct and efficient methods for the characterization of the flocculation behavior (sedimentation velocity, packing density of the sludge, particle size distribution) are necessary and will be described.

Finally, the most advanced applications for PECs are discussed.

Keywords Dual system · Flocculation · Polyanion · Polycation · Polyelectrolyte complex · Pre-mixed complexes

G. Petzold and S. Schwarz (✉)
Leibniz-Institut für Polymerforschung Dresden e.V., Hohe Strasse 6, 01069 Dresden, Germany
e-mail: simsch@ipfdd.de

Contents

Abbreviations and Symbols

AFM	Atomic force microscopy
CD	Charge density
CMC	Carboxymethylcellulose
cmc	Critical micelle concentration
CNT	Carbon nanotubes
CPR	Carboxylated phenolic resin
DCS	Dissolved colloidal substances
DLS	Dynamic light scattering
DMAPAA	*N*,*N*-Dimethylaminopropylacrylamide
DSC	Differential scanning calorimetry
FTIR	Fourier transform infrared spectroscopy
GPE	Short-chained guest PEL
HA	Humic acid
HCS	Highly cationic starches
HMW	High molecular weight
HPE	Long-chained host PEL
LCST	Lower critical solution temperature
LMW	Low molecular weight

MMW	Medium molecular weight
NaPA	Poly(sodium acrylate)
NaPAMPS	Poly(sodium 2-acrylamido-2-methylpropanesulfonate)
NaPSS	Poly(styrene-*p*-sodium sulfonate-sodium salt)
NIPEC	Nonstoichiometric interpolyelectrolyte complex dispersion
NPEC	Nonstoichiometric polyelectrolyte complex
OM-PEI	Oligo-maltose-modified PEI
P(MSP)	Poly(maleic acid-*co*-propylene)
P(MS-α-MeSty)	Poly(maleic acid-*co*-α-methylstyrene)
PA	Polyanion
PAA	Poly(acrylamide)
PAC	Poly(acrylic acid)
PAE	Polyamideamine epichlorohydrine condensate
PAMPS	Poly(sodium 2-acrylamido-2-methylpropanesulfonate)
PC	Polycation
PC/D/PA	Polycation/dye/polyanion complexes
PCA5	Polycations containing *N*,*N*-dimethyl-2-hydroxypropylene ammonium chloride
PCA5D1	Polycations containing *N*,*N*-dimethyl-2-hydroxypropylene ammonium chloride with different hydrophobic units
PDADMAC	Poly(*N*,*N*-diallyl-*N*,*N*-dimethyl-ammonium chloride)
PEC	Polyelectrolyte complex
PEI	Poly(ethyleneimine)
PEL	Polyelectrolytes
PEO	Poly(ethylene oxide)
PI	Polydispersity index
PMADAMBQ	Copolymer of *N*-methacryloyloxyethyl–*N*-benzyl-*N*,*N*-dimethyl-ammonium chloride
PNIAA	Poly(isopropylacrylamide-*co*-acrylic acid)
PNIPAAM	Poly(*N*-isopropylacrylamide)
PNVCL	Poly(*N*-vinylcaprolactam)
PPEI	Phosphonomethylated derivative of PEI
PR2540	Poly(acrylamide-*co*-sodium acrylate)
PSC	Polyelectrolyte–surfactant complex
PSS	Poly(styrene sulfonate)
PTMMAC	Poly[*NNN*-trimethyl-*N*-(2-methacryloxyethyl) ammonium chloride]
PVA	Poly(vinyl alcohol)
Quartolan	Dodecyl-amidoethyl-dimethylbencyl-ammonium chloride
SDS	Sodium dodecylsulfate
siRNA	Small interfering RNA
TC	Trash content
TOC	Total organic carbon content
XPS	X-ray photoelectron spectroscopy

XRD X-ray diffraction

Polycation 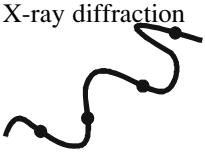

Polyanion 

Negatively charged particle 

Polyelectrolyte complex 

Micelle 

Negatively charged waste 

Surfactant 

Star-like polymer 

1 Introduction

Solid–liquid separations are an important part of many industrial processes such as papermaking, water treatment, or mineral processing.

For the separation of particles or unwanted components from a dispersion, it is necessary to add flocculants. Salts, such as ferrous (III) or aluminum salts, which were used as flocculants in the past, have many drawbacks such as high demand for salt, the formation of small, unstable flocs, and a large volume of sludge. Therefore, they were replaced by water-soluble polymers (or were used in combination with them). Small polymer concentrations can produce large aggregates that can be separated easily. Numerous flocculating agents with different chemical properties are commercially available. Their flocculation mechanism as well as the results of the separation process are influenced by the properties of the polymers, such as their charge and molecular weight, and of the dispersed material. Nearly every solid–liquid system is different from every other. Therefore, there is no general rule on how to treat them. In different fields of application, the solid–liquid systems can be extremely different. So, the particle size can range from a few nanometers up to micrometers, or the solid content from parts per million up to 20%. The removal of solids of nanometer-size range from the dispersion is a crucial stage in many environmental technologies. Such colloidal particles are too small to be effectively separated by filtration, flotation, or sedimentation. Therefore, the most effective way to remove them is to cause the particles to flocculate so that larger units are formed.

As already mentioned, an effective separation can be realized by using only one polymer (monoflocculation). But, because water is becoming an increasingly scarce and limiting resource, the demand for treatment technologies has grown and, in recent years, there has been considerable interest in cases where more than one polymer is used. Such combinations of polymers can have significant benefits over the use of single polymers. Moreover, we will show that some of the new challenges in the industry can only be solved by using new types of flocculants.

We will discuss the possible interactions of such polymer mixtures from polycations (PC) and polyanions (PA), which can form polyelectrolyte complexes (PECs) or can be applied as “dual systems”.

There are some different possibilities for the appearance of PECs in flocculation applications. The most important options are presented in Fig. 1.

The first option is the application of two-component flocculants of opposite charge, which are added step by step (Fig. 1, top). During the flocculation process an interaction can occur between the two flocculants PA and PC, resulting in the formation of PECs, as well as between the polymer (mostly PC) and the suspension (inorganic particles or fibers). A summary of former results and recent developments will be presented in Sect. 2.

The complex formation between a (mostly negative) charged suspension and PC (Fig. 1, center) will be described in Sect. 3. The “basic” type of flocculation, i.e., the interaction between a negatively charged particle suspension and PC has often been studied and is not the topic of this review. But, instead of a particle suspension, the PC

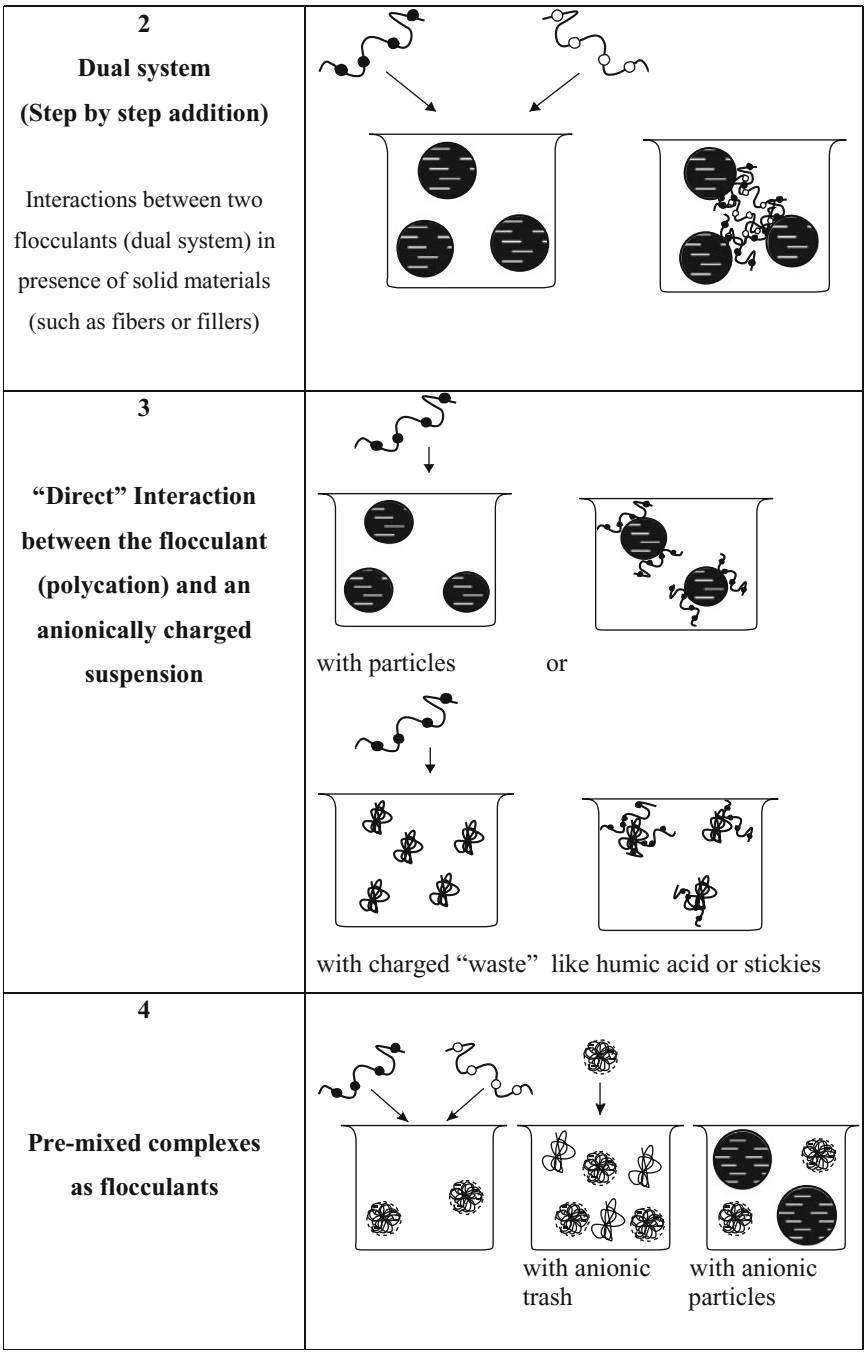

Fig. 1 Different types of polyelectrolyte complexes (PECs) in flocculation applications

can interact also with colloidal detrimental substances such as stickies (Fig. 1, center). Relatively few systematic investigations of such interactions have been reported.

The third possibility is the formation and application of pre-mixed PECs in a first step, which can then be applied as flocculants (Fig. 1, bottom).This will be described in Sect. 4.

The use of polymer combinations for the improvement of flocculation efficiency is not new and was described earlier [1–24]. Two or even more components, added in sequence as flocculant systems, produce synergistic effects on the flocculation. Many different systems have been applied in the paper industry, and also in other fields like peat dewatering [1], flocculation of harbor sediments [2], wastewater [3], or sugar beet washings [4].

But, in the meantime, the importance of flocculation applications has been growing because of increasing requirements in several fields, such as for:

The paper industry:

- Excellent dewatering combined with good retention
- Reduction of high anionic trash content in combination with the reduction of water use in paperprocessing (due to the closure of circuits)

In other fields, flocculation is used in the following processes:

- Separation of ultrafine- or nanoparticles
- Separation of uncharged and/or colored materials
- Purification of fruit and vegetable wash water
- Reduction of the moisture content in separated sludge
- Sorption of low concentrated organic molecules from water, such as enzymes or hazardous materials
- Removal of humic acid from drinking water
- Preparation of carrier materials with great potential in health care and environmental sciences
- Splitting of emulsions and the removal of oil from oily sludge

The next three sections show that some of the problems that flocculation is required to deal with can only be solved with new types of flocculants like polymer combinations or aggregates.

2 Dual Systems (Step-by-Step Addition)

Flocculants are usually applied to accelerate separation processes, such as the drainage process during paper making, and to increase the retention of the finely dispersed material in the paper. Flocculation is one of the most important factors and influences both the machine runability and paper quality. Many chemical and physical factors influence flocculation in a complex way.

Usually, cationic polymers of high molar mass are used for flocculating the anionically charged suspension. However, the improved effect of dual systems is also appreciated. The application of two or even more components, added in sequence

as flocculant systems, produces synergistic effects on the flocculation. Many different systems have been applied, especially in the paper industry.

The so-called dual system was first described in literature in the 1970s and consists of two oppositely charged polymers. It can produce distinct improvements in retention and dewatering [5, 6]. From the 1980s until now, much work has been done to improve our knowledge about such systems. This has been especially true in research areas like paper forming and floc shear stability. A special type of dual system, the so-called microparticle containing system, has been developed. In this system, the addition of a cationic polymer is followed by the addition of an anionic submicron particle suspension. Examples of this type of retention aid system are cationic starch used in conjunction with anionic colloidal silica or anionic colloidal alumina hydroxide and cationic copolymers of acrylamide used together with sodium montmorrilonite. Several systems of this type are commercially available. They are said to be very efficient flocculants, which give smaller flocs at an equal degree of flocculation compared to single-component systems.

Very good reviews, which include a survey of some aggregation mechanisms and comparisons between different dual systems, are available [7–12].

This chapter focuses on polymer–polymer systems, mainly in the paper industry. But, current approaches used in other fields of flocculation will also be mentioned.

2.1 Interaction with Cellulose (Paper Industry)

An example of an early and very detailed investigation of such a dual system is the work of Moore [13], in which different types of cationic polymers were combined with hydrolyzed polyacrylamides at various alumina concentrations. In contrast to other workers, Moore studied the charge relationship of the various charged species. He discovered that a combination of cationic and anionic polymers can give very high levels of retention with high shear resistance only in the case of a proper balance of charges and concentrations.

Müller and Beck [14] have investigated cationic polyethylene imine (PEI) or polyamidoamine in combination with an anionic polyacrylamide. They explained that under conditions of optimum performance, two mechanisms are operating: charge patch formation and bridging. The relatively short-chain PC produces a very fine flocculation of the particles via a charge patch destabilization mechanism. If a long-chain polyacrylamide (PAA) is then added to the stock, the negatively charged chains "get a good grip" on the positive patches of the primary floc and bring further linkages by forming bridges. Other aspects of the floc formation mechanism were studied by Petäjä [15], including the influence of the type and amount of PC, the time delay between cationic and anionic addition, and the degree of turbulence. It was shown that the agitation level and control of floc formation after cation addition are very important for good sheet formation.

In Table 1, a wide variety of examples of polymer–polymer systems from the literature are listed. The most commonly used systems are those in which the PC is added prior to a high molar mass PA. It was confirmed by different authors that the

Table 1 Examples of different types of polymer–polymer dual-systems

Type of polycation (PC)	Type of polyanion (PA)	Remarks/reference
PEI or PAAm; LMW; 0.2–0.3 wt%	PAA; HMW; 0.02–0.04 wt%	Optimum ratio is necessary; for waste paper [14]
PEI or other PC; LMW up to HMW	"PA"	Dual systems are not the solution to all retention problems [15]
PDADMAC of MMW, high charge density or dimethyl-amino-epichloro-hydrin resin of LMW; 0.07 wt%	PAA, HMW; medium charge density; 0–0.12 wt%	Three different dual systems are compared [16]; cationic polymer should be added before the anionic
LMW polymers, e.g., polyamines (highly cationic)	PAA	Dual systems need better control in terms of optimum polymer ratio [17]
Polyacrylamide copolymer	PAA (medium or HMW)	The cationic charge density of the polymer affected initial flocculation as well as reflocculation; fiber fines and filler responded differently on flocculation [18]
Starch 2 wt%	PAA; 0–0.08 wt%	Classical dual systems are both less reversible and show a lower dewatering compared with microparticle systems [19]
PDADMAC; MMW	PAA; HMW; low or medium charge density	The necessary amount of PC depends on the charge of the suspension [20, 21]
Cationically modified PVA	PAA-derived PA; HMW; low charge density	Improvement in the flocculation of fine clay particles [22]
PC with low charge density of 6 mol%	PA with high charge density of 35 mol%	Optimum at a 1:1 mass ratio, corresponding to about sixfold excess of negative over positive charges in the adsorbed layer [23]
PAA-derived PC with charge density 50%	Three different synthetic PAA-based PA	It is necessary to consider the overall system of sedimentation and filtration of the sludge; PC followed by PA is more effective than PA followed by PC [2]
Cationic starch (degree of substitution > 0.5)	Synthetic PAs	The results of [24] are comparable to those in [2]

The quantity of polymers used is mostly given in weight percent

order of addition is essential for efficacy. Drainage and retention are significantly increased if the PC is added before adding the PA, a treatment usually superior to the addition of a single PC. However, the dose rates of such systems are said to be often higher than those for single polymers [9]. It may be that the optimum polymer balance was not reached in these cases.

Table 1 demonstrates the large differences in the composition of dual systems. The quantity of polymers is mostly given in weight percent (wt%) without consideration of the charge content of the systems to be flocculated.

In contrast to microparticle-containing systems, which were widely used in the paper industry, the "classical" dual retention aid systems (polymer–polymer) are said to give high retention combined with a poor dewatering [19]. But, some researchers were able to show that an optimized polymer–polymer system has many advantages, such as good dewatering, superior retention, and shear-resistant flocs.

These effects are obtained by a combination of charge patch formation and bridging. The behavior especially depends on the concentration of PC (according to the anionic character of the suspension) and the molar ratio of anionic and cationic charges.

We have studied the mechanism of such polymer–polymer interactions as well as the interaction between polymers and fibers or particles [20]. After investigating the reaction between the strong PC poly(diallyl-dimethyl-ammonium chloride) (PDADMAC) and two cellulosic model suspensions with low or high anionic trash content, the influence of added PA on flocculation and dewatering was studied [20, 21]. As shown in Fig. 2a, for both suspensions, the drainage volume increased with increasing polymer (PC) concentration in the suspension up to a maximum. The charge of the suspension is slightly negative at this point, as shown in Fig. 2b. However, at higher polymer dosage the efficiency of flocculation decreases. Something like a plateau can be found; however, at the polymer dosage where the system is neutral, the volume V_{SR} strongly decreases. The polymer amount that is necessary for optimum flocculation depends on the charge of the suspension to be flocculated. For instance, the optimum polymer concentration (cationic demand) significantly increases with increasing trash content, but the drainage behavior (maximum of the drainage volume) was similar in both cases (Fig. 2a). The amount of PC necessary for optimum flocculation is of great importance for the optimization of the whole dual system and, as a rule, it should be determined first.

It was also found that the molar mass of the added PA has large influence on flocculation and dewatering. The higher the molar mass, the better the efficiency in flocculation. In contrast to this observation, the charge density of the PAs should not be very high. Most excellent results were obtained with PAA having a low (less than about 30%) anionic charge. The difference between a step-by-step addition of polymers to cellulosic suspension and the addition of pre-mixed complexes [25] will be discussed in Sect. 4.

2.2 *Interaction with Humic Acid*

The influence of charge and molar mass on the flocculation mechanism was also confirmed by results obtained for water treatment, where the influence of humic acid on the flocculation of clay was investigated [26]. The separation of clay particles was influenced by the presence of humic compounds, which act like an additional PA in the clay dispersion. Owing to their adsorption on clay and the higher anionic charge

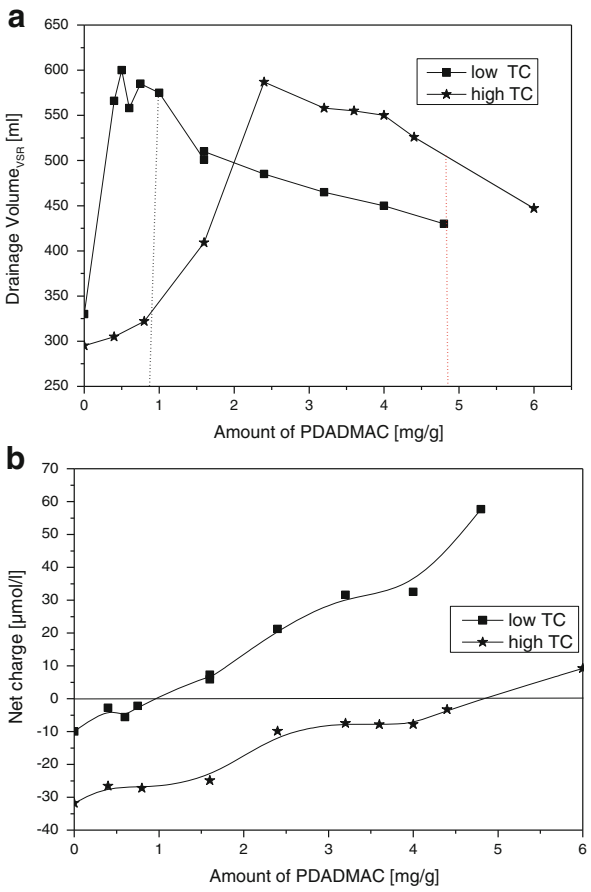

Fig. 2 Drainage behavior of cellulosic model suspensions with low or high anionic trash content (TC) in the presence of PDADMAC. (**a**) Drainage volume V_{SR} in dependence on the amount of PDADMAC; the *dotted lines* exhibit the point of zero charge in the suspension. (**b**) Net charge of the residual solution/mixture in dependence on the amount of added PDADMAC

of the system to be flocculated, the optimum PC concentration is higher compared with clay in water. PCs with high charge density are efficient at removing humic acid owing to complex formation and precipitation. It was shown that the complexes formed by the highly charged PDADMAC and the weak PA humic acid are also able to collect fine particles. Most effective removal of humic acid was obtained by a combination of the highly charged PC and small amounts of a high molar mass PA (dual system). In this case, a broad flocculation window (Fig. 3) was obtained because of the bridging mechanism, as well as larger flocs than obtained with monoflocculation [26].

2.3 Removal of Minerals or Heavy Metals

Dual systems were also used for the flocculation of mineral suspensions [27, 28] or for the precipitation of heavy metals such as Cu^{2+}, Co^{2+}, Zn^{2+}, Ni^{2+}, and Pb^{2+} [29, 30]. Glover [27] investigated the effect of a dual system on the compressive yield stress and

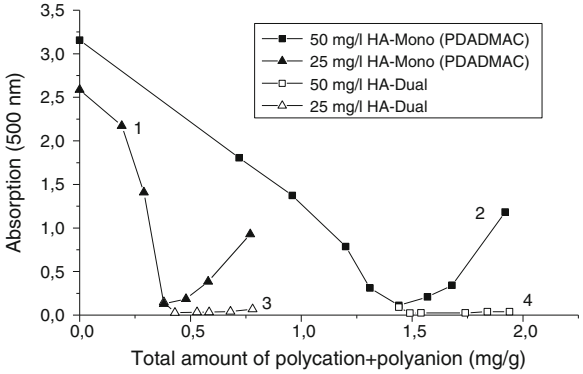

Fig. 3 Monoflocculation (*curves 1* and *2*) compared with dual flocculation (*curves 3* and *4*) of clay (10 g/L) in solutions of humic acid (HA) in water (25 or 50 mg/L) showing dependence of the absorption of the supernatant on the total amount of polymer used. PDADMAC was used for monoflocculation; PDADMAC + HMW PA were used as dual system. Figure adapted from [26]

hindered settling function of positively charged alumina suspensions, as measured by a filtration technique.

The removal of various heavy metal ions such as Cu^{2+}, Co^{2+}, Zn^{2+}, Ni^{2+}, and Pb^{2+} from aqueous solutions was conducted [29]. Heavy metal binding with a phosphonomethylated derivative of PEI (PPEI) was initially allowed to occur and then, upon equilibration, PEI was added to initiate precipitation of the PEC together with the heavy metal ion. The PPEI–PEI system was found effective for heavy metal scavenging purposes, even in the presence of high concentrations of non-transition metal ions like Na^{+}. The PPEI–PEI PEC was found to be more effective than traditional precipitation methods; however, the result was not obtained by the application of premixed complexes, but by a step-by-step addition of PPEI and PEI (similar to other dual systems described here).

Gohlke described the separation of heavy metal ions with a PEC comprising a polycation and a polyphosphone compound [30].

Another field of an advanced separation is the flocculation and efficient dewatering of ultrfine coal (>150 μm) with a polymer blend (unmodified and sonicated flocculant) as dual system [31]. The authors proved that ultrasonic conditioning may be an effective alternative for a dual system in which two different flocculants are used.

2.4 Dual Systems Using "New Polymers"

In contrast to studies where most advantageous results were obtained by an optimization of the polymer amount and properties (molar mass, charge density) [20, 21], other groups have been trying to improve the results by the application of "new" polyelectrolytes. Water-soluble starch derivatives with a high degree of substitution up to 1 (containing quaternary ammonium groups) were used in combination with a high molar mass PAA for the flocculation of harbor sediment suspensions [32].

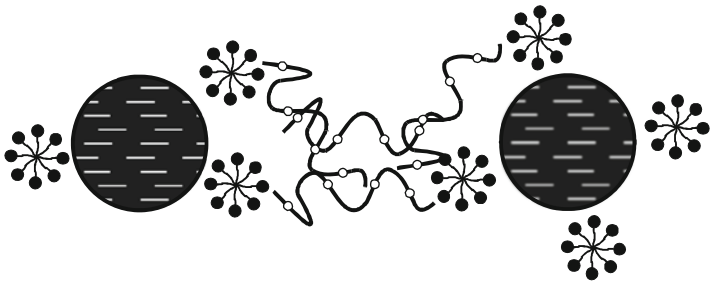

Fig. 4 Clay flocculation induced by dual-polymer system based on Star-P(MeDMA) polymers. Adapted from [33]

Li et al. [33] investigated the application of cationic star polymer with 21 arms as part of a novel component in a dual-component flocculation system for fine clay particles. Several cationic star polymers with different hydrodynamic sizes were applied as both single- and dual-component flocculation systems. The results indicated that the dual-component systems were superior to the single-component systems. In combination with a PAA-based anionic polymer (Percol 173) with high molar mass, very effective flocculation was achieved using the star polymer. Electrostatic interactions between the clay and Star-P(meDMA) polymers, as well as those between the Star-P-pretreated clay and anionic polymer, were studied via the determination of adsorption isotherms. It was concluded that the star polymers played an important role in inducing highly effective bridging flocculation (Fig. 4). Moreover, the reported system also removed soluble aromatic compounds simultaneously with the flocculation.

A new type of dual system was also described by Sang [22]. In conjunction with an anionic PAA-based polymer with high molar mass and low charge density, cationic modified PVA induced effective flocculation of fine clay particles.

As mentioned above, two-component flocculants often present advantages over a single-component flocculant, such as better control of flocculation kinetics and improved floc strength. Most dual-component flocculants consist of two polyelectrolytes, two polymers, or a polyelectrolyte and a nanocolloid. Usually, one of the components adsorbs on the surface of the particles to be flocculated and the second component bridges these polymer-coated particles. Therefore, this combination of "patching" and "bridging" is believed to be responsible for excellent results, as described for instance for retention systems (Fig. 5) [10].

2.5 Dewatering and Sludge Conditioning

Sludge conditioning by single and dual polymers has been investigated [34, 35]. Capillary suction time (CST) or specific resistance to filtration (SRF) were used to assess sludge dewaterability. Experimental results showed that sludge conditioned with dual polymers showed a better dewaterability, with less chance of overdosing

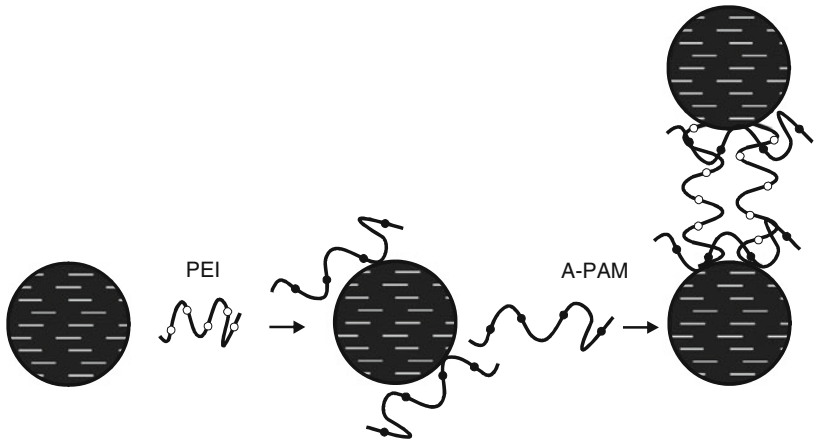

Fig. 5 Combinations of polyelectrolytes with different charge. Primary flocs are formed with the help of patching, after which primary flocs are linked together by bridging. *PEI* poly(ethyleneimine), *A-PAM* anionic polyacrylamide copolymer. Adapted from [10]

compared with sludge conditioned using a single polymer. In addition, sludge conditioned with dual polyelectrolytes (PEL) performed better in fine particle capture and in the formation of larger aggregates, which resulted in a better dewaterability and less chance of overdosing [34, 35].

The formation and breakage of flocs using dual systems was also investigated by Yukselen and Gregory. In the case of cationic–anionic polymers, the re-growth of flocs was fully reversible and the breakage factors were smallest, indicating highest floc strength. In contrast, flocs formed using nonionic polymer together with anionic or cationic polymer did not produce strong flocs [36].

Wang et al. [37] investigated the dual conditioning of activated sludge utilizing a polyampholyte in combination with ferric chloride or cationic PEL. The investigations indicated that dual conditioning of sludge exhibited better dewaterability at lower doses compared with single conditioning. The advantages of PDADMAC over ferric chloride as applied in dual systems were also discussed [38].

As shown for clay [39], the sediment height and therefore the density of the sediment can be measured quantitatively using the separation analyzer LUMiFuge. The results obtained agreed very well with other methods like the JAR-Test, which is not so convenient.

One example of a very special dual-component polymeric flocculant is poly (ethylene oxide) (PEO) and carboxylated phenolic resin (CPR), usually referred to as a cofactor. It has been shown that this dual flocculant can induce a richness of flocculation behavior depending on the concentration of the two components [40, 41]. Flocculation, deflocculation, and reflocculation of cellulose particles were studied for various CPR:PEO ratios. It was found that reflocculation is a strong function of this ratio. For low ratios, no reflocculation occurs after a few cycles, whereas for high ratios very limited flocculation and reflocculation occurs.

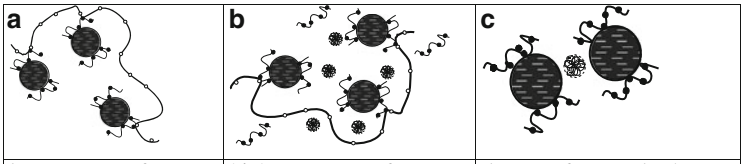

low amount of polycation	higher amount of PC (than in 6a), formation of PEC as an additional flocculant	dosage of PC and PA at the same time

Fig. 6 Different types of interaction between PC and PA in the presence of particles, depending on the amount of PC and the order of addition: (**a**) low amount of polycation, (**b**) higher amount of PC (than in **a**), formation of PEC as an additional flocculant, (**c**) dosage of PC and PA at the same time

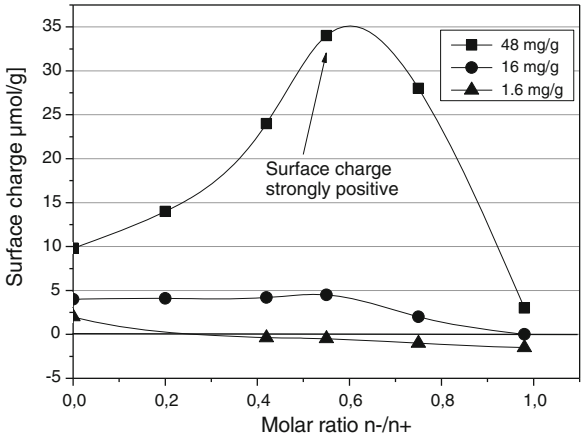

Fig. 7 Surface charge of sulfite cellulose, modified with PDADMAC/P(MS-α-MeSty) in dependence on the molar ratio of PA and PC at different dosage levels of the PC

2.6 Surface Modification

We have described how a step-by-step addition of oppositely charged PEL can improve the quality of flocculation. A possible flocculation mechanism is described (Fig. 5) and is also shown for comparison in Fig. 6a. However, an increase in the PC amount can also lead to the formation of PEC in solution (Fig. 6b), which can be used as an additional flocculant. In the case that the PC and PA are added at the same time, the complex formation is favored (Fig. 6c).

The situation shown in Fig. 6b can also be applied for a strong surface modification of particles or fibers [42–45]. As demonstrated [43], in the presence of cellulose the complex formation between the two PEL is favored in the solution, and this complex itself is adsorbed on the surface by electrostatic interactions, which also causes flocculation. Under the condition that a large quantity of PC is still in solution when the PA is added dropwise, it is possible that the incorporation of the PC into the expanded complex takes place. As shown in Fig. 7, the surface charge of flocculated

cellulose increases and has a maximum at a molar ratio of negative to positive charges ($n-/n+$) of about 0.55–0.6.

Clay particles whose surfaces have been modified by the PC PDADMAC and the sodium salt of the weak PA poly(maleic acid-*co*-α-methylstyrene), P(MS-α-MeSty), were used as sorbents for removal of surfactants from aqueous solutions [46].

2.7 Dual Systems with Thermosensitive Polymers

A novel strategy for faster and better flocculation in solid–liquid separation processes has been reported. The natural polyelectrolyte chitosan was used in combination with a biocompatible thermosensitive polymer [poly(*N*-vinylcaprolactam); PNVCL]. The flocculation of silica dispersions (Aerosil OX50) was evaluated using laser diffraction and turbidimetry studies. The sedimentation velocity, which was determined with an analytical centrifuge, was doubled by addition of PNVCL. Furthermore, at 45°C the density of the sediment was 33% higher than when chitosan was used. This results from the temperature-sensitive behavior of PNVCL, which phase-separates expelling water at temperatures higher than its lower critical solution temperature (LCST; 32–34°C). By using this strategy, the sediment is more compact, contains less water, and contains a very small amount of biodegradable chitosan and biocompatible PNVCL.

The flocculation of clay using mixtures of chitosan and a thermosensitive polymer was investigated as a function of the polymer concentrations and the temperature at different pH values [47].

The compaction of TiO_2 suspensions [48] as well as the dewatering of inorganic drinking water treatment sludge using dual ionic thermosensitive polymers was described by Sakhohara [48, 49]. By using both cationic and anionic modified PNIPAAm, the anionic thermosensitive polymer poly(NIPAM-*co*-AAC) in combination with cationic poly(NIPAM-*co*-AAC), the dewatering rate was remarkably increased at relatively low temperatures. This increase was attributed to the formation of a polymer complex that decreased the LCST of the polymer molecules adsorbed on the sludge.

3 “Direct” Interaction Between the Flocculant (PC) and an Anionically Charged Suspension

In contrast to the situation shown in Fig. 1 and described in Sect. 2, where different interactions between two oppositely charged PEL on one side and the solid material (fibers or particles) on the other side can occur, in this section we describe the “direct” interaction between a flocculant (PC) and a charged suspension, which acts like a PA. But, as shown in Fig. 1, the suspension can contain particles as well as “soluble” anionically charged material.

Those interactions are very important in the paper industry [50, 51] because the effectiveness of cationic polymers as retention and drainage aids in the manufacture of paper is strongly affected and sometimes even limited by anionic macromolecules, which dissolve in the white water. Such polymers are, for example, lignin or carbohydrates from wood. Therefore, the application-relevant effect of pine xylan on the use of PEI, and acrylamide copolymer as retention and drainage aid, for an unbleached sulfite pulp was investigated [50]. The formation of PECs between pine xylan and three cationic polymers has been studied as a function of pH and ionic strength [51]. Complex formation was found to be nonstoichiometric and both soluble and insoluble complexes are formed, with maximum precipitation occurring when the complexes are neutral. A tentative structure of the complexes was suggested.

3.1 Paper Recycling

The problems of complex formation are growing because the increasing use of de-inked pulps, in combination with the closure of paper machine circuits in pulp and paper industry processes, is leading to an accumulation of so-called trash material or tacky substances. The formation of a high amount of these substances affects paper production negatively due to lower retention of the filler or increased deposition on paper machines. These substances are brought into the process through many different sources. The recycling of paper is one of the most important ways of producing paper.

The variety of tacky materials present in papermaking systems have different names: for instance, the accumulated pollutants in the water recycling system are called dissolved and colloidal substances (DCS). The composition of DCS, which mainly come from pulp, filler, recycled water, and the chemicals added during the papermaking process, is very complex.

Pelton [40] describes PEC formation as an important part of paper technology. One example is the strategy for removing the anionic PEL components of the DCS by adding oppositely charged polymers to form PEC. Oppositely charged PEL will form complexes over a broad range of stoichiometric ratios. However, the complexes tend to be water-soluble unless they are nearly stoichiometric because an excess of either positive or negative particle charge will confer water solubility. This behavior is illustrated by the interaction of PDADMAC, a linear cationic PEL, with kraft lignin, which is a branched anionic phenolic polymer resulting from the decomposition of lignin in the kraft pulping process. The formation and the amount of precipitated kraft-lignin–PDADMAC complex were investigated as a function of the mass ratio (kraft lignin/PDADMAC) and the pH [40]. But, kraft lignin is not ideally suited for fundamental studies of PEC formation because lignin is a polydisperse polymer with a complicated structure; hence, most of the basic information about PEC comes from investigations on well-defined synthetic polymers [52] (see Sect. 4).

3.2 Sticky Removal

The appearance of so-called stickies is described for instance by Hubbe [53]. These are most often the result of synthetic polymers used in pressure-sensitive label adhesives. The full characterization of stickies is not easy to assess since there are many different types of stickies that have to be considered [54].

The existence of primary stickies (from raw materials) and secondary stickies, which were built by the interaction in such systems, has been described, together with many different characterization methods(including mechanical methods) for quantifying the efficiency of different fixing agents [55, 56]. In addition, physico-chemical methods such as measuring the cationic demand, the zeta-potential, or the turbidity of wastewater have been applied.

Unfortunately, none of the sticky test methods investigated was found to be universally applicable, i.e., suitable for all types of stickies. Therefore, the most suitable method must be chosen for each particular case and problem area [56].

Previous articles or reviews (such as [53, 57]) have considered the origin, the nature, as well as the removal of DCS.

Among the organic polymers used in the paper industry to combat deposit problems are polymers with a huge ranges of molecular mass, charge, and hydrophilic versus sparingly soluble character. The effects of these polymers are greatly dependent on how these materials interact with the suspension or with surfaces [53]. Important classes of polymers are cationic polymers with very high mass, e.g., acrylamide polymers (well known as retention aids) or high charge cationic polymers [58, 59]. Hydrophilic polymers of intermediate mass are applied as well as PEL with partially hydrophobic character or surfactants. The adsorption tendency of PEL onto tacky materials can be increased by derivatization with hydrophobic substituent groups. Various copolymers of cationic, hydrophilic monomers, and hydrophobic monomers have shown promise as detackifying agents for resinous material [60, 61].

According to Meixner et al. [62], tailor-made cationic polymers are very effective for fixing interfering substances because they reduce the tendency of adhesive, hydrophobic substances to agglomerate and slow down the rate at which secondary stickies are formed. Using different types of models (hydrophilic or hydrophobic) and fixing agents, Meixner et al. were able to demonstrate that, for efficient sticky removal, not only is the cationic charge necessary but also the hydrophobicity. Whether (or not) a certain polymer is effective depends on the type of detrimental substances.

3.3 Natural Polymers for Sticky Removal

A few articles describe the application of starch, modified starch, or other carbohydrate polymers as flocculant for sticky removal [63–66]. The role of charge on the destabilization of microstickies was investigated by Huo by comparing the strong PC

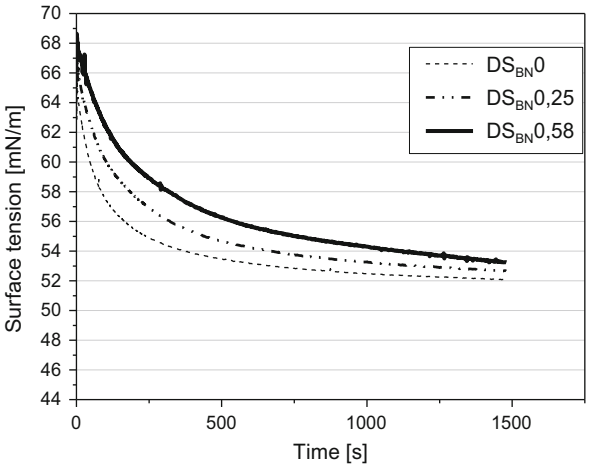

Fig. 8 Dynamic surface tension of mixtures between a highly surface-active model suspension and modified starches having the same cationicity, but different degrees of benzylation, DS_{BN}, at a mixing ratio (volume suspension:volume starch) of 10:1; surface tension was measured using a profile analysis tensiometer (t = 1,200 s) [67]

PDADMAC with commercial cationic starch. The agglomeration of microstickies with PDADMAC occurred mainly via a charge neutralization mechanism. In contrast, the agglomeration of microstickies with cationic starch "had a more complicated behavior" [64].

Luo and Wang [65] prepared highly cationic starches (HCS) with different branching degrees and molar mass. The DCS controlling effects were investigated using zeta-potential, cationic demand, drainage speed, and turbidity. The study indicated that the degraded linear HCS had better performance in controlling microstickies than the branched HCS, which had better performance in paper strengthening.

Recently, we have investigated the interaction between tailored cationic starches wearing hydrophobic groups and model extracts of recycled newspaper and sticky material [67–69]. The properties of the prepared extracts differed in turbidity, total organic carbon (TOC), and charge. The surface tension was established as a useful tool for characterizing the surface activity and, therefore, the sticky content of the suspension. The interaction of three modified starches with the same "medium" cationic charge, but different hydrophobicity (degree of substitution by benzyl groups, DS_{BN}) with model suspensions was investigated. The interaction and complex formation was confirmed by complex precipitation, resulting in a decrease in turbidity and TOC, but an increase in surface tension. The most important consequence of this work was the finding that the amount of cationic charge is essential for sticky removal, especially for the reduction of turbidity and TOC, but that sticky removal can be improved by a higher degree of starch hydrophobicity. The highest surface tension of the mixture between the model suspension and different starch types (mentioned above) was obtained with the benzyl starch, having the highest DS_{BN} (Fig. 8).

The surface tension of this mixture between modified starch and the suspension with a very high sticky content can be further increased by the addition of bentonite (Aquamont) [72], so that the resulting supernatant is almost free of surface-active substances (surface tension about 70 mN/m). It is also important that the mixing

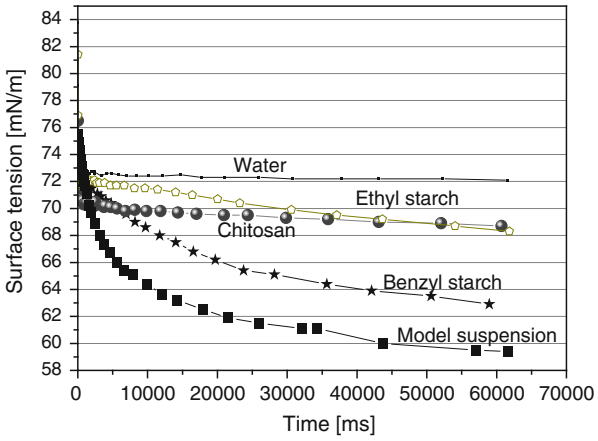

Fig. 9 Dynamic surface tension of mixtures between a highly surface-active model suspension and solutions (1 g/L) of modified natural polymers at the same mixing ratio (volume suspension: volume polymer) of 10:1; dynamic surface tension, was measured by bubble pressure tensiometer ($t = 60$ s)

ratio significantly influences the properties. Despite the fact that the turbidity removal is good in most cases, differences in the surface tension were obtained. The most effective composition (lowest TOC and highest surface tension) was obtained at a mixing ratio were the system is neutral.

Sticky removal with different natural polymers has been compared [69]. Tailored starches, with benzyl as well as with ethyl substituents, from very low to high cationic starch density, were investigated as well as benzylated chitosan.

In contrast to previous results [67, 68], the bubble pressure method, a relative simple and time-saving test method, was used for the dynamic surface tension measurement [69]. For comparison it was shown that the addition of unmodified starch did not have any positive influence on sticky removal: neither for decreasing the turbidity or TOC content, nor for the reduction of surface activity. In contrast, the interaction between the functionalized starches and DCS, and therefore the sticky removal, is significantly influenced by the main properties of the modified starches, i.e., their cationic charge density and their hydrophobicity. As already described, the stickies were removed due to complex formation between the tailored modified starch and the colloidal substances in the suspension having anionic charge. As demonstrated in Fig. 9, the surface tension of a sticky-containing model suspension increases due to the addition of modified natural polymers bearing cationic charge. As already shown [67, 68], the efficiency of sticky removal depends on the charge ratio (anionic:cationic charge), which means that it depends on polymer dosage. Most effective removal was obtained when the mixture between the starch and the SCS was neutral.

Consequently, the results shown in Fig. 9 do not show an optimum because the natural polymers have different cationic charge densities. Whereas the modified starch with low cationic charge (benzyl starch) is more effective at higher polymer dosage, the modified chitosan, having higher cationic charge, has optimum sticky removal at the dosage shown in Fig. 9. The ethyl starch, despite its low cationic charge, is also effective in reducing the surface activity due to its hydrophobicity [69].

4 Pre-mixed PECs as Flocculants

4.1 Complex Formation and Characterization

It is well known that oppositely charged PEL will form complexes over a broad range of stoichiometric ratios.

Such interactions were investigated, among others, by Tsuchida [70], Dubin [71], Philipp and Dautzenberg [72, 73], Müller [74–76], Pergushov and Müller [77], Dragan [12], and the group of Kabanov [78, 79]. Some of the most important PEL used for complex formation are summarized in Table 2 and in works by Dragan [12] and Jaeger et al. [80].

Kabanov et al. described the formation of water-soluble nonstoichiometric PECs (NPEC) as a result of the interaction of oppositely charged PEL in nonequivalent ratios. They are obtained by the interaction of polyions with different degree of polymerization, i.e., different molar masses. The polyions are introduced into the reaction in nonequivalent ratios so that a relatively long-chained host PEL (HPE) is incorporated into an NPEC particle in some excess in comparison with the opposite charged relatively short-chained guest PEL (GPE). Such NPEC are water-soluble because of their big differences in molar mass, and their properties can be studied by classical methods. An NPEC can be represented as a peculiar block copolymer with alternating hydrophobic double-strand blocks and hydrophilic single-strand blocks composed of sequences of HPE units incorporated in NPEC in excess (Fig. 10). One of the most important properties of NPEC is their ability to participate in intermacromolecular exchange and substitution reactions in aqueous solutions, as described by Kabanov [77]. These properties can be used to flocculate and separate materials such as dyes.

PEC nanoparticles, prepared by mixing solutions of the commercial low-cost PEL components PEI and PAC, were described by Müller et al. [75]. It was found that the size and internal structure of PEI/PAC particles can be regulated by process, media, and structural parameters. The mixing order, mixing ratio, PEL concentration, pH, and molar mass were found to be especially sensitive parameters for regulating the size (diameter) of spherical PEI/PAC nanoparticles, in the range between 80 and 1,000 nm, in a defined way.

The formation of PECs using structurally uniform and strongly charged cationic and anionic modified alternating maleic anhydride copolymers was described by Mende [81]. The hydrophobicity of the PEL was changed by the comonomers (ethylene, isobutylene, and styrene). Additionally, the $n-/n+$ ratio of the molar charges of the PEL and the procedure of formation were varied. Dynamic light scattering indicates that, besides large PEC particle aggregates, distinct smaller and more compact particles were formed by the copolymers having the highest hydrophobicity (styrene). These findings could be proved by AFM. Measurements of fractal dimension, root mean square roughness, and the surface profiles of the PEC particles adsorbed on mica allow the following conclusions: the higher the hydrophobicity of the polyelectrolytes, the broader the particle size distribution and

Table 2 Structures of some of the most commonly used types of PEL for complex formation

Polycation (PC)	
Name	Structure
PDADMAC: poly(*N*,*N*-diallyl-*N*,*N*-dimethyl-ammonium chloride)	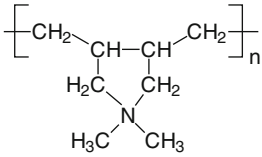
PEI: poly(ethyleneimine)	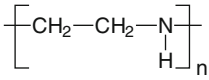
PAA: polyacrylamide (cationic)	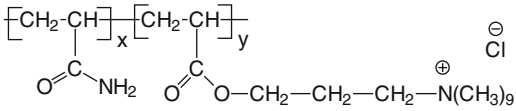
PMADAMBQ: copolymer of *N*-methacryloyloxy-ethyl-*N*-benzyl-*N*,*N*-dimethyl-ammonium chloride	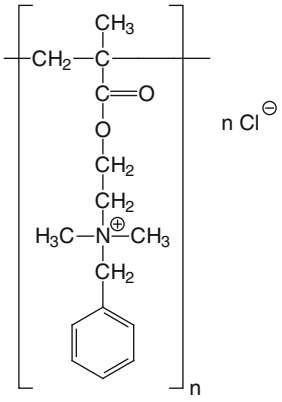
Poly(ethylene-trimethylammonium-iodidepropylmaleimide)	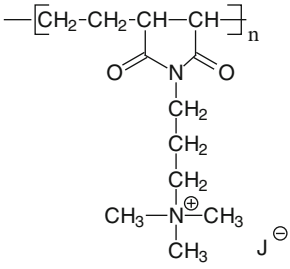
Polyanions (PA)	–

(continued)

Table 2 (continued)

Polycation (PC)	
Name	Structure
Maleic anhydride copolymers	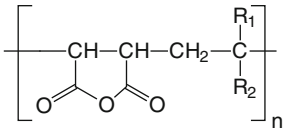
NaPAMPS: poly(sodium 2-acrylamido-2-methylpropanesulfonate)	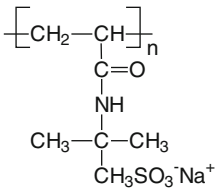
PAC: polyacrylic acid	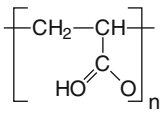
PVS: poly(vinylsulfonate)	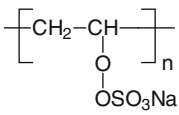
PAA: polyacrylamide (anionic)	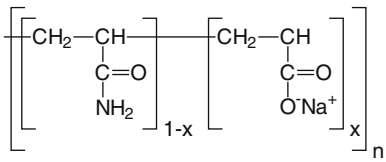
PSS: poly(styrene sulfonate)	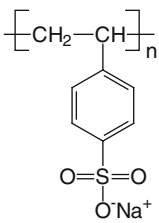

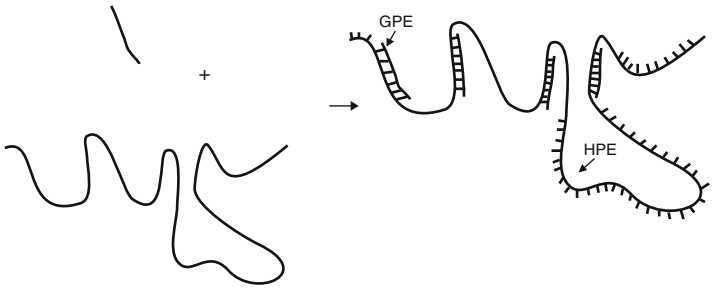

Fig. 10 Fragment of a nonstoichiometric PEC particle having hydrophilic as well as hydrophobic units. *GPE* guest PEL, *HPE* host PEL. Adapted from [82]

the minor the swelling of the PEC particles. Hence, the most compact particles were formed with the very hydrophobic copolymers.

4.2 Influence of Polymer Type on Complex Properties

From basic research on PECs, we can summarize the following important points.
There are many parameters that can influence the formation of PECs:
Charge density of the polyelectrolytes

- Strong polyelectrolytes (the charge does not depend on pH) with high charge density have a rod-like structure; they form complexes with a ladder-like-structure.
- In strong polyelectrolytes with low charge density, the polymer is coiled. In the case of a weak PEL such as PEI, PAC, or chitosan as a natural polymer, the complex formation is influenced by the pH dependence of the polymer charge. In such cases, the complexes are formed between coils of PC and coils of PA.

Molar mass

Complexes made from polyelectrolytes with low and medium molar mass (such as PDADMAC, PSS, PEI, PAC) are studied very often and are used in different fields of application.

Complexes made from PEL with very high molar masses (more than 10^6 g/mol) are used in paper production; such complexes are formed from big polymer coils and therefore such PECs are very large.

Polyelectrolytes with big differences in their molar mass form PECs that are water-soluble.

Substances bearing hydrophobic parts such as PSS, PMBQ, styrene or surfactants and micelles form complexes that are very dense or compact. The stability is often low.

Other parameters that can influence complex formation are the mixing conditions such as mixing speed, order of addition, ionic strength, and pH.

4.3 Application of Pre-mixed Complexes as Flocculants

For a long time, the application of pre-mixed PECs as flocculants seemed to be a field of academic work that had not found a practical application [20]. But, as found earlier [82], such complexes made from oppositely charged polymer solutions have interesting properties and are very effective for the flocculation of finely dispersed inorganic particles. A reflocculation was not noticed in a wide range of concentrations. Investigations on PECs as flocculants for inorganic particles like silica are important for the understanding of flocculation mechanism. But, PECs will never be applied as flocculant for such inorganic particles in practice. Nevertheless, PECs play an important role as flocculants in certain applications for special problems in wastewater treatment, such as low content of solids, soluble detrimental substances, or small amount of dye that can color a big volume of water. Therefore their removal is important.

As one of the first to study this, Somasundaran and coworkers [83] found that combinations of polystyrene sulfonate and cationic polyacrylamide enhanced the flocculation of (positively charged) alumina suspensions. The weight ratio of the two polymers was kept at 1:1 for all experiments. But, pre-mixing of the two polymers did not give as good results as those obtained when the polymers were added step by step [82]. In our opinion, the charge ratio of both PECs is extremely important and influences the flocculation mechanism. Effective flocculation can be found with highly charged complexes as well as with complexes near the 1:1 ratio of charges.

Onabe [84] analyzed the drainage behavior of pulp suspensions with a two-component system, with attention to polyion complex formation. With cationic and anionic polyacrylamides (molecular weights 3,000,000 and 1,000,000 g/mol) added individually, a polyion complex with an irregular three-dimensional structure was precipitated on the fiber surface. This reduced the homogeneity of the paper sheets. In contrast to this, a pre-mixed system of an anionic and cationic polyacrylamide [83] resulted in an improvement in pulp retention and paper quality (paper strength). Because of the very high molar mass and thus the big coil diameter, the formed PECs are very big and are therefore good flocculants.

Wagberg and coworkers [85] described the preparation and characterization of complexes for dry and wet strength improvement of paper. They investigated the structure of complexes formed by two oppositely charged PEL commonly used in the paper industry: polyamideamine epichlorohydrine condensate (PAE) and carboxymethylcellulose (CMC). They found that complexes can have a good resistance to PEC aggregation/dissolution at high salt concentrations and that it was possible to adjust the net charge of the complex particle solutions, making the PEC of great value in papermaking for covering the fibers with a high amount of material in a one-step procedure.

CMC-rich cellulose sheets were prepared by Uematsu [86] with a cationic retention aid. When 5% poly(*NNN*-trimethyl-*N*-(2-methacryloxyethyl) ammonium

chloride (PTMMAC) and 5% CMC were added to cellulose slurries, approximately 94% of the polymers were retained in the sheets by formation of a polyion complex.

PEC dispersions have been used as a fixing agent, flocculant, or retention aid to increase the water resistance of paper [87].

Detailed studies of particle (silica) flocculation using pre-mixed complexes were done by Buchhammer [88], Schwarz and Dragan [89], and Mende et al. [90, 91].

The flocculation efficiency of some nonstoichiometric interpolyelectrolyte complex dispersions synthesized by the interaction between poly(sodium 2-acrylamido-2-methylpropanesulfonate) (NaPAMPS) and three strong PCs bearing quaternary ammonium salt centers in the backbone on a stable monodisperse silica dispersion have been tested. The PCs PDADMAC and PCA5 alone showed a very narrow range of flocculation. In the case of the most hydrophobic PC, PCA5D1, the window of optimum flocculation concentration was broader compared with other PCs [88].

Mende investigated the flocculation of silica dispersions in dependence of the properties of nonstoichiometric PECs with different charge excess and hydrophobicity as well as different average hydrodynamic particle size. PDADMAC as PC and different PAs such as poly(styrene-*p*-sodium sulfonate) (NaPSS) and poly(acrylamide-*co*-sodium acrylate), were used so that PECs with different charge excess and hydrophobicity as well as different average hydrodynamic particle size could be prepared. The work was focused especially on the stability of complexes and it was pointed out that a higher tendency to instability results for complexes with PAs that have a Π-system (phenyl-) in the polymer chain [94]. The average hydrodynamic particle size and the polydispersity indices (PI), determined by dynamic light scattering were strongly influenced by the mixing conditions of the PECs and the nature of the used polyelectrolytes. It was found that particles with narrow or monodisperse distribution can be prepared under the condition that the PC is the starting solution, as shown in Fig. 11. Dispersions with PI values between 0.03 and 0.06 are described as monodisperse, whereas a narrow particle size distribution is found at PI values between 0.1 and 0.2. A broad particle size distribution is represented by PI values between 0.25 and 0.5; at PI > 0.5 the result is not analyzable [89].

The reaction process between silica and the used flocculants can be divided into three intervals (destabilization, flocculation optimum, and restabilization) as known for all other polymer flocculants. For an effective flocculation of a charged substrate, both electrostatic as well as hydrophobic interactions play an important role. The interval up to the beginning of the flocculation optimum is mainly influenced by electrostatic interactions (the charge density of the flocculant) but the broadness of the flocculation optimum depends largely on hydrophobic interactions. Hydrophobic interactions also play an important role in the shear stability of the formed flocs.

As shown in Fig. 12, the floc size rapidly increases in dependence of flocculant charge added to the silica dispersions. The size of flocs obtained with complexes is larger than the size of flocs obtained with the pure PC. The monomodal particle size distribution for the silica dispersion ($n = 0$) changes to bimodal or multimodal under the influence of the amount of cationic charge. With increasing amount of cationic charge, the volume proportion of single silica particles decreases and the fraction of bigger aggregates increases (Fig. 12a). The beginning of the flocculation optimum

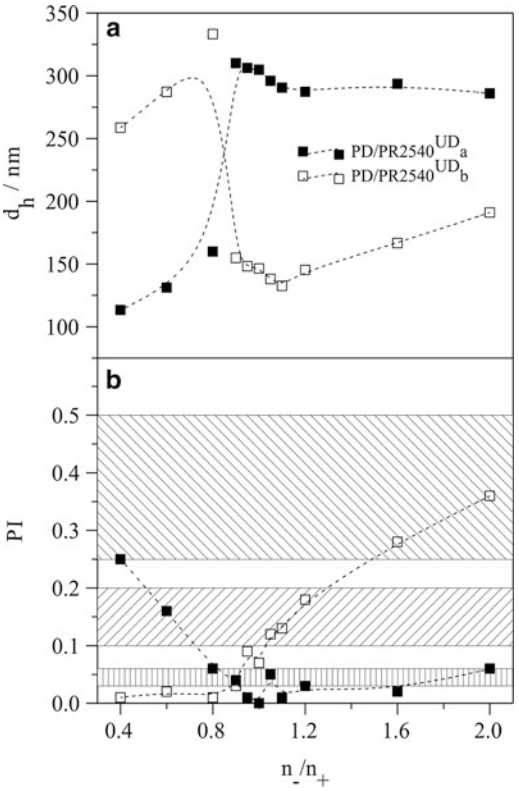

Fig. 11 Average hydrodynamic particle size d_h (*top*) and polydispersity index (PI) (*bottom*) of the studied stable PEC dispersions in dependence on the molar ratio $n-/n+$. PDADMAC (PD) as PC is combined with a commercial polyacrylamide copolymer (*PR2540*): (**a**; filled quares): PD is the starting solution, (**b**; empty squares): PR2540 is the starting solution

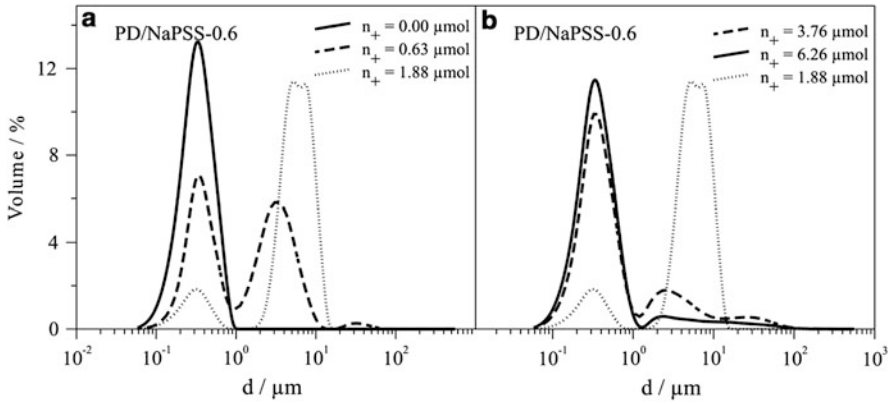

Fig. 12 Particle size (diameter; % volume distribution) of silica dispersions without flocculant ($n+ = 0.00$ µmol) and treated with PD/NaPSS complexes with $n-/n+$ ratio of 0.6 in dependence on the flocculant charge ($n+$) added to silica dispersions: (**a**) low cationic charge (0–1.88 µmol/L); (**b**) higher cationic charge (1.88–6.26 µmol/L)

was found at $n+ = 0.63$ µmol, where the peaks of both fractions have nearly the same size. At very high concentrations of cationic charge (Fig. 12b), the particle size distribution becomes smaller again. It was also confirmed by sedimentation analysis that the broadness of the so-called flocculation window (range of optimum flocculant concentration) depends on the hydrophobicity of the flocculant [90].

Nyström et al. [92, 93] correlated the observed flocculation behavior of calcium carbonate, induced by mixtures of cationic starch and anionic poly(sodium acrylate) (NaPA) at various electrolyte concentrations, with the complex properties. A strong correlation exists between the properties of the PEL mixture, primarily the amount of complexes formed, and the flocculation behavior. Several mechanisms are involved in this flocculation process induced by the two polymers. However, interparticle bridging by the PECs and charge neutralization induced by the deposition of the complexes were found to be the main reasons for the enhanced flocculation.

As already mentioned, the removal of different dyes is one of the fields where complexes can successfully be applied [94–97]. The "direct" formation of complexes between a PC and anionic dyes with two, three, or six sulfonic groups was investigated using UV–vis spectrophotometry and viscosimetry. Dragan et al. [12] also reported the formation of complexes having three components. They were formed by the interaction between nonstoichiometric PC/dye complexes with PAs. PCs differed in their content of the *N*,*N*-dimethyl-2-hydroxypropylene ammonium chloride units in the main chain. NaPA, NaPAMPS, and NaPSS were used as PAs. Crystal Ponceau 6R and Ponceau 4R with two or three sulfonic groups were used as anionic dyes. The formation of the three component PC/dye/PA complexes takes place mainly by the electrostatic interaction between the PA and the free positive charges of the PC/dye complex. The stoichiometry and the stability of such complexes depends on the PC structure, the structure and molar mass of PA, the dye structure, and the P:dye molar ratio. A high amount of the dye was excluded from the complex before the end point, when a branched PC was used. The higher the solubility of the dye, the lower the stability of the PC/dye/PA complexes [12].

The mechanism of dye incorporation into triple complexes was also intensively studied by Zemaitaitiene et al. It was shown that cationic polymer tends to react with anionic textile finishing chemicals and auxiliaries such as anionic detergents, forming intermolecular complexes of different stoichiometry. Under controlled conditions, these complexes can incorporate the dye and precipitate. Surprisingly, the disperse dye (which was uncharged) also seemed to be bound by polymer–polymer complexes [98, 99].

Buchhammer et al. [100] investigated the flocculation behavior of two PCs in comparison with pre-mixed PEC nanoparticles. These results show that depolarization of the dye solution can be achieved with the PCs as well as with the complex dispersions, depending on the type and quantity of the flocculant used. However, significant differences with regard to the removing efficiency and the usable range for effective flocculation exist. For both PCs used, which differed markedly in terms of their structure and chain length, a relatively narrow flocculation window was found. It was also interesting that the concentration ratio $c_{dye}/c_{polymer}$ is determined essentially from the properties of the PC. The concentration ratio is shifted significantly to lower

values with the long chain PMADAMBQ that is sterically stabilized. For application, this means that long chains as well as branched polymers are particularly effective when used as flocculants for depolarization of textile effluents containing, e.g., disperse dyes at low concentration. Further, it was shown that the dye structure had a marked influence. The dye content after separation was at least 15% for the disperse dye Celliton Fast Blue, whereas the degree of dye removal was much better for Cibacet Red [104]. Solid–liquid separation processes in general use highly hydrophilic linear polyelectrolytes with excellent water solubility as processing aids, but not all flocculation processes can be carried out with sufficient efficiency. These disadvantages may be overcome using associating or aggregating cationic polyelectrolytes as flocculants. A significant enhancement of the flocculation properties can be achieved by introduction of hydrophobic functionalities into the PEL backbone [101–103].

4.4 Polymer–Surfactant Complexes

It was also interesting to investigate the application of pre-mixed polymer–surfactant complexes (PSCs). Such mixtures of polymers and surfactants are common in many industrial formulations. The interaction between surfactants and water-soluble polymers provides special effects, e.g. enhancing the surface activity, stabilizing foams and emulsions, etc. It is, therefore, very important to study the interaction between surfactants and water-soluble polymers, especially between components of opposite charge. The first results were described in the literature of the 1970s, and from 1980 until now much work has been done to improve the understanding of such systems [104–107]. Very detailed investigations using different characterization methods such as surface tensiometry, light scattering, neutron scattering, NMR or ESR, and surface rheological methods [108–123] are mentioned. Usually, mixed solutions at fixed PEL and variable surfactant concentrations are investigated and it can be shown that the association between PEL and oppositely charged surfactant starts at very low surfactant concentration (typically one to three orders of magnitude below the cmc of the surfactant). The degree of surface tension lowering depends not only on the type of PEL (on their hydrophobicity, charge density, molar mass), but also on the mixing conditions (order of addition, influence of time) and salt content [124]. In most studies, a fixed polyelectrolyte amount was added to solutions of an oppositely charged surfactant (the "polymer to surfactant regime" [123]). Because the interaction between polymer and surfactant starts at very low surfactant concentration, basic research is often carried out below the cmc, but for industrial applications the interaction with polymers at higher surfactant concentration is also important. However, despite the importance and common use of PSCs there are only very few publications about application-relevant properties. As mentioned above, it is possible to tailor stable, differently charged dispersions made from oppositely charged polyelectrolytes and surfactants that can be used for different applications, such as surface modification of powders, sorption of organic molecules from wastewater, or as flocculants. As an example, complexes with PDADMAC as PC and sodium dodecylsulfate (SDS) as an anionic surfactant are shown in Fig. 13.

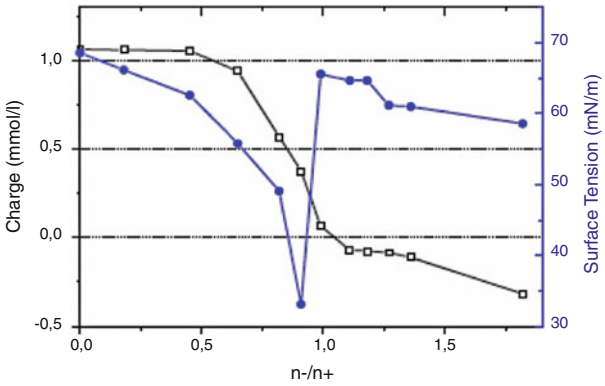

Fig. 13 Charge and surface tension of PSCs made from PDADMAC and SDS in dependence on $n-/n+$

Whereas the charge continuously decreases with increasing SDS content, the surface tension has a minimum near the 1:1 charge ratio. Such complexes were used for the separation of silver particles on zeolite. The separation of such fine particles was impossible with commercial flocculants, but successful with PCSs.

The interactions between a technical cationic surfactant (dodecyl-amidoethyl-dimethylbencyl-ammonium chloride) and anionic polyelectrolytes were investigated [123, 125]. The cationic surfactant strongly interacts with different PAs such as copolymers of maleic acid or PSS. This makes it possible to tailor complex dispersions with different properties that are sufficiently stable and can be used for the separation of dyes or dye-containing wastewater. Such nanoparticles are able to bind disperse dyes effectively due to their size (i.e., in the same range as the dye molecules) and their structure. They can bind the individual dye aggregates via hydrophobic as well as electrostatic interaction forces. The more stable dispersion with poly(maleic acid-*co*-propylene), P(MSP), compared with the α-methylstyrene copolymer P(MS-α-MeSty) is favorable for use in different applications. PSCs are very effective flocculants [124]. Whereas not more than 85% of Celliton Fast Blue could be removed with PECs, this value can be increased up to more than 95% by using PSCs. The supernatant is clear and seems to be colorless. Factors affecting the quality of flocculation are the charge and the hydrophobicity of the components and, as a consequence, the particle size. The application of "neutral" complexes results in a broad flocculation window.

The flocculation performance of polyampholytes (terpolymers containing hydrophobically modified cationic, hydrophilic nonionic, and anionic monomer units, always with an excess of cationic charges) was investigated [126]. The results were compared with homopolymers and with those obtained using nonstoichiometric (PSC) dispersions with adjustable surface charge density. The polyampholytes as well as the PSC can successfully remove the dye Celliton Fast Blue (Dispers Blue 3). The efficiency of dye separation is mainly influenced by the charge of polymers or complexes, demonstrating that charge neutralization is one possible flocculation mechanism. However, PSC, which are almost neutral, are also able to remove the dye due to their size and structure. In this case, the degree of dye removal is a little

better and the so-called flocculation window is broader, as in the case of charge neutralization.

The removal of dye was also investigated [127]. PECs, described as "new particle forming flocculants", were used in comparison with PCs to separate dyes from sludge (mixture of organic and inorganic components). The charge of the system to be flocculated was shown to be the most important property for influencing flocculation behavior. Therefore, sludge with strong anionic charge could be separated with commercial PC according to a patch mechanism, whereas for the removal of nearly "uncharged" sludge or dye the complex particles were more effective. The latter can be easily tailored with different properties by the interaction between aqueous solutions of dodecylamidoethyl-dimethylbencyl-ammonium chloride (Quartolan), which carries a positive charge, and a PA such as PSS. In dependence on the mixing ratio $n-/n+$ as well as on the dosage, these complexes can effectively eliminate commercial dyes such as Acid Yellow 3 or Acid Blue 74 due to their hydrophobicity and structure.

PSCs can be also used as flocculants in montmorrilonite dispersions [128]. An anionic surfactant (SDS) was combined with a cationic polymer (PDADMAC). At a 1:1 molar ratio, optimal flocculation was obtained owing to the formation of an insoluble surfactant–polymer complex in the presence of particles. Such interactions may lead to a flocculation mechanism that combines polymer adsorption, charge neutralization, and hydrophobic interactions. Other experiments have shown that a similar flocculation process can be achieved by using a cationic surfactant and anionic polymer [127].

4.5 Removal of Organic Pollutants

Buchhammer [129] described the design of new materials for removing organic pollutants such as *p*-nitrophenol or dyes from wastewater. The sorption of solved organic molecules on previously formed PSCs or PECs (PC/PA) was studied. The scheme of complex formation and possible structures is presented in Fig. 14. The sorption capability of such macromolecular assemblies increases with increasing molar mass and hydrophobicity of the macromolecules used.

The solubilization of hydrophobic molecules such as pyrene (a fluorescence probe), or Nile Red (a solvatochromic probe) in nanoparticles was investigated by Nizri et al. [130]. They studied the morphology of the resulting nanoparticles and their ability to solubilize hydrophobic materials. As shown by AFM and SEM imaging, the particles are spherical, having a diameter of about 20 nm. From pyrene solubilization it appeared that the hydrophobicity of the nanoparticles depends on the ratio between SDS molecules and the charge unit of the polymer and therefore they confirmed the results described by other authors [128].

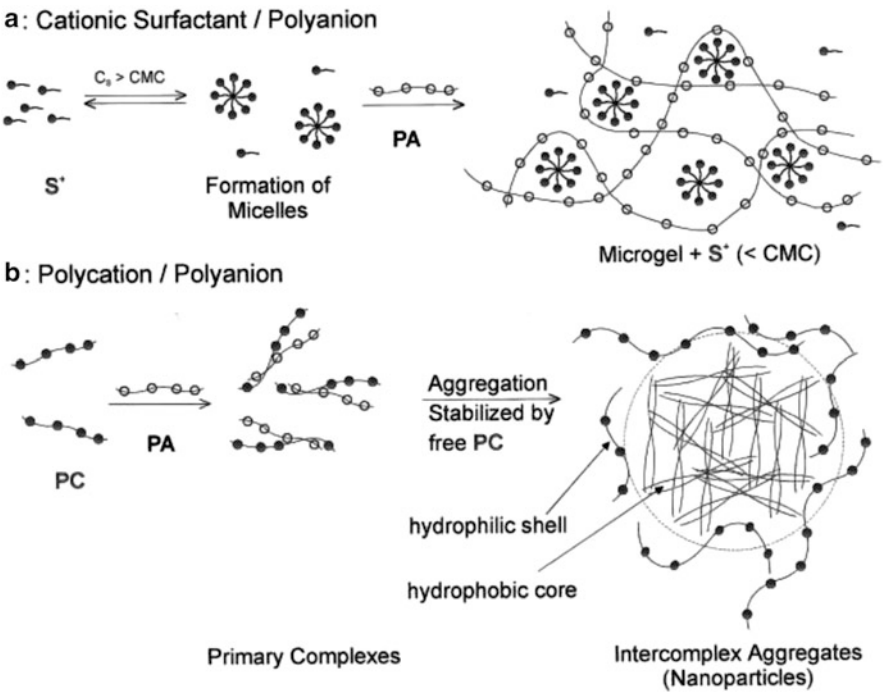

Fig. 14 Scheme of complex formation and possible structures: (**a**) cationic surfactant/PA; (**b**) PC/PA. Adapted from [128]

5 Current Trends and Future Research Directions

5.1 Advanced Characterization Methods

In contrast to previous research in the field of flocculation, which mostly investigated the direct interaction between one substrate and one polymer, today we have to deal with multicomponent mixtures and formulations. Therefore, a direct and efficient method for the characterization of the sedimentation behavior is necessary. It is demonstrated that the separation analyzers LUMiFuge and LUMiSizer can be used for a pre-selection of flocculants [131, 132]. The LUMiSizer is a microprocessor-controlled analytical centrifuge that allows determination of space- and time-resolved extinction profiles during the centrifugation of up to 12 samples simultaneously [133]. This multisample analytical batch centrifugation with optical detection proved to be a versatile tool for the determination of the characteristic material properties related to the sedimentation and consolidation behavior of dispersions. This was demonstrated for the sedimentation and consolidation of rigid non-interacting particles and also for the consolidation of interacting network-forming particles.

The evaluation of ceramic dispersions using analytical centrifugation (STEP-Technology), combined with multisample analytical centrifugation is described [134]. The shear-dependent sedimentation rate, consolidation, and packing behavior are directly analyzed. In addition, the particle size distribution can be obtained with high resolution. Application studies on kaolin, silicon carbide, and silica dispersions show the high potential of this method. The potential of multisample analytical centrifugation for formulation design (stability as well as flocculation) was demonstrated in investigations on the effect of particle (silica, calcium carbonate) and polymer (PAA) concentration on dispersion properties of different stabilized suspensions [135].

The dispersibility of carbon nanotubes (CNTs) was assessed by studying the sedimentation of CNTs dispersed in aqueous surfactant solutions at different ultrasonication treatment times using a LUMiSizer. Different commercially available multiwalled CNTs, such as Baytubes C150P or Nanocyl NC7000, showing quite different kinetics, were compared. In addition, the particle size distributions were analyzed using dynamic light scattering and centrifugal separation analysis [136].

As described, the application of flocculants with two or more components is of growing importance for solid–liquid separation processes, including the dewatering of ultrafine materials (sludge from clay, coal, or gravel pits) or sewage sludge. Through various examples involving the preparation of well-characterized model systems, it has been demonstrated that the removal of detrimental substances such as colored materials (dyes) or stickies is favorable by the formation of PECs. In addition, PECs as well as PSCs can be used as materials for the sorption of hydrophobic materials such as organic compounds.

5.2 Use of Natural Polymers

For many years, in most cases synthetic polyelectrolytes such as PDADMAC or PEI as PC, and PAC, PAMPS, or PSS as PA were used for complex formation. But at present, the application of so-called natural polymers is of growing importance in the field of complex formation. Natural polymers occur in nature and can be extracted. Examples are chitosan as well as polysaccharides such as starch, pectin, or alginate. Natural polymers are used because of their good biodegradability and high biocompatibility in a wide range of applications in industry. They can have cationic charge (chitosan) [137] or can be modified with cationic as well as hydrophobic units [74].

The interaction between modified starch and sticky-containing wastewater was mentioned in Sect. 3.2. of this article [67, 68]. Mihai [141] investigated chitosan-based nonstoichiometric PECs (NPECs) as specialized flocculants. Such NPEC were more effective than chitosan in kaolin separation. Their main advantage is the increase in critical concentration for kaolin restabilization. The NPEC particles were adsorbed on the kaolin surface, protecting them more efficiently against re-dispersion.

The physicochemical properties of biopolymer-based PECs with controlled pH and/or thermoresponsiveness were described by Glampedaki et al. [138, 139]. The study [138] illustrates a novel combination between negatively charged pH- and thermoresponsive microparticles of poly(isopropylacrylamide-*co*-acrylic acid) (PNIAA) and positively charged chitosan chains. Morphological and physicochemical aspects of the stimuli-responsiveness of the complexes were investigated through scanning electron microscopy, polyelectrolyte titration, UV–vis spectroscopy, analytical centrifugation, and tensiometry. The PNIAA thermoresponsiveness kinetics was found to be both temperature- and pH-dependent. Chitosan/PNIAA complexes appeared more hydrophobic below LCST and more hydrophilic above LCST, compared with PNIAA alone. Their demixing behavior revealed that chitosan/PNIAA complexes are more sensitive to pH and temperature changes than their individual components. Finally, complexes were found to be surface-active, with their surface activity lying between those of chitosan and PNIAA. The information obtained about hydrophilicity/hydrophobicity aspects of the studied systems is considered essential, as they are intended for interesting applications such as polyester surface functionalization.

The preparation of pH- or thermoresponsive microgels of NIPAAm copolymerized with acrylic acid, either alone or complexed with chitosan is described [138]. All properties of the microgels are in very good correlation with those expected from the chemical structure of the polymers used for their preparation.

A new type of a dual system using mixtures of chitosan and a thermosensitive polymer has been described in Sect. 2.7 [47–50].

PECs also have been the focus of an expanding number of studies for their wide use in medicine. For instance, biopolymer nanoparticles have been described as very promising nanosized carrier materials with great potential in health care and environmental sciences [140].

Müller et al. [141] described PEC nanoparticles prepared by mixing solutions of oppositely charged PEL, whose size and shape can be regulated by external and media parameters. An improved preparation protocol for PEC nanoparticles based on consecutive centrifugations was elaborated, resulting in better reproducibility and lower polydispersity. Experimental and simulation evidence showed that salt and PEL concentration are sensitive parameters for size regulation of spherical PEC nanoparticles. The authors outline certain advantages of dispersed PEC particles for life science applications due to easy preparation, graded nanodimensions, achievable solid content, and uptake/release properties for proteins and drugs.

The physicochemical and biological properties of DNA and small interfering RNA (siRNA) complexes prepared from a set of maltose-, maltotriose-, or maltoheptaose-modified hyperbranched PEIs [termed (oligo-)maltose-modified PEIs; OM-PEIs] were investigated [142]. The authors showed that pH-dependent charge densities of the OM-PEIs correlate with the structure and degree of grafting and with the length of the oligomaltose. Decreased zeta-potentials of OM-PEI-based complexes and changes in the thermodynamics of DNA complex formation are observed, while the complex sizes are largely unaffected by maltose grafting and the presence of serum proteins.

But, these aspects of complex application in medicine are not addressed in this review and therefore they are not referred to in detail here.

6 Summary and Outlook

Polyelectrolytes and their complexes play a central role in solid–liquid separation processes such as paper making or waste water treatment.

A lot of different products are available – synthetic as well as natural polymers. Worldwide, the use of PECs is a fast growing market for treating water in different spheres of life, such as the supply of drinking water, the purification of wash water, or the dewatering of sludge.

The main message of this review is that many different ideas based on an understanding of colloid–polymer interactions have been developed for solving different problems, at first in the paper industry, but also for other technologies such as the separation of metals (like alumina) or minerals, the dewatering of sludge, or the removal of dyes.

The direct interactions between a flocculant (PC) and a charged particle suspension have been investigated for many years and are not the topic of this review. But, it is important to know (also for dual flocculation) that polymers with low molar mass can flocculate via neutralization or patch flocculation mechanism, whereas polymers with higher molar mass can flocculate via bridging. Decreasing the charge density of polymers makes the flocculation range broader and the flocs bigger.

Because the separation problems have become more and more complex, new principles of flocculation must be used to meet all requirements, such as the removal of heavy metals, dyes, or natural colloids. Instead of monoflocculation with one polycation, pre-mixed PECs (made from PC and PA), which are effective flocculants due to their size and structure, are used. Because hydrophobic interactions are of growing importance for the removal of hydrophobic substances such as oil, it is necessary to introduce hydrophobic parts into the flocculants or, alternatively, to use pre-mixed PSCs.

Last but not least, the flocculation efficiency of synthetic polymers should be compared with natural polymers like chitosan, or with polysaccharides such as modified starch, pectin, or alginate.

Acknowledgements We are indebted to many long-term collaborators and colleagues, especially to Dr. Stela Dragan and her group (Institute Petru Poni, Iasi, Romania) and to Dr. Svetlana Bratskaya (Far East Department of Russian Academy of Sciences, Institute of Chemistry, Vladivostok, Russia). The investigations with tailored polymers, especially hydrophobic PCs, were undertaken in collaboration with Prof. Laschewsky and his group (Fraunhofer IAP Golm, Germany). Above all, we would like to thank our unforgettable colleague and friend Dr. Werner Jaeger.
Financial support from the BMBF and AiF is gratefully acknowledged.

References

1. Ringqvist L, Igsell P (1994) Dual polymer system in peat dewatering. Energy Fuel 8:953
2. Kulicke WM, Lenk S, Detzner D et al (1993) Anwendung von Polyelektrolyten bei der mechanischen Fest/Flüssig-Trennung. Chem Ing Technol 65:541
3. Böhm N, Kulicke WM (1997) Optimization of the use of polyelectrolytes for dewatering industrial sludges of various origins. Colloid Polym Sci 275:73
4. Zhang X (1992) A new polymer flocculant for dyes. Water Treat 7:33
5. Arno J, Frankle W, Sheridan J (1974) Zeta potential and its application to filler retention. Tappi 57:97
6. Britt KW, Unbehend J (1974) Electrophoresis in paper stock suspensions as measured by mass transport analysis. Tappi 57:81
7. Hagedorn R (1988) The combination of highly charged polyelectrolytes with retention agents: retention in the presence of interfering substances. Tappi 71:131
8. Andersson K, Sandström A, Ström K, Barla P (1986) The use of cationic starch and colloidal silica to improve the drainage characteristics of kraft pulp. Nordic Pulp Paper Res J 2:26
9. Swerin A, Ödberg L (1996) An extended model for the estimation of flocculation efficiency factors in multicomponent flocculant systems. Colloids Surf A 113:25
10. Eklund D, Lindström T (1991) Paper chemistry. DT Paper Science Publications, Grankulla
11. Gregory J, Barany S (2011) Adsorption and flocculation by polymers and polymer mixtures. Adv Colloid Interface Sci 169:1
12. Dragan ES (2007) New trends in ionic (co)polymers and hybrids. Nova Science, New York
13. Moore E (1976) Charge relationship of dual polymer retention aids. Tappi 59:120
14. Müller F, Beck U (1978) Dual-Produktsysteme zur Retention und Entwässerung in der Papierindustrie. Das Papier 32:V25
15. Petäjä T (1980) Fundamental mechanisms of retention with retention agents. Kemia-Kemi 5:261
16. Wagberg L, Lindström T (1987) Some fundamental aspects on dual component retention aid systems. Nordic Pulp Paper Res J 2:49
17. Gill RI (1991) Development in retention aid technology. Paper Technol 32:34
18. Krogerus B (1993) Dynamic flocculation studies on fibre fines and filler clay. Nordic Pulp Paper Res J 8:135
19. Hedborg F, Lindström T (1996) Some aspects on the reversibility of flocculation of paper stocks. Nordic Pulp Paper Res J 4:254
20. Petzold G (1999) Dual addition schemes. In: Farinato RS, Dubin P (eds) Colloid-polymer interactions: from fundamentals to practice. Wiley, New York, pp 83–100
21. Petzold G, Buchhammer HM, Lunkwitz K (1996) The use of oppositely charged polyelectrolytes as flocculants and retention aids. Colloids Surf A 119:87
22. Sang Y, Xiao H (2008) Clay flocculation improved by cationic poly(vinyl alcohol)/anionic polymer dual-component system. J Colloid Interface Sci 326:420
23. Barany S, Meszaros R et al (2011) Effect of polyelectrolyte mixtures on the electrokinetic potential and kinetics of flocculation of clay mineral particles. Colloids Surf A 383:48
24. Oelmeyer G, Krentz O, Kulicke WM (2001) Kombinierte Flockungshilfsmittelsysteme mit kationischen Stärken in der Fest/Flüssig-Trennung von Hafenschlick. Chem Ing Technol 73:546
25. Petzold G, Lunkwitz K (1995) The interaction between polyelectrolyte complexes made from poly(dimethyldiallylammoniumchloride) (PDMDAAC) and poly(maleic acid-co-α-methylstyrene) (P(MS-α-MeSty)) and cellulosic materials. Colloids Surf A 98:225
26. Petzold G, Schwarz S, Geißler U, Smolka N (2004) Influence of humic acid on the flocculation of clay. Colloid Polym Sci 282:670
27. Glover S, Yan D, Jameson G, Biggs S (2004) Dewatering properties of dual-polymer flocculated systems. Int J Min Process 73:145
28. Fan A, Turro N, Somasundaran P (2000) A study of dual polymer flocculation. Colloids Surf A 162:141

29. Navarro R, Wada S, Tatsumi K (2005) Heavy metal precipitation by polycation–polyanion complex of PEI and its phosphonomethylated derivative. J Hazard Mater B 123:203
30. Gohlke U (2000) Separation of heavy metal ions from aqueous solutions. German Patent DE19829827
31. Lemanowicz M, Jach Z, Kilian E (2011) Dual-polymer flocculation with unmodified and ultrasonically conditioned flocculant. Chem Eng J 168:159
32. Haack V, Heinze T, Oelmeyer G (2002) Starch derivatives of high degree of functionalization, 8 – synthesis and flocculation behaviour of cationic starch polyelectrolytes. Macromol Mater Eng 287:495
33. Li J, Modak PR, Xiao HN (2006) Novel flocculation system based on 21-arm cationic star polymer. Colloids Surf A 289:172
34. Lee CH, Liu JC (2001) Sludge dewaterability and floc structure in dual polymer conditioning. Adv Environ Res 5:129
35. Lee CH, Liu JC (2000) Enhanced sludge dewaterability by dual polyelectrolytes conditioning. Water Res 34:4430
36. Yukselen MA, Gregory J, Soyer E (2006) Formation and breakage of flocs using dual systems. Water Sci Technol 53:217
37. Wang J, Liu J, Lee DJ (2005) Dual conditioning of sludge utilizing polyampholyte. J Environ Eng 131:1659
38. Wei JC, Gao B, Yue Q (2009) Comparison of coagulation behaviour and floc structure characteristic of different polyferric-cationic polymer dual coagulants in humic acid solution. Water Res 43:724
39. Petzold G, Schwarz S, Lunkwitz K (2003) Combinations of flocculants for the improvement in the efficiency of flocculation processes. Chem Eng Technol 26:48
40. Pelton R (1999) Polymer-colloid interactions in pulp and paper manufacture. In: Farinato RS, Dubin P (eds) Colloid-polymer interactions: from fundamentals to practice. Wiley, New York
41. Wu M, van de Veen T (2009) Flocculation and reflocculation: interplay between the adsorption behavior of the components of a dual flocculant. Colloids Surf A 341:40
42. Buchhammer HM, Petzold G, Lunkwitz K (1993) The interaction between oppositely charged polyelectrolytes in the presence of solid surfaces. Colloids Surf A 76:81
43. Oertel U, Petzold G, Buchhammer HM (1991) Introduction of surface charge into polymers by polyelectrolyte complexes. Colloids Surf A 57:375
44. Petzold G, Schwarz S, Buchhammer HM, Lunkwitz K (1997) A very effective method for the cationic modification of cellulose. Die Angew Makromol Chem 253:1
45. Schmidt S, Buchhammer HM, Lunkwitz K (1997) Surface modification of glass and viscose fiber with non-stoichiometric surfactant/polyelectrolyte complexes and polyelectrolyte/polyelectrolyte complexes. Tenside Surf Det 34:267
46. Lukaszczyk J, Lekawska E, Lunkwitz K, Petzold G (2004) Sorbents for removal surfactants from aqueous solutions. Surface modification of natural solids to enhance sorption ability. J Polym Sci 92:1510
47. Schwarz S, Ponce-Vargas S, Licea-Claverie A, Steinbach C (2012) Chitosan and mixtures with aqueous biocompatible temperature sensitive polymer as flocculants. Colloids Surf A 413:7–12. doi:10.1016/j.colsurfa.2012.03.048
48. Sakohara S, Hinago R, Ueda H (2008) Compaction of TiO_2 suspension by using dual ionic thermosensitive polymers. Sep Purif Technol 63:319
49. Sakohara S, Yagi S, Lizawa T (2011) Dewatering of inorganic sludge using dual ionic thermosensitive polymers. Sep Purif Technol 80:148
50. Ström G, Barla P, Stenius P (1982) The effect of pine xylan on the use of some polycations as retention and drainage aids. Svensk Papperstidning 85:R100
51. Ström G, Barla P, Stenius P (1985) The formation of polyelectrolyte complexes between pine xylan and cationic polymers. Colloids Surf 13:193
52. Kötz J (1993) Phase behavior of polyanion–polycation aggregates. Nordic Pulp Paper Res J 8:11

53. Hubbe MA, Rojas O, Venditti RA (2006) Control of tacky deposits on paper machines – a review. Nordic Pulp Paper Res J 21:154
54. Blanco A, Miranda R (2007) Full characterization of stickies in a newsprint mill: the need for a complementary approach. Tappi J 6:19
55. Putz HJ, Hamann A, Gruber E (2003) Examination of sticky origin and sticky removal. Wochenbl Papierfabrikat 131:883
56. Putz HJ, Hamann A (2003) Comparison of sticky test methods. Wochenbl Papierfabrikat 131:218
57. Glazer JA (1991) Overview of deposit control. Tappi J 74:72
58. Strauß J, Großmann H (1997) Kreislaufwasserreinigung unter besonderer Berücksichtigung klebender Verunreinigungen. Wochenbl Papierfabrikat 125:468
59. Richardson PF (1995) New technology for pitch and stickies control. In: Proceedings papermakers conference. TAPPI Press, Atlanta, p 205
60. Fink MR, Greer CS, Ramesh M (1993) Hydrophobic polyelectrolyte coagulants for the control of pitch in pulp and paper systems. US Patent 5,246,547
61. Murray G, Stack K, McLean D, Shen W, Garnier G (2009) Mechanism of pitch adsorption on carboxy methyl dextran surfaces. Appita J 1:64
62. Meixner H, Auhorn W, Gercke M (1998) Tailor-made cationic polymers for fixing detrimental substances of primary and secondary origin. Das Papier 52(10A):36–41
63. Knubb S, Zetter C (2002) Deposit study of alkylether dimer dispersions. Nordic Pulp Paper Res J 17:164
64. Huo X, Venditti RA, Chang HM (2001) Effect of cationic polymers, salts and fibres on the stability of model micro-stickies. J Pulp Paper Sci 27:207
65. Luo LZ, Wang LJ (2010) DCS controlling and paper strengthening effects of highly cationic starches with different branching degrees and molecular weights. Appita J 63:37
66. Glittenberg D, Hemmes JL, Bergh NO (1993) Synergism between synthetic agents and cationic starches in wood-containing systems. Wochenbl Papierfabrikat 121:1000
67. Petzold G, Schönberger L, Schwarz S (2011) Die Bindung von Stickies mit kationischen Stärken unterschiedlicher Hydrophobie. Wochenbl Papierfabrikat 139:592
68. Petzold G, Schönberger L, Genest S, Schwarz S (2012) Interaction of cationic starch and dissolved colloidal substances from paper recycling, characterized by dynamic surface measurements. Colloids Surf A 413:162
69. Petzold G, Petzold-Welcke K, Qi H, Stengel K, Schwarz S, Heinze T (2012) Sticky removal with natural based polymers – highly cationic and hydrophobic types compared with unmodified ones. Carbohydr Polym 90:1712
70. Tsuchida E, Abe K (1982) Interactions between macromolecules in solution and intermacromolecular complexes. Adv Polym Sci (Springer, Berlin) 45:1
71. Li Y, Dubin PL, Spindler R, Tomalia T (1995) Complex formation between poly(dimethyldiallylammonium chloride) and carboxylated starbust dendrimers. Macromolecules 28:8426
72. Philipp B, Dautzenberg H, Linow K (1991) Formation and structure of polyelectrolyte complexes. Prog Polym Sci 14:91
73. Dautzenberg H, Jaeger W, Kötz J, Philipp B (1994) Polyelectrolytes: formation, characterization and application. Carl Hanser, München
74. Müller M, Starchenko V, Lebovka N, Ouyang W, Keßler B (2010) Preparation and life science applications of polyelectrolyte complex nanoparticles. Curr Trends Polym Sci 13:1
75. Müller M, Kessler B, Fröhlich J, Poeschla S, Torger B (2011) Polyelectrolyte complex nanoparticles of poly(ethyleneinine) and poly(acrylic acid): preparation and applications. Polymers 3:762
76. Müller M (2012) Sizing, shaping and pharmaceutical applications of polyelectrolyte complex nanoparticles. Adv Polym Sci. doi:10.1007/12_2012_170
77. Schacher F, Betthausen E, Walther A, Schmalz A, Pergushov D, Müller A (2009) Interpolyelectrolyte complexes of dynamic multicompartment micells. ACS Nano 3:2095

78. Kabanov VA, Zezin AB, Izumrudov VA (1985) Cooperative interpolyelectrolyte reactions. Makromol Chem Macromol Chem Phys 13:137
79. Zezin AB, Izumrudov VA, Kabanov VA (1989) Interpolyelctrolyte complexes as new family of enzyme carriers. Makromol Chem Macromol Symp 26:249
80. Jaeger W, Bohrisch J, Laschewsky A (2010) Synthetic polymers with quaternary nitrogen atoms-synthesis and structure of the most used type of cationic polyelectrolytes. Prog Polym Sci 35:511
81. Mende M, Schwarz S, Zschoche S, Petzold G, Janke A (2011) Influence of the hydrophobicity of polyelectrolytes on polyelectrolyte complex formation and complex particle structure and shape. Polymers 3:1363
82. Petzold G, Nebel A, Buchhammer HM, Lunkwitz K (1998) Preparation and characterization of different polyelectrolyte complexes and their application as flocculants. Colloid Polym Sci 276:125
83. Xiang Y, Somasundaran P (1993) Enhanced flocculation with double flocculants. Colloids Surf A 81:17
84. Onabe F (1983) Effect of the polyion-complex formation on the drainage behavior of pulp suspensions: an interpretation of the dual-polymer system. Mokuzai Gakkaishi 29:60
85. Gernandt R, Wagberg L, Gärlund L (2003) Polyelectrolyte complexes for surface modification of wood fibres. Colloids Surf A 213:15
86. Uematsu T, Matsui Y, Kakiuchi S, Isogai A (2011) Cellulose wet wiper sheets prepared with cationic polymer and carboxymethyl cellulose using a papermaking technique. Cellulose 18:1129
87. Champ S, Auweter H, Leduc M (2004) Method for the production of aqueous polyelectrolyte complex dispersions, and use thereof for increasing the water resistance. Patent WO2004096895
88. Buchhammer HM, Petzold G, Lunkwitz K (1999) Salt effect on formation and properties of interpolyelectrolyte complexes and their interactions with silica particles. Langmuir 15:4306
89. Schwarz S, Dragan ES (2004) Nonstoichiometric interpolyelectrolyte complexes as colloidal dispersions based on NaPAMPS and their interaction with colloidal silica particles. Macromol Symp 210:185
90. Mende M, Buchhammer HM, Schwarz S, Petzold G, Jaeger W (2004) The stability of polyelectrolyte complex systems of PDADMAC with different polyanions. Macromol Symp 211:121
91. Mende M, Schwarz S, Petzold G, Jaeger W (2007) Destabilization of model silica dispersions by polyelectrolyte complex particles with different charge excess, hydrophobicity, and particle size. J Appl Polym Sci 103:3776
92. Nyström RS, Rosenholm JB, Nurmi K (2003) Flocculation of semidilute calcite dispersion induced by anionic sodium polyacrylate-cationic starch complexes. Langmuir 19:3981
93. Nyström R, Hedström G, Gustafsson J, Rosenholm JB (2004) Mixtures of cationic starch and anionic polyacrylate used for flocculation of calcium carbonate-influence of electrolytes. Colloids Surf A 234:85
94. Dragan ES, Ghimici L, Cristea M (1999) Polyelectrolyte complexes III. Binding characteristics of some polycations. Acta Polym 50:260
95. Dragan ES, Cristea M (2003) Polyelectrolyte complexes. Formation, characterizationand application. In: Gayathri A (ed) Recent research developments in polymer science, vol 7. Research Signpost, Trivandrum, pp 149–181
96. Dragan ES, Mihai M (2007) Polyanion structure and mixing conditions-useful tool to tailor the characteristics of PEC particles. J Optoelectron Adv Mater 9:3927
97. Dragan ES, Dragan D, Christea M (1999) Polyelectrolyte complexes. II. Specific aspects of the formation of polycation/dye/polyanion complexes. J Polym Sci A 37:409
98. Zemaitaitiene RJ, Zliobaite E, Klimaviciute R, Zemaitaitis A (2003) The role of anionic substances in removal of textile dyes from solutions using cationic flocculant. Colloids Surf A 214:37

99. Zliobaite E (1998) Binding of dyes with cationic polyelectrolytes in textile wastewater. Ph.D. Thesis, Kaunas University of Technology, Lithuania
100. Buchhammer HM, Oelmann M, Petzold G (2001) Flocculation of disperse dyes in effluents with polyelectrolyte complexes. Melliand Engl 82:E104
101. Zhao HZ, Luan ZK, Gao BY, Yue QY (2002) J Appl Polym Sci 84:335
102. Schwarz S, Lunkwitz K, Kessler B, Spiegler U, Killmann E, Jaeger W (2000) Adsorption and stability of colloidal silica. Colloids Surf A 163:17
103. Schwarz S, Bratskaya S, Jaeger W, Paulke BR (2006) Effect of charge density, molecular weight and hydrophobicity on adsorption and flocculation. J Appl Polym Sci 101:3422
104. Goddard ED, Ananthapadmanabhan KP (1993) Interactions of surfactants with polymers and proteins. CRC, Boca Raton
105. Kabanov VA, Dubin P, Bock J, Devies JM, Schulz DN (1994) Macromolecular complexes in chemistry and biology. Springer, Berlin
106. Holmberg K, Jönsson B, Kronberg B, Lindman B (1998) Surfactants and polymers in aqueous solution. Wiley, Chichester
107. Piculell L, Thuresson K, Lindman B (2001) Mixed solutions of surfactant and hydrophobically modified polymer. Polym Adv Technol 12:44
108. Ritacco H, Kurlat DH (2003) Critical aggregation concentration in the PAMPS (10%)/DTAB system. Colloids Surf A 218:27
109. Jain NJ, Albouy PA, Langevin D (2003) Study of adsorbed monolayers of a cationic surfactant and an anionic polyelectrolyte at the air–water interface. Langmuir 19:5680
110. Jain NJ, Trabelsi S, Guillot S, McLoughlin D, Langevin L, Letellier P, Turmine M (2004) Critical aggregation concentration in mixed solutions of anionic polyelectrolytes and cationic surfactants. Langmuir 20:8496
111. Krishnan R, Sprycha R (1999) Interactions of acetylenic diol surfactants with polymers – Part 1. Maleic anhydride co-polymers. Colloids Surf A 149:355
112. Olea AF, Gamboa C, Acevedo B, Martinez B (2000) Synergistic effect of cationic surfactant on surface properties of anionic copolymers of maleic acid and styrene. Langmuir 16:6884
113. Zimin D, Craig VSJ, Kunz W (2004) Adsorption and desorption of polymer/surfactant mixtures at solid–liquid interfaces: substitution experiments. Langmuir 20:8114
114. Kasaikin VA, Litmanovich EA, Kabanov VA (1999) Self-organisation of micellar phase upon binding of sodium dodecyl sulfate with polydimethyldiallylammonium chloride in dilute aqueous solution. Doklady Phys Chem 367:205
115. Staples E, Tucker I, Penfold J, Warren N, Thomas RK, Taylor DJF (2002) Organization of polymer-surfactant mixtures at the air–water interface: sodium dodecyl sulfate and poly (dimethyldiallylammonium chloride). Langmuir 18:5147
116. Taylor DJF, Thomas RK (2002) The adsorption of oppositely charged polyelectrolyte/ surfactant mixtures: neutron reflection from dodecyl trimethylammonium bromide and sodium poly(styrene sulfonate) at the air/water interface. Langmuir 18:4748
117. Li F, Li GZ, Xu GY, Wang HQ, Wang M (1998) Studies on the interactions between anionic surfactants and polyvinylpyrrolidone: surface tension measurement, ^{13}C NMR and ESR. Colloid Polym Sci 276:1
118. Prioetti N, Amato ME, Masci G, Segre AL (2002) Polyelectrolyte/surfactant interaction: an NMR characterization. Macromol 35:4365
119. Taylor DJF, Thomas RK, Li PX, Penfold J (2003) Adsorption of oppositely charged polyelectrolyte/surfactant mixtures. Neutron reflection from alkyl trimethylammonium bromides and sodium poly(styrenesulfonate) at the air/water interface: the effect of surfactant chain length. Langmuir 19:3712
120. Ritacco H, Kurlat D, Langevin D (2003) Properties of aqueous solutions of polyelectrolytes and surfactants of opposite charge: surface tension, surface rheology, and electrical birefringence studies. J Phys Chem B 107:9146

121. Noskov BA, Loglio G, Miller R (2004) Dilational visco-elasticity of polyelectrolyte/surfactant adsorption films at the air/water interface: dodecyltrimethylammonium bromide and sodium poly(styrene sulfonate). J Phys Chem 108:18615
122. Noskov BA, Loglio G, Lin SY, Miller R (2006) Dynamic surface elasticity of polyelectrolyte/surfactant adsorption layers at the air/water interface: dodecyltrimethylammonium bromide and copolymer of sodium 2-acrylamido-2-methyl-1-propansulfonate with N-isopropyl-acrylamide. J Colloid Interface Sci 301:386
123. Naderi A, Claesson PM, Bergström M, Dėdinaitė A (2005) Trapped non-equilibrium states in aqueous solutions of oppositely charged polyelectrolytes and surfactants: effect of mixing protocol and salt concentration. Colloids Surf A 253:83
124. Petzold G, Dutschk V, Mende M, Miller R (2008) Interaction of cationic surfactant and anionic polyelectrolytes in mixed aqueous solutions. Colloids Surf A 319:43
125. Petzold G, Mende M, Kochurova N (2007) Polymer-surfactant complexes as flocculants. Colloids Surf A 298:139
126. Petzold G, Jaeger W, Schwarz S, Mende M (2007) Dye flocculation using polyampholytes and polyelectrolyte-surfactant nanoparticles. J Appl Polym Sci 104:1342
127. Petzold G, Schwarz S (2006) Dye removal with polyelectrolytes and polyelectrolyte – surfactant complexes. Sep Purif Technol 51:318
128. Magdassi S, Rodel BZ (1996) Flocculation of montmorillonite dispersions based on surfactant–polymer interactions. Colloids Surf A 119:51
129. Buchhammer HM, Petzold G, Lunkwitz K (2000) Nanoparticles based on PEL. Colloid Polym Sci 278:841
130. Nizri G, Magdassi S (2005) Solubilization of hydrophobic molecules in nanoparticles formed by polymer-surfactant interactions. J Colloid Interface Sci 291:169
131. Sobisch T, Lerche D (2002) Pre-selection of flocculants by the LUMiFuge separation analyser. Water Sci Technol 46:441
132. Lerche D, Sobisch T (2011) Direct and accelerated direct and accelerated characterization of formulation stability. J Dispersion Sci Technol 32:1799
133. Lerche D (2002) Dispersion stability and particle characterization by sedimentation kinetics in a centrifugal field. J Dispersion Sci Technol 23:699
134. Küchler S, Sobisch T, Detloff T, Lerche D (2011) Direct characterization of ceramic dispersions. Ceram Forum Int 88:E27
135. Sobisch T, Lerche L (2008) Thickener performance. Colloids Surf A 331:114
136. Krause B, Mende M, Pötschke P, Petzold G (2010) Dispersability and particle size distribution of CNTs in an aqueous surfactant dispersion as a function of ultrasonic treatment time. Carbon 48:2746
137. Mihai M (2009) Chitosan based nonstoichiometric polyelectrolyte complexes as specialized flocculants. Colloids Surf A 346:39
138. Glampedaki P, Petzold G, Dutsch V, Miller R, Warmoeskerken MCG (2012) Physicochemical properties of biopolymer-based polyelectrolyte complexes with controlled pH/thermo responsiveness. React Funct Polym 72:458
139. Glampedaki P, Krägel J, Petzold G, Dutschk V, Miller R (2012) Textile functionalization through incorporation of pH/thermo – responsive microgels. Part 1. Microgel preparation. Colloids Surf A 413:334
140. Rutkaite R, Bendoraitiene J, Klimaviciute R, Zemaitaitis A (2012) Cationic starch nanoparticles based on polyelectrolyte complexes. Int J Biol Macromol 50:687
141. Müller M, Starchenko V, Lebovka N, Ouyang W, Keßler B (2009) Nanoparticles of polyelectrolyte complexes with narrow size distribution: preparation and life science applications. Polym Mater Sci Eng 101:1514
142. Höbel S, Loos A, Appelhans D, Schwarz S, Seidel J, Voit B, Aigner A (2011) Maltose- and maltotriose-modified, hyperbranched poly(ethylene imine)s (OM-PEIs): physicochemical and biological properties of DNA and siRNA complexes. J Controlled Release 149:146

Adv Polym Sci (2014) 256: 67–102
DOI: 10.1007/12_2012_201

Published online: 4 April 2013

Spontaneous Assembly and Induced Aggregation of Food Proteins

Saïd Bouhallab and Thomas Croguennec

Abstract Beyond their nutritional value, food proteins are a versatile group of biopolymers with a considerable number of functionalities throughout their extensive structures, conformations and interaction–aggregation behaviour in solution. In the present paper, we give an overview of the induced aggregation and spontaneous reversible assembly of food proteins that lead to a diversity of supramolecular structures. After a brief description of the properties of some food proteins, the first part summarises the aggregation processes that lead to supramolecular structures with a variety of morphologies and sizes. The second part reports on the requirements that drive spontaneous assembly of oppositely charged proteins into reversible supramolecular structures. The promising new applications of these structures in food and non-food sectors are also mentioned.

Keywords Aggregation · Food proteins · Interactions · Self-assembly · Supramolecular structures

Contents

S. Bouhallab (✉) and T. Croguennec
INRA, UMR1253 Science et Technologie du Lait et de l'œuf, 35042 Rennes, France

Agrocampus Ouest, UMR1253 Science et Technologie du Lait et de l'œuf, 35042 Rennes, France
e-mail: Said.bouhallab@rennes.inra.fr

Abbreviations

α-La α-Lactalbumin
β-Lg β-Lactoglobulin
BSA Bovine serum albumin
Lf Lactoferrin
LYS Lysozyme
Ova Ovalbumin

1 Introduction

Protein assembly in food science has been studied for long time because it contributes to the characteristics and specific sensory properties of food. In the past decades, improving knowledge on the mechanism of protein assembly has been responsible for the design of specific but still limited numbers of supramolecular structures (fibres, spheres, nanotubes, etc.) [1–5]. These structures could extend the functional properties of proteins by the development of new sensory properties in food or the encapsulation, protection and delivery of bioactives. Anyway, obtaining such supramolecular structures from protein solutions tightens the evidence that proteins constitute ideal building blocks for obtaining assemblies of various size and architectures [6]. These supramolecular structures are not specific to one (or a group of) protein(s) but are obtained from very distinct proteins, indicating that the way that proteins assemble into supramolecular structures is a generic property of proteins that is, de facto, independent of the amino acid composition of proteins [7]. In addition, one selected protein will self-assemble into various different supramolecular structures only by modifying the physicochemical conditions of the medium. Hence, even if protein assembly follows universal mechanisms, the selection of the physicochemical conditions of the medium, by affecting the rate of the different steps occurring during protein assembly, influences the size, shape and characteristics of the supramolecular structure formed (reactivity, internal structure, etc.); these physicochemical conditions being specific to each protein system [8].

In contrast to model solutions of protein, food systems have a complex composition that contains proteins, polysaccharides, lipids, minerals, etc., of different types and mixes at different concentrations and ratios. The presence of molecules other than proteins in the medium, such as small solutes (specific ions, amino acids, fatty acids, etc.), strongly affects their assembly process [9–12]. The assembly process is also affected when working with mixtures of proteins [13–15]. These parameters constitute putative, still underestimated, means for controlling the characteristics and functionalities of new supramolecular structures. All these parameters must be considered for the interpretation of data on the protein assembly process. In fact, combining the large diversity in protein structure (stability, repartition of hydrophobic and hydrophilic patches, net charge, localisation of charged group onto the protein surface, etc.) and in medium composition offers endless possibilities for protein self-assembly into supramolecular structures. In these conditions, the control of supramolecular structure formation becomes a real challenge, though examples from biological systems inform us that food technology has just entered this new scientific area.

Prediction of protein assembly needs for its perfect control an understanding of the physicochemical parameters affecting protein–protein and/or protein–aggregates and/or aggregates–aggregates interactions at different length scales, from molecular to nano- and mesoscopic, and at different time scales. One of the key issues for controlling the formation of supramolecular structures with defined size and shape is to identify the initial events that promote the later stages of the process of protein assembly. Having proteins with well-characterised molecular structure (identification of residues and atoms accessible to the solvent and available for protein–protein interaction) is helpful for understanding and predicting the mechanism of protein assembly at a molecular level [16]. Forces and energies developed at a higher range scale could be different since intrinsic properties of aggregates change throughout the progress of the assembly. Identifying the type and intensity of inter-protein and inter-supramolecular structure interactions acting simultaneously and/or sequentially in both space and time constitutes important knowledge for understanding protein behaviour in complex systems [17].

Induced assemblies and spontaneous assemblies (self-assemblies) are two distinctive routes to the formation of supramolecular structures. Induced assemblies occur when proteins are destabilised consecutively to an induced unfolding and/or hydrolysis that triggers protein assemblies. They are obtained under physicochemical conditions that are different from physiological conditions, i.e., under elevated temperatures and/or extreme pH conditions, by changing solvent quality, etc. [18–23]. Induced assemblies are often irreversible. In contrast, protein self-assemblies dictated by thermodynamics involve the spontaneous and hierarchical association of the proteins into ordered supramolecular structures without the contribution of external energy input and/or denaturing agents. The driving forces for self-assembly involve either attractive intermolecular interactions or an indirect entropy contribution resulting from the release of counter-ions and water molecules [24, 25]. Self-assembly phenomenon is widespread in nature and is the basis of numerous biological functions (structure, regulation, transport, protection, etc.). Apart from mimicking nature, using the self-assembly potential of proteins for the

design of specific supramolecular structures (new biomaterials), leading to new functionalities, constitutes great scientific and technologic challenges in food science and also in various fields such as in nano- and medical technologies. The main advantages of the self-assembly approach compared to other ways used for the production of supramolecular structures (high temperatures, unpleasant chemicals or solvents, mechanical stresses, etc.) lie in the step-by-step control of polymer association (bottom-up approach) and a reduction of energy costs [26, 27]. Other specificities are that protein self-assembly is usually reversible, i.e. that assembly or disassembly may be triggered by modifications of the physicochemical conditions of the aqueous solution. In addition, the composition and yield of formation of supramolecular structures resulting from self-assembly are precise and are adjustable by slight changes in the physicochemical conditions of the medium [12, 28].

Literature reviews describing experimental and/or theoretical polymer–polymer assembly is abundant and diversified regarding the nature of the polymers and physicochemical conditions used and the supramolecular structures obtained [29–35]. In this review, we will focus on recent data on food protein assembly. After a description of the structure and main properties of some important food proteins, we will describe first the protein-induced assemblies that lead to regular supramolecular structures and, in a second part the spontaneous protein self-assembly potential with a special emphasis on systems containing more than one protein.

2 Structure and Properties of Some Food Proteins

In this section, a brief overview of the structural characteristics of the food proteins most widely used in studies on protein–protein complex formation is presented. Proteins presented below and in Table 1 are from milk [β-lactoglobulin (β-Lg), α-lactalbumin (α-La), bovine serum albumin (BSA), lactoferrin, caseins] or egg white (ovalbumin, lysozyme), even if proteins from other sources (including gelatin and soy and wheat proteins) are also used for self-assemblies and complex formation studies. The proteins presented are mainly monomers, but are able to self-assemble into oligomers or aggregates in some specific conditions. These conditions are also addressed.

2.1 General Aspects of Proteins

Proteins are complex natural macromolecules made up of successive amino acids that are covalently bonded together in a head-to-tail arrangement through amide bonds. Each protein molecule is composed of an exact sequence of amino acids determined by the genetic code and arranged in a linear fashion. Proteins are zwitterions because they contain both positive and negative charges in a proportion that depends on the amino-acid composition. Hence, proteins are weak

Table 1 Physicochemical properties of various food proteins

Protein	Mw (kDa)	p*I*	Charge at neutral pH	Aggregation state	~T_m (°C)
β-Lactoglobulin	18.3	5.2	−16	Dimer	75
Bovine serum albumin	66.3	5.0	−7 to −10	Monomer	80
α-Lactalbumin					
Apo	14.2	4.3–4.7	−4	Monomer	26
Holo					64
Ovalbumin	45.5	4.5	−12	Monomer	84.5
Casein					
α_{S1}	23.6	4.9	−21	Micellar	–
α_{S2}	25.2	5.2	−15	Micellar	–
β	24	5.4	−12	Micellar	–
κ	19	5.6	−3	Micellar	–
Lactoferrin					
Apo	83	8.5	+14	Monomer	60–65
Holo					~90
Lysozyme	14.3	10.7	+7.5	Monomer	74

pI isoelectric point, T_m denaturation temperature

polyelectrolytes whose charge sign and density show a strong dependence on the pH. Proteins are distinguished from each other by their amino acid sequence, their folding (globular folded form, fibrous form, intrinsically unfolded conformation) and their biological function. One of the key features of proteins is their ability to acquire distinctive secondary and three-dimensional (3D) structures dictated by the amino acid sequence.

The primary structure of a protein is the succession of amino acids bonded together by peptide bonds between the carboxyl group of the amino acid *N* and the amine group of the amino acid *N* + 1. The acid hydrolysis of proteins releases 20 amino acids, each having a lateral chain with specific reactivity. Some lateral chains are hydrophobic, others are hydrophilic, neutral or carry an electric charge (positive or negative). The presence of hydrophobic residues confers to proteins an affinity towards hydrophobic surfaces. The charge on the lateral chain of the amino acids gives the protein a net charge that is positive, negative or null according to the pH value. At a certain pH, referred to as the isoelectric point (p*I*), the numbers of positive and negative charges on a protein are equal and the protein is electrically neutral. Proteins have an excess of positive charges below its p*I* and an excess of negative charges above its p*I*. Basic proteins (high p*I*) are rich in arginine and lysine residues whereas acidic proteins are rich in glutamic and aspartic acid residues. Figure 1 illustrates an example of how the theoretical net charge of a globular protein (α-La) evolves according to pH, with a zero net electric charge (p*I*) around 4.6.

The secondary structure consists of the local spatial arrangement of the polypeptide chain into repeating structures stabilised by hydrogen bonds, i.e. α-helices and β-sheets. In α-helices, hydrogen bonds are shared by amino acid residues close to each other in the primary sequence of the protein whereas in β-sheets, they involved distant residues. In addition proteins exhibit local non-repeating structures, i.e. turns.

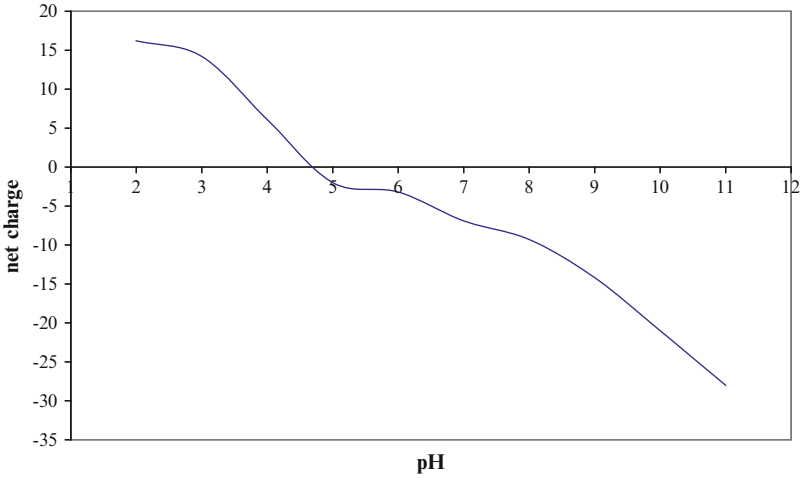

Fig. 1 Evolution of the theoretical net charge of a protein (α-lactalbumin) according to pH, determined using ExPASy Bioinformatics Resources Portal. Theoretical isoelectric point (p*I*) of α-lactalbumin is 4.7

The tertiary structure of the proteins is the 3D organisation of the proteins, involving the repartition of the secondary structure units of the proteins with respect to each other. The driving force for the folding into tertiary structure is dependent on the physicochemical properties of the medium. In aqueous solutions, the hydrophobic residues of the proteins are hidden in the core of the proteins in order to minimise contacts with water molecules. The protein tertiary structure is stabilised by hydrophobic interactions, salt bridges, hydrogen bonds and, for some proteins, disulfide bonds.

Behind these three structural levels, some proteins have a quaternary structure that results from the association of two or more identical or different polypeptide chains (protein subunits).

In solutions, the overall protein conformation fluctuates between a large number of conformations that are very similar to each other. The native protein structure is defined as the structure of lowest energy or structure of highest probability. Away from their p*I*, proteins in solution are stable because the protein molecules carry charges of the same sign and repel each other. In contrast to intrinsically unfolded proteins, numerous globular proteins are also stable close to their p*I* at low or medium ionic strength due to the presence of residual charged patches on the protein surface that counterbalance short-range attractive interactions. In some conditions (elevated temperatures, presence of denaturants, etc.), the native protein unfolds (loses its native conformation) or denatures. Each protein (except intrinsically unfolded proteins) has a denaturation temperature that is dependent on the conditions of the medium (pH, ionic strength, dielectric constant). Upon denaturation, the hydrodynamic size, the flexibility and also the reactivity of the proteins increase because of the exposure of reactive groups to the surface of the proteins.

This denaturation may lead to protein aggregation. One other consequence for globular proteins is a loss of solubility close to the p*I*.

2.2 β-Lactoglobulin

β-Lg is a globular protein of 162 amino acids and a molar mass of 18.3 kDa. It belongs to the lipocalin superfamily, sharing the common β-barrel calyx structural feature as an ideal binding site for hydrophobic ligands [36–38]. Its molecular structure is well established [36]: basically, β-Lg has 10–15% α-helix, 43% β-sheet and 47% unordered structures, including β-turn. Its structure contains nine β-strands (labelled A–I) that are organised into two β-sheets facing each other and a C-terminal α-helix, as determined by X-ray crystallography [39]. β-Lg has two disulfide bonds, which play an important role in the reversibility of β-Lg denaturation [40]. β-Lg also contains one free sulfhydryl group, which is buried within the protein structure on the β-strand H and plays an important role in stabilising the protein structure [41]. Its p*I* is about 5.2. At neutral pH (5.5–7.5) and room temperature, native β-Lg exists as a stable non-covalent dimer but its oligomerisation sate is dependent on the medium conditions. At pH below 3.5 and above 7.5, β-Lg is mainly monomer; between pH 3.5–5.5, it is mainly associated as octamer. These pH ranges also vary according to the ionic strength, temperature and the presence of hydrophobic ligands in the central cavity of the protein. Changes that occur in protein structure when heated have been described [42].

2.3 Serum Albumin

BSA consists of a polypeptide chain of 582 amino acids and a molar mass of 66.4 kDa. It is mainly a helical protein having a p*I* of 4.9 [43]. BSA is a monomer containing one sulfhydryl group and 17 disulfide bonds, which stabilise the structure of the protein. All the disulfide bonds are relatively close to each other in the polypeptide chain, which is therefore organised in a series of short loops. BSA exhibits several binding sites for hydrophobic ligands on its surface.

2.4 α-Lactalbumin

α-La consists of 123 amino acids and has a molecular weight of 14.2 kDa. Its isoelectric point is between 4.2 and 4.5. α-La has close homology in sequence with hen egg-white lysozyme [44]. Among the 123 amino acid residues, 54 are identical to corresponding residues in lysozyme and a further 23 residues are structurally similar. α-La consists of 26% α-helix, 14% β-sheet and 60% unordered structure. α-La

contains eight cysteine residues, all engaged in disulfide bonds that stabilize the tertiary structure of the protein. In addition, α-La binds one calcium ion per molecule ($K_A = 2.9 \times 10^8$ M^{-1} [45]) in a pocket containing four aspartate residues [46]. When the pH is decreased below 5, the aspartate residues are progressively protonated and α-La ability to bind calcium decreases. The calcium-free apo form of α-La is highly heat-sensitive and it denatures rapidly when the temperature increases. The denaturation temperature of apo α-La is around 30°C [47] whereas holo α-La is stable up to around 60°C [48, 49] (see Table 1). The apo α-La self-associates at pH close to 5.0 at about 50°C to give microscopic aggregates.

2.5 Ovalbumin

Ovalbumin (Ova) is a phosphoglycoprotein of 385 amino acids and a molar mass of about 45 kDa [50]. Its amino acid sequence contains about 50% hydrophobic residues and about 33% charged residues, mostly acidic, giving the protein a p*I* of 4.5 [51]. The sequence includes six cysteine residues, two of which are involved in a disulfide bond, and the N-terminal residue of the protein is an acetylated glycine [52]. Ova has one glycosylation site and two phosphorylation sites [53]. Ova contains 32% β-sheets and 30% α-helix as determined by X-ray crystallography [54, 55]. Some evidences indicate that Ova molecules self-assemble depending on protein concentration and pH. Ova is monomer at concentrations lower than about 0.1% and forms oligomers (dimer, trimer and tetramer) at higher protein concentrations; the association behaviour is favoured when pH decreases from a neutral value to the protein p*I* [56].

2.6 Caseins

Caseins (α_{S1}, α_{S2}, β, κ) are a group of flexible proteins of about 20–24 kDa (from 169 to 209 amino acids) sharing some common features such as the presence of ester-bound phosphate (organic phosphate) in their structure and rather high number of charged (glutamic acid, lysine) and uncharged (leucine, isoleucine, proline) residues, but low number of sulphur-containing amino acids. They are often considered as intrinsically unstructured proteins [57] or rheomorphic proteins [58] as the structure of caseins is sensitive to environmental variations. In addition, caseins consist of well-separated hydrophobic and hydrophilic domains, especially β-casein and κ-casein. The caseins also exhibit microheterogeneity regarding their degree of phosphorylation and glycosylation [59]. α_S- and β-caseins are extensively phosphorylated whereas κ-casein has only one or two ester-bound phosphates but is glycosylated. Due to the presence of a high amount of phosphoseryl groups, α_S- and β-casein precipitate in the presence of calcium. In contrast, κ-casein is still soluble even in the presence of high amount of calcium. Casein aggregation state also depends

on pH and temperature. Caseins precipitate when the pH is reduced to 4.6 and β-casein self-assembles as small aggregates in a temperature-dependent manner.

2.7 Lactoferrin

Lactoferrin (Lf) is an iron-binding glycoprotein composed of 689 amino acids and has a molar mass of about 80 kDa. It has approximately 41% α-helix and 24% β-sheets and the polypeptide chain is folded in two homologous lobes (N- and C-lobes) connected to each other by a three turns of an α-helix (residues 334–344) [60]. Each lobe is composed by two domains (N_1, N_2 and C_1, C_2) forming a cleft in between; the interdomain cleft forms a binding site for one iron ion or other metallic ion concomitantly to a synergically bound carbonate anion [61, 62]. Lf tertiary structure is stabilised by 17 disulfide bonds. Compared to the holo form, which is conformationally rigid, the metal-free apo form of Lf is much more flexible and more susceptible to denaturation. Lf is a basic protein with a p*I* of 8.6–8.9 and consequently carries a positive net charge at neutral pH. The charge distribution on Lf surface is uneven with some highly positive patches on the N-lobe and the inter-lobe region [62]. Additional negative charges on the Lf surface are also carried by sialic moieties [60, 63, 64], which increase the hydration volume on the protein surface and stabilise Lf [65]. Lf exhibits ionic strength-dependent aggregation behaviour [66, 67]. These studies reported an Lf monomer–aggregate equilibrium that is sensitive to variation in ionic strength. At low ionic strength (and neutral pH), Lf molecules are mainly monomer and positively charged. When ionic strength increased, Lf forms neutral [66] or negatively charged aggregates (p*I* ~6) [67].

2.8 Lysozyme

Lysozyme (C-type family without a specific metal binding site; LYS) is a globular protein of 129 amino acids (14.3 kDa) and a strongly basic character (p$I = 10.7$). It is a protein consisting of two domains (domains α and β) linked together by a long helix–loop–helix (residues 87–114). The secondary structure of the protein is formed by 39% α-helix gathered mainly in the domain α and 11% β-sheet involved in a three-strand antiparallel β-sheet that constitutes, with some helices, the β-domain [68]. LYS has eight cysteine residues, all of which are involved in intramolecular disulfide bonds making the protein compact and stable [69]. It was noticed that under specific conditions of protein concentration, temperature and ionic strength, LYS forms transient clusters [70, 71]. Clusters result from short-range attractions, leading to surface energy reduction upon cluster formation, and long-range repulsions that increase the Coulomb energy of the clusters and thus limits their growth [72].

3 Induced Assemblies of Food Proteins

This section focuses on fibrils, ribbons, spherulites, nanotubes and particulate aggregates, which are the most regular macromolecular structures obtained from food protein solutions. The structure (shape, size) of induced assemblies may be changed by controlling parameters such as protein concentration, temperature and time of heating, pH, presence of small solutes, etc. The structures of induced assemblies are generic forms of proteins aggregation as long as the conditions for protein aggregation are defined: these conditions may change depending on the protein system [7]. For instance, under appropriate conditions, β-Lg is able to form fibrils, ribbons, spherulites or particulate aggregates. Similar supramolecular structures may be obtained with proteins having different structures and properties. This means that the supramolecular structure of the induced assemblies is independent of the primary structure of the proteins; it results from identical aggregation mechanisms occurring for different physicochemical conditions of the medium [8].

3.1 Fibrils

Amyloid-type fibrils are linear polymers of about 3–10 nm width and range in length from hundreds of nanometres to micrometres (Fig. 2a) [23, 76]. Protein fibrils are extensively studied and theoretical models have been proposed that explain and predict their behaviour. Fibril formation follows a nucleation/growth mechanism [77–81] where nucleation constitutes a lag phase in which no significant growth is measurable. Fibril nucleation is usually the limiting step but the lag phase is reduced by shearing, adding fibril seeds or increasing the temperature [18, 82, 83]. Fibril growth is hierarchical and unidirectional. During this step, proteins form linear β-sheet-organised aggregates in which β-sheet conformation is perpendicular to the growth direction of the fibrils. Protein fibril formation requires specific physicochemical conditions allowing the proteins to expose hydrophobic patches to the solvent and to conserve some net charge on the surface. For this reason, peptides and intrinsically unfolded proteins such as κ-casein are well adapted to fibril formation. Fibrils of κ-casein are obtained at neutral pH and physiological temperature (37°C) after reducing protein disulfide bonds [13, 14, 84]. Fibril formation from globular proteins such as whey, egg white and soy proteins require a preliminary step of unfolding and/or hydrolysis of the proteins in order to expose on the protein surface residues prone to establish intermolecular β-sheets. Even if protein hydrolysis was suggested to be an essential preliminary step for fibril formation [85, 86], experimental evidence indicates that fibril formation also occurs under conditions where an absence of protein hydrolysis is expected [19–21, 87]. In vitro, fibrils from globular proteins are obtained under elevated temperatures, low pH and low ionic strength [23, 85], in the presence of urea [21, 87] or at high concentration of alcohol [20]. Arnaudov et al. [88] indicated that fibrils formed after a short heating time but not after long heating periods are unstable and disintegrate on cooling. For numerous

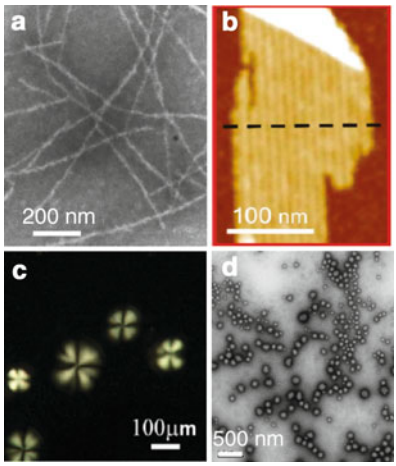

Fig. 2 Diversity of supramolecular structures obtained from food proteins. (**a**) TEM micrograph of fibrils obtained after heating a mixture of β-lactoglobulin (β-Lg) and α-lactalbumin (α-La) (2.5 wt% with ratio β-Lg to α-La of 90:10) at pH 2 [adapted with permission from Bolder et al. [73] © (2006) from ACS]. (**b**) AFM micrograph of β-Lg ribbons obtained after heating β-Lg (2 wt%) at 90°C and pH 2 [reprinted with permission from Lara et al. [23] © (2011) from ACS]. (**c**) Polarised light microscopy micrograph of spherulites formed from β-Lg [reproduced with permission from Krebs et al. [74] © 2009 from The Biochemical Society]. (**d**) TEM micrograph of β-Lg dispersion (1 wt%) after heating at 85°C for 15 min at pH 5.8 [adapted with permission from Schmitt et al. [75] © (2009) from ACS]

proteins, reducing the pH of the protein solution subjected to heat treatment speeds up the formation of fibrils regardless of the p*I* of native protein, for instance LYS (10.7) and α-La (4.2–4.5). Heat treatment under acidic pH conditions induces some cleavage in the polypeptide backbone [76, 82, 85] and generates some succinimidyl residues from aspartic acid [76], both reactions being preponderant at low pH. Peptides are considered to be the major building blocks of fibrils, but the contribution of succinimdyl residues is much more speculative. For β-Lg, the yield of incorporation of the peptides into fibrils is low because only the most hydrophobic peptides with β-sheet propensity are involved [85]. The shape and size of the fibrils are also tuned by ionic strength. Screening of the electrostatic charges by salts fastens the aggregation stage, resulting in shorter and more curved fibrils [89]. However, according to these authors, the fibrils exhibited similar thicknesses of around 3.5 nm and a periodic structure, with a period of about 25 nm whatever the ionic strength in the range 10–100 mM.

3.2 Multistranded Ribbons and Spherulites

The above fibrils are also able to order into larger structures that are either linear (helical ribbons) (Fig. 2b) or spherical (spherulites) (Fig. 2c). Under specific conditions, the larger structures coexist with fibrils in solution [73].

Ribbons result from the lateral stacking of fibrils. They are observed only after a prolonged heating at acid pH of globular proteins as different as LYS or β-Lg. The formation of multistranded ribbons occurs concomitantly with an extensive hydrolysis of the proteins into low molecular weight peptides [23]. Such small peptides are hypothesised to be responsible for the formation of multistranded ribbons.

Spherulites result from the radial arrangement of unbranched protein fibrils and are characterised by a semi-crystalline structure [90, 91]. Because of their inner structure, spherulites exhibit a Maltese cross pattern when they are observed between crossed polarizers in a light microscope [92]. The spherulites can reach several hundred micrometres in diameter. In the larger spherulites, it is possible to distinguish two regions: an amorphous nucleus and a semi-crystalline surrounding corona [91, 93]. In contrast to the surrounding corona, the core progressively loses its birefringence during the radial growth of the spherulite. Assuming that the growth of the spherulite occurs through the periphery and that the radially ordered fibrils do not convert into amorphous aggregates, it was hypothesised that a distortion of fibrils in the core of the spherulite occurs during the growth, resulting in a progressive loss of birefringence [8]. Although the mechanism triggering the association of single fibrils into spherulites is not totally elucidated, it was hypothesised that the balance between electrostatic, hydrophilic and hydrophobic interactions is preponderant; heating temperature and pH are preponderant factors in reducing the lag phase for spherulite observation [94]. In addition, the morphology of the spherulites is affected by the presence of salt, which favours larger spherulites with a larger nucleus [74].

3.3 Particulate Aggregates

Globular proteins (BSA, β-Lg, LYS, etc.) are able to form irreversible, well-defined, particulate aggregates of several tenths to hundreds of nanometres when heated close to their p*I* or in the presence of salts (Fig. 2d) [95–97]. Heating induces the exposure to the solvent of hydrophobic patches initially buried in the interior of the protein structure. Hydrophobic interactions constitute the main driving force for protein assembly, even if some authors underline the importance of electrostatic interactions [10]. As for fibrils, proteins are held together by intermolecular β-sheets in the particulate aggregates. However, intermolecular β-sheets are shorter in the particulate aggregates and they have random orientations due to a faster aggregation step (low electrostatic barriers for protein aggregation) [8]. Experiments on β-Lg indicate that heat treatment of the unfolded proteins first causes aggregation into oligomers and then into soluble aggregates [98, 99]. On prolonged heating, soluble aggregates interact and form particulate aggregates of about one to several hundred nanometres in diameter. These particulate aggregates self-assemble when the electrostatic repulsions are too low for their stabilisation in solution [100]. The aggregation of β-Lg slows down rapidly and even stops when the proportion of native proteins in solution is lower than 10% [101].

The low electrostatic repulsion between proteins during the heat-induced assembly process favours the growth of the aggregate into spherical structures [102]. Then, particulate aggregates are formed at close to protein p*I* or in the presence of salts due to the screening of exposed ionised groups. pH, ionic strength, hydrophilic–hydrophobic balance in the polypeptide chain, protein concentration, heating temperature ramp and heating time are factors tuning the size of the particulate aggregates formed [74, 100, 103] and governing their assembly behaviour and stability in solution [100]. Stable suspensions of particulate aggregates of β-Lg (absence of sedimentation) are obtained after heating β-Lg solution at low ionic strength and at pH slightly below (pH 4.5–4.7) or slightly above (pH 5.7–5.9) the isoelectric point. Under these conditions, the particulate aggregates are individualised and monodispersed, with an average diameter of around 200 nm. Their size is slightly higher at pH 4.6, under which conditions the net charge of the particulate aggregates is lower than at pH 5.8 (+30 mV at pH 4.6 versus −40 mV at pH 5.8) [75]. It was hypothesised that the charge of the particulate aggregates limits their growth and prevents their assembly into larger supramolecular structures. A macroscopic phase separation appears rapidly when the repulsion between the particulate aggregates decreases [100]. In another study, aggregates with different sizes and morphologies were produced by heating β-Lg at 80°C in the pH range between 6 and 6.8. Large spherical aggregates with an average hydrodynamic diameter of 96 nm were formed at pH 6 against smaller and linear aggregates with an average hydrodynamic diameter of 42 nm at pH 6.8 [104]. Particulate aggregates are also formed by heating a mixture of β-Lg and α-La (ratio 80:20) at pH 5.7. For higher proportion of α-La in the mixture, the yield of conversion of native proteins into particulate aggregates decreases and the particles lose their spherical shape and/or aggregation [15]. At pH 5.7, both proteins are negatively charged but it was suggested that the presence of α-La in the aggregates reduces the hydrophobic attractive interactions for the formation of round and dense particles. The yield of conversion of native proteins into particulate aggregates increases in the presence of salts because salts promote aggregation [15]. This indicates that mineral composition and protein composition influence the assembly process. A suspension of spherical aggregates, with core–shell structure of diameter around 100 nm, is also obtained by heating a mixture of oppositely charged proteins (Ova/LYS or ovotransferrin/LYS) [105, 106]. Interestingly, these studies described lysozyme-rich core and ovalbumin-rich shell particles whose charge depend on the medium pH: at pH 5–10 the core carries positive charges and the shell carries negative charges; at pH around 5, formed particles are neutral; below pH 5, particles with homogeneous positive charge are formed; and above pH 10, particles with homogeneous negative charge are formed. The mechanism of protein assembly is not understood yet, but under the same physicochemical conditions it is not possible to obtain the same supramolecular structures with only one protein. This indicates the prevalence of the interactions between proteins of opposite charge. The procedure for the formation of nanoparticles of Ova and LYS consists first of the pH adjustment of the solution at 5.3, between the p*I* of the two proteins, promoting Ova–LYS interactions (Fig. 3). Then, the pH is increased and, when the value comes close to the p*I* of LYS, the LYS molecules aggregate

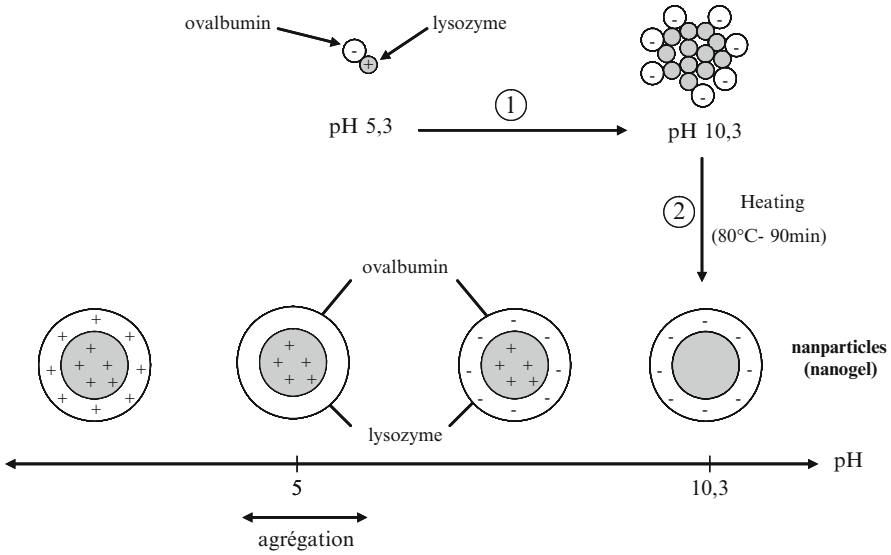

Fig. 3 Illustration of the mechanism of formation of core–shell nanoparticles between ovalbumin and lysozyme according to the pH value (constructed from [105])

due to the decrease in electrostatic repulsions (Fig. 3, step 1). After 1 h of gentle stirring, nanoparticle formation is triggered by heating the solution at 80°C for 90 min (Fig. 3, step 2). Finally, the nanoparticles are constituted, with an Ova-rich shell entrapping an inner structure composed mainly of LYS. The nanoparticles have a positively charged surface at pH <5 and a negatively charged surface at pH >6. Between pH 5.0 and 6.0, the nanoparticles are weakly charged and aggregate reversibly (Fig. 3). Stable spherical nanoparticles of LYS and β-casein are obtained by heating the protein mixture under specific pH conditions and appropriate ratio [107]. Between pH 5 and 11, the two proteins carry opposite charges and form complexes after mixing. However, the pH suitable for nanoparticle formation is around the p*I* of the two proteins, i.e. in the pH ranges 4.0–6.0 and 9.0–12.0 (Fig. 4). After heating, β-casein molecules are trapped in the core of the nanoparticles and are covered by a gelated shell of LYS. In these pH ranges, the protein conversion yield into nanoparticles decreases if the pH decreases towards 4.0 or increases towards 12. Between pH 6.0 and 9.0, the charge of the two proteins have similar magnitude and a coagula instead of nanoparticles is obtained after heating.

3.4 Nanotubes

In contrast to fibrils, the formation of nanotubes from proteins is much less frequently observed and far less well understood [108]. Concerning food proteins, to date nanotubes have so far only been reported for α-La, the second most abundant protein in the whey fraction of bovine milk. Ten years ago, Ipsen et al. [109]

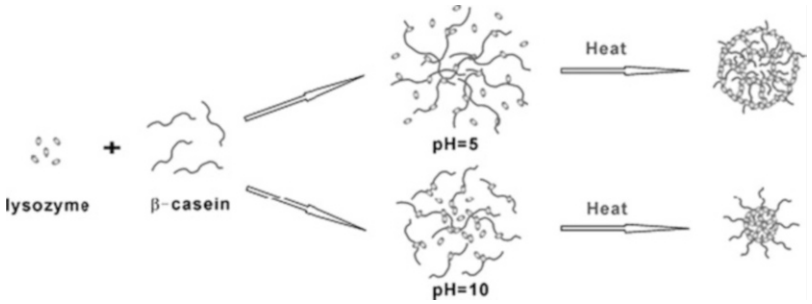

Fig. 4 Mechanism of formation of lysozyme/β-casein nanoparticles at pH 5.0 and 10 [reprinted with permission from Pan et al. [107] © (2007) from Elsevier]

showed that α-La self-assembles into long and tubular strands of 20 nm in diameter upon limited proteolysis by a specific serine protease. The nanotube structure of these tubular strands was further described in detail a few years later [1]. These authors showed that the formation of nanotubes from hydrolysed α-La requires the control of protein concentration, presence and concentration of specific divalent cations such as calcium and hydrolysis conditions (for details see [2]). The presence of a small percentage of other proteins as well as the use of certain divalent cations such as magnesium inhibit the self-assembly process into nanotubes and lead instead to random aggregates [2]. These nanotube structures are described to be stable towards processing and could, for example, withstand conditions similar to pasteurisation. Consequently, they exhibit some interesting futures for food and non-food applications. As an example, because of their linearity, these nanotubes form strong gels with a high storage modulus, even at a weight protein fraction as low as 3% [1]. The reversibility and disassembly properties of these nanotubes provide other potential applications such as encapsulation and controlled release of nutritional and bioactive components [2].

4 Spontaneous Assemblies of Food Proteins

For self-assembly, proteins have to diffuse in the medium and establish specific and/or non-specific interactions when meeting a counterpart. Interactions occur through the protein surface (absence of denaturation step) and protein–protein interactions are mainly of low energy, i.e. non-covalent (electrostatic interactions, van der Waals bonds, hydrogen bonds, salt bridges). Protein–protein interaction energy is only slightly higher than thermal energy kT (with k is the Boltzmann constant and T the temperature), enabling the proteins to rearrange locally with each other for adoption of preferential orientations. In the later stages, minimisation of the free energy of the protein aggregates drives the assembly to ordered supramolecular structures [110]; this mainly involves the surface energy of the

supramolecular structure and the strain energy [26]. In addition, most self-assembled objects are near-equilibrium systems and then evolve slowly with time and with local variations in the surrounding of the supramolecular structures. These different steps could explain why the rate of supramolecular structure formation through protein self-assembly is relatively slow. The final state depends on the equilibrium of attractive and repulsive interaction between proteins inside the overall structure and the forces between the supramolecular structures [17]:

- Repartition of attractive and repulsive zones onto the protein surface is responsible for the shape and size of the supramolecular structure; hence, depending on the protein system and the physicochemical conditions of the medium, the size (from nanometre to micrometre) and shape (fibres, spheres, etc.) are able to change.
- Energy and nature of attractive and repulsive interactions between self-assembled proteins control the stability and reversibility of the formed supramolecular structures.

4.1 Oppositely Charged Proteins and Polyelectrolytes

Several recent reviews deal with the fundamental self-assembly between proteins and natural polyelectrolytes, e.g. DNA and polysaccharides [30, 31, 34, 111]. The applications in the food sector of protein and polysaccharide complexes and coacervates are also well covered elsewhere [35, 112]. Given these abundant recent reviews, this field is deliberately excluded from the present review.

The literature on the interactions and assembly between synthetic polyelectrolytes and proteins with opposite charges is also abundant (for reviews see [31, 113, 114]). The initial interactions in these systems involve short-range interactions like van der Waals and longer-range interactions, especially electrostatic interactions. At the thermodynamic level, for oppositely charged systems of protein and polyelectrolyte, interaction and assembly is generally found to be an exothermic process due to favourable electrostatic interactions [115], although an endothermic process has been reported for a BSA/polyelectrolyte system [116]. In addition to electrostatic interactions, the entropic contribution of the release of small counterions and water molecules has also been reported. For synthetic polyelectrolytes interacting with proteins, it is postulated that the interaction process is the result of a competition between the attractive electrostatic interactions between polyelectrolytes and proteins in one hand, and the polymer characteristics on the other hand. This was modelled by Muthukumar [117], taking into account the charge densities, size, Debye length and the molecular weight of involved macromolecules.

Control of these interactions is of importance for the design of a variety of supramolecular structures with different intrinsic properties. Before considering the cross-assembly between proteins, we first present some general elements on the interaction of proteins with linear polyelectrolytes. Some examples published during the last 10 years on dual systems involving a mixture of protein and

Table 2 Some indicative examples of protein/polyelectrolytes self-assembly and generation of various supramolecular structures

Protein	Synthetic polyelectrolyte	Structures	Reference
Lysozyme	Poly(acrylic acid)/poly(vinyl sulfonic acid)	Insoluble complexes	[118]
Lysozyme	Poly(methacrylic acid)/poly (acrylic acid)	Insoluble complexes	[119]
Lysozyme	Poly(styrenesulfonate)	Spherical complexes, dense globules	[120]
Lysozyme	Gold nanoparticle/serum albumin	Aggregates	[121]
Cytochrome c	Gold nanoparticle/aspartic acid	Conventional aggregates or core–shell nanoparticles	[122]
Caseins	Dodecyl-trimethylammonium	Insoluble aggregates or soluble complexes	[123]
BSA	Gold nanoparticle	Trimers/complexes	[124]
Lysozyme	Hyaluronan	Rod-like complexes	[125]
Poly (L-lysine)	Poly(vinylsulfate)/poly (methacrylic acid)	Spherical or needle-like particles	[126]
BSA	Poly(allylamine hydrochloride)	Positively or negatively charged aggregates	[116]

polyelectrolyte are given in Table 2. Several teams are interested in studying the connections between proteins and mineral nanoparticles modified by chemical polymers. These works explore the diversity of shapes and sizes of protein molecules that constitute the building blocks for the creation of bio-hybrid nanomaterials. For example, the electrostatic complementarities between cytochrome c (a basic protein) and gold nanoparticles facilitate the controlled design and manufacture of micrometre-sized composite materials [122]. In that study, the protein is used as an orientating agent for the assembly into nanoparticles. The difference in protein conformation between apo form and holo form allowed the formation of nanocomposites with different supramolecular architecture, i.e. from conventional aggregated nanoparticles with the apo form to well-defined gold-nanoparticles surrounded by a layer of cytochrome c when used in its holo form. Environmental changes, e.g. pH or enzymatic digestion, induce a remodelling of the nanocomposites. This study clearly confirms that selective surface recognition by protein molecules provides programmed bottom-up assembly of synthetic nanomaterials. In another study, Chen et al. [121] explored the ability of LYS to assemble with gold nanoparticles grafted with human serum albumin as a means of detection of LYS in complex food products [121]. The concentration of serum albumin and the working pH value were shown to be the main factors affecting the selectivity of the interaction with the LYS as well as the detection limit. This cross-assembly approach allowed the detection of LYS concentrations as low as 50 μM. Concerning the interactions in this assembly system, the surface of gold nanoparticles covalently bonded with serum albumin became neutral after addition of LYS and resulted in the aggregation of gold nanoparticles via the London–van

der Waals attractive forces. The assembly of casein, either in monomer or micellar states, with a cationic polymer of dodecyltrimethylammonium has been described [123]. Repeating units of the cationic polymer at low concentrations bind to acidic amino acids of the casein molecules, making the casein micelles more compact due to the reduction of the overall net surface charge. Increasing the concentration of cationic polymer induced aggregation and formation of insoluble casein–surfactant complexes. A re-solubilisation of these complexes was reached for a large excess of polymer with respect to the casein because of the repulsion caused by an excess of positive charges at the surface of assembled particles. The re-solubilised complexes exhibited new physicochemical properties compared to the initial complexes, which may, according to the authors, broaden the application range of casein micelles in food science, as well as in the cosmetic and medical domains. This study illustrates the key effect of the relative proportions of mixed oppositely charged molecules on the final properties of formed supramolecular structures. The use of neutron scattering provides access to the internal structure of objects resulting from the mixture of a protein and a polyelectrolyte with opposite charge. Studies of mixtures of an anionic polyelectrolyte with LYS showed that the assembly leads to the formation of several types of supramolecular structures depending on the concentration, pH and the size of the polyelectrolyte chain [120]. The study clearly shows that the initial charge ratio and the polyelectrolyte concentration are the main factors governing the assembly. Under certain conditions, the two molecules form dense primary complexes with an internal positive/negative charge ratio close to 1. According to the initial charge ratio, either free protein in solution or polyelectrolyte forming a crown around the assembled structure were detected. The variation of physicochemical parameters allowed the authors to draw the following three conclusions: (a) the inner charge ratio of formed complex remains close to 1 whatever the initial charge ratio; (b) the assembled complexes exhibit a very high density when the charge density of mixed molecules is maximum; and (c) the finite size of complexes (up to several microns) is limited by the electrostatic repulsions and can therefore be modulated by the ionic strength of the medium. These laws of interaction have been also reported in the case of two synthetic oppositely charged polyelectrolytes [127]. A strong or a weak assembly was reached according to the charge and concentration ratio of the constituents. The stoichiometry between the two partners found in the assembled supramolecular structures depends on the system studied. The difference in size between mixed molecules was assumed to be important for the stoichiometry in the supramolecular structures. This is well illustrated during cross-assembly of LYS with different polyelectrolytes [118]. One LYS molecule self-assembles with either 20 mol of poly(vinyl sulfonic acid) or 500 mol of poly(acrylic acid). The apparent energy associated with the formation of the complexes is very high but once normalised by the number of involved molecules, it accounts for about 10 kcal/mol, corresponding to the energy of a normal Coulombic interaction between two electrical charges in solution. This explains the low salt concentration typically required for total dissociation of the formed supramolecular structures.

Several theoretical models describing the interactions and assembly between two charged polymers are available. However, the application of these models is often difficult when proteins are involved because of their structural complexity. Chain flexibility and electric charge density are the main structural parameters of a given synthetic polyelectrolyte that influence its interacting properties. The importance of molecular flexibility for self-assembly and complex formation is well illustrated when mixing synthetic polyelectrolyte poly(vinylsulfate) or poly (methacrylic acid) with oppositely charged poly(L-lysine), whose conformation can be modulated by pH or salt concentration change [126]. Spherical particles were obtained with random coil conformation of the polypeptide chain whereas α-helical conformation resulted in needle-like particles. Concerning proteins, the situation is much more complex due to the presence of charges of opposite sign distributed all over the surface of the molecule, with specificity in local charge density. In general, proteins carry patches of negative and positive charges on their surface. For acidic proteins, the number of negative residues on the surface is larger than the number of positive residues. Hence, the overall charge of these proteins under neutral pH condition is negative (see [114]). The inverse is true for basic proteins that carry positive charge under the same conditions. The presence of positive (negative) patches on the surface of acidic (basic) proteins regulates the surface concentration of counterions of opposite charges that affect subsequent interaction and assembly processes between oppositely charged partners.

4.2 Oppositely Charged Proteins

The physicochemical laws that govern protein assembly in a system containing more than one protein are presumably different from those described for the single protein systems. In binary protein systems, there is a range of pH for which the two proteins carry opposite net charges. This is especially true when mixing a basic protein and an acidic protein. Under these conditions, electrostatic interactions between the two proteins of opposite charge are attractive and can lead to supramolecular assembly. For a visual illustration, Fig. 5 summarizes how ionic strength affects the assembly of proteins in system containing one type of protein (all proteins carry the same net charge at a given pH) or a mixture of proteins with opposite net charge at a given pH.

The interaction and spontaneous assembly between food proteins with opposite charge under mild conditions are poorly described. Some published examples are summarised in Table 3. In contrast to protein assemblies induced by drastic conditions (see above), the advantage of mild conditions is the possibility of fabricating reversible supramolecular assemblies because only weak non covalent interactions are involved. This offers a real opportunity for better control of both the assembly process of proteins into nano- and microstructures and the disassembly process.

Kobayashi's group and Lewis's group were the first to report the formation of turbid solutions by mixing two oppositely charged globular proteins from

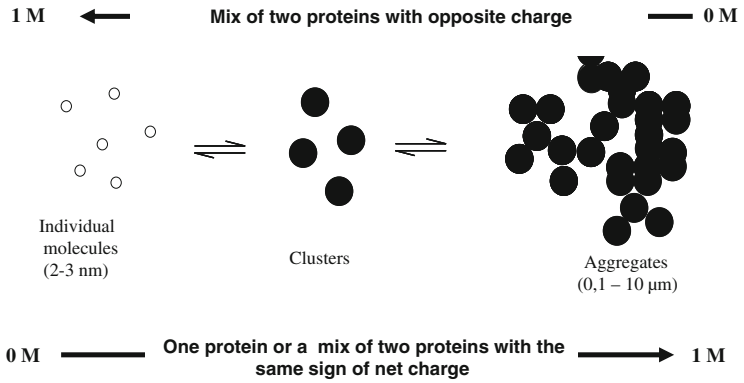

Fig. 5 Illustration of how an increase in ionic strength affects protein self-assembly according to the net charge of proteins at a given pH

Table 3 Self-assembly between oppositely charged food proteins and the shape of formed supramolecular objects

Acidic, negatively charged protein	Basic, positively charged protein	Shape of formed supramolecular structures	References
Pre-denatured ovalbumin	Lysozyme	Undetermined	[128]
Ovalbumin	Lysozyme	No self-assembly	[128]
Holo α-lactalbumin	Lysozyme	Undetermined	[129]
β-Lactoglobulin	Lysozyme	Undetermined	[129]
Succinylated lysozyme	Native lysozyme	Undetermined	[130, 131]
Caseins	Lactoferrin	Coacervates	[132]
Gelatin B	Gelatin A	Coacervates	[133]
Holo α-lactalbumin	Lysozyme	No self-assembly	[3, 12, 134, 135]
Apo α-lactalbumin	Lysozyme	Amorphous aggregates	[3, 12, 134, 135]
Apo α-lactalbumin	Lysozyme	Microspheres	[3, 12, 134, 135]
Ovalbumin	Lysozyme	Microspheres	[5]
Ovalbumin	Avidin	Microspheres	[5]
BSA	Lysozyme	Microspheres	[5]
β-Lactoglobulin	Lactoferrin	Microspheres or aggregates	Bouhallab et al. (unpublished data)
β-Lactoglobulin	Lysozyme		
Apo α-lactalbumin	Lactoferrin		

egg-white and milk whey, respectively [128, 129]. They suggest liquid–liquid phase separation throughout cross-protein aggregation. Howell et al. [129] underlined the strong dependence of such assembly between mixed native proteins on the physico-chemical conditions of the medium. Assembly between LYS and β-Lg, but also between LYS and α-La, were shown to be modulated by several physicochemical parameters such as protein molar ratio, pH and ionic strength of the solution, suggesting the involvement of electrostatic interactions between these proteins. Working on egg-white proteins, Matsudomi et al. [128] showed that pre-denaturation

of Ova was essential to initiate cross-assembly when mixed with LYS at pH 7.6 and low ionic strength. A LYS:Ova molar ratio of 1.5 was found in the formed supramolecular structures. No turbidity (aggregation) was detected by these authors when LYS was mixed with native (unheated) Ova. The aggregation between LYS and denatured Ova was also inhibited through the decrease of the positive net charge of LYS by chemical acetylation. Similarly, an increase in ionic strength beyond 50 mM strongly reduces the aggregation between the two proteins. The authors conclude that electrostatic interactions are important during cross-assembly of LYS with the unfolded chain of Ova. Electrostatic cross-assembly between oppositely charged molecules was also reported for binary systems involving unstructured proteins. This is the case when mixing gelatin-A ($pI = 9$) and gelatin-B ($pI = 5$) at molar ratio gelatin-A:gelatin-B of 1.5 [133]. This pH-controlled electrostatic cross-assembly was explored by these authors for encapsulation and release of a hydrophilic drug.

Electrostatic interactions are also described to be the main driving force in the self-assembly of structures between Lf (a globular protein) and α-casein, β-casein or κ-casein (unstructured proteins) at neutral pH [132]. As expected for electrostatic-driven complexes, the size of the formed complexes is affected by pH and ionic strength. The size of the complex decreases with increasing salt or when the pH shifts away from the pH for charge equilibration. For this latter case, it is assumed that the growth of the complexes is limited by the accumulation of charge on the surface of the self-assembled structures.

Recent and fundamental studies have been done on the physical chemistry of aggregation and assembly between proteins with opposite charge. Biesheuvel et al. [130] have shown the importance of the surface properties of proteins for their interaction and subsequent assembly and phase separation in the case of a binary protein mixture. For this, they studied the assembly between native LYS, with an overall charge at neutral pH of +7, and succinylated LYS, with an overall opposite charge at neutral pH of −7. The study was conducted under conditions whereby the overall conformation of proteins are not affected. By combining experimental and modelling approaches, these authors showed that the assembly between these two proteins was modulated by different physicochemical factors such as pH, ionic strength, the molar ratio of the two proteins and the temperature [130, 131]. The assembly process between these two protein forms decreases with increasing ionic strength and is inhibited for pH values where the overall charges of the two proteins has the same sign. A complete phase diagram, depending on the ionic strength and protein concentration, was described and commented on by the authors. In this protein mixture, electrostatic interactions and temperature are shown to be the main driving forces for protein interaction, for subsequent aggregation and then for phase separation. The theoretical model used to describe the assembly of oppositely charged proteins takes into account electrostatic interactions, steric effects and temperature. Optimal conditions for liquid–liquid phase separation in this system include: low ionic strength, low temperature, a symmetrical charge ratio, high protein concentration and a pH value at which the protein charge densities are highest, i.e. pH 7.5. In this work, protein aggregation and phase separation were assessed by turbidimetry measurements but no structural characterisation of the

supramolecular structures formed under the different physicochemical conditions of the medium tested was performed.

Our research group had further extended these interaction studies using a multiscale approach from molecular to microscopic level. The mechanism of cross-assembly between oppositely charged proteins was investigated using various mixtures of globular proteins derived from milk or egg white (Table 3). We thus studied in depth the process of interaction–assembly between α-La from bovine milk and egg-white LYS. The use of the α-La in its two conformational forms holo (with calcium) and apo (without calcium) aimed to clarify the role of protein conformation in the assembly process. At the molecular level, LYS interacts with holo and apo forms of α-La at pH 7.5 to form oligomeric structures with a dissociation constant in the micromolar range in both cases [135]. The affinity constant between the two proteins decreases with increasing ionic strength, reflecting the involvement of electrostatic interactions. However, only the apo α-La/LYS mixture spontaneously assembles into supramolecular objects, leading to liquid–liquid phase separation.

In the case of the α-La–LYS system, the cross-assembly mechanism between these two proteins is controlled by both (a) the conformation of α-La and (b) the molecular interaction with LYS, leading to the formation of oligomers of specific conformations [135]. Characterisation of interactions at the molecular level was further performed to understand the driving forces behind such protein assembly. The early steps of assembly were characterised through the identification of the amino acid involved in the interacting surfaces of the proteins. This was monitored by NMR chemical shift perturbations by titrating one ^{15}N-labelled protein with its unlabelled partner [136]. These authors showed that α-La has a narrow interaction site on the formed heterodimers, whereas LYS exhibited interaction sites scattered on a broader surface. Further assembly into tetramers requires additional interaction sites between apo α-La–LYS heterodimers. The absence of bound calcium on apo α-La exposes another negatively charged patch on the protein surface, which gives a second site for interacting with LYS. Within the formed tetramers, most of the electrostatic charge patches on the protein surface are shielded, enhancing the contribution of the hydrophobic patches on the tetramer surface for further assemblies. Again, the increased flexibility of apo α-La compared to holo α-La favourably exposes some hydrophobic residues on the surface of tetramer. Then, hydrophobic interactions are assumed to contribute to subsequent assembly throughout the formation of larger oligomers of LYS and apo α-La. These experimental results agree and match well with Monte Carlo simulations that show preferential alignment between proteins resulting from the strength of their dipole moments [136].

Interestingly, the morphology of cross-assembled objects between apo α-La and LYS was found to be temperature dependent: polydisperse amorphous aggregates are obtained by mixing the two proteins at a temperature below 25°C compared with well-ordered spherical particles when the mixing is carried out above 30°C [3]. It is well-established that the apo form of α-La changes its conformation above 27°C from “native-like” to a “molten globule” conformation that is more flexible.

Thus, the 3D structure of apo α-La directs the nature of the supramolecular structures resulting from its assembly with LYS. Hence, as already underlined by Chiti and Dobson [79], subsequent self-assembly of proteins is highly promoted by conformational change and/or formation of small oligomers. Behind these structural considerations, the nature of some other constituents such as small ions is quite important. Theoretical approaches confirm the main role of molecular structure as well as of the surrounding environment. To predict the morphology of cross-assembled particles at a given thermodynamic condition, explicit access to the effective interactions between the macromolecules and the surrounding solutes is of crucial importance. Several studies indicate that this can be reached by the coarse-grained Monte Carlo approach that provides such access through a judicious choice of the interaction parameters [137].

Recent kinetic investigations showed that the temperature, in the range 20–45°C, affects only the structural re-organisation of the formed final supramolecular structures. Whatever the temperature, small homogeneous aggregates form rapidly when the two proteins are mixed that subsequently grow by collision and fusion, as evidenced by dynamic and static light scattering [138]. However, the amorphous aggregates formed at 25°C are rapidly converted to well-defined microspheres once the temperature is increased above 30°C [138].

Working on this protein system, we demonstrated for the first time the possibility of spontaneous formation of microspheres between two oppositely charged proteins, under conditions of charge compensation. The final size of formed spheres seems to be highly dependent on the initial protein concentration. Microspheres of about 3–5 μm are classically obtained starting with a total protein concentration around 0.2–0.5 mM. Decreasing the initial total protein concentration to 0.02 mM leads to the formation of nanospheres with a diameter of about 100–200 nm. Hence, the particle size is directly correlated to the initial protein concentration. Quantification of proteins in formed microspheres shows a perfect stoichiometry with α-La: LYS molar ratio of 1, and the two proteins exhibited a perfect spatial co-localisation in the microspheres [134]. Moreover, the effect of ionic strength on both the formation and the stability of the microspheres has been described [12]. An ionic strength above 100 mM completely inhibits the assembly between the two proteins. However, once formed, a higher salt concentration is needed to dissociate the microspheres. In this sense, the divalent ions (calcium, magnesium) are more effective than monovalent ions in the disassembly of the microspheres. Starting from these published experimental results, Persson and Lund [139] conducted a pioneering theoretical study on the self-assembly between these two proteins using Monte Carlo simulations. For such a simulation study, the two proteins, counterions and salt particles are immersed in a spherical simulation cell containing a continuum solvent described by the dielectric constant of water (Fig. 6). The authors suggest that the highly uneven charge distribution on α-La is responsible for the formation of strongly ordered heterodimers that facilitate the formation of structured mesoscopic aggregates through electrostatic steering [139]. The process is described as similar to the interaction between an ion and a dipole; LYS has a clear preference for interaction to the negative end of α-La, which coincides with

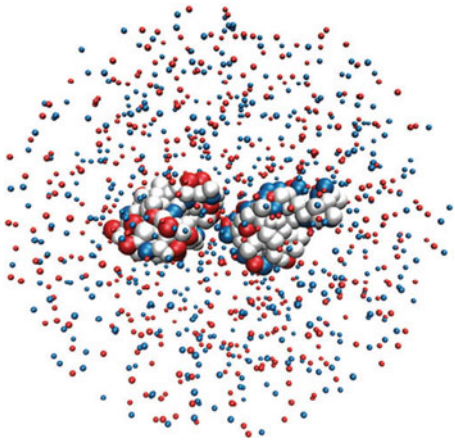

Fig. 6 Illustration of the model used for simulating two proteins in a salt solution. The solvent is treated as a dielectric continuum while salt particles and proteins are described as (clusters of) hard, charged spheres. For clarity, the salt size has been reduced [reproduced with permission from Persson and Lund [139] © (2009) from RSC]

the negative pole of the molecular dipole moment. The authors evaluated the free energy of interaction minima at around $-9\ kT$ (where k is the Boltzmann constant and T the temperature) at low ionic strength and neutral pH. When apo α-La binds calcium, the dipole moment decreases significantly from 400 to 330 D. Such a decrease, in combination with a screening of negative charges by calcium and the reduction in α-La flexibility, could explain the absence of oligomerisation subsequent to the protein cross-assembly observed experimentally. According to the developed model, the presence of calcium on α-La reduces the orientation with positively charged LYS. This would explain the experimentally observed absence of supramolecular structures between LYS and holo form of α-La. The model also simulates the effectiveness of divalent ions in destabilising the supramolecular structures in agreement with experimental finding. These data underline the crucial role of protein charge anisotropy for orientational assembly, as also described for other systems such as protein/cationic polyelectrolyte coacervation [140]. In that work, a clear relationship between protein charge anisotropy (BSA versus β-Lg), binding affinity to polyelectrolyte and selective coacervation was found experimentally and using computer modelling.

The formation of the original microspheres in dual protein systems was investigated by mixing various proteins in a pH range where the two proteins carry opposite net charge. The work carried out has shown that it is possible to generate spherical structures in other binary protein mixtures, providing the experimental conditions were adapted [5]. Microspheres are obtained at low ionic strength in dual systems such as Ova/LYS, BSA/LYS and Ova/avidin. In the case of Ova/LYS, spherical particles were formed between pH 7.4 and pH 8.6 with an optimum cross-assembly yield at pH 8. The formed microspheres contained twofold excess of LYS, i.e. the protein molar ratio LYS:Ova was 2. When Ova is mixed with avidin, microspheres with an equimolar ratio of the two proteins are obtained in the pH range between 6.4 and 8. In addition, the total protein needed to form Ova/avidin microspheres is then fold lower than that required to detect Ova/LYS

microspheres. For BSA/LYS mixture, microspheres are obtained between pH 7.4 and 9.2, with an optimal yield of cross-assembly at pH 8.9. The formed microspheres contained 3 mol of LYS per mole of BSA. According to the considered dual protein mixtures, well-defined microspheres are observed for a narrow pH window. Far from this window, either amorphous aggregates or no cross-assembly are detected, according to the system. Comparing the conditions of formation of the microspheres in the three binary systems reveals the following three similarities:

1. Existence of a pH value for maximum efficiency of cross-assembly
2. High sensitivity to the ionic strength, no assembly was detected above an ionic strength of 30 mM
3. Microspheres are gently obtained at 25°C, a temperature significantly lower than that required to form apo α-La/LYS microspheres, i.e. above 30°C [3]

The three dual systems also reveal some specificities with differences in:

1. The total protein concentration required to observe microspheres
2. The optimum pH for microsphere formation
3. The final stoichiometry in the formed microspheres

Whatever the considered binary system, a phenomenon of protein surface charge compensation seems to prevail in the mechanism that governs microsphere formation. This is consistent with the complexation theory between biopolymers involving short- and long-range interactions [102]. However, this theory does not completely explain the dual protein dependency of the final stoichiometry found in microspheres. Fine examination of protein stoichiometries in various binary systems shows that protein charge compensation by itself is necessary but not sufficient. The results we obtained recently suggest that the difference in the surface area available for interaction between two proteins is also an essential parameter that could explain the change in the final stoichiometry. For each protein, this interacting surface is assumed to be proportional to the molecular weight or size of the protein. Perfect charge compensation is expected with a molar ratio of one between two proteins of similar size, e.g. apo α-La/LYS or Ova/avidin. This is exactly what is seen experimentally. The sizes of Ova and BSA are respectively two and three times higher than that of LYS. This would explain the molar ratios of 2 and 3 observed in the microspheres obtained with Ova/LYS and BSA/LYS, respectively [5]. These results are in agreement with those reported for microspheres formed between gold nanoparticles (grafted with positive charges) and negatively charged proteins of different sizes [124]. When the nanoparticles are larger than the protein, several protein molecules assemble with one gold nanoparticle and the inverse is true in the case where the proteins are larger than the gold nanoparticles. In the case where the dimensions of the nanoparticle and protein are in the same order of magnitude, extended aggregates are observed [124]. Thus, the stoichiometry found in microspheres of cross-assembled proteins depends, among other considerations, on the extent of the relative size difference between mixed proteins. Consequently, as well as charge compensation, size compensation is a key parameter that guides protein assembly and their stoichiometry in microspheres in dual systems.

As shown throughout these results on dual protein systems, the experimental conditions for optimum cross-assembly are specific for each system because of the required charge and size compensation. This could explain the earlier results reported in 1990 that showed that Lf interacts and forms complexes with β-Lg and BSA but not with α-La [141]. A specific optimum pH value favouring Lf/α-La cross-assembly was probably missing in this work. We have recently confirmed this assumption by showing that, once the conditions are optimised, LF interacts with α-La as well as with β-Lg, as revealed by isothermal titration calorimetry experiments (unpublished data). Indeed, we also observed self-assemblies into microspheres of β-Lg/LF, α-La/LF and β-Lg/LYS binary mixtures at specific, system-dependent pH values (unpublished data).

The visualisation of protein microspheres by confocal microscopy showed that, for all the dual systems described above, the two proteins are perfectly co-localised in the three dimensions of the microsphere [5, 134]. This is probably related to the fact that the building blocks initiating the cross-assembly are hetero-oligomers (dimers, trimers, tetramers) formed by the two proteins involved, as shown experimentally in the case of apo α-La/LYS [135, 136].

Kinetically speaking, even if the reaction of spontaneous interaction–assembly between proteins is very fast, experimental evidence shows that microspheres are not formed immediately after mixing the two proteins [142]. At a given total protein concentration, the organisation into microspheres is a dynamic, kinetically controlled process. This is well illustrated by the work conducted by our group on α-La and LYS using confocal microscopy [142]. As shown in Fig. 7, branched aggregates or "clusters of nanospheres" are formed rapidly after protein mixing. Then, the clusters of nanospheres progressively re-organize into well-defined spherical particles of a few micrometres when protein concentration is in the sub-millimolar range. In these experimental conditions, the process takes about 20 min to reach the final particle organisation.

The formation of spherical structures in mixtures of oppositely charged globular proteins seems to be a generic process. Beyond the binary systems, we have shown that it is also possible to form microspheres by mixing three different proteins, provided the mixing is performed in suitable proportions. This is the case, for example, for a mixture containing negatively charged Ova and positively charged avidin and LYS. This offers the possibility to design these new supramolecular structures in complex protein mixtures. Interestingly, Sugimoto et al. [143] were able to form amyloid-like fibrils in dual globular protein system including native LYS and pre-denatured Ova. The fibrils were obtained at pH 7.5 with an initial molar ratio LYS:Ova of 3. However, the exact stoichiometry recovered in the formed fibrils was not indicated. This would be of interest for comparison with the protein stoichiometry of 2 recovered in the LYS/Ova microspheres (see above). Furthermore, the authors identified the exact peptidic sequence of Ova that interacts with LYS. The self-assembly of various macromolecules such as proteins in structures with very specific geometries requires the development of highly specific interactions combining kinetic and thermodynamic aspects. Different models exist that describe the laws of oriented molecular assembly between various

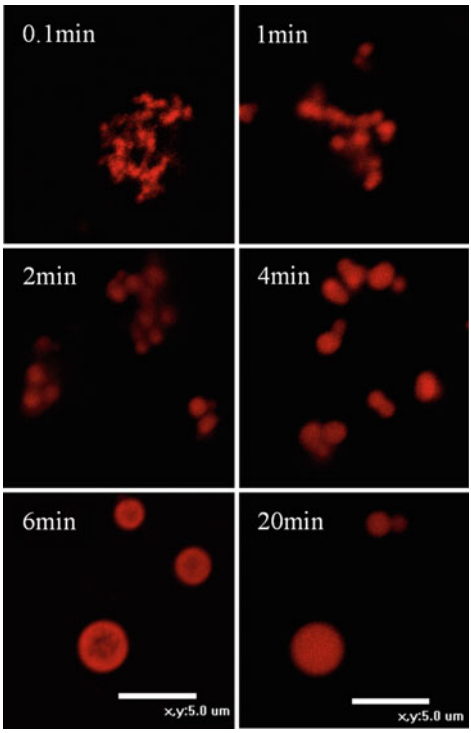

Fig. 7 Dynamics of apo α-lactalbumin/lysozyme cross-assembly. Re-organisation of the supramolecular structures over time, as assessed by confocal scanning laser microscopy. Solution of apo α-lactalbumin (0.2 mM) was mixed with lysozyme (0.2 mM) and aliquots were taken at various times: (**a**) 0.1 min, (**b**) 1 min, (**c**) 2 min, (**d**) 4 min, (**e**) 6 min and (**f**) 20 min. For visualisation, one of the two proteins were labelled by a fluorescent probe. Scale bars 5 μm [reproduced with permission from Nigen et al. [142] © (2010) from Elsevier]

macromolecules from basic blocks. At the thermodynamic level, assembly into structures with spherical shape is advantageous because the process is controlled by the surface tension at the interface between the solution and the condensed phase. Sphere formation leads to surface energy gain throughout the minimisation of the overall surface of the particles [144].

5 Conclusion

The application of fundamental physicochemical concepts for rational design of functional assemblies from food materials constitute, first, a response to the growing trend toward the development of new and innovative food products and, second, an opportunity to generate new structures with new applications. Food proteins are particularly interesting substrates because they are biocompatible and biodegradable. They can be manipulated to create either irreversible or, more recently, reversible supramolecular assemblies. Irreversible supramolecular structures, involving covalent bonds, are induced throughout processing (i.e. energy input), which mimes the industrial practices such as heat treatment, high shear, high pressure, chemical and enzymatic cross-linking or degradation, etc. Stable dispersions of self-assembled

proteins with a variety of structures can be formed by heating aqueous solutions of food proteins. The design of specific supramolecular structures may enable several new functions in food science. For instance, supramolecular structures could encapsulate and protect bioactive ingredients during processing and/or passage through the gut and, at the same time, allow desired mouth feeling. Concerning the latter property, controlling the shape and size of constitutive particles is important for several reasons, one of which is the desired viscosity. The viscosity of solutions containing linear assembly of proteins increases with the length and rigidity of the fibrils. If a viscous aspect is required, linear protein assembly can result in the desired texture even at low protein concentrations. In contrast, if an absence of viscosity is required, even for high protein content, the design of spherical particles is required. The size of the spherical particles has to be controlled because a coarse mouth feeling texture appears for particles of several tenths of micrometres. For instance, in the case of whey proteins, diversely sized structures ranging from rigid rods to homogeneous spheres and branched flexible strands can be created (for more details, see the review by Nicolai et al. [145]). This is because whey proteins undergo denaturation (via processing) and the denatured forms re-assemble to covalently linked larger structures like fibrils, spheres or aggregates, which in turn can be assembled to form gel networks (e.g. yogurt).

During the last few years, there has been an increasing interest in designing new and efficient food vehicles for encapsulation and protection of sensitive substances and for their targeted oral delivery. This involves a good control of the formation of such vehicles, their stability and the conditions of their disassembly. Spontaneous assembly of food proteins into microspheres, micelles or nanotubes are good candidates for such applications. Similarly, taking advantage of their availability, low cost and natural and safe origin, food proteins have been proposed as drug nanocarriers for oral delivery [133, 146]. However, prior to these applications, some challenges still need to be met including: (a) understanding the physicochemical forces governing the kinetics and dynamics of the self-assembly processes. We need to investigate not only protein–protein interactions and self-assembly but also various molecular interactions between protein molecules and the solute to be protected; (b) the stability of formed objects toward processing (concentration, lyophilisation, presence of other components inside food matrix) and storage; and (c) physicochemical (physiological) conditions of their disassembly, which is essential for the drug-releasing step. Although the challenge is great, the knowledge accumulated on the self-assembly and structure of chemical polyelectrolytes and polyelectrolytes–biomolecules in the field of medical, pharmaceutical and electronics etc. could help to move rapidly towards these new applications.

Acknowledgements Many thanks to our collaborators: M. Nigen, D. Salvatore, P. Hamon and M.N. Madec. Part of the work performed in our laboratory was supported by INRA and by the French National Research Agency (Agence Nationale de la Recherche, grant ANR-07-PNRA-010, project LACLYS).

References

1. Graveland-Bikker JF, Ipsen R, Otte J et al (2004) Influence of calcium on the self-assembly of partially hydrolyzed α-lactalbumin. Langmuir 20:6841–6846
2. Graveland-Bikker JF, de Kruifs CG (2006) Unique milk protein based nanotubes: food and nanotechnology meet. Trends Food Sci Technol 17:196–203
3. Nigen M, Croguennec T, Renard D et al (2007) Temperature affects the supramolecular structures resulting from alpha-lactalbumin-lysozyme interaction. Biochemistry 46:1248–1255
4. Ipsen R, Otte J (2007) Self-assembly of partially hydrolysed alpha-lactalbumin. Biotechnol Adv 25:602–605
5. Desfougères Y, Croguennec T, Lechevalier V et al (2010) Charge and size drive spontaneous self-assembly of oppositely charged globular proteins into microspheres. J Phys Chem 114:4138–4144
6. Zhang S (2003) Fabrication of novel biomaterials through molecular self-assembly. Nat Biotechnol 21(10):1171–1178
7. Donald AM (2008) Aggregation in β-lactoglobulin. Soft Matter 4:1147–1150
8. Krebs MRH, Domike KR, Cannon D et al (2008) Common motif in protein self-assembly. Faraday Discuss 139:265–274
9. Dickinson E, Semenova MG, Belyakova LE et al (2001) Analysis of light scattering data on the calcium ion sensitivity of caseinate solution thermodynamics: relationship to emulsion flocculation. J Colloid Interface Sci 239(1):87–97
10. Unterhaslberger G, Schmitt C, Sanchez C et al (2006) Heat denaturation and aggregation of beta-lacto globulin enriched WPI in the presence of arginine HCl, NaCl and guanidinium HCl at pH 4.0 and 7.0. Food Hydrocolloid 20:1006–1019
11. Yang F Jr, Zhang M, Zhou BR et al (2006) Oleic acid inhibits amyloid formation of the intermediate of alpha-lactalbumin at moderately acidic pH. J Mol Biol 362:821–834
12. Nigen M, Croguennec T, Bouhallab S (2009) Formation and stability of alpha-lactalbumin-lysozyme spherical particles: involvement of electrostatic forces. Food Hydrocolloid 23:510–518
13. Thorn DC, Meehan S, Sunde M et al (2005) Amyloid fibril formation by bovine milk k-casein and its inhibition by the molecular chaperones αs- and β-casein. Biochemistry 44:17027–17036
14. Léonil J, Henry G, Jouanneau D et al (2008) Kinetics of fibril formation of bovine κ-casein indicate a conformational rearrangement as a critical step in the process. J Mol Biol 381:1267–1280
15. Schmitt C, Bovay C, Vuilliomenet A-M et al (2011) Influence of protein and mineral composition on the formation of whey protein heat-induced microgels. Food Hydrocolloid 25:558–567
16. Keskin O, Gursoy A, Ma B (2008) Principles of protein-protein interactions: what are the preferred ways for proteins to interact? Chem Rev 108(4):1225–1244
17. Min Y, Akbulut M, Kristiansen K et al (2008) The role of interparticle and external forces in nanoparticle assembly. Nat Mater 7:527–538
18. Krebs MRH, Wilkins DK, Chung EW et al (2000) Formation and seeding of amyloid fibrils from wild-type hen lysozyme and a peptide fragment from the β-domain. J Mol Biol 300:541–549
19. Gosal WS, Clark AH, Pudney (2002) Novel amyloid fibrillar networks derived from a globular protein: β-lactoglobulin. Langmuir 18:7174–7181
20. Gosal WS, Clark AH, Ross-Murphy SB (2004) Fibrillar β-lactoglobulin gels: part 1: fibril formation and structure. Biomacromolecules 5:2408–2419
21. Rasmussen P, Barbiroli A, Bonomi et al (2007) Formation of structured polymers upon controlled denaturation of β-lactoglobulin with different chaotropes. Biopolymers 86:57–72
22. Akkermans C, van der Goot AJ, Venema P et al (2007) Micrometer-sized fibrillar protein aggregates from soy glycinin and soy protein isolate. J Agric Food Chem 55:9877–9882

23. Lara C, Adamcik J, Jordens S et al (2011) General self-assembly mechanism converting hydrolyzed globular proteins into giant multistranded amyloid ribbons. Biomacromolecules 12:1868–1875
24. Gummel J, Cousin F, Boué F (2007) Counterions release from electrostatic complexes of polyelectrolytes and proteins of opposite charge: a direct measurement. J Am Chem Soc 129:5806–5807
25. Semenova MG (2007) Thermodynamic analysis of the impact of molecular interactions on the functionality of food biopolymers in solution and in colloidal systems. Food Hydrocolloid 21:23–45
26. Viney C (2004) Self-assembly as a route to fibrous materials: concepts, opportunities and challenges. Curr Opin Solid State Mater Sci 8:95–101
27. Velikov KP, Pelan E (2008) Colloidal delivery systems for micronutrients and nutraceuticals. Soft Matter 4:1964–1980
28. Gummel J, Boué F, Clemens D et al (2008) Finite size and inner structure controlled by electrostatic screening in globular complexes of proteins and polyelectrolytes. Soft Matter 4(8):1653–1664
29. Doubliez JL, Garnier C, Renard D et al (2000) Protein-polysaccharide interactions. Curr Opin Colloid Interface Sci 5:202–214
30. de Kruif CG, Weinbreck F, de Vries R (2004) Complex coacervation of proteins and anionic polysaccharides. Curr Opin Colloid Interface Sci 9:340–349
31. Cooper CL, Dubin PL, Kayitmazer AB et al (2005) Polyelectrolyte-protein complexes. Curr Opin Colloid Interface Sci 10:52–78
32. de Vries R, Cohen Stuart M (2006) Theory and simulations of macroion complexation. Curr Opin Colloid Interface Sci 11:295–301
33. Hales K, Pochan DJ (2006) Using polyelectrolyte block copolymers to tune nanostructure assembly. Curr Opin Colloid Interface Sci 11:330–336
34. Turgeon SL, Schmitt C, Sanchez C (2007) Protein-polysaccharide complexes and coacervates. Curr Opin Colloid Interface Sci 12(4–5):166–178
35. Jones GO, McClements DJ (2010) Functional biopolymer particles: design, fabrication, and application. Compr Rev Food Sci Food Safety 9:374–397
36. Brownlow S, Cabral JHM, Cooper R et al (1997) Bovine β-lactoglobulin at 1.8 Angstrom resolution – still an enigmatic lipocalin. Structure 5(4):481–495
37. Sawyer L, Kontopidis G (2000) The core lipocalin, bovine β-lactoglobulin. Biochem Biophys Acta 1482:136–148
38. Kontopidis G, Holt G, Sawyer L (2002) The ligand-binding site of bovine β-lactoglobulin: evidence for a function? J Mol Biol 318(4):1043–1055
39. Papiz MZ, Sawyer L, Eliopoulos EE et al (1986) The structure of beta-lactoglobulin and its similarity to plasma retinol-binding protein. Nature 324:383–385
40. Kitabatake N, Wada R, Fujita Y (2001) Reversible conformational change in beta-lactoglobulin modified with N-ethylmaleimide and resistance to molecular aggregation on heating. J Agric Food Chem 49:4011–4018
41. Jayat D, Gaudin JC, Chobert JM et al (2004) A recombinant C121S mutant of bovine β-lactoglobulin is more susceptible to peptic digestion and to denaturation by reducing agent and heating. Biochemistry 43:6312–6321
42. Qi XL, Holt C, Mcnulty D et al (1997) Effect of temperature on the secondary structure of beta-lactoglobulin at pH 6.7, As determined by CD and IR spectroscopy: a test of the molten globule hypothesis. Biochem J 324:341–346
43. Mattison KW, Dubin PL, Brittain IJ (1998) Complex formation between bovine serum albumin and strong polyelectrolytes: effect of polymer charge density. J Phys Chem B 102:3830–3836
44. Brew K, Vanaman TC, Hill RL (1967) Comparison of the amino acid sequence of bovine α-lactalbumin and hen egg white lysozyme. J Biol Chem 242:3747–3748

45. Hendrix T, Griko YV, Privalov PL (2000) A calorimetric study of the influence of calcium on the stability of bovine α lactalbumin. Biophys Chem 84:27–34
46. Hiraoka Y, Secawa T, Kuwajima K et al (1980) α-Lactalbumin: a metalloprotein. Biochem Biophys Res Commun 95(3):1098–1104
47. Bernal V, Jelen P (1984) Effect of calcium binding on thermal denaturation of bovine α-lactalbumin. J Dairy Sci 67:2452–2454
48. DeWit JN, Klarenbeek G (1984) Effects of various heat treatments on structure and solubility of whey proteins. J Dairy Sci 67:2701–2710
49. Griko YV, Remeta DP (1999) Energetics of solvent and ligand induced conformational changes in α-lactalbumin. Protein Sci 8(3):554–561
50. Warner RC (1954) In: Neurath H, Bailey K (eds) The proteins, vol 2. Academic, New York, p 443
51. Li Chan E, Nakai S (1989) Biochemical basis for the properties of egg white. Crit Rev Poult Biol 2:21–57
52. Narita K, Ishii J (1962) N terminal sequence in ovalbumin. J Biochem (Tokyo) 52:367–373
53. Nisbet AD, Saundry RH, Moir AJ et al (1981) The complete amino acid sequence of hen ovalbumin. Eur J Biochem 115:335–345
54. Stein PE, Leslie AG, Finch JT et al (1990) Crystal structure of ovalbumin as a model for the reactive centre of serpins. Nature 347:99–102
55. Stein PE, Leslie AG, Finch JT et al (1991) Crystal structure of uncleaved ovalbumin at 1.95 Å resolution. J Mol Biol 221:941–959
56. Matsumoto T, Chiba J, Inoue H (1992) Effect of pH on colloidal properties of native ovalbumin aqueous systems. Colloid Polym Sci 270:687–693
57. Farrel HM Jr, Qi PX, Uversky VN (2006) New views of protein structure: applications to the caseins: protein structure and functionality. In: Fishman ML, Qi PX, Wisker L (eds) Advances in biopolymers: molecules, clusters, networks, and interactions. American Chemical Society, Washington, DC, pp 52–70
58. Holt C, Sawyer L (1993) Caseins as rheomorphic proteins: interpretation of the primary and secondary structures of the α_{S1}, β and κ-caseins. J Chem Soc Faraday Trans 89:2683–2692
59. Fox PF, Brodkorb A (2008) The casein micelle: historical aspects, current concepts and significance. Int Dairy J 18:677–684
60. Moore SA, Anderson BF, Groom CR et al (1997) Three-dimensional structure of diferric bovine lactoferrin at 2.8 Å resolution. J Mol Biol 274(2):222–236
61. Baker EN (1994) Structure and reactivity of transferrins. Adv Inorg Chem 41:389–463
62. Baker EN, Baker HM (2009) A structural framework for understanding the multifunctional character of lactoferrin. Biochimie 91(1):3–10
63. Spik G, Coddeville B, Mazurier J et al (1994) Primary and three-dimensional structure of lactotransferrin (lactoferrin) glycans. Adv Exp Med Biol 357:21–32
64. Antonini G, Rossi P, Pitari G et al (2000) Role of glycan in bovine lactoferrin. In: Shimakaki K, Tsuda H, Tomita M, Kuwata T, Perraudin JP (eds) Lactoferrin: structure, function and applications. Elsevier Science, Amsterdam, pp 3–16
65. Rossi P, Giansanti F, Boffi A et al (2002) Ca^{2+} Binding to bovine lactoferrin enhances protein stability and influences the release of bacterial lipopolysaccharide. Biochem Cell Biol 80:41–48
66. Chaufer B, Rabiller-Baudry M, Lucas D et al (2000) Selective extraction of lysozyme from a mixture with lactoferrin by ultrafiltration. Role of the physico-chemical environment. Lait 80:197–203
67. Mela I, Aumaitre E, Williamson A-M et al (2010) Charge reversal by salt-induced aggregation in aqueous lactoferrin solutions. Colloids Surf B 78(1):53–60
68. Wang J, Dauter M, Alkire H (2007) Triclinic lysozyme at 0.65 Å resolution. Acta Cristallogr D 63(12):1254–1268
69. Canfield RE, Liu AK (1965) The disulfide bonds of egg white lysozyme (muramidase). J Biol Chem 240:1997–2002

70. Stradner A, Sedgwick H, Cardinaux F et al (2004) Equilibrium cluster formation in concentrated protein solutions and colloids. Nature 432(7016):492–495
71. Liu Y, Porcar L, Chen J (2011) Lyzosyme protein solution with an intermediate range order structure. J Phys Chem B 115(22):7238–7247
72. Stradner A, Cardinaux F, Schurtenberger P et al (2006) A small angle scattering study on equilibrium clusters in lysozyme solution. J Phys Chem B 110(42):21222–21231
73. Bolder SG, Hendrickx H, Sagis LMC et al (2006) Fibril assemblies in aqueous whey protein mixtures. J Agric Food Chem 54:4229–4234
74. Krebs MRH, Domike KR, Donald AM (2009) Protein aggregation: more than just fibrils. Biochem Soc Trans 37(9):682–686
75. Schmitt C, Bovay C, Vuilliomenet A-M et al (2009) Multiscale characterization of individualized β-lactoglobulin microgels formed upon heat treatment under narrow pH range conditions. Langmuir 25:7899–7909
76. Trexler AJ, Nilsoon MR (2007) The formation of amyloid fibrils from proteins in the lysozyme family. Curr Protein Pept Sci 8:537–557
77. Lomakin A, Chung DS, Benedek GB et al (1996) On the nucleation and growth of amyloid α-protein fibrils: detection of nuclei and quantitation of rate constants. Proc Natl Acad Sci USA 93:1125–1129
78. Lomakin A, Teplow DB, Kirschner DA et al (1997) Kinetic theory of fibrillogenesis of amyloid b-protein. Proc Natl Acad Sci USA 94:7942–7947
79. Chiti F, Dobson CM (2006) Protein misfolding, functional amyloid, and human disease. Annu Rev Biochem 75:333–366
80. Pellarin R, Guarnera E, Caflisch A (2007) Pathways and intermediates of amyloid fibril formation. J Mol Biol 374:917–924
81. Arnaudov LN, de Vries R (2007) Theoretical modeling of the kinetics of fibrilar aggregation of bovine beta-lactoglobulin at pH 2. J Chem Phys 126:145106
82. Bolder SG, Sagis LMC, Venema P et al (2007) Effect of Stirling and seeding on whey proteína fibril formation. J Agric Food Chem 55:5661–5669
83. Loveday SM, Wang XL, Rao MA et al (2012) β-Lactoglobulin nanofibrils: effect of temperature on fibril formation kinetics, fibril morphology and the rheological properties of fibril dispersions. Food Hydrocolloid 27:242–249
84. Farrell H, Cooke P, Wickham E et al (2003) Environmental influences on bovine κ-casein: reduction and conversion to fibrillar (amyloid) structures. J Protein Chem 22:259–273
85. Akkermans C, Venema P, van der Goot AJ et al (2008) Peptides are building blocks of heat-induced fibrillar proteins aggregates of β-Lg formed at pH 2. Biomacromolecules 9:1474–1479
86. Kroes-Nijboer A, Venema P, Bouman J et al (2011) Influence of protein hydrolysis on the growth kinetics of β-Lg fibrils. Langmuir 27:5753–5761
87. Hamada D, Tanaka T, Tartaglia GG et al (2009) Competition between folding, native-state dimerisation and amyloid aggregation in β-lactoglobulin. J Mol Biol 386:878–890
88. Arnaudov LN, de Vries R, Ippel H et al (2003) Multiple steps during the formation of beta-lactoglobulin fibrils. Macromolecules 4:1614–1622
89. Arnaudov LN, de Vries R (2006) Strong impact of ionic strength on the kinetics of fibrilar aggregation of β-lactoglobulin. Biomacromolecules 7:3490–3498
90. Bromley EHC, Krebs MRH, Donald AM (2005) Aggregation across the length scales in β-lactoglobulin. Faraday Discuss 128:13–27
91. Krebs MRH, Bromley EHC, Rogers SS et al (2005) The mechanism of amyloid spherulite formation by bovine insulin. Biophys J 88:2013–2021
92. Domike KR, Hardin E, Armstead DN et al (2009) Investigating the inner structure of irregular β-lactoglobulin spherulites. Eur Phys J E 29:173–182
93. Rogers SS, Krebs MRH, Bromley EHC, van der Linden E, Donald AM (2006) Optical microscopy of growing insulin amyloid spherulites on surfaces in vitro. Biophys J 90:1043–1054

94. Domike KR, Donald AM (2007) Thermal dependence of thermally induced protein spherulite formation and growth: kinetics of β-lactoglobulin and insulin. Biomacromolecules 8:3930–3937
95. Bromley E, Krebs M, Donald A (2006) Mechanisms of structure formation in particulate gels of β-lactoglobulin formed near the isoelectric point. Soft Matter 21:145–152
96. Krebs MRH, Devlin GL, Donald AM (2007) Protein particulates: another generic form of protein aggregation? Biophys J 92:1336–1342
97. Bengoechea C, Peinado I, McClements DJ (2011) Formation of nanoparticles by controlled heat treatment of lactoferrin: factors affecting particles characteristics. Food Hydrocolloid 25:1354–1360
98. Baussay K, Le Bon C, Nicolai T et al (2004) Influence of ionic strength on the heat-induced aggregation of the globular protein β-lactoglobulin at pH 7.0. Int J Biol Macromol 34:21–28
99. Pouzot M, Nicolai T, Visschers RW et al (2005) X-ray and light scattering study of the structure of large protein aggregates at neutral pH. Food Hydrocolloid 19:231–238
100. Donato L, Schmitt C, Bovetto L et al (2009) Mechanism of formation of stable heat-induced β-lactoglobulin microgels. Int Dairy J 19:295–306
101. Le Bon C, Nicolaï T, Durand D (1999) Growth and structure of aggregates of heat-denatured β-lactoglobulin. Int J Food Sci Technol 34:451–465
102. Mossa S, Sciortino F, Tartaglia P et al (2004) Ground-state clusters for short-range attractive and lon-range repulsive potentials. Langmuir 20:10756–10763
103. Sun XS, Wang D, Zhang L et al (2008) Morpholgy and phase separation of hydrophobic clusters of soy globular protein polymers. Macromol Biosci 2008:295–303
104. Zuniga RN, Tolkach A, Kulozik U et al (2010) Kinetics of formation and physicochemical characterization of thermally-induced β-lactoglobulin aggregates. J Food Sci 75:E261–E268
105. Yu S, Yao P, Jiang M et al (2006) Nanogels prepared by self-assembly of oppositely charged globular proteins. Biopolymers 83:148–158
106. Hu J, Yu S, Yao P (2007) Stable amphoteric nanogels made of ovalbumin and ovotransferrin via self-assembly. Langmuir 23:6358–6364
107. Pan XY, Yu S, Yao P et al (2007) Self-assembly of β-casein and lysozyme. J Colloid Interface Sci 316:405–412
108. Scanlon S, Aggeli A (2008) Self-assembling peptide nanotubes. Nano Today 3:22–30
109. Ipsen R, Otte J, Qvist KB (2001) Molecular self-assembly of partially hydrolysed α-lactalbumin resulting in strong gels with a novel microstructure. J Dairy Res 68:277–286
110. Ubbink J, Burbidge A, Mezzenga R (2008) Food structure and functionality: a soft matter perspective. Soft Matter 4:1569–1581
111. Jones GO, McClements DJ (2011) Recent progress in biopolymer nanoparticle and microparticle formation by heat-treating electrostatic protein–polysaccharide complexes. Adv Colloid Interfac 67:49–62
112. Schmitt C, Turgeon SL (2011) Protein/polysaccharide complexes and coacervates in food systems. Adv Colloid Interface 167:63–70
113. Voets IK, de Keizer A, Cohen Stuart MA (2009) Complex coacervate core micelles. Adv Colloid Interface 147–148:300–318
114. Becker AL, Henzler K, Welsch N et al (2012) Proteins and polyelectrolytes: a charged relationship. Curr Opin Colloid Interface Sci 17:90–96
115. Sperber BLHM, Cohen Stuart MA, Schols HA et al (2010) Overall charge and local charge density of pectin determines the enthalpic and entropic contributions to complexation with β-lactoglobulin. Biomacromolecules 11:3578–3583
116. Ball V, Winterhalter M, Schwinte P et al (2002) Complexation mechanism of bovine serum albumin and poly(allylamine hydrochloride). J Phys Chem B 106:2357–2364
117. Muthukumar M (1995) Pattern recognition by polyelectrolytes. J Chem Phys 103:4723–4731
118. Romanini D, Braia M, Angarte RG et al (2007) Interaction of lysozyme with negatively charged flexible chain polymers. J Chromatogr B 857:25–31

119. Ivinova ON, Izumrudov VA, Muronetz VI et al (2003) Influence of complexing polyanions on the thermostability of basic proteins. Macromol Biosci 3:210–215
120. Gummel J, Boué F, Deme B et al (2006) Charge stoichiometry inside polyelectrolyte-protein complexes: a direct SANS measurement for the PSSNa-lysozyme system. J Phys Chem B 110:24837–24846
121. Chen YM, Yu CJ, Cheng TL et al (2008) Colorimetric detection of lysozyme based on electrostatic interaction with human serum albumin-modified gold nanoparticles. Langmuir 24:3654–3660
122. Bayraktar H, Srivastava S, You C et al (2008) Controlled nanoparticle assembly through protein conformational changes. Soft Matter 4:629–904
123. Liu Y, Guo R (2007) Interaction between casein and the oppositely charged surfactant. Biomacromolecules 8:2902–2908
124. De M, Miranda OR, Rana S et al (2009) Size and geometry dependent protein–nanoparticle self-assembly. Chem Commun 2009(16):2157–2159
125. Morfin I, Buhler E, Cousin F et al (2011) Rodlike complexes of a polyelectrolyte (hyaluronan) and a protein (lysozyme) observed by SANS. Biomacromolecules 12:859–870
126. Müller M, Ouyang W, Bohata K et al (2010) Nanostructured complexes of polyelectrolytes and charged polypeptides. Adv Eng Mater 12:B519–B528
127. Mengarelli V, Auvray L, Zeghal M (2009) Phase behaviour and structure of stable complexes of oppositely charged polyelectrolytes. Eur Phys Lett 85:58001
128. Matsudomi N, Yamamura Y, Kobayashi K (1987) Agregation between lysozyme and heat-denatured ovalbumin. Agric Biol Chem 51(7):1811–1817
129. Howell N, Yeboah N, Lewis D (1995) Studies on the electrostatic interactions of lysozyme with α-lactalbumin and β-lactoglobulin. Int J Food Sci Technol 30:813–824
130. Biesheuvel PM, Lindhoud S, de Vries R et al (2006) Phase behavior of mixtures of oppositely charged nanoparticles: heterogeneous Poisson-Boltzmann cell model applied to lysozyme and succinylated lysozyme. Langmuir 22:1291–1300
131. Biesheuvel PM, Lindhoud S, Cohen Stuart MA et al (2006) Phase behavior of mixtures of oppositely charged protein nanoparticles at asymmetric charge ratios. Phys Rev E 73(4):041408
132. Anema SG, de Kruif CG (2012) Co-acervates of lactoferrin and caseins. Soft Matter 8(16):4471–4478
133. Tiwari A, Bindal S, Bohidar HB (2009) Kinetics of protein-protein complex coacervation and biphasic release of salbutamol sulfate from coacervate matrix. Biomacromolecules 10:184–189
134. Nigen M, Croguennec T, Madec MN et al (2007) Apo alpha-lactalbumin and lysozyme are colocalized in their subsequently formed spherical supramolecular assembly. FEBS J 274:6085–6093
135. Nigen M, Le Tilly V, Croguennec T et al (2009) Molecular interaction between apo or holo α-lactalbumin and lysozyme: formation of heterodimers as assessed by fluorescence measurements. Biochim Biophys Acta 1794:709–715
136. Salvatore D, Duraffourg N, Favier A et al (2011) Investigation at residue level of the early steps during the assembly of two proteins into supramolecular objects. Biomacromolecules 12(6):2200–2210
137. Shinoda W, DeVane R, Klein ML (2012) Computer simulation studies of self-assembling macromolecules. Curr Opin Struct Biol 22:1–12
138. Salvatore D, Croguennec T, Bouhallab S et al (2011) Kinetics and structure during self-assembly of oppositely charged proteins in aqueous solution. Biomacromolecules 12(5):1920–6192
139. Persson BA, Lund M (2009) Association and electrostatic steering of α-lactalbumin–lysozyme heterodimers. Phys Chem Chem Phys 11:8879–8885
140. Xu Y, Mazzawi M, Chen K et al (2011) Protein purification by polyelectrolyte coacervation: influence of protein charge anisotropy on selectivity. Biomacromolecules 12:1512–1522

141. Lampreave F, Piñeiro A, Brock JH et al (1990) Interaction of bovine lactoferrin with other proteins of milk whey. Int J Biol Macromol 12(1):2–5
142. Nigen M, Gaillard C, Croguennec T et al (2010) Dynamic and supramolecular organisation of α-lactalbumin/lysozyme microspheres: a microscopic study. Biophys Chem 146:30–35
143. Sugimoto Y, Kamada Y, Tokunaga Y et al (2011) Aggregates with lysozyme and ovalbumin show features of amyloid-like fibrils. Biochem Cell Biol 89:533–544
144. Maresov EA, Semenov AN (2008) Mesoglobule morphologies of amphiphilic polymers. Macromolecules 41:9439–9457
145. Nicolai T, Britten M, Schmitt C (2011) β-lactoglobulin aggregates: formation, structure and applications. Food hydrocolloid 25:1945–1962
146. Bachar M, Mandelbaum A, Portnaya I (2012) Development and characterization of a novel drug nanocarrier for oral delivery, based on self-assembled β-casein micelles. J Control Release 160:164–171

Adv Polym Sci (2014) 256: 103–196
DOI: 10.1007/12_2013_218

Published online: 16 May 2013

Polyelectrolyte Complexes of DNA and Polycations as Gene Delivery Vectors

Annabelle Bertin

Abstract This review gives representative examples of the various types of synthetic cationic polymers or polyampholytes (chemical structure, architecture, etc) that can be used to complex DNA (forming polyplexes) for their application in gene delivery. In designing polycations for gene delivery, one has to take into account a balance between protection of DNA versus loss of efficiency for DNA condensation and efficient condensation versus hindering of DNA release. Indeed, if the polyplexes are not stable enough, premature dissociation will occur before delivery of the genetic material at the desired place, resulting in low transfection efficiency; on the other hand, a complex that is too stable will not release the DNA, also resulting in low gene expression. The techniques generally used to determine these properties are gel electrophoresis to test the DNA/polymer complexation, ethidium bromide or polyanion displacement to test the affinity of a polymer for DNA, and light scattering to determine the extent of DNA condensation. Moreover, with the development of more precise instruments for physico-chemical characterization and appropriate biochemical and biophysical techniques, a direct link between the physico-chemical characteristics of the polyplexes and their in vitro and in vivo properties can be drawn, thus allowing tremendous progress in the quest towards application of polyplexes for gene therapy, beyond the research laboratory.

Keywords Colloidal stabilization · DNA · Gene delivery vectors · Polyampholytes · Polycations · Polyelectrolyte complexes · Polyplexes

A. Bertin (✉)
Division 6.5 "Polymers in Life Science and Nanotechnology", Federal Institute for Materials Research and Testing (BAM), Unter den Eichen 87, 12205 Berlin, Germany

Department of Biology, Chemistry, and Pharmacy, Freie Universität Berlin, Takustrasse 3, 14195 Berlin, Germany
e-mail: annabelle.bertin@bam.de

Contents

Abbreviations

AFM	Atomic force microscopy
Arg	Arginine
bp	Base pair
CAC	Critical aggregation concentration
CMC	Critical micelle concentration
CMV	Cytomegalovirus
COS (cells)	CV-1 (simian) cell line carrying the SV40 genetic material
ctDNA	Calf thymus DNA
Da	Dalton, $g.mol^{-1}$
DLS	Dynamic light scattering
DLVO	Derjaguin, Landau, Verwey, and Overbeek theory
DNA	Deoxyribonucleic acid
DP	Degree of polymerization
ds	Double stranded
EGFP	Enhanced green fluorescent protein
EM	Electron microscopy
EtBr	Ethidium bromide
Glu	Glutamic acid
HEK (cells)	Human embryonic kidney cell line
HepG2 (cells)	Human hepatocarcinoma cell line with epithelial morphology
His	Histidine
HIV	Human immunodeficiency virus
IPEC	Interpolylectrolyte complex
LPEI	Linear polyethyleneimine
LS	Light scattering
Luc	Luciferase
Lys	Lysine
MPC	2-Methacryloxyethyl phosphorylcholine

MPS	Mononuclear phagocyte system
NCP	Nucleosome core particle
NMR	Nuclear magnetic resonance
PAMAM	Poly(amido amine)
PCL	Poly(ε-caprolactone)
PDI	Polydispersity index
PDMAEMA	Poly[(2-dimethylamino) ethyl methacrylate]
pDNA	Plasmid DNA
PEC	Polyelectrolyte complex
PEG	Poly(ethylene glycol)
PEI	Polyethyleneimine
PHEMA	Poly(2-hydroxy ethyl methacrylate)
PHPMA	Poly(2-hydroxy propyl methacrylate)
PLL	Poly(L-lysine)
PLLA	Poly(L-lactide)
PMMA	Poly(methyl methacrylate)
PNIPAM	Poly(*N*-isopropyl acrylamide)
PPI	Poly(propylene imine)
PTMAEMA	Poly[(*N*-trimethylammonium) ethyl methacrylate]
PVP	Poly(4-vinylpyridine)
RNA	Ribonucleic acid
SV	Simian virus
TEM	Transmission electron microscopy

1 Introduction

The subject of this review is complexes of DNA with synthetic cationic polymers and their application in gene delivery [1–4]. Linear, graft, and comb polymers (flexible, i.e., non-conjugated polymers) are its focus. This review is not meant to be exhaustive but to give representative examples of the various types (chemical structure, architecture, etc.) of synthetic cationic polymers or polyampholytes that can be used to complex DNA. Other interesting synthetic architectures such dendrimers [5–7], dendritic structures/polymers [8, 9], and hyperbranched polymers [10–12] will not be addressed because there are numerous recent valuable reports about their complexes with DNA. Natural or partially synthetic polymers such as polysaccharides (chitosan [13], dextran [14, 15], etc.) and peptides [16, 17] for DNA complexation or delivery will not be mentioned.

Since the first generation of polycations for cell transfection, such as poly (ethylene imine) (PEI, commercially available as ExGen500 or jetPEI in its linear form or as Lipofectamine, which is hyperbranched PEI incorporated in cationic lipids) [18, 19], poly(L-lysine) (PLL) [20], poly(amido amine) (PAMAM, Starburst) [8], poly(propylene imine) (PPI) [21, 22], and their derivatives, various other architectures and structural motifs have been designed in order to surpass the

efficiency of these commercial products but unfortunately none of them have succeeded [23]. To date, no gene carrier has been approved for use in vivo despite the increasing numbers of clinical trials in this direction worldwide, and therefore research in the field of polycations as non-viral gene delivery vectors is still of prime importance.

It is to be noted that not only water-soluble polymers can be used to complex DNA, amphiphilic polymers, which depending on the relative ratio of hydrophilic to hydrophobic block, can also form various self-assembled structures, from spherical micelles to vesicles (polymersomes). This review will be restricted to micelle-forming polymers and will exclude polymersomes, which can both encapsulate (in their aqueous interior) and complex DNA [24, 25].

Since the early years of DNA complexation with cationic polymers, pioneers from the field of polyelectrolyte complexes between surfactants and/or polymers led solid physico-chemical studies on the complexation of DNA with polymers. But it is only more recently, with the rise of more precise instruments for physico-chemical characterization and appropriate biochemical and biophysical techniques, that the published studies are allowing a direct link to be drawn between physico-chemical characteristics (such as size, charge, etc.) of the DNA/polymer (mostly polycations) complexes, also called polyplexes, and their in vitro and in vivo properties, thus allowing tremendous progresses in the quest towards polyplexes for gene therapy and their application beyond research laboratories.

The Introduction will give a brief description of DNA as a biopolymer (structure, conformations, topologies), some definitions in the field of polyelectrolytes (weak and strong polyelectrolytes), some generalities about DNA/polycation complexes (factors influencing the complexation, models describing the structure of the polyplexes, methods adapted to their characterization), and a description of the parameters to take into consideration for their use in gene therapy.

Then in Sect. 2, the interpolyelectrolyte complexes (IPEC) between polycationic polymers and DNA will be addressed as a function of the chemical structure of the polymer (most of the DNA being used is plasmid DNA, consisting of many thousands of base pairs). Water-soluble and amphiphilic polymers will be discussed and then other properties will be taken into consideration such as the polyelectrolyte's nature (strong or weak), the presence of steric stabilizers, etc. Section 3 will deal with complexes of polyamphoteric polymers with DNA. In both parts, the working line is the correlation between physico-chemical properties and efficiency in vitro (transfection potency).

Finally, we will give some perspectives on the field opened by new polymerization techniques, and consequently new types of polymers, and on recent discoveries about how to interfere with the expression of specific genes with oligonucleotides.

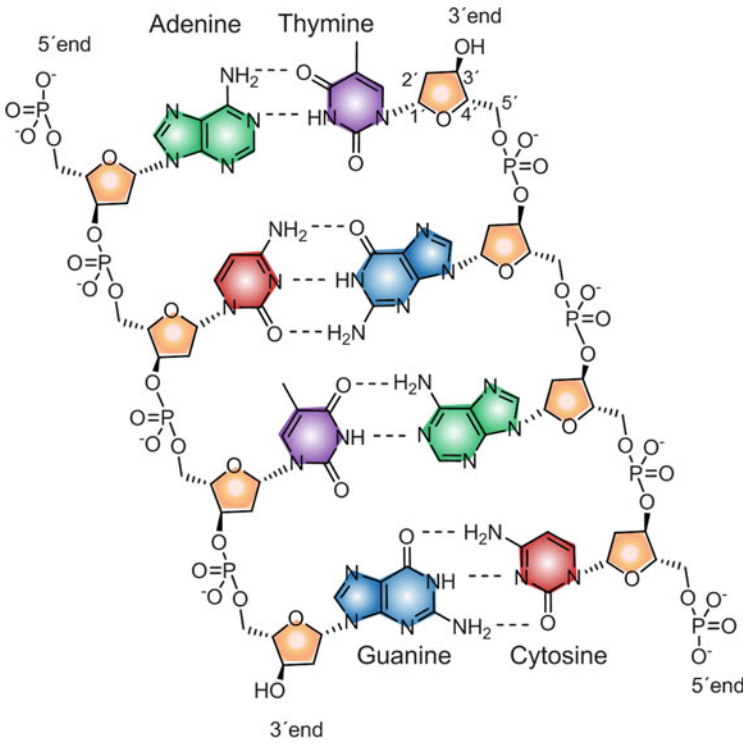

Scheme 1 Chemical structure of DNA

1.1 DNA

1.1.1 Structure of DNA

DNA (deoxyribonucleic acid) is a biopolymer containing the genetic information [26, 27]. Deoxyribonucleotides are the monomers of DNA and are all composed of three parts: a nitrogenous base also called nucleobase, a deoxyribose sugar, and one phosphate group (negatively charged at physiological pH). The nucleobase is always bound to the 1′-carbon of the deoxyribose and the phosphate groups bind to the 5′-carbon of the sugar. There are four different nucleobases: two purines [adenine (A) and guanine (G)], and two pyrimidines [cytosine (C) and thymine (T)]. The deoxyribonucleotides are linked with one another via 3′–5′-phosphodiester bounds.

DNA is composed of two antiparallel complementary strands, which build a double helix. Pairing of the bases, which grant stability to the helix, takes place via hydrogen bonds. The base pairs (bp) are A–T (two bonds) and G–C (three bonds), and constitute the inner side of the double helix (Scheme 1). The backbone of the helix is composed of the sugar-phosphate chain. Another important contribution to the stability of the helix comes from the base stacking of the aromatic rings of the

nucleobases. The length of the strands also plays a role: the longer the strands (i.e., the more nucleobases there are to interact), the more stable is the double helix.

1.1.2 Conformations of DNA

DNA can have different conformations (A-, B-, or Z-DNA), which vary in handedness, number of base pairs per helix turn, and diameter as proved by X-ray diffraction studies [28]. DNA in its native state is a semi-flexible long thin rod, only about 2 nm in diameter (B- and Z-DNA), with a persistence length (mechanical property quantifying the stiffness of a polymer) of about 50 nm [29, 30], which depends on ionic strength [31], DNA sequence [32], and temperature [33].

The conformation of the double helix can be studied using various spectroscopic methods such as circular dichroism (CD) [34], infrared (IR), Raman, ultraviolet (UV), visible absorption spectroscopy, and nuclear magnetic resonance (NMR) spectroscopy [35].

1.1.3 Topologies of DNA

DNA can be chromosomal or extra-chromosomal (plasmid DNA). Plasmid DNA (pDNA) is a double-stranded DNA (dsDNA) that can replicate independently of the chromosomal DNA, and is usually constituted of hundreds to a few thousand base pairs. Artificial plasmids are widely used in gene therapy in order to drive the replication of recombinant DNA sequences within host organisms. pDNA can adopt various conformations (linear, circular, or supercoiled) according to the over- or underwinding of a DNA strand (Scheme 2). DNA supercoiling is important for DNA packaging within all cells. Because the length of DNA can be thousands of times that of a cell, supercoiling of DNA allows DNA compaction, therefore much more genetic material can be packaged into the cell or nucleus (in eukaryotes).

The commercial calf thymus DNA (ctDNA) often used in physico-chemical studies is a linear DNA that can be isolated from calf thymus, an organ that has a very high yield of DNA.

The various topologies of DNA (supercoiled, circular, linear) can be discriminated by various methods such as electrophoresis and by microscopy techniques such as electron microscopy (EM) [36], cryogenic transmission electron microscopy (cryo-TEM) [37], and atomic force microscopy (AFM) [38].

1.1.4 DNA Condensation in Nature

Interpolyelectrolyte complexes form spontaneously upon mixing of solutions of oppositely charged polyelectrolytes, the main driving force being the gain of entropy because of the release of small counterions as well as the electrostatic interactions. This entropy-driven process creates an exceedingly tricky problem of how to package the genetic material in a stable non-aggregating form with synthetic

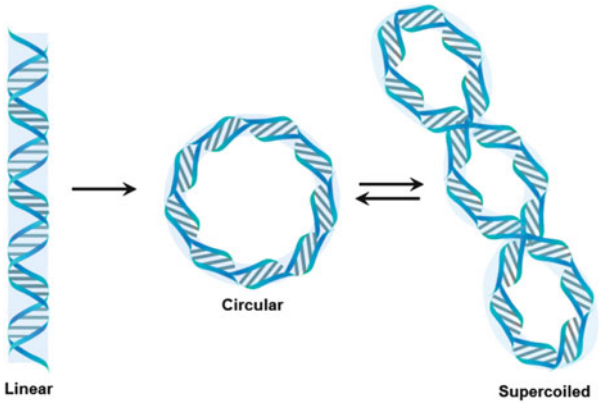

Scheme 2 Various topologies of dsDNA molecule: linear, circular, and supercoiled

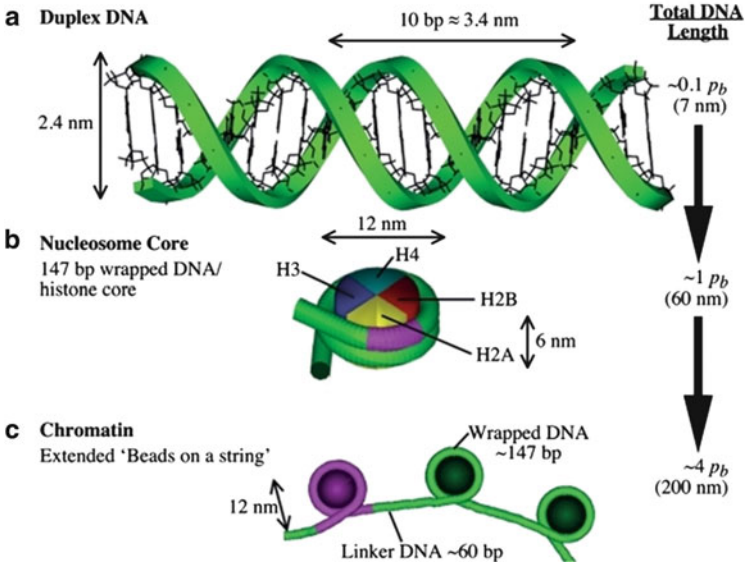

Scheme 3 Schematic view of some levels of DNA folding in the cell. (**a**) On length scales much smaller than the persistence length (p_b), DNA can be considered straight. (**b**) In eukaryotic cells, DNA wraps around a core of histone proteins to create a nucleosome structure. (**c**) Structure of chromation with "beads-on-a-string" configuration. Reprinted with permission from [243]. Copyright 2012 American Society for Biochemistry and Molecular Biology

polymers. On the other hand, the way Nature deals with the complexation of genetic material by proteins is extremely efficient: the genome of eukaryotic cells is packaged in a topologically controlled manner in the form of fibrous superstructures known as chromatin, and this allows DNA with a contour length of 2 m to be packaged in the nucleus of cells only a few micrometers in diameter [39]. The nucleosome core particle (NCP) is the fundamental building block of chromatin

and contains approximatively 147 bp of DNA wrapped in roughly two superhelical turns around an octamer of four core histones (H2A, H2B, H3, H4) (Scheme 3b): the DNA that links two neighboring nucleosomes is called linker DNA (55 bp) [40]. The structure adopts a "beads-on-a-string" configuration (Scheme 3c).

The H1 protein interacts with NCPs and organizes linker DNA, helping stabilize the zig-zagged 30 nm chromatin fiber. This is a nice example found in Nature of controlled complexation of genetic material [negatively charged DNA and histones, constituted mainly of positively charged amino acids such as arginine (Arg) and lysine (Lys)].

The selective binding of a protein to a particular DNA sequence requires the recognition by the protein of an ensemble of steric and chemical features that delineate the binding site [41]. DNA–protein recognition occurs very often by insertion of an R-helix into the major groove of dsDNA. A specific DNA sequence is then recognized through:

1. Formation of extensive hydrogen bonding and van der Waals interactions with the bases ("direct readout")
2. Recognition of sequence-dependent conformational features through electrostatic interactions with the negatively charged phosphodiester backbone ("indirect readout")

The structure of these DNA-binding proteins and the way they bind to DNA can be taken as inspiration for the rational design of synthetic polymers as DNA complexants.

1.2 Polyelectrolytes

Due to the presence of negatively charged phosphate groups, DNA is a strong polyanion and can forms complexes with positively charged polymers. DNA is usually defined by its number of base pairs and molecular weight (in Daltons) per charge (two charges per bp, ~650 Da/bp). It is important to mention that the polyelectrolyte character of DNA largely controls its behavior in solution.

1.2.1 Weak and Strong Polyelectrolytes

Polyelectrolytes are polymers whose repeating units bear an ionizable group. These groups will dissociate in aqueous solutions, making the polymers charged. Polyelectrolytes can be divided into weak and strong polyelectrolytes. Strong polyelectrolytes dissociate completely in solution for most reasonable pH values, whereas weak polyelectrolytes have a dissociation constant (pK_a) in the range of ~2 to 10, meaning that they will be partially dissociated at intermediate pH.

In the case of strong polyelectrolytes, the number and position of charges is fixed; variation of pH or ion concentration will not affect the number of charges. On the other hand, weak polyelectrolytes are not fully charged in solution, and their average degree of charges is given by the dissociation–association equilibrium

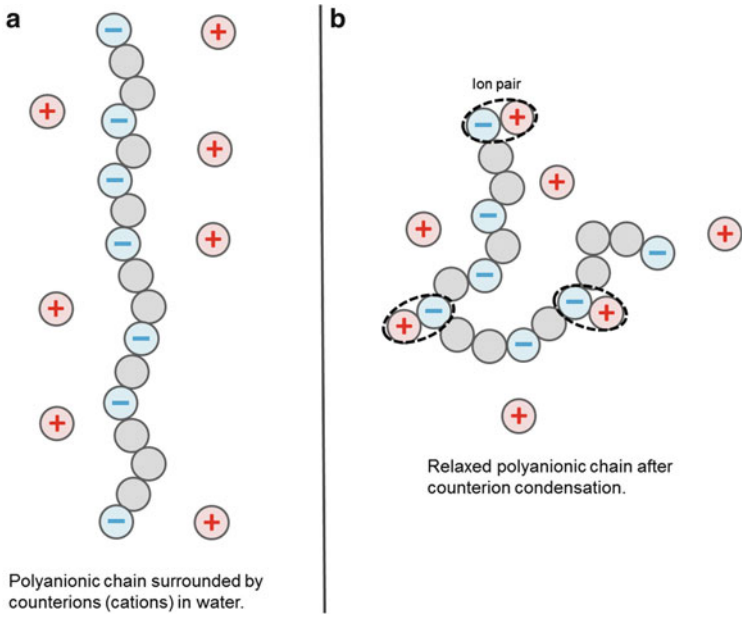

Scheme 4 Counterion condensation on a polyelectrolyte

constant and is governed by the pH of the solution, counterion concentration, and ionic strength; the charges are mobile within the polyelectrolyte.

The conformation of any polymer is affected by a number of factors, including the polymer architecture and the solvent affinity. In the case of polyelectrolytes, an additional factor is present: charge [42, 43]. In solution, whereas an uncharged linear polymer chain is usually found in a random conformation (theta solvent), a linear polyelectrolyte will adopt a more expanded, rigid-rod-like conformation due to the coulomb repulsion (the charges on the chain will repel each other) (Scheme 4a).

The structure of the polyelectrolyte itself depends on the grafting density, degree of dissociation with counterions, and ionic strength of the medium. If the ionic strength of a solution is high enough, the charges will be screened and consequently the polyelectrolyte chain will collapse to adopt the conformation of a neutral chain in good solvent (Scheme 4b).

1.2.2 Manning Condensation and Effective Charge Density

The properties of polyelectrolyte solutions depend strongly on the interactions between the polymers and the surrounding counterions. Manning's theory of counterion condensation predicts that a certain quantity of counterions condenses onto a polymer, whose charge density exceeds a critical value [44]. This leads to an effective decrease in the polymer charge. The macroscopic properties of the polyelectrolyte are not determined by its bare charge but by an effective charge. In particular, the flexibility and hydrophobicity of the polyelectrolyte chain, the

chemical nature of the counterions, the solvent quality, and concentration effects may well influence the "Manning condensation" [45]. Condensation occurs whenever the average distance between co-ions (assumed to be monovalent) on the polymer backbone is smaller than the Bjerrum length λ_B (distance between two dissociated ion pairs) defined as:

$$\lambda_B = \frac{q^2}{4\pi\varepsilon\varepsilon_0 k_B T},$$

where q is the elementary charge, $k_B T$ the thermal energy, and ε the dielectric constant of the solvent. This condensation is expected to lead to an average charge density of q/λ_B on the polymer backbone.

Since the polyelectrolyte dissociation releases counter-ions, this affects the solution's ionic strength and consequently the Debye length (distance over which significant charge separation can occur). The Debye length κ^{-1} (in nm) can be expressed as:

$$\kappa^{-1} = \frac{1}{\sqrt{8\pi\lambda_B N_A I}},$$

where N_A is the Avogadro number, λ_B is the Bjerrum length of the medium (in nm), and I is the ionic strength of the medium (in mol L^{-1}).

At room temperature, in water, the relation gives [46]:

$$\kappa^{-1} = \frac{0.304}{\sqrt{I}}.$$

These are parameters that should be taken into account when considering the individual polyelectrolytes (DNA and polycations) before complexation.

1.3 DNA/Polycation Complexes

Polyanions and polycations can co-react in aqueous solution to form polyelectrolyte complexes via a process closely linked to self-assembly processes [47]. Despite progresses in the field of (inter-) polyelectrolyte complexes [47] (IPEC from Gohy et al. [48], block ionomer complexes BIC from Kabanov et al. [49], polyion complex PIC from Kataoka and colleagues [50, 51], and complex coacervate core micelles C3M from Cohen Stuart and colleagues [52], understanding of more complex structures such as polyplexes (polyelectrolyte complexes of DNA and polycations) [53] is rather limited [54]. It has also to be considered that the behavior of cationic polymers in the presence of DNA and their complexes can be unpredictable, particularly in physiological environments due to the presence of other polyelectrolytes (i.e., proteins and enzymes) and variations in pH, etc.

1.3.1 Factors Influencing the Complexation of DNA by Cationic Polymers

The complexation of DNA and polycations is a function of the intrinsic properties of the two components. For instance, from the use of synthetic polycations for complexing DNA also arises the problem of polydispersity of polymers (a polymer sample is usually composed of macromolecular species of differing molar masses) compared with DNA, which is monodisperse. Because the polydispersity of the polycation could be an issue in studies of IPECs, sugar-based polymers (usually polydisperse except if fractionated), conjugated polymers (polydispersity, $M_w/M_n > 2$), branched PEI derivatives, and hyperbranched polymers are out of the scope of this review, as already mentioned. Only polymers synthesized via controlled or living polymerization methods will be discussed [55–57].

Although the interaction between multivalent polymeric cations with DNA is electrostatic in origin, the flexibility of the polymer backbones (rigid versus flexible) and molecular architectures also show great impact on the properties of the final polyplexes [58]. The molecular weight and topology of both the polymer (which can possess various architectures such as linear, brush, star, etc.) and the DNA (linear, circular, and supercoiled) has to be taken into account. On the polymer side, the composition (block, statistical, random, etc.) and its strength as a polyelectrolyte also play a role, as its charge density is varied.

As already mentioned, the main driving force of complex formation is the gain in entropy caused by the release of low molecular weight counterions, but other interactions such as hydrogen bonding and hydrophobic interactions can also contribute to the complexation process. Thus, the hydrophilicity/hydrophobicity of the polymer (influencing both the solubility of the polymer in aqueous media and its complexation with DNA via hydrophobic interactions) as well as its H-bonding capacity have to be taken into consideration. Moreover, the importance of counterions or substituents (inducing screening of charges) is often neglected in the formation of polyplexes.

Extrinsic factors (environment) such as the medium conditions also play a large part in the complexation process, especially pH and ionic strength (salt and polyelectrolyte concentrations). Also of prime importance is the way that the complexation itself is conducted, i.e., mixing parameters such as the stoichiometry of the components, the addition rate, and order of addition of the components (kinetic versus thermodynamic). Even if this process is fast and kinetically controlled (in water without added salt), i.e., far from the thermodynamic equilibrium, it can be followed by a slower stage in which the chains redistribute to a IPEC conformation closer to equilibrium [59].

1.3.2 Condensation of DNA by Cationic Polymers

DNA can be more simply considered as a particular case of a stiff anionic linear polyelectrolyte. Monovalent cations will condense on DNA (condensation) but do

not cause DNA compaction, which is the collapse of DNA into a compact structure. The compaction of DNA by an incompatible polymer has been modeled as a coil–globule transition such as observed in other polymers [60], and is also the topic of recent studies by the group of Dias, Lindman and colleagues [61, 62].

What seems to be the predominant method for polyplex formation is the addition of a polymer solution to a DNA solution. Some of the consequences of this procedure are that the concentration of the DNA solution changes in course of the addition (increase in volume) and DNA is consumed by the ongoing complexation process. Despite the importance of the addition rate, it is often not mentioned in polyplex studies. For instance, from IPEC studies it was found that the higher the titrant addition rate, the higher the storage stability of the complexes in the case of random copolymers of sodium 2-acrylamido-2-methylpropanesulfonate with either *t*-butyl acrylamide or methyl methacrylate complexed with poly(diallyldimethylammonium chloride) or with an ionene-type polycation containing 95 mol% *N*,*N*-dimethyl-2-hydroxypropyleneammonium chloride repeat units [63]. Moreover, by addition of a polycation to DNA, the zeta potential increases from negative values (DNA) to positive values (nanoparticles with excess of polycations).

The behavior of both DNA and polyplexes is also a function of the starting concentration of DNA, which can be in the dilute (polymers act as individual units without intermolecular interactions), intermediate, or semi-dilute regime (polymer chains overlap each other and form a transient network). IPEC studies of the complexation of poly(allylamine hydrochloride) and the two polyanions poly (acrylic acid) and poly(methacrylic acid) have shown that the higher the concentration, the larger and denser are the complexes formed [64]. Unfortunately, this type of study with complexes of DNA and polycations are still scarce.

Structural Models

Two structural models are discussed in the literature for polyelectrolyte complex (PEC) formation, depending on the components (weak or strong polyelectrolyte, stoichiometry, molecular weight) and the external conditions (presence of salts, etc.): ladder-like (complex formation takes place on a molecular level via conformational adaptation) or "scrambled egg" structure (large number of chains in a particle) (Scheme 5) [65].

The ladder-like structure results from the mixing of polyelectrolytes having weak ionic groups and large differences in molecular dimensions. It is the result of the propagation of the complex reaction as a "zippering action," since the ionic sites next to the first reacted ones would be the most likely to react next. The "scrambled egg" structure refers to complexes that are the product of the combination of polyelectrolytes having strong ionic groups and comparable molecular dimensions. These models have been extensively discussed and most experimental structures lie between these two models, though probably closer to the scrambled egg than the ladder model [66], especially in the case of complexes of DNA with polycations.

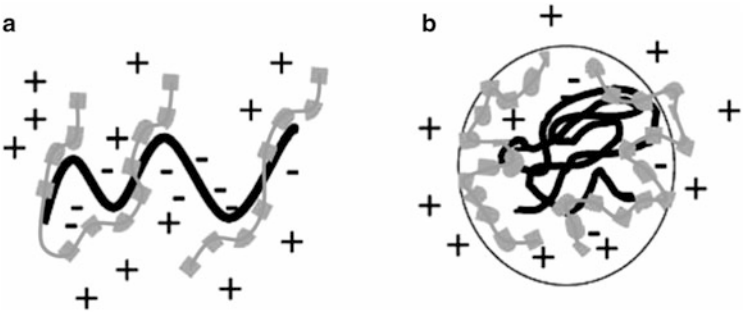

Scheme 5 Representation of ladder and scrambled egg structures. *Black line*s represent large polyions (negative), while *gray lines* with *squares* represent polyions of opposite charge (positive). (**a**) Ladder representation, where insufficient ion pairing occurs under certain stoichiometric conditions leading to macromolecular aggregates, insoluble, and soluble PECs. (**b**) Scrambled egg model, where polymers of comparable size complex to yield insoluble PECs under certain conditions. Reprinted with permission from [65]. Copyright 2007 Springer

Cooperative Versus Non-cooperative Binding

The binding itself can occur either via cooperative or non-cooperative binding (Scheme 6). A macromolecule (DNA, protein, synthetic polymer) exhibits cooperative binding if its affinity for its ligand changes with the amount of ligand already bound. The cooperativity is positive if the binding of ligand at one site increases the affinity for ligand at another site, whereas the cooperativity is negative if the binding of ligand at one site lowers the affinity for ligand at another site. A macromolecule exhibits non-cooperative binding if the ligand binds at each site independently.

In complexation of DNA with polycations, both scenarios can be found. In the case of cooperative binding, some of the DNA is totally complexed, while the rest of DNA is left "naked." In the case of non-cooperative binding, all individual DNA chains are roughly equally complexed by polycations.

1.3.3 Structure of Polyplexes

Condensates of polycation with DNA (polyplexes) can adopt various shapes, the most commonly observed being toroidal, rod-like, and globular (examples of some of these structures are presented in Scheme 7) [68–71]. The different structures that IPECs can adopt can be categorized into different subtypes: water-soluble, colloidally stable, and insoluble. The type of complex formed is governed by all the factors mentioned in the previous paragraphs. Moreover, it should be noted that the polycation/DNA charge ratio influences the size, charge, and solubility of the polyplexes. As a consequence, in some cases, the polyplexes can be consecutively water soluble, then colloidally stable, and eventually precipitate.

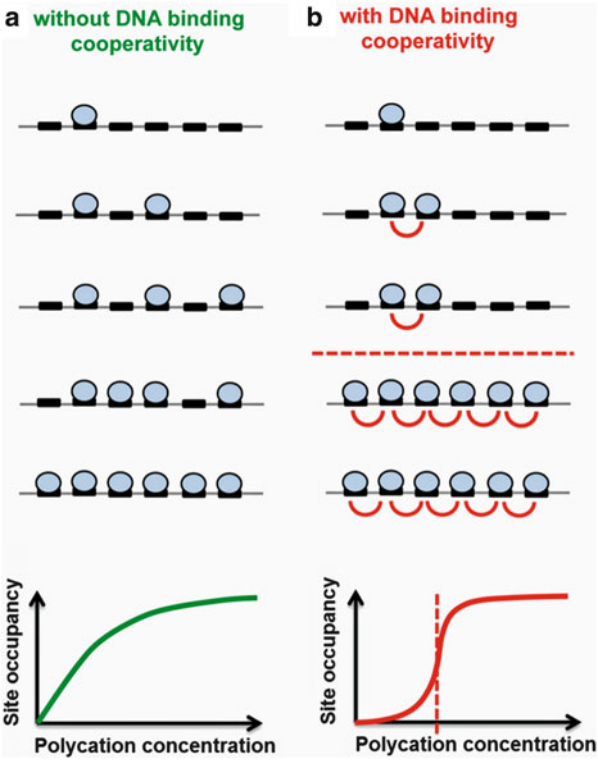

Scheme 6 (**a**) If a polycation binds to a cluster of DNA binding sites in a non-cooperative manner, a gradual increase in polycation concentration generates a gradual increase in the average occupancy of the cluster. (**b**) Conversely, if the polycation binding to adjacent sites is cooperative, a gradual increase in polycation concentration generates a "digital" on/off response as the concentration sweeps a threshold value (*dashed line*). The higher the binding cooperativity, the steeper the transition between the "off" and the "on" states. Adapted and reprinted with permission from [67]. Copyright 2010 Elsevier

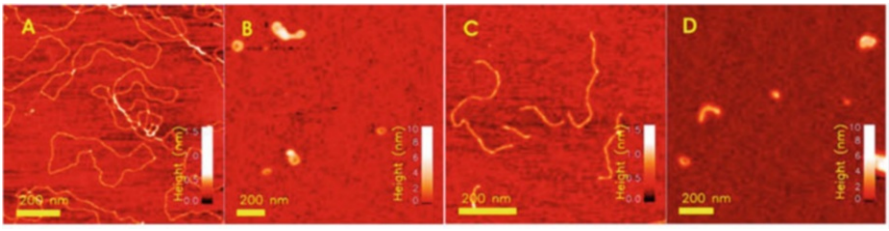

Scheme 7 Tapping mode AFM height topographs of (**A**) uncomplexed pBR322, (**C**) linear DNA, and (**B**, **D**) the respective complexes of these formed when mixed with chitosan. $C_{DNA} = 4$ μg mL^{-1}. Reprinted with permission from [68]. Copyright 2004 American Chemical Society

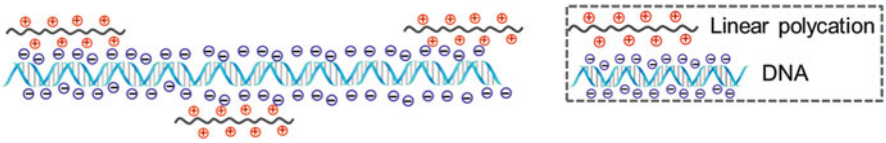

Scheme 8 Proposed model for water-soluble polyplexes with sequentially hydrophilic (polyanion) and hydrophobic segments (complex of polyanion and polycation). The bending or compaction of DNA are not taken into account in this scheme

In the schemes included hereafter DNA is represented as linear (but can have other topologies and is compacted within the polyplexes), and the type of binding (cooperative or not) is not taken into account, except if mentioned.

Water-Soluble Polyplexes

Soluble polyplexes are macroscopically homogeneous systems containing small PEC aggregates. Due to the strong polyanionic nature of DNA, water-soluble polyplexes are formed when the polycation is present in non-stoichiometric proportions under certain concentration (dilute) and/or salt conditions and with significantly different molecular weights [72, 73]. The complex adopts a conformation similar to that of the ladder model with hydrophilic (polyanion) and hydrophobic segments (complex of polyanion and polycation) (Scheme 8). This type of polyplexes is the key to forming polyplexes monomolecular in one component.

Colloidally Stable Polyplexes

Colloidally stable polyplexes are PEC systems in the transition range to phase separation, exhibiting an observable light scattering or Tyndall effect [65]. These systems can be stable because of electrostatic stabilization, steric stabilization, or a combination of both called electrosteric stabilization.

Without Steric Stabilization

IPEC formation between (strong) polyelectrolytes results in highly aggregated and/or macroscopic flocculated systems. Nevertheless, the aggregation can be stopped at a colloidal level in extremely dilute solutions, and a polydisperse colloidally stable system of nearly spherical particles can usually be achieved [47].

Due to the entropy-driven charge neutralization rather than a strictly located binding, charges can sometimes be "buried," leading to a mismatching of the charge densities even at 1:1 charge ratio. Furthermore, the stoichiometry depends on the polymer flexibility because rigid polymers that are less able to change their conformation are more likely to form non-stoichiometric IPECs. Polymers with nonlinear architectures (graft, hyperbranched, etc.) are also prone to the formation

of non-stoichiometric IPECs, since charges at sites in the inner parts of the molecules can be inaccessible to the oppositely charged polyelectrolyte. Mismatching charge densities leads to a higher degree of swelling of the colloidal particles. It is proposed that these colloidally stable IPEC particles consist of a charge-neutralized core, in which 1:1 stoichiometry and high entanglements prevails, and an outer shell consisting of a few polyelectrolyte layers whose charges are not completely compensated, giving the complex its net charge, stabilizing the particles, and preventing them from further aggregation. The number of polymer chains included in a single IPEC particle varies from hundreds of chains in extremely dilute systems up to several thousands for more concentrated component solutions [47].

With Steric Stabilization

In the previous situation, the particles were stabilized mainly by the charges in the outer shell (electrostatic stabilization). Another type of stabilization for colloids is steric stabilization, which can be introduced in the case of polyplexes by the presence of a neutral hydrophilic block in the polycation. Micelle-like structures are thus obtained consisting of a charge-neutralized core, in which 1:1 stoichiometry and high entanglements prevails, and an outer shell consisting of a neutral hydrophilic block, stabilizing the particles via steric interactions. These IPEC micelles are also called complex coacervate core micelles (CCCM or C3M) [52]. This allows, even at charge neutralization and despite possible secondary aggregation, the colloids to stay in solution stabilized by their polymeric hydrophilic shell. Secondary aggregation occurs when the particles in solution try to minimize contact with their surroundings (water) at charge neutralization; the particles will adhere with each other and finally the entire dispersion may coalesce. Usually, the higher the molecular weight of the polymer and the larger the thickness of its hydration shell, the more stable are the colloids. In the most efficient cases of steric stabilization, secondary aggregation can be avoided and single particles are present in solution, even if neutral. If the stabilization is slightly less efficient, the aggregates that are nevertheless stable can be redispersed by the addition of more polycation. The additional polymer is included in the polyplexes leading to a positive net charge, which introduces repulsion between the particles (Scheme 9).

Poly(ethylene glycol) (PEG) is the polymer that is most used for steric stabilization due to its biocompatibility. It should be noted that random copolymers are usually not as effective in steric stabilization as block or graft copolymers.

In most of the studies, unfortunately, physico-chemical characterization is not conducted in enough detail that the size and surface charge of the various species present in solution are determined; usually, only the properties of the colloidal suspensions (sum of species) are determined. Indeed, when polycations are added in high excess to polyplexes after charge neutralization, it seems that in most cases polycations and neutral polyplexes coexist in solution because the polycations do not adsorb at the surface of the polyplexes. A way of determining the real size and surface charge of the polyplexes would be to separate the colloids from the

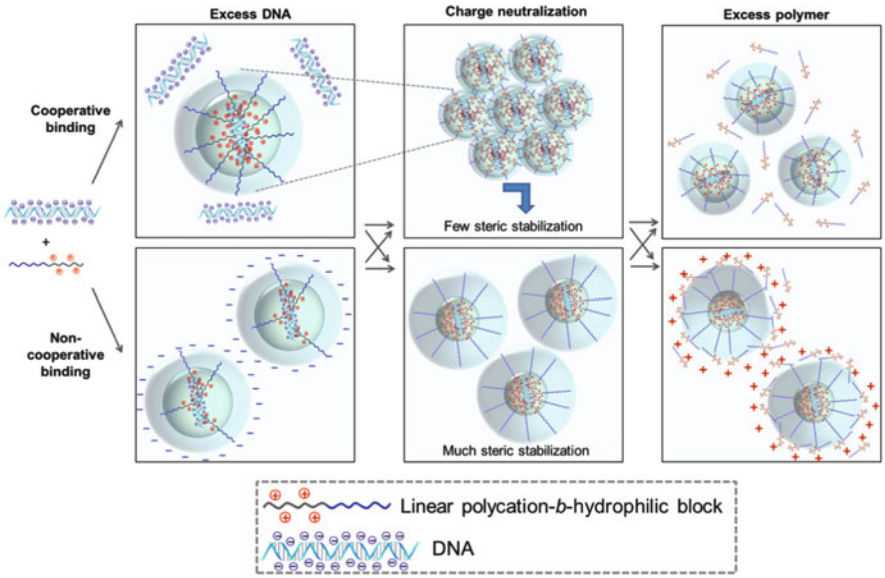

Scheme 9 Proposed model for sterically stabilized polyplexes as function of the charge ratio polycation:DNA. When an excess of DNA is present in solution, if the binding is cooperative then neutral polyplexes (charge neutralized DNA/polymer complexes) and DNA molecules will coexist in solution. If the binding is not cooperative, negatively charged polyplexes will be present in solution (where the charges of DNA are not compensated by the polycations). In both cases negative zeta potentials are obtained. At charge neutralization, if the steric stabilization is not sufficient, aggregation of the neutral polyplexes will take place and they will precipitate (they can eventually in some cases be redispersed following further addition of polymer).If the steric stabilization is sufficient, polyplexes can stay as individual nanoparticles in solution. When an excess of polymer is present in solution, two cases are possible: either the polycations and neutral polyplexes coexist in solution because the polycations do not adsorb at the surface of the polyplexes, or the polycations adsorb on the polyplexes surfaces (usually when the steric barrier is sufficient) leading to positively charged polyplexes (until a certain point where the polycations do not adsorb on the positively charged polyplexes due to electrostatic repulsion). In both cases positive zeta potentials are obtained

individual polycations, for instance by means of dialysis (dilution could eventually have an influence on the stability of the polyplexes by influencing the equilibrium between polycation and PIC micelle). In both cases (excess polycation adsorbed or not at the surface of the polyplex), this would explain the big discrepancies between the physico-chemical characteristics of polyplexes and their performances in vitro. Even if the mixture of polymer and polyplex shows a positive zeta potential, this does not mean that the polyplex containing the therapeutic gene is positively charged. As a consequence, if the polyplex itself is neutral, it will not interact favorably with the cell membrane and thus will not lead to high transfection because of the low cellular uptake. Also, even if the polyplex has a positive zeta potential due to the polycations adsorbed on the surface of the neutral polyplexes, the polycation would probably be easily displaced after intravenous injection,

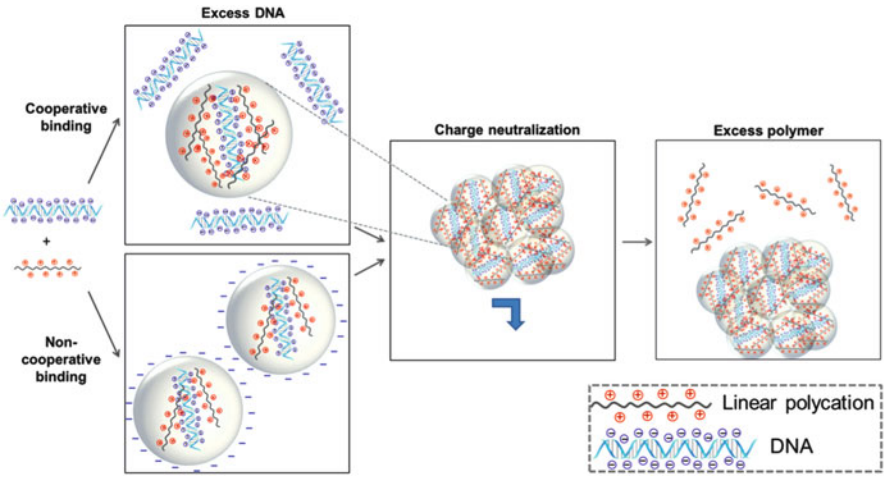

Scheme 10 Proposed model for non-sterically stabilized polyplexes as function of the charge ratio strong polycation:DNA. When an excess of DNA is present in solution, if the binding is cooperative neutral polyplexes (charge neutralized DNA/polymer complexes) and DNA molecules will coexist in solution. If the binding is not cooperative, negatively charged polyplexes will be present in solution (where the charges of DNA are not yet compensated by the polycations). In both cases negative zeta potentials are obtained. At charge neutralization, aggregation of the neutral polyplexes will take place and they will precipitate (macroscopically visible). These aggregates of polyplexes cannot be redispersed and addition of more polymer will lead to positive zeta potential because the polycation is the only specie present in solution

i.e., in vivo (dilution effect and competition with other polyanions or polycations present in the blood stream).

Insoluble Polyplexes

Insoluble polyplexes are the result of a two-phase system of supernatant liquid solution (containing either polycation as in Scheme 10, or DNA as in Scheme 11) or colloidal suspension (in the particular case of polymeric micelles in solution as shown in Scheme 11, case 1) from which the polyplexes precipitate. For non-sterically stabilized polyplexes, when the molar mixing ratio approaches unity or a low quantity of salt is added (screening of charges of the polyplex) [74] and therefore the electrostatic stabilization is insufficient, secondary aggregation occurs and the aggregates precipitate (this is also a function of the density of the polyplexes) (Scheme 10) [47].

Polyplexes Based on Amphiphilic Polycations

Polymeric micelles are colloidal particles formed by the self-assembly of amphiphilic block polymers (at certain hydrophilic/hydrophobic ratio of the blocks

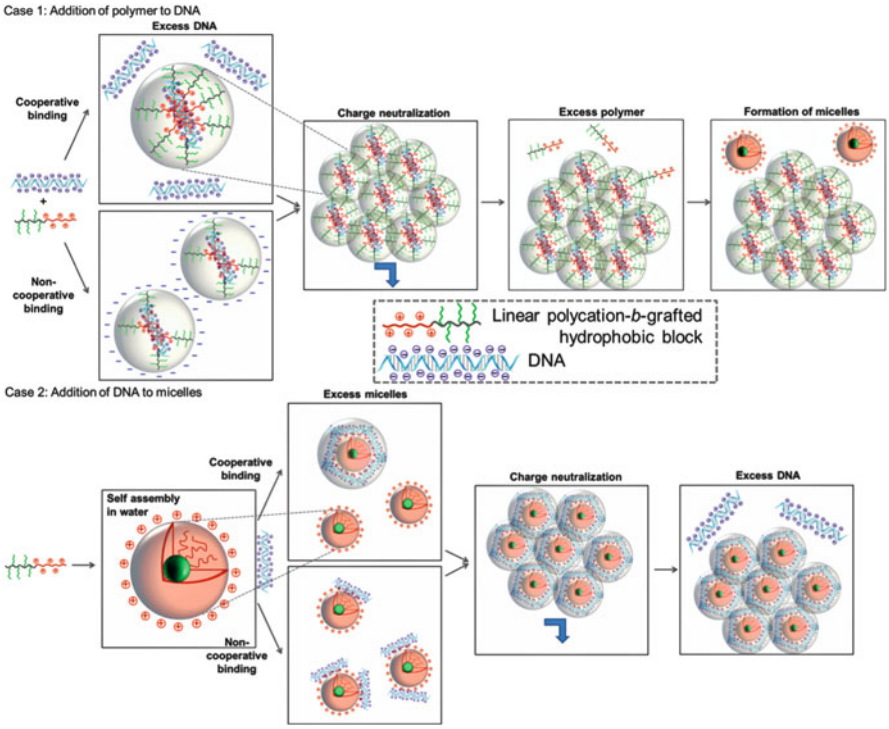

Scheme 11 Proposed models for polyplexes based on amphiphilic polycations as a function of the charge ratio. *Case 1*: When an excess of DNA is present in solution, if the binding is cooperative neutral polyplexes with hydrophobic shell and DNA molecules will coexist in solution. As these core–shell structures possess hydrophobic shells, their range of stability is reduced and they nearly immediately aggregate and precipitate. If the binding is not cooperative, negatively charged polyplexes with hydrophobic shell will be present in solution (where the charges of DNA are not yet compensated by the polycations). At charge neutralization, aggregation of the neutral polyplexes will take place and they will precipitate. With further addition of polymer, amphiphilic polycations are present in solution as unimers until the CMC is reached, where polycationic micelles are the only colloidal specie in solution. *Case 2*: When DNA is added to a polymer micellar solution, if the binding is cooperative neutral polyplexes with a micellar core composed of the cationic amphiphilic and a shell composed of DNA are formed. If the binding is not cooperative, overall positively charged polyplexes with DNA as shell will be present in solution. At charge neutralization, aggregation of the neutral polyplexes will take place and they will precipitate. With further addition of DNA, the zeta potential of the solution will be negative because DNA is the only specie present in solution

constituting the polymer) in an aqueous environment and have sizes ranging from 10 to 100 nm [75]. Micelles can form only above a given concentration, which is known as the critical micelle concentration (CMC) [76]. If the concentration of amphiphilic polymer in the sample is under its CMC, the observed behavior is roughly that presented in previous cases, except that, due to the amphiphilic nature

of the polycation, the stability of the polyplex will be more limited in an aqueous environment.

If the concentration of the amphiphilic polymer in the sample is above its CMC, there are two cases to consider: the micellar solution is added to the DNA solution or the DNA solution is added to a micellar solution. In the first case, where the micellar solution of polycation is added to DNA, the micelles are immediately diluted in the DNA solution, which on one hand can mean that the polymer concentration is under its CMC and therefore that the polymer is only present as individual chains in solution (unimers), on the other hand, that there is concurrence between self-assembly of micelles versus electrostatic interactions with a large quantity of negatively charged material. In this case, the micelles are usually destabilized as soon as they reach the DNA solution (Scheme 11, case 1).

In the case of DNA added to a micellar solution of polycation, the micelles can stay stable in some cases: (it depends on the hydrophobicity of the micellar core and strength of the electrostatic interactions). This can be proven if pyrene or other hydrophobic molecules entrapped in the hydrophobic interior are not released even after addition of DNA [77]. It has to be noted that micelles are in thermodynamic equilibrium with unimers and that both species can form electrostatic interactions with DNA. When the micelles do not undergo a structural change, no rearrangement into a "scrambled eggs" structure takes place between the amphiphilic polycation and DNA, and because DNA is in minority, it adds to the positive shell of the structure until neutralization (Scheme 11, case 2).

Influence of Salts

After changes in ionic strength (due to the addition of salt), swelling or deswelling of IPECs occurs immediately, whereas coagulation (i.e., destabilization of colloids by neutralizing the electric charge of the dispersed nanoparticles, which results in aggregation of the colloidal particles) is a much slower process and is dependent on the concentration of the colloidal particles [74]. Two major effects on the formation of IPECs in the presence of salt were found by Dautzenberg [77]. On the one hand, the presence of a very small amount of salt during formation dramatically decreased the level of aggregation, probably due to the less stiff and more coiled structure that the polymers can adopt. On the other hand, a higher ionic strength resulted in macroscopic flocculation, explained by the contribution of two factors: particle swelling because of charge screening of the stabilizing outer shell and particle aggregation due to colloidal instability. However, the internal structure of most IPECs is marginally affected by salt [77]. With a further increase in ionic strength, the point is reached where charges are screened at the level of the polymers, and polycations and DNA are dissolved as individual polymers.

As already mentioned, counterions seem to be important for the interaction between polyelectrolytes (uni- or multivalent) and the specific ions involved (size, chaotropic/kosmotropic) [78, 79].

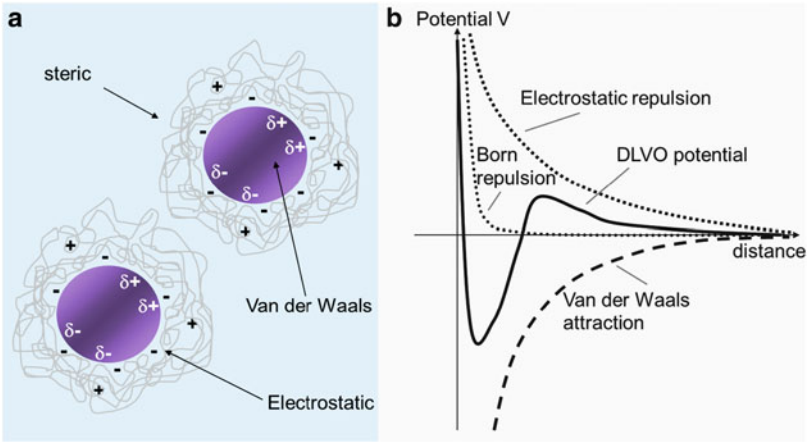

Fig. 1 Interactions between nanoparticles. (**a**) Traditional forces for colloidal stabilization (e.g., electrostatic, van der Waals, steric) that occur when particles are dispersed in aqueous media. (**b**) The van der Waals forces are attractive whereas the electrostatic forces are repulsive over a typical length scale. The Derjaguin–Landau–Verwey–Overbeek theory in colloid science considers the sum of these forces. Reprinted with permission from [80]. Copyright 2011 Elsevier

1.3.4 Characterization of Polyplexes

The final polyplexes either precipitate if they are water insoluble or form a colloidal system (particles that have a diameter less than a micrometer evenly dispersed in aqueous media in this case) if they are sufficiently stabilized even after complexation. In both cases, these polymer–DNA complexes can be characterized using a variety of analytical techniques, which will be presented in the next paragraph.

In the case that the polyplexes form a colloidal system, the Derjaguin, Landau, Verwey and Overbeek theory (DLVO theory) can be used to describe their colloidal stability and aggregation behavior. The DLVO theory describes the force between charged surfaces interacting through a liquid. It takes into account the effects of the van der Waals attraction and the electrostatic repulsion due to the double layer of counterions, but additional forces have also been reported to play a major role in determining colloid stability (Fig. 1) [80]. This topic is addressed in more detail by Lebovka in another chapter of this volume [81].

Structural Characterization

Light scattering (LS) provides information related to the dimensions of the polyplexes (hydrodynamic radius R_h), their shape (radius of gyration R_g and shape factor $\rho = R_g/R_h$), as well as weight-average molecular weight (M_w) of the aggregates and polydispersity of the sample.

Atomic force microscopy (AFM) and electron microscopy techniques allow imaging the polyplexes. The electron microscopy techniques used, as for other nanoparticles, are transmission electron microscopy (TEM) and cryo-TEM.

Charge Determination

In the case of strong polyelectrolytes, the number of ionized units corresponds to the number of dissociable ionic units (see Manning condensation) and is independent of the pH. For weak polyelectrolytes, the number of ionized units at a given pH is dependent on the pK_a. From acid/base titration, their pK_a as well as buffering capacity (illustrated by plotting the pH of a solution containing a polymer as a function of the volume of acid added) can be determined. The following equation reported by Patchornik et al. can be used to determine the number of ionized units, i.e., the protonation state of a polycation, at a specific pH [82]:

$$\mathrm{pH} = \mathrm{p}K_a + \log\left[\frac{(1-\alpha)}{\alpha}\right] - 0.868\, n \times \alpha \times w,$$

where pK_a is the intrinsic pK of the protonatable moiety, n is the average number of protonatable moieties per polymer chain, α is the fraction of protonated moieties, and w is an electrostatic interaction factor defined as:

$$w = \frac{e^2}{2DkT}\left(\frac{1}{b} - \frac{K}{1+Ka}\right)$$

assuming a spherical molecule with radius b and a distance of closest approach a; D is the dielectric constant of water, k the Boltzmann constant, T the absolute temperature, e the electronic charge and k has its usual significance in the Debye theory. By solving it in an iterative fashion, one can determine the percentage of groups on the polymer that are protonated at physiological pH and therefore are potentially available to assist in the condensation of DNA.

Z or φ is the charge ratio at a given pH (also called +/−), meaning the ratio of ionized units of the cationic polymers at the given pH by the number of negative charges of the DNA. N:P ratio, which is the ratio of nitrogen atoms in the polycation to phosphorus atoms in DNA, is usually employed in the case of polyplexes based on weak polyelectrolytes when the number of ionized units is not determined. Unfortunately, it does not best reflect the polyelectrolyte behavior. Also used are the molar or weight ratios of polymer:DNA.

Zeta potential (ζ) analysis can be used to measure the relative surface charges of nanoparticles such as polyplexes. It helps define a range of stability for colloids, when steric stabilization does not take place (only electrostatic stabilization). Zeta potential, as well as dynamic light scattering (DLS) are useful methods for determining if various fractions are present in solution (with different surface charge or size, respectively).

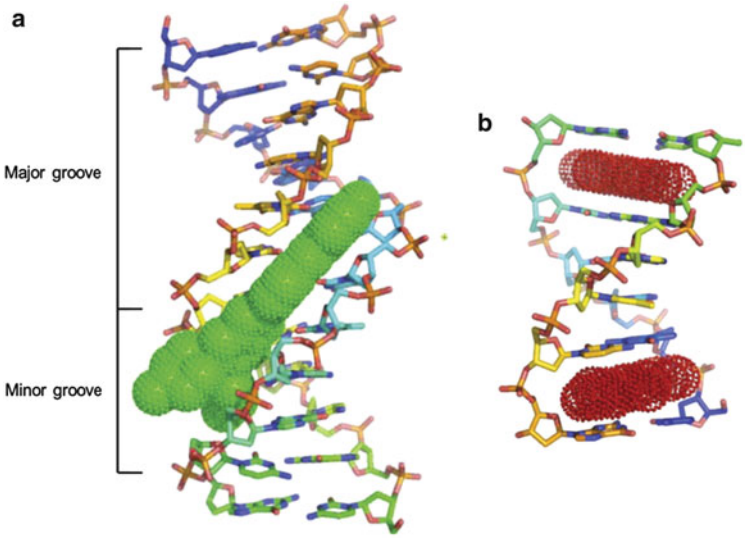

Fig. 2 (**a**) Groove binding of Hoechst 33258 to the minor groove of DNA. (**b**) Intercalation of ellipticine into DNA. Adapted and reprinted with permission from [83]. Copyright 2007 Elsevier

Agarose gel electrophoresis separates macromolecules on the basis of both charge and size, and the immobilization of DNA on a gel in the presence of cationic polymer can be used to determine the conditions under which self-assembly and/or charge neutralization occurs. It should be noted that retardation of polyplexes can be due to neutralization of the positive charge or to an increase in mass.

Strength of the Complexation

Ethidium bromide (EtBr) is commonly used as a fluorescent nucleic acid stain in techniques such as agarose gel electrophoresis. When excited by 530 nm light, EtBr emits fluorescence at 610 nm, with an almost 20-fold increase in intensity after intercalating into DNA base pairs due to π-stacking with the nucleobases (see Fig. 2b for an example of a DNA intercalator) [84]. When polymers interact tightly with DNA to form polyplexes and condense DNA, EtBr is released into solution, where its fluorescence is far inferior to that when intercalated in DNA. Thus, EtBr is a good indicator for evaluating the strength of condensation of DNA by polycations. Some other dyes such as Hoechst stains are (minor) groove binding agents (see Fig. 2a), and therefore give less information about the strength of complexation.

The coil–globule transition of DNA (reflecting the compaction of DNA) can be followed by thermal analysis or spectroscopic methods such as UV.

Competition binding can be used to test the stability of the polyplexes. The release rate of DNA from a polyplex by competitive binding between

the components of the gene delivery vector with charged components (for instance polyanions such as heparin) is an indicator of the strength of the complexation (necessary for the extracellular milieu) as well as the possibility of release (in intracellular milieu, favorable for gene expression).

Testing the efficiency of a polymer in protecting DNA from enzymatic degradation (by nuclease, etc.) gives information about the efficiency of compaction of DNA by the polycation and/or the steric protection of the polyplex. The protection of DNA in the polyplex from its degradation by enzymes is essential for in vivo delivery.

1.4 Application in Gene Therapy

One of the many applications of polymers capable of complexing but also condensing DNA is their use as transfection agents (introduce genetic material into cells).

1.4.1 Introduction to Gene Therapy

Gene therapy aims to cure inherited and acquired diseases by correcting the overexpression or underexpression of defective genes, and its success depends largely upon the development of vectors that deliver and efficiently express a therapeutic gene in a specific cell population [85, 86]. Gene therapy protocols were originally designed to correct inheritable disorders such as adenosine deaminase deficiency, cystic fibrosis, Gaucher's disease, and Duchenne muscular dystrophy [87, 88]. However, gene therapy is not exclusively used in an attempt to supply a missing gene product to a patient with a given inborn error of metabolism. Indeed, gene therapy has been considered more recently as a promising tool for treating acquired diseases such as cancer [89] and human immunodeficiency virus (HIV) infections [90]. Clearly, different applications have distinct needs, and tailoring gene delivery vectors to the specific requirements of a therapeutic application is still a challenge. For example, the ideal gene vector for treating genetic disorders should not only deliver intact pDNA efficiently to the nucleus of most of the target cells, but also, once delivered, the transgene should be maintained in the nucleus without disrupting host gene expression or signaling pathways. By contrast, anticancer gene therapy trials are in progress in which the aim is high transgene expression in as many tumor cells as possible, rather than sustained gene expression.

Two types of vectors are used in gene delivery: viral [91] and non-viral [92, 93]. Viral-mediated DNA vehicles (infection) have played a major role in gene therapeutics. Unfortunately, the initial enthusiasm associated with the high infection yields has been tempered by growing concerns regarding safety issues such as toxicity, immunogenicity, and oncogenicity. On the other hand, synthetic gene vectors (transfection), with dimensions in the nanometer range, provide potential alternatives for gene therapy because these vectors (based on lipids, dendrimers, peptides, or polymers) are more easily produced and at lower cost. Moreover, they

work reasonably well in vitro and overcome some of the disadvantages of viral-based gene delivery systems such as immunological response, fatal infections, etc.

The genetic material for treatment of a variety of genetic disorders can be of three types: (1) pDNA, to express a gene of interest under the control of a suitable promoter (has to reach the nucleus), which will result in the increased production of a protein [94, 95]; (2) oligomeric genetic material such as antisense OligoDeoxy-Nucleotides (ODN), short RNA molecules such as small interfering RNA (siRNA) micro-RNA (miRNA) or short hairpin RNA (shRNA), or a DNAzyme in order to silence a specific gene by reducing the target/protein activity. The short RNA molecules as well as DNAzyme have to reach the cytoplasm and more precisely the RNA-induced silencing complex (RISC) without being destroyed in the late endosomes or lysosomes [96–98].

1.4.2 Requirements for Efficient Gene Therapy

Complexation and Compaction/Condensation

For most cell types, the size requirement for particle uptake via endocytosis is of the order of 200 nm or less. As DNA has a R_h of a few hundred nanometers when its molecular weight is a few thousand base pairs, the polymers should not only complex DNA but also condense or compact it into smaller particles. The polymer remains unable to condense DNA until the neutralization of a critical amount of negative charges on the DNA. For instance, Wilson and Bloomfield have calculated that in order to condense DNA, 90% of the phosphonate moieties have to be neutralized when the condensing agent is spermine or spermidine [99].

For condensation, strong (quaternary ammonium, etc.) as well as weak polyelectrolytes (containing amino acids such as Arg, Lys, etc. or poly[(2-dimethylamino) ethyl methacrylate], PDMAEMA [100]) can be used, which should possess a minimum number of cationic charges at physiological pH. For instance, as a weak polyelectrolyte, linear PEI (LPEI, 22 kDa) has 75% of its amino groups protonated at physiological pH [101]. At pH 8, with a degree of polymerization (DP) of 32, PDMAEMA has approximately 24% of its amino groups protonated [102].

Extracellular Barriers and Physico-chemical Aspects

A major drawback of current transfection vectors is that they have poor in vivo transfection efficiency and only confer transient gene expression. Indeed, poor transfection efficiency is due, in part, to the lack of stability of the non-viral vector–DNA complex under physiological conditions and its ability to interact with blood plasma proteins after intravenous injection, the extracellular matrix, and undesirable cells, and its possible degradation by enzymes, even before reaching the intracellular compartment (Scheme 12). In order to overcome these problems and to enable the carrier to translocate across cellular membranes (thus

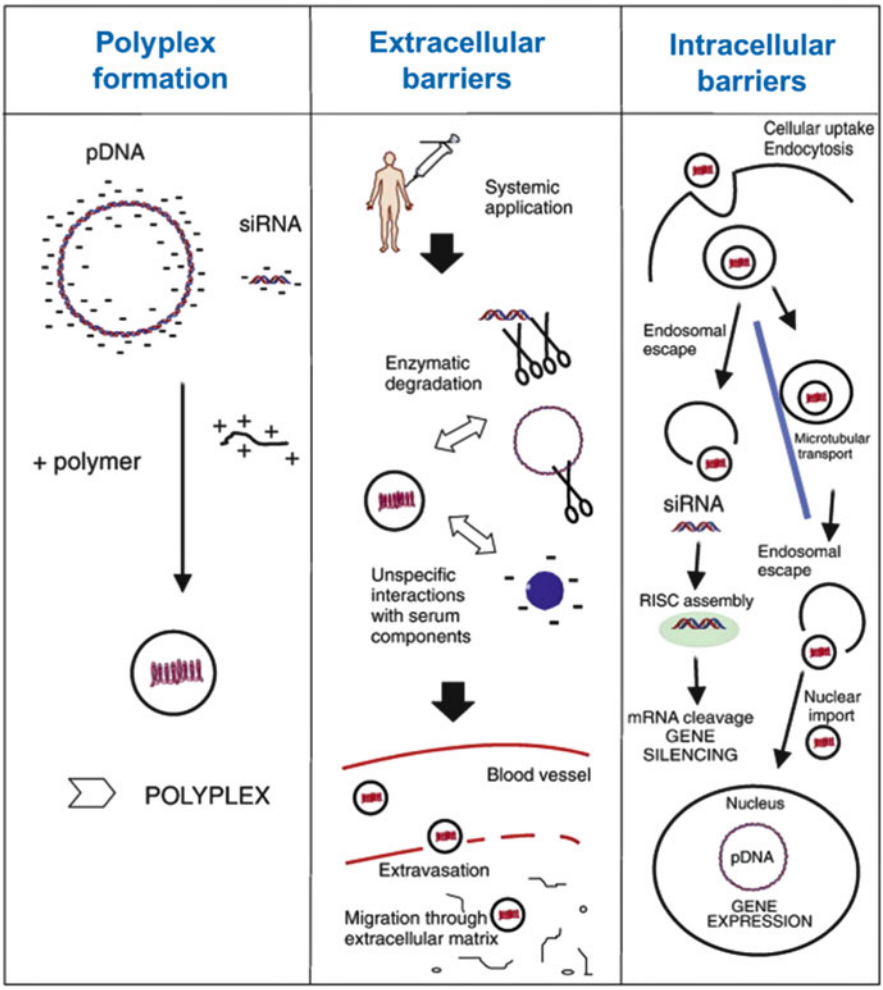

Scheme 12 Nucleic acid nanoparticle formation and delivery barriers. Adapted and reprinted with permission from [95]. Copyright 2012 Elsevier

further influencing its biodistribution, cell internalization, and trafficking properties), it is of prime importance to engineer the polyplex (polymer/DNA complex) in terms of chemical structure, molecular weight, hydrophilicity/hydrophobicity, size, surface groups, charge density, and concentration. This is the main aspect that will be treated in this review, i.e., the chemical engineering of polycations and the physico-chemical aspects of polyplexes. Various publications address the topic of structure–property relationships by modification of the polymer via processes such as acetylation [103, 104], introduction of an hydrophilic block through PEGylation [105, 106], control of charge density [102, 107], incorporation of hydrogen bonding [107, 108], or varying the topology

of the polymer [109, 110]. It is important to note that internalization of positively charged polyplexes is facilitated, given that the cell surface is negatively charged (because of the presence of proteoglycans) so, in general, nanoparticles with smaller size and higher zeta potential are most likely to be uptaken by cells.

Once in the blood stream, hydrophobic nanospheres are rapidly opsonized and extensively cleared by the mononuclear phagocyte system (MPS). This problem can be prevented by surface modification, such as coating with hydrophilic polymers, or by formulating nanospheres with biodegradable copolymers with hydrophilic characteristics [111]. Moreover, the introduction of hydrophilic polymers, such as oligo(ethylene glycol) or poly(ethylene glycol) (PEG, probably the most widely used), or others such as the zwiterrionic 2-methacryloxyethyl phosphorylcholine (MPC) or poly(hydroxyethyl methacrylate) (PHEMA) can provide steric stabilization to otherwise unstable polyplexes in water. They can also protect DNA against protein adsorption and degradation by enzymatic nucleases.

Active targeting to certain cells or organs can be attained by the recognition at the molecular level between a ligand and receptors overexpressed on cell membranes through specific interactions. Once the molecules bind to the receptors, the complex is internalized via receptor-mediated endocytosis, facilitating the cellular uptake of the carrier of this ligand. This will not be treated in this review because, most of the time, active targeting with nanoparticles is achieved by conjugating an antibody or protein to a polymer, thus influencing the physicochemical properties of the polymer and polyplex formed thereof. Nevertheless, this is an extremely important aspect of gene delivery for in vivo applications [112].

Intracellular Processes

As previously mentioned, for most cell types, the size requirement for particle uptake via endocytosis is in the order of 200 nm or less, and a net positive charge on the surface of the conjugate has been shown to be important for triggering uptake. Moreover, to be effective, these polyplexes must be optimized at all stages of the delivery process, ranging from target-cell recognition (attachment of targeting ligands in order to be recognized and taken up by specific cells) [113–115] to their escape from the endosome-enclosed milieu, resistance to cytoplasmic degradative enzymes such as nucleases, and release of the genetic material at the desired site of action [116]. Thus, polymers should bind efficiently and protect the genetic material against nonspecific interactions with proteins and cell membranes in blood, but efficiently release it in the cytosol in order to favor gene expression (Scheme 13) [117]. Indeed, when the polycation binds too strongly, it results in impaired gene expression.

Concerning the intracellular trafficking of polyplexes, it begins in early endosomal vesicles. These early endosomes subsequently fuse with sorting endosomes, which in turn transfer their contents to the late endosomes. Late endosomal vesicles are acidified (pH 5–6) by membrane-bound proton-pump ATPases. The normal process is that the endosomal content is then relocated to

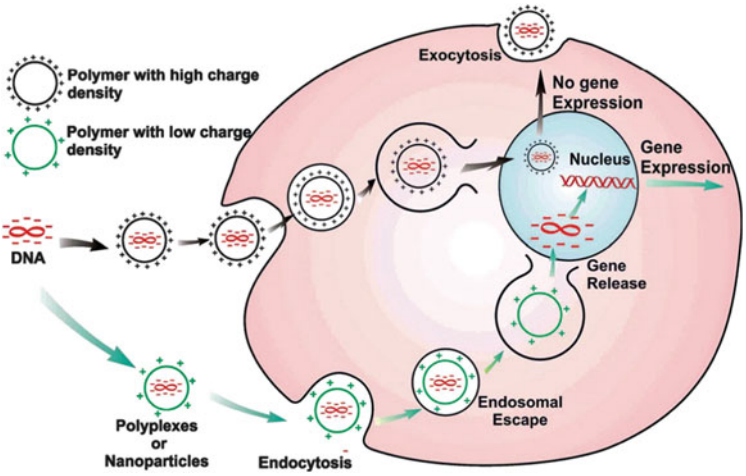

Scheme 13 Intracellular trafficking of polyplexes. The size of a polyplex is generally a few hundred nanometers (100–200 nm). Reprinted with permission from [100]. Copyright 2012 Elsevier

the lysosomes, which are further acidified (pH ~4.5) and contain various nucleases that promote the degradation of the DNA. To avoid lysosomal degradation, the genetic material (free or complexed with the carrier) must escape from the endosome into the cytosol (endosomal escape, Scheme 13) [118].

Release into the cytosol can be achieved by using bioresponsive polymers for triggered release (responsive to conditions or components present in the intracellular milieu) [118]. This type of polymer, such as those containing disulfide bonds, will not be discussed here because they are of little relevance to polyelectrolyte interactions and DNA complexation. Another way to favor endosomal escape is to use polymers that have a pH-buffering effect or "proton sponge effect." These polymers must contain amines that can act as a "proton sponge" in endosomes, preventing acidification of endosomal vesicles and thereby increasing the ATPase-mediated influx of protons and counter-ions (which enter the vesicles to balance the proton flux), leading to osmotic swelling, endosomal membrane rupture, and the eventual leakage of the polyplex into the cytosol (Scheme 14) [120].

Toxicity, Biocompatibility, and Biodegradability

The challenge is not limited to bringing the polyplex inside cells: even if the polyplexes overcome the extracellular barriers, it is not useful if, due do its intrinsic toxicity, the polyplex kills cells after uptake. This is in many cases the reason why the overall transfection efficiency of a polyplex is rather low, despite a high value for its cellular uptake. Thus, it is of prime importance to study the intracellular uptake, for example with fluorescence imaging, as well as the toxicity of both the

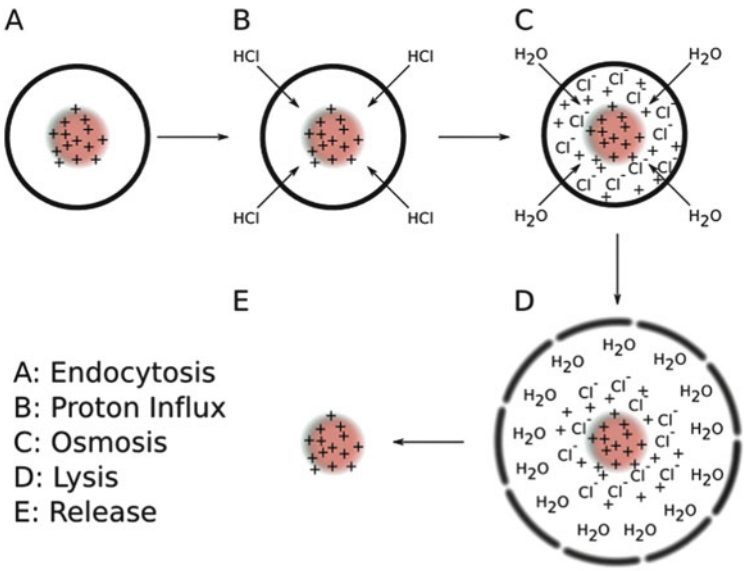

Scheme 14 The proposed proton sponge mechanism of endosomal escape. (**A**) Polyplexes enclosed in an endosome after endocytosis. (**B**) Due to the pH buffering in the endosome, the protons continue to be pumped into the vesicle, resulting in Cl^- influx and an increase in the osmolarity inside the endosomal vesicle. (**C**) Because of the osmolarity increase, water passes into the endosomal vesicle. (**D**) The increase in water volume results in the swelling of the endosomal compartment until it ruptures. (**E**) Release of the polyplex into the cytoplasm, which leads to nuclear uptake of DNA. Reprinted with permission from [119]. Copyright 2011 Elsevier

polymer and polyplex and the transfection efficiency of the polyplex at relevant concentrations and times of exposure. Almost as important is the comparison with a relevant standard such as PEI, because usually more than one parameter is varied (cell line, concentration, etc.) from one study to another and therefore the results are difficult to compare. In toxicity tests, the half maximal inhibitory concentration or IC_{50} is the quantitative measure used (in some of the publications IC_{50} also means the charge ratio causing 50% reduction of EtBr fluorescence). The cell lines most commonly used are: COS cell lines (CV-1, simian in origin, and carrying the SV40 genetic material), which resemble human fibroblast cells; human embryonic kidney 293 cell line (HEK 293), which is originally derived from human embryonic kidney cells grown in tissue culture; and HepG2 cell line that is a human liver hepatocellular carcinoma cell line.

It is to be mentioned that, as a general rule, strong polycations are highly toxic [121]. It is nevertheless possible to limit immediate toxicity by "masking" the non-biocompatible part to its environment via the introduction of hydrophilic biocompatible segments (such as PEG) into the construct. Biocompatibility is the ability of a polymer or material to perform with an appropriate host response (local and systemic) in a specific application and by not producing a toxic, injurious, or immunological response in living tissue. This is strongly determined by the primary

chemical structure. Sugar-based polymers (chitosan, dextran, etc.) are a great example of biocompatible materials. Increasing the biodegradability is of course an alternative way to limit toxicity (for instance, by incorporation of acid labile groups such as β-amino esters and ortho esters) because the byproducts of degradation can be eliminated by the body via natural pathways.

It is important to keep following criteria in mind for efficient polymer-mediated gene delivery: efficient compaction of genetic material (size <200 nm); stability of the polyplexes under physiological conditions (i.e., presence of salts, pH 7.4) because particles that precipitate under these conditions are not suitable for in vivo applications; high uptake by cells and intracellular release; and efficient transfection without inducing cytotoxicity. Moreover, biodegradability and targeting of the polyplexes are important properties for in vivo applications.

2 Polycation/DNA Complexes

2.1 Water-Soluble Polycations

2.1.1 Strong Polyelectrolytes

Strong polyelectrolytes are salts of quaternary ammonium cations (alkyl), pyridinium, or imidazolium with an anion. Charge neutralization is usually achieved at or close to a 1:1 stoichiometry for strong polycations and DNA.

Containing Aromatics or Having a Charged Backbone

In the pioneering work of Izumrudov and Zhiryakova, the shorter the PEVP (Fig. 3a) the less resistant was the polyplex to the addition of salts; this effect was much more pronounced for chain lengths between 10 and 100 than above [122]. Interestingly, the stability of the PEC was virtually independent of the length of the nucleic acid in the studied region (500 bp, DNA from salmon testes; 10,000 bp, calf thymus DNA). The longer the substituent (methyl, ethyl, and propyl), the longer was the distance between charges of DNA and quaternized PVP because of the shielding, and the less was the complexation efficiency. Also, a decrease in charge density (PEVP-β, quaternization degree $\beta = 23$ or 46%) led to a decrease in PEC stability and a decrease in the critical salt concentration (salt concentration at which half of the EtBr molecules are intercalated in DNA-free sites).

Given that poly(1-vinylimidazole) (PVIm) has a pK_a of around 5.5, this polymer does not complex DNA at physiological pH. Thus, Allen et al. quaternized the imidazole ring with various substituents such as bromoethanol in order to obtain permanently charged imidazolium-containing copolymers [107]. As the quaternization degree was increased, fewer sites were available for protonation,

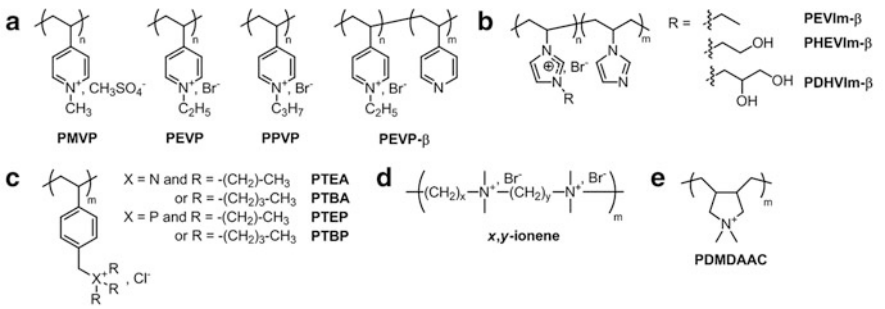

Name of the polymer	Abbreviation	Description of the polymer	DNA used	Ref
Poly(4-vinylpyridine)	PVP	DP_w = 10, 20, 40, 70, 100, 120, 340, 4000	ctDNA (10kbp) for EtBr Salmon testes DNA (500bp)	[122]
Poly(*N*-methyl-4-vinylpyridinium methyl sulfate)	PMVP	DP_w = 10, 20, 40, 70, 100, 120, 340, 4000, M_w/M_n = 1.1-1.2		
Poly(*N*-ethyl-4-vinylpyridinium bromide)	PEVP			
Poly(*N*-propyl-4-vinylpyridinium bromide)	PPVP			
Poly[(*N*-ethyl-4-vinylpyridinium bromide)-*co*-(4-vinylpyridine)]	PEVP-β	DP_w = 100, β = 23, 46%		
Poly(1-vinylimidazole)	PVIm	M_n = 23kDa, M_w/M_n = 1.89	pDNA: gWiz-Luc	[107]
Poly[(1-hydroxyethyl-3-vinylimidazolium bromide)-*co*-(1-vinylimidazole)]	PHEVIm-β	β = 13, 25, 50, 65, 100		
Poly[(1-ethyl-3-vinylimidazolium bromide)-*co*-(1-vinylimidazole)]	PEVIm-β	β = 25		
Poly[[1-(1,2-propanediol)-3-vinylimidazolium bromide]-*co*-(1-vinylimidazole)]	PDHVIm-β	β = 25		
Poly[triethyl-(4-vinylbenzyl)ammonium chloride]	PTEA	M_n = 230kDa, M_w/M_n = 1.67	pDNa: gWiz-Luc	[125]
Poly[tributyl-(4-vinylbenzyl)ammonium chloride]	PTBA	M_n = 224kDa, M_w/M_n = 1.74		
Poly[triethyl-(4-vinylbenzyl)phosphonium chloride]	PTEP	M_n = 304kDa, M_w/M_n = 1.59		
Poly[tributyl-(4-vinylbenzyl)phosphonium chloride]	PTBP	M_n = 254kDa, M_w/M_n = 1.82		
Aliphatic ionenes via Menshutkin polyaddition reaction between *N,N,N′,N′*-tetramethylethylene diamine (TMED) and dibromoalkanes	*x,y*-ionene	x = 2, y = 4, 8, 10, DP = 10- 30	ctDNA (10kbp) pDNA: pCMV-Luc	[126]
Poly(*N,N′*-dimethyldiallylammonium chloride)	PDMDAAC	DP = 1400	ctDNA not specified	[127]

Fig. 3 Strong polycations containing aromatics or having a charged backbone: (**a**–**c**) Vinyl polymers containing aromatics and other architectures such as (**d**) ionenes, and (**e**) poly (*N,N′*-dimethyldiallylammonium chloride)

thus the buffering capacity of the polymer decreased. With an increase in the quaternization percentage of PHEVIm-β, (Fig. 3b) the N:P ratio necessary for complexation with DNA decreased as well as the polyplex size (accompanied by a slight increase in zeta potential), suggesting a tighter binding between the polymer and pDNA. These effects reached a plateau at around 50% quaternization. At the same time, by increasing the quaternization percentage, the cytotoxicity increased (typical case). The maximum gene expression was observed for 25% quaternization for PHEVIm, which can be attributed to the right balance between PEC stability and efficient DNA release. To study the effects of adjacent hydroxyl number on transfection efficiency, two additional 25% quaternized copolymers, PEVIm-25, which did not contain hydroxyl groups, and PDHVIm-25 containing two hydroxyl groups for every four repeat units ($n = 2$) were compared to PHEVIm-25, which contained on average one hydroxyl group for every four repeat units ($n = 1$). As the number of hydroxyl groups increased, the initial N:P ratio required for polyplex formation decreased, suggesting hydrogen bond formation between the polycation and pDNA (Scheme 15). Indeed, previously, Reineke and colleagues found that the incorporation of hydroxyl groups further enhanced the

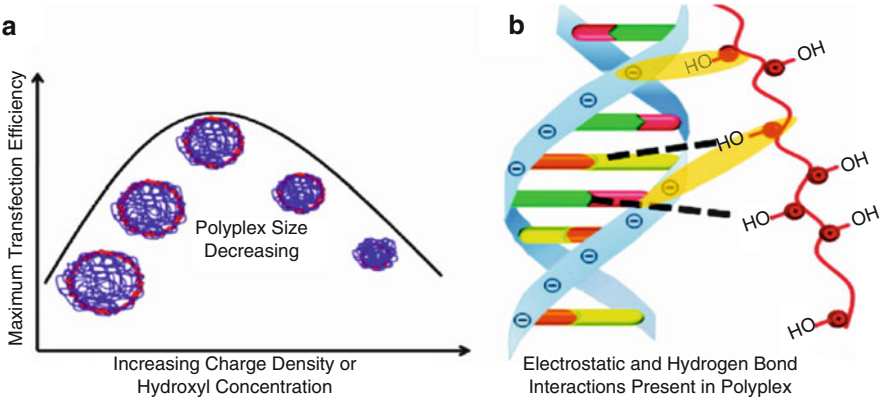

Scheme 15 (**a**) Structure–property–transfection relationships for imidazolium copolymers with controlled charge density and side chain hydroxyl number. (**b**) Cationic polymers electrostatically bind and condense anionic pDNA, forming a polyplex. Various factors, including hydrogen bonding, impact polyplex stability. Reprinted with permission from [107]. Copyright 2011 American Chemical Society

binding of polymer to pDNA through hydrogen bonding and concluded that hydrogen bond formation between polymers and pDNA would serve as a less toxic alternative to high charge density polyelectrolytes [108].

Regarding transfection efficiency, PEVIm-25 was two orders of magnitude less efficient than SuperFect tranfection reagent, while PHEVIm-25 was less than one order of magnitude less efficient and two orders more efficient than naked DNA in COS-7 cells; however, PDHVIm-25 was slightly less efficient than PHEVIm-25. Therefore, a balance has to be found between the hydrogen bonding properties of the polycation (facilitating DNA binding but not its release) and the shielding of the positive charge by the presence of hydroxyl groups, which reduces the protein adsorption and cytotoxicity but also the transfection efficiency. For the PVIm copolymers, one hydroxyl group in the form of PHEVIm seemed to be the optimal choice. This approach using hydroxyl groups to benefit from the hydrogen bonding capacity and decrease in toxicity has also been used with weak polyelectrolytes based on polymethacrylates [123, 124].

Ammonium- and phosphonium-containing polyelectrolytes (PTEA, PTBA, PTEP, and PTBP) differing in the nature of the quaternized group (ammonium versus phosphonium) and the length of their substituents (triethyl versus tributyl) were studied by the group of Long (Fig. 3c) [125]. According to gel electrophoresis, the ammonium polyelectrolytes bound DNA at higher +/− ratio compared to the phosphonium polyelectrolytes, which suggested improved DNA binding of phosphonium cations over ammonium cations. The authors proposed that a combination of different charge densities and cation sizes (phosphonium is a larger cation with less diffuse positive charge than ammonium) were responsible for the better DNA binding affinity of the phosphonium polyelectrolytes compared to ammonium. All polyelectrolytes condensed DNA into polyplexes of about 200 nm or less

at +/− ratio of 4, except for PTBP, which condensed DNA into polyplexes of this size at +/− ratio of 6, meaning that the binding is less tight. PTEA, PTBA, and PTEP also exhibited a plateau in their zeta potential (positive) without significant change from a +/− ratio of 2. PTBP polyplexes generated at +/− ratio of 2 had zeta potentials near neutral, and then a positive plateau starting at +/− ratio of 4. The presence of a plateau in the polyplex diameter and zeta potential suggests that the additional polymer remained as free polymer in the solution, uncomplexed to DNA. The zeta potentials of the triethyl-based polyplexes were more positive than those of the tributyl-based polyplexes due to hydrophobic screening of the cationic charge with longer alkyl chains. All polymers exhibited similar toxicities due to their 100% charge densities, approximately like that of the transfection reagent jetPEI. PTEA and PTEP displayed poor transfection efficiency compared with SuperFect, whereas PTBA and PTBP exhibited excellent transfection, similar to SuperFect. Given that the entry into the cell of all polyplexes was successful, the higher transfection efficiency of tributyl-containing polyelectrolytes over triethyl-based polyelectrolytes could be due to a higher endosomolytic activity.

Ionene are polycations with charged quaternized nitrogen atoms in the polymer backbone (Fig. 3d). Izumrudov and colleagues synthesized ionenes via Menshutkin polyaddition reaction between *N*,*N*,*N*′,*N*′-tetramethylethylenediamine (TMED) and dibromoalkanes such as 1,4-dibromobutane and 1,8-dibromooctane [126]. For [ionene]/[DNA] < 1, the increase in ionene content was accompanied by a substantial decrease in PEC particle size (from 500 to 100 nm), up to a charge ratio of unity, where the particles were neutral and formed aggregates. With excess polycation, the positively charged PEC did not aggregate, and at charge ratios of the polymers of 2:1 the particle size was again ~100 nm, regardless of the charge density or chain length of the polycation. Nevertheless, a difference could be observed in the protection of DNA against nuclease attack: the polymers with the highest DP offered better protection and, at a given DP, the shortest spacer (i.e., the highest charge density) was preferred. These results correlated with the stability of the polyplexes, even if upon lengthening of the ionene chains (DP > 20), the difference in PEC stability between ionenes with different spacers became relatively small. The transfection efficiency in COS-7 cells followed the same trend for the ionenes as the PEC stability.

By comparing the DNA/polycation complexes based on various architectures such as PEVP (Fig. 3a), ionene (Fig. 3d) and PDMDAAC, which is a polycation of pendant type (Fig. 3e), Galaev and colleagues suggested that phase separation in solutions of DNA-containing PECs (with strong polycations without steric stabilization) follows the general rules ascertained from PECs formed by flexible vinyl polyanions. However, the high rigidity of the double helix of native DNA appears to be responsible for significant extension of the region of insoluble PECs at the expense of the region in which soluble PECs are formed [127].

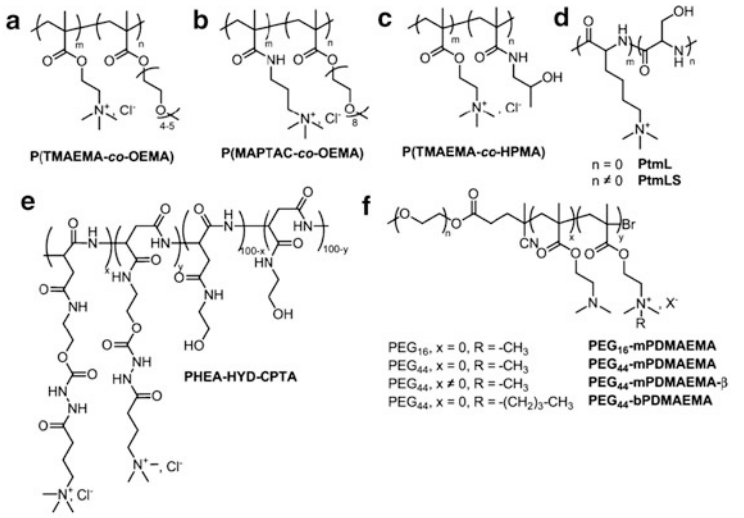

Name of the polymer	Abbreviation	Description of the polymer	DNA used	Ref
Poly(trimethylammonio ethylmethacrylate)	PTMAEMA	M_w = 300kDa	Salmon DNA (Sigma)	
Poly{(trimethylammonio ethylmethacrylate)-*co*-[oligo(ethylene glycol)methyl ether methacrylate]}	P(TMAEMA-*co*-OEMA)	M_w = 280kDa, 15% POE	Salmon DNA (Sigma) $M_w = 10.4 \times 10^6$ g.mol^{-1}	[128]
Poly{[(3-methacrylcylamino propyl) trimethylammonium chloride]-*co*-[oligo(ethylene glycol)methyl ether methacrylate]}	P(MAPTAC-*co*-OEMA)	mol.% POE: 68; mol.% POE: 89, $M_w = 1.8 \times 10^6$Da; mol.% POE: 94, $M_w = 3.5 \times 10^6$Da	ctDNA: 2-2.5kbp	[129]

Poly{(trimethylammonio ethylmethacrylate)-*co*-[*N*-(2-hydroxypropyl)methacrylamide]}	P(TMAEMA-*co*-HPMA)	mol.% TMAEMA: 5, M_w = 35kDa;
		mol.% TMAEMA: 15, M_w = 41kDa;
		mol.% TMAEMA: 50, M_w = 13kDa;
		mol.% TMAEMA: 100. M_w = 34kDa
			ctDNA for EtBr and zeta potential: pDNA 5.5kb encoding β-galactosidase for the rest of the stucies	[130]

Poly(L-lysine)	PLL	M_w = 18700, M_w/M_n = 1.8	pEGFP-N1 pT7-Luc Salmon testis DNA	[131]
Poly(trimethylated L-lysine)	PtmL	M_w = 24800, M_w/M_n = 1.4		
Poly(L-lysine-*co*-serine)	PLS	86:14, M_w = 23.4kDa, M_w/M_n = 3.4		
Poly(trimethylated L-lysine-*co*-serine)	PtmLS	86:14, M_w = 30.6kDa, M_w/M_n = 2.2		
α,β-Poly[(N-2-hydroxyethyl/carbazate)-D,L-aspartamide]	PHEA-HYD	mol.% HYD: 20.2, M_w = 40kDa, M_w/M_n = 1.81 mol.% HYD: 40.6, M_w = 40.5kDa, M_w/M_n = 1.78	ctDNA	[132]
α,β-Poly[(*N*-2-hydroxyethyl)-*N*-carbazate[*N*-(3-trimethylammonium chloride)propylhydrazide]-D,L-aspartamide}	PHEA-HYD-CPTA	mol.% CPTA: 20, M_w = 46kDa, M_w/M_n = 1.69 mol.% CPTA: 40, M_w = 40.5kDa, M_w/M_n = 1.66		
PEG_{16}-methylated PDMAEMA	PEG_{16}-mPDMAEMA	M_n = 28kDa, 90 CG per molecule	pCV-Tat average mass per charge: 330Da	[133]
PEG_{44}-methylated PDMAEMA	PEG_{44}-mPDMAEMA	M_n = 91kDa, 300 CG per molecule		
PEG_{44}-partially methylated PDMAEMA	PEG_{44}-mPDMAEMA-β	55%, M_n = 56.4kDa, 127 CG per molecule 30%, M_n = 48.2kDa, 70 CG per molecule		
PEG_{44}-butylated PDMAEMA	PEG_{44}-bPDMAEMA	M_n = 80.6kDa, 230 CG per molecule		

Fig. 4 (**a**–**f**) Strong polycations with side chains containing quaternary ammoniums: Methyl methacrylate and amide backbones

With Side Chains Containing Quaternary Ammoniums

In regular DNA/polycation systems, at a charge ratio close to unity, macroscopic phase separation occurs: the cationic units of the polymers will form ion pairs with the anionic phosphate groups of DNA to yield charge-neutralized complexes. By the introduction of a sufficient amount of steric stabilizer such as PEG in the polycation (as block copolymer or grafts), this macroscopic phase separation can be avoided due to the lyophilizing effect of the PEG segments and the complexes will remain stable in solution. This was observed for P(TMAEMA-*co*-OEMA), $M_w = 2.8 \times 10^5$ g mol^{-1}, 15 mol% oligo(ethylene glycol) grafts (OE), and 4–5 oligo(ethylene glycol)methyl ether units per graft (Fig. 4a) [128] compared

to the non-PEGylated polymer at a ratio close to unity and for similar polymers, P(MAPTAC-*co*-OEMA), with higher degree of OE substitution, 8 oligo(ethylene glycol)methyl ether units per graft, $M_w = 1.8 \times 10^6$ g mol^{-1} for 89 mol% OE, and $M_w = 3.5 \times 10^6$ g mol^{-1} for 94 mol% OE (Fig. 4b) [129]. Complete binding of DNA by these polycations occurred at a ratio of more than 1 due to the presence of PEG, which partially screens the charges of the polycation (the higher the PEG content, the higher the ratio for complete binding). At a charge ratio of ~2 for these P(MAPTAC-*co*-OEMA) copolymers, the zeta potential reached a plateau at a neutral value and the hydrodynamic diameter stayed constant, meaning that the excess polycation was not incorporated into the polyplex. On the contrary, for the examples of the last paragraph that did not possess a steric component and for which the same phenomenon had mainly an electrostatic explanation, the lack of incorporation of the excess polycation into the polyplex occurred in this case mainly because of the steric repulsion produced by the PEG corona. Moreover, the DNA present in these polyplexes was inaccessible to DNAse I, which clearly indicates that the PEG segments present in the outer part of the polyplexes protect the DNA inside the polyplexes. Nevertheless, it is surprising that despite the high content of PEG in the polycation, the DNA binding was still efficient. By contrast, for P(MAPTAC-*co*-OEMA) the zeta potential was positive at a high charge ratio of random copolymers, P(TMAEMA-*co*-HPMA) (Fig. 4c) [130]. Nevertheless, only binding of DNA is not enough and a tight binding is desired. The copolymers P (TMAEMA-*co*-HPMA) containing the lowest degree of ammonium (5 and 15%) showed virtually no ability to displace EtBr and also did not protect DNA from degradation by endonucleases, probably because their association with DNA was too weak. The inverse tendency has been observed for PLL and PLS and their trimethylated derivatives (PtmL and PtmLS, respectively; Fig. 4d) [131]: the complexes with trimethylated peptides seemed to be looser (according to EtBr complexation and exchange reaction with anions) but the compaction of DNA occured at lower charge C/A ratio, due to their higher charge density.Interestingly, the transfection efficiency of the trimethylated PtmLS into COS-1 cells was better than that of PtmL and the non-quaternized derivatives, despite their similar intracellular distribution. Thus, it seems that a loose structure for the release of DNA from the complex (at best from endosome into the cytoplasm) is necessary, as well as the presence of functional groups such as serine residues that impart hydrophilicity and hydrogen bonding capacity.

A similar construct to PLL, based on a slightly different amide backbone, a polyaspartamide derivative containing a quaternary ammonium, α,β-poly{(*N*-2-hydroxyethyl)-*N*-carbazate[*N*-(3-trimethylammonium chloride) propylhydrazide]-D,L-aspartamide} (PHEA-HYD-CPTA) (Fig. 4e) [132], also revealed itself to efficiently complex DNA and reduce its rate of degradation by DNAse. Similar polymers but with a block structure were also efficient at protecting DNA against enzymatic degradation. Indeed, partially methylated PEG-mPDMAEMA-β and completely methylated PEG-mPDMAEMA or butylated PEG-bPDMAEMA with PEG blocks of various lengths (Fig. 4f) [133] formed, as previously explained, micellar-type

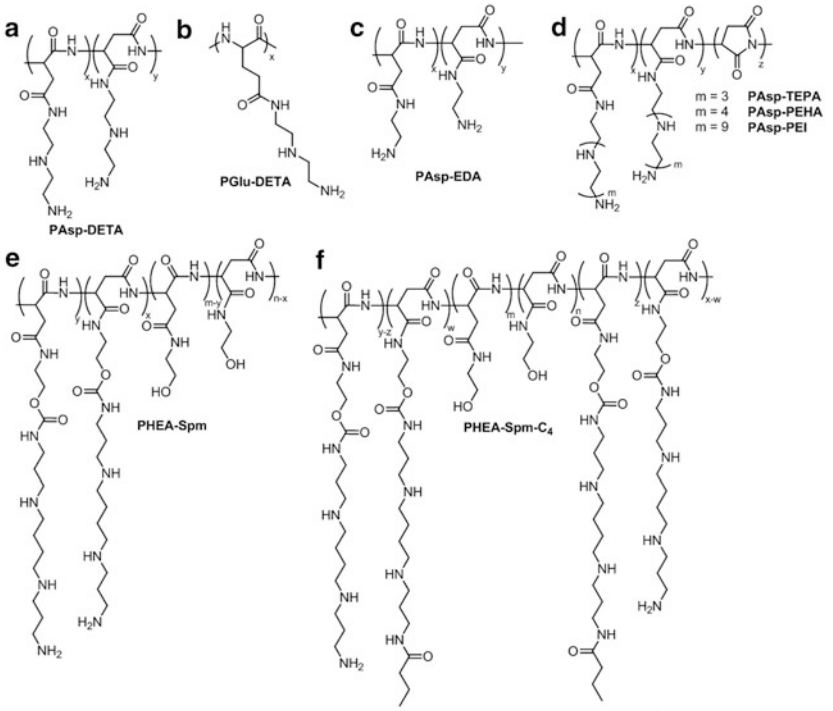

Name of the polymer	Abbreviation	Description of the polymer	DNA used	Ref
Poly[*N*-[*N*-(2-aminoethyl)-2-aminoethyl]aspartamide]	PAsp-DETA	Precursor: DP = 102, M_w/M_n = 1.06, M_w ~ 20kDa	pDNA: pGL4.13 (encoding firefly luciferase) pRL-CMV(encoding renilla luciferase)	[134]
Poly[*N*-[*N*-(2-aminoethyl)-2-aminoethyl]glutamide]	PGlu-DETA	Precursor: DP = 89, M_w/M_n = 1.11, M_w ~ 20kDa		
Polyaspartamide modified with ethylene diamine	PAsp-EDA	M_w = 17.8kDa	pDNA: pRE-Luc, 11.9kb	[135]
Polyaspartamide modified with tetraethylene pentamine	PAsp-TEPA	m = 3, M_w = 9.8kDa		
Polyaspartamide modified with pentaethylene hexamine	PAsp-PEHA	m = 4, M_w = 10.9kDa		
Polyaspartamide modified with polyethyleneimine	PAsp-PEI	m = 9, M_w = 14.5kDa		
α,β-Poly[(*N*-2-hydroxyethyl)-D,L-aspartamide] modified with spermine	PHEA-Spm	M_w = 40kDa, M_w/M_n = 1.6	pDNA: pCMV-Luc	[136]
α,β-poly[(*N*-2-hydroxyethyl)-D,L-aspartamide] modified with spermine-butyramide	PHEA-Spm-C_4	M_w = 36kDa, M_w/M_n = 1.8		

Fig. 5 (**a**–**f**) Weak polycations without steric stabilizer: Polyaspartamide and polyglutamide and their derivatives

structures with a PEG protective shell that is more difficult to achieve for polymers grafted with oligoethylene glycol segments.

2.1.2 Weak Polyelectrolytes

Without Steric Stabilizer

Polyaspartamide Derivatives

PAsp-DETA (Fig. 5a), a polyaspartamide derivative [134] that is degradable and thus causes minimal toxicity, shows a higher transfection efficiency in

HUVEC cells after repeated administration compared to linear PEI (22 kDa) and PGlu-DETA (Fig. 5b) that are non-biodegradable. Among polyaspartamides modified with oligoethyleneimine side chains of various lengths [ethylene diamine (PAsp-EDA) in Fig. 5c, and triethylene pentamine (PAsp-TEPA), pentaethylene hexamine (PAsp-PEHA), and polyethyleneimine (PAsp-PEI) in Fig. 5d] [135], PAsp-PEHA showed the highest capacity of condensation, similar to PAsp-PEI (diameter <300 nm), while PAsp-EDA showed the lowest DNA condensation capacity. Full retardation of DNA migration occurred at N:P = 1:1 for PAsp-TEPA, PAsp-PEHA, and PAsp-PEI, and only at 5:1 for PAsp-EDA. This trend was also observed for the transfection efficiency in HEK293 cells, meaning that the length of oligoethyleneimine side chains is an important factor and that a side chain with four ethylene imine repeating units was enough for condensation. Similar polyaspartamide derivatives (α,β-poly[(*N*-2-hydroxyethyl)-D,L-aspartamide]) but with spermine side chains (and not oligoethylene imine) were studied by the group of Cavallaro, i.e., α,β-poly[(*N*-2-hydroxyethyl)-D,L-aspartamide] modified with spermine (PHEA-Spm) (Fig. 5e) and α,β-poly[(*N*-2-hydroxyethyl)-D,L-aspartamide] modified with spermine-butyramide (PHEA-Spm-C_4) (Fig. 5f) [136]. In this case, full retardation of DNA migration was observed at C:P = 0.75 for PHEA-Spm and 2 for Spm-C_4. The zeta-potential values became positive at a polycation:DNA weight ratio above 1.5 for PHEA-Spm, and 2.5 for PHEA-Spm-C_4. These values are in agreement with the lower amount of free primary amino groups present in PHEA-Spm-C_4 compared with PHEA-Spm. A nearly total quenching of EtBr was reached at C:P = 8 for PHEA-Spm, and at 10 for Spm-C_4, but at the same time the condensing ability of PHEA-Spm-C_4 was superior to that of PHEA-Spm; at C:P = 1 the polyplex diameter was 600 nm for PHEA-Spm and 130 nm for PHEA-Spm-C_4. It seems that the introduction of a short hydrophobic chain in the structure enabled an increased condensing capacity, probably conferred by hydrophobic interactions with DNA, which in turn led to a decrease in transfection efficiency, which could be due to the stability of the polyplex (even if EtBr displacement shows equivalent performances).

Other Polyamide Backbones

Poly(amidoamine)s with pendant primary amines [amino ethane (PA-AE), amino butane (PA-AB), and amino hexane (PA-AH)] (Fig. 6a) [137] all had a better buffering capacity than branched PEI of 25 kDa. Those with the longest alkyl chains had higher buffering capacity than PA-AE in the pH range 5–7, which is important for endosomal release. Cytotoxicity in 293T and COS-7 cells was concentration dependent and proportional to the length of the alkyl chain: the longer the chain, the more toxic. As in the case of polyaspartamide modified with oligoethyleneimine side chains of various lengths [135], the shortest chain showed the lowest condensation capacity (even if no secondary amines were present in the side chains of these poly(amidoamine)s with pendant primary amines). This suggests that the condensation capacity (size of the polyplex) was mainly a function of the accessibility and degree of protonation of the primary and tertiary amines.

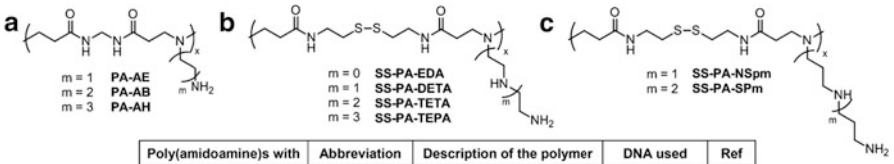

Poly(amidoamine)s with	Abbreviation	Description of the polymer	DNA used	Ref
pendant amino ethane	PA-AE	M_w = 18kDa, M_w/M_n = 1.50	pDNA: pGL-3 PEGFP-C1	[137]
pendant amino butane	PA-AB	M_w = 11.7kDa, M_w/M_n = 2.80		
pendant amino hexane	PA-AH	M_w = 11.7kDa, M_w/M_n = 2.51		
ethylene diamine	SS-PA-EDA	M_w = 3.5kDa, M_w/M_n = 1.92	pCMCLacZ	[139]
diethylene triamine	SS-PA-DETA	M_w = 3.0kDa, M_w/M_n = 1.25		
triethylene tetramine	SS-PA-TETA	M_w = 4.6kDa, M_w/M_n = 1.53		
tetraethylene pentamine	SS-PA-TEPA	M_w = 5.1kDa, M_w/M_n = 1.39		
norspermidine	SS-PA-NSpm	M_w = 6.2kDa, M_w/M_n = 1.33		
spermine	SS-PA-Spm	M_w = 5.3kDa, M_w/M_n = 1.17		

Fig. 6 (**a**–**c**) Weak polycations without steric stabilizer: Polyamide backbones

Polymers with longer chains showed better performances until a certain chain length, given that when the flexibility of the chains was sufficient, no further improvements were observed (zeta potentials had the same profile). These results showed that these poly(amidoamine)s with pendant primary amines were a bit less efficient than polyaspartamide derivatives of comparable length regarding full retardation of DNA migration. Indeed, DNA was fully retarded at N:P = 5 for PA-AE, 3 for PA-AB, and 2 for PA-AH; this could be explained by the absence of secondary amines in the side chains. Despite the better performances of PA-AH, its transfection efficiency in 293T cells was lower than that of PA-AB, probably due to its higher cytotoxicity or its slightly lower buffering capacity. It is important to note that the transfection efficiency of these polymers was dependent on the cell type (low transfection efficiency in COS-7 cells compared to 293T).

Comparable bioreducible [138] poly(amidoamine)s with oligoamine side chains (ethyleneimine or spermine type) were studied by Engbersen and coworkers [139]. The introduction of disulfide linkages in the backbone is a way to reduce the cytotoxicity by promoting its biodegradability in the reducing intracellular environment, in contrast to the last example [137]. Moreover, the cleavage of the backbone is supposed to promote DNA release intracellularly, thus improving the transfection. Indeed, poly(amidoamine)s with pendant ethylene diamine (SS-PA-EDA), diethylene triamine (SS-PA-DETA), triethylene tetramine (SS-PA-TETA), and tetraethylene pentamine (SS-PA-TEPA) (Fig. 6b) showed extremely low cytotoxicity in COS-7 cells even at 50 μg/mL (more than 90% cell viability reported, but duration of exposure was not clear) [139]. Nevertheless, poly(amidoamine)s with pendant norspermidine (SS-PA-NSpm) or spermine (SS-PA-Spm) (Fig. 6c) showed much higher toxicities. The enlargement of the alkyl spacer between the amino groups in the side chain from ethylene to propylene seems to be responsible for the higher cytotoxicity. When one compares the cytotoxicity of SS-PA-EDA, SS-PA-DETA, SS-PA-TETA, and SS-PA-TEPA in COS-7 cells to PA-AE, PA-AB, and PA-AH [137], the two last polymers showed much higher toxicities at the same concentration after 24 h exposure, which might only be an effect of duration of exposure and a time-dependent cytotoxicity.

If not the duration, this could be a positive effect of the disulfide bond or the lower M_w. Except for SS-PA-EDA, these poly(amidoamine)s showed comparable or slightly higher buffering capacities than branched PEI of 25 kDa. Similar results as for poly (amidoamine)s with pendant primary amines concerning DNA retardation in gel electrophoresis were obtained with the best polymer, SS-PA-TEPA (N:P = 2). All these polycations condensed pDNA in a similar manner as regards the diameter of the polyplexes (<150 nm). The polyplexes of the SS-PA bearing secondary amines in their side chain (SS-PA-DETA, SS-PA-TETA, and SS-PA-TEPA) induced relatively high transfections, but those of SS-PA-EDA with only a terminal primary amino group in the side chain gave only low transfection efficiency, reinforcing the idea that a minimum chain length is needed and/or the presence of secondary amines and higher buffering capacities of the polymers, suggesting a more facilitated endosomal escape of their polyplexes. Enlargement of the alkyl spacer between the amino groups in the side chain from ethylene to propylene (SS-PA-NSpm and SS-PA-Spm) had a negative effect on transfection efficiency. The reason was unclear given that polyplex size, surface charge, and buffering capacity did not deviate significantly from the other SS-PA. This could be due to their inherent cytotoxicity.

PDMAEMA and Derivatives

Poly[2-(dimethylamino)ethyl methacrylate] (PDMAEMA) is usually used as weak polyelectrolyte for gene delivery and has the additional property of being temperature sensitive [140, 141]. The study by Stolnik and coworkers on PDMAEMA (Fig. 7a) emphasized the condensation behavior of PDMAEMA as a function of pH [102]. As can be intuitively understood, the ionization of PDMAEMA increases from pH 8 (only 24% ionization) to pH 4 (polycation nearly completely ionized), therefore the binding of PDMAEMA with DNA is tighter (EtBr displacement assay) at lower pH, which is "counterproductive" when it comes to release of the genetic material. But, this effect is balanced by its buffering capacity via the tertiary amine groups, which is favorable for endosomal escape.

PDMAEMA of various molecular weights were tested by the group of Hennink for their transfection efficiency [142]. In COS-7 and OVCAR-3 cells, high molecular weight polymers (M_w < 300 kDa) were more efficient in transfection than the low molecular weight polymers (M_w < 60 kDa), which was related to their property as condensing agents. Low molecular weight polymers led to polyplexes with sizes bigger than 300 nm (up to 1 μm), while high molecular weight polymers gave polyplexes with sizes in the range 150–200 nm, and these smaller particles seemed to enter the cells more easily.

PDMAEMA and its derivatives PDMAPMAm, PDMAPMA, PDMAEMAm, and PTMAEMA of higher molecular weight (M_n > 25 kDa) than in the first study or of comparable molecular weight in the case of PDMAEA and PDEAEMA (M_n < 10 kDa) (Fig. 7b–e) were studied by Hennink and colleagues [143]. The methacrylate/methacrylamide derivatives of PDMAEMA of high molecular weight were able to condense pDNA, yielding polyplexes with sizes of

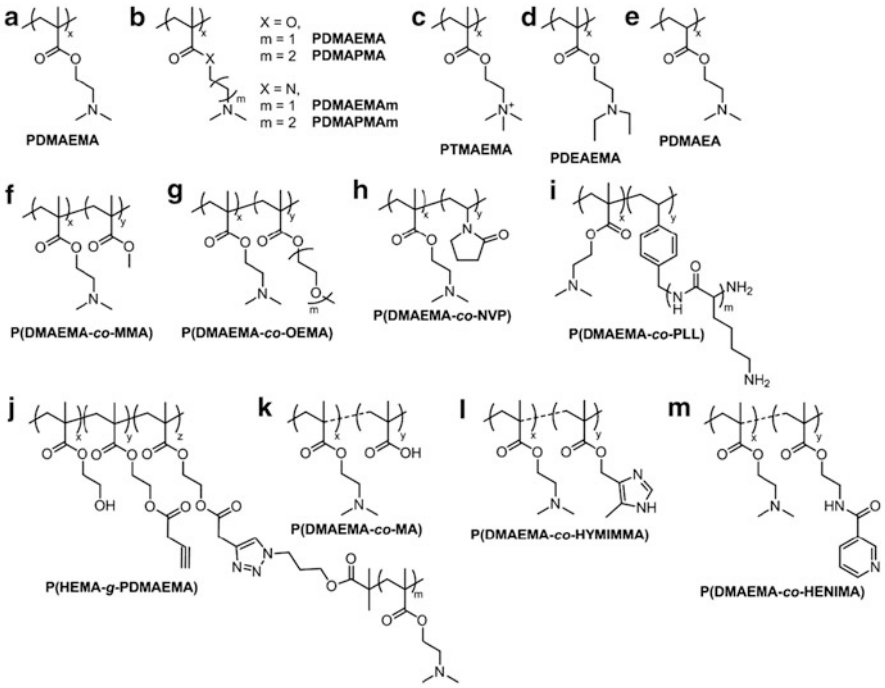

Name of the polymer	Abbreviation	Description of the polymer	DNA used	Ref
Poly[2-(dimethylamino)ethyl methacrylate]	PDMAEMA	M_n = 5.13kDa, M_w/M_n = 1.18	ctDNA	[102]
Poly[2-(dimethylamino)ethyl methacrylate]	PDMAEMA	M_n = 50 ± 30kDa, M_w = 550 ± 200kDa, av. pK_a = 7.4	pDNA: pCMV-LacZ	[143]
Poly[2-(dimethylamino)ethyl methacrylamide]	PDMAEMAm	M_n = 27 ± 12kDa, M_w = 120 ± 60kDa, av. pK_a = 7.8		
Poly[2-(dimethylamino)propyl methacrylate]	PDMAPMA	M_n = 27 ± 6kDa, M_w = 275 ± 90kDa, av. pK_a = 8.4		
Poly[2-(dimethylamino)propyl methacrylamide]	PDMAPMAm	M_n = 30 ± 19kDa, M_w = 220 ± 180kDa, av. pK_a = 8.8		
Poly[2-(dimethylamino)ethyl acrylate]	PDMAEA	M_n = 7 ± 1kDa, M_w = 25 ± 4kDa, av. pK_a = 8.2		
Poly[2-(diethylamino)ethyl methacrylate]	PDEAEMA	M_n = 8 ± 2kDa, M_w = 90 ± 20kDa, av. pK_a = 7.5		
Poly[2-(trimethylamino)ethyl methacrylate]	PTMAEMA	M_n = 70 ± 24kDa, M_w = 845 ± 145kDa, av. pK_a = no pK_a		
Poly{[2-(dimethylamino)ethyl methacrylate]-*co*-(methyl methacrylate)}	P(DMAEMA-*co*-MMA)	mol.% MMA = 20, M_n = 42kDa, M_w = 92kDa	pCMV-LacZ	[142]
Poly{[2-(dimethylamino)ethyl methacrylate]-*co*-(ethoxy triethylene glycol methacrylate)}	P(DMAEMA-*co*-OEMA)	mol.% OEMA = 21, M_n = 45kDa, M_w = 106kDa mol.% OEMA = 48, M_n = 48kDa, M_w = 111kDa		
Poly{[2-(dimethylamino)ethyl methacrylate]-*co*-(*N*-vinyl pyrrolidone)}	P(DMAEMA-*co*-NVP)	mol.% NVP = 14, M_n = 54kDa, M_w = 108 kDa mol.% OEMA = 54, M_n = 50kDa, M_w = 113 kDa		
Poly{[2-(diethylamino)ethyl methacrylate]-*co*-poly(L-lysine)}	P(DMAEMA-*co*-PLL)	PLL: P_n = 20, mol.% PLL = 2.5, 4.3, 8.8, M_n =40kDa	ctDNA	[144]
		PLL: P_n= 30, mol.% PLL = 1.5, M_n = 40kDa		
Poly[(hydroxyethyl methacrylate)-*g*-poly(2-(dimethylamino)ethyl methacrylate]	P(HEMA-*g*-PDMAEMA)	N_3-pDMAEMA: M_n = 8.7kDa, M_w = 10.0kDa pHEMA: M_n = 6.9kDa, M_w = 8.2kDa %clickable HEMA in backbone = 52% P(HEMA-*g*-PDMAEMA): M_n = 45.2kDa, M_w = 79.3kDa	pCMV-LacZ	[145]
		N_3-pDMAEMA 2: M_n = 8.7kDa, M_w = 10.0kDa pHEMA: M_n = 13.2kDa, M_w = 18.7kDa %clickable HEMA in backbone = 23% P(HEMA-*g*-PDMAEMA): M_n = 52.7kDa, M_w = 589kDa		
Poly(dimethylaminoethyl methacrylate)	PDMAEMA	M_w = 93kDa, M_w/M_n = 1.6	ctDNA (23kb)	[146]
		M_w = 110kDa, M_w/M_n = 1.3		
		M_w = 166kDa, M_w/M_n = 1.3		
		M_w = 201kDa, M_w/M_n = 1.4		
Poly{(dimethylaminoethyl methacrylate)-*co*-(methacrylic acid)}	P(DMAEMA-*co*-MA)	DMAEMA:MA = 82:18, M_w = 108kDa, M_w/M_n = 1.3		
		DMAEMA:MA = 65:35		
Poly{(dimethylaminoethyl methacrylate)-*co*-[4-(5-methylimidazoyl) methyl methacrylate]}	P(DMAEMA-*co*-HYMIMMA)	DMAEMA:HYMIMMA = 94:6, M_w = 99.5kDa, M_w/M_n = 1.4		
		DMAEMA:HYMIMMA = 88:12, M_w = 72kDa, M_w/M_n = 1.5		
		DMAEMA:HYMIMMA = 81:19, M_w = 54kDa, M_w/M_n = 1.3		
Poly{(dimethylaminoethyl methacrylate)-*co*-[*N*-(2-hydroxyethyl) nicotinamide methacrylate]}	P(DMAEMA-*co*-HENIMA)	DMAEMA:HENIMA = 90:10, M_w = 140kDa, M_w/M_n = 1.3		
		DMAEMA:HENIMA = 89:11, M_w = 164kDa, M_w/M_n = 1.4		

Fig. 7 (**a**–**m**) Weak polycations without steric stabilizer (except (**g**) and (**j**) for comparison): PDMAEMA and derivatives

100–300 nm and a slightly positive zeta potential, while PDMAEA and PDEAEMA were not capable of condensing pDNA to small particles, possibly due to their relatively low molecular weight (and low solubility of PDEAEMA at pH 7). The transfection efficiency and the cytotoxicity of the polymers differed widely: the highest transfection efficiency and cytotoxicity were observed for PDMAEMA. As PDMAEMA is capable of condensing DNA to small particles and has the lowest average pK_a value (7.5) of all condensing derivatives, PDMAEMA has the highest buffering capacity and probably behaves as the best candidate for endosomal escape. Furthermore, molecular modeling showed that, of all studied polymers, PDMAEMA has the lowest number of interactions with DNA. Therefore, the authors hypothesized that the superior transfection efficiency of its polyplexes can be ascribed to the intrinsic property of this polymer to destabilize endosomes combined with an easy dissociation of the polyplex once present in the cytosol and/or nucleus.

Hennink and colleagues also studied copolymers of DMAEMA with various monomers such as the hydrophobic methyl methacrylate (MMA) in P(DMAEMA-*co*-MMA) (Fig. 7f), or hydrophilic *N*-vinyl pyrrolidone (NVP) in P(DMAEMA-*co*-NVP) (Fig. 7h), and OEGMA in P(DMAEMA-*co*-OEMA) (Fig. 7g) of $M_w > 90$ kDa [142]. A copolymer with 20 mol% of MMA showed reduced transfection efficiency and a substantially increased cytotoxicity compared with PDMAEMA of the same molecular weight. A copolymer with OEGMA (48 mol%) showed both a reduced transfection efficiency and a reduced cytotoxicity (presence of OEMA), whereas a copolymer with NVP (54 mol%) yielded smaller particles at a lower P:DNA ratio than PDMAEMA or than the other copolymers with equivalent degree of modification (as NVP interacts with DNA via hydrogen bonding) and showed an increased transfection and decreased cytotoxicity.

Further derivatives of PDMAEMA were synthesized in order to improve its condensation ability at physiological pH, such as a comb-type polycation consisting of P(DMAEMA-*co*-PLL) (Fig. 7i) [144]. This copolymer possessed a pH-dependent behavior due to the presence of PDMAEMA (pK_a 7.5) and PLL (pK_a 10). The presence of the PLL segments prevented precipitation of the copolymer at pH > 7.5, as is the case for PDMAEMA homopolymer, and this comb-type polymer was capable of DNA condensation at pH 8 (as observed using circular dichroism).

Poly(hydroxyethyl methacrylate) backbones, onto which poly [2-(dimethylamino)ethyl methacrylate] of various lengths were grafted via click chemistry [P(HEMA-*g*-PDMAEMA), $M_w > 75$ kDa; Fig. 7j], were able to condense DNA into small particles (90–190 nm, at a polymer to plasmid mass ratio of 6) [145] and the sizes as well as the zeta potentials of the P(HEMA-*g*-PDMAEMA)-based polyplexes were independent of the molecular weight of P(HEMA-*g*-PDMAEMA) (for M_w of 75 kDa and above). P(HEMA-*g*-PDMAEMA) showed more EtBr quenching than the starting PDMAEMA, indicating a weaker binding of this low molecular weight polymer to the pDNA. However, it showed similar quenching as high molecular weight PDMAEMA, but less toxicity.

A study comparing PDMAEMA with PEGylated derivatives and different functional groups such as tertiary amine, pyridine, imidazole, and acid groups was conducted by Schacht and colleagues [146]. They found that the presence of methacrylic acid in P(DMAEMA-*co*-MA) (Fig. 7k) increased the amount of polymer needed for DNA condensation with increasing amount of acid groups, which can be explained by the repulsive effect between anionic DNA and the negatively charged carboxylate groups. A similar effect was observed for imidazole-containing polymers, as the imidazole groups are not protonated under the experimental conditions. These results also correlated with the zeta potential measurements: the greater the amount of these groups (negatively charged or neutral), the lower the zeta potential of the polyplexes. P(DMAEMA-*co*-MA), P(DMAEMA-*co*-HYMIMMA) (Fig. 7l), and P(DMAEMA-*co*-HENIMA) (Fig. 7m) were able to condense DNA into nanoparticles with size <300 nm at a charge ratio of 2:1 but with bimodal or trimodal distributions (not well-defined, possibly due to aggregation).

PNIPAM Derivatives

Homopolymers of PNIPAM have a lower critical solution temperature (LCST) around body temperature. The LCST of copolymers of PNIPAM such as P(DMAEMA-*co*-NIPAM (Fig. 8a) gradually increased with increasing content of DMAEMA (hydrophilic monomer) and was independent of the molecular weight (38.3–45.7°C for a DMAEMA content of 15–30% and >80°C for a content of 80%) [147]. All P(DMAEMA-*co*-NIPAM) copolymers (M_w > 91 kDa), even with a low DMAEMA content of 15 mol%, were able to bind to DNA. With increasing NIPAM content, the charge density of the copolymer decreased and the P:DNA ratio needed for condensation to occur increased. Concerning the polyplexes, with increasing NIPAM content, the zeta potential of the polyplexes at the optimum P:DNA ratio decreased, as did the cytotoxicity and transfection efficiency. The authors postulated that these polyplexes interacted less with the negatively charged membrane, thus leading to lower transfection efficiency. At 37°C, even if the LCST was not passed, complexes made from low molecular weight polymers (independent of the content) or of high molecular weight with low DMAEMA content (15%) showed poor properties as transfection agents, which was linked to their poor stability.

The condensation properties of PLL-*g*-PNIPAM (Fig. 8b) were governed, like in the last case, by the PNIPAM content related to the condensing units such as lysine (higher content of PNIPAM, less condensation efficiency) but the molecular weight of the PNIPAM grafts did not have a significant effect [148]. As also observed in the previous study [147], the size of the complexes increased with increasing PNIPAM content at 25°C due to an internal swelling of the hydrated PNIPAM chains. At 38°C (above the phase transition of PNIPAM), the size of the polyplexes decreased as a consequence of the collapse of PNIPAM chains, accompanied by a higher structural density and thus a more difficult release of DNA.

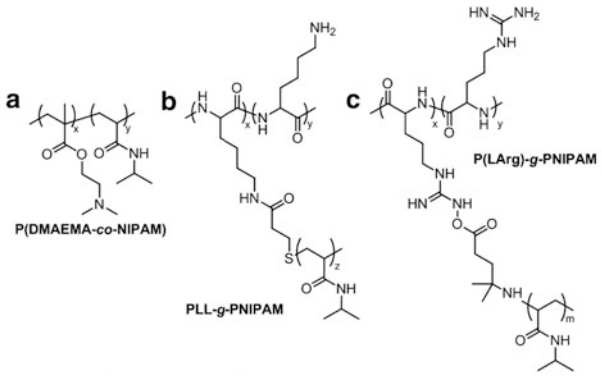

Name of the polymer	Abbreviation	Description of the polymer	DNA used	Ref
Poly([2-(dimethylamino)ethyl methacrylate]-*co*-(*N*-isopropylacryl amide))	P(DMAEMA-*co*-NIPAM)	DMAEMA/NIPAM ~ 0/100, 15/85, 30/70, 80/20, 100/0 M_n ~ 9-138kDa, M_w ~ 91-1237kDa	pDNA: pCMVLacZ	[147]
Poly(L-lysine)-*g*-poly(*N*-isopropylacryl amide)	PLL-*g*-PNIPAM	M_nPNIPAM grafts = 4.2kDa %wt. PNIPAM in copolymer = 21, M_w = 110kDa; %wt. PNIPAM in copolymer = 42, M_w = 150kDa; %wt. PNIPAM in copolymer = 62, M_w = 230kDa	pDNA: pGL3-control (5.2kb)	[148]
		M_nPNIPAM grafts = 12.4 kDa %wt. PNIPAM in copolymer: 21, M_w = 110kDa; %wt. PNIPAM in copolymer: 42, M_w = 150kDa; %wt. PNIPAM in copolymer: 55, M_w = 190kDa		
Poly(L-arginine)-*g*-poly(*N*-isopropylacryl amide)	P(LArg)-*g*-PNIPAM	M_nPNIPAM = 2.1kDa, M_w/M_n = 1.88 M_nPArg = 7.5kDa	pDNA: pGL3-control pEGFP-C1	[149]

Fig. 8 (**a–c**) Weak polycations without steric stabilizer: PNIPAM derivatives

Similar architectures based on polyarginine of shorter length than PLL, P(LArg)-*g*-PNIPAM (Fig. 8c), showed comparable results concerning the physico-chemical characteristics of the polyplexes and were influenced by the LCST of PNIPAM (LCST of P(LArg)-*g*-PNIPAM was 35.2°C) [149]. The low cytotoxicity of P(LArg)-*g*-PNIPAM was also attributed to the reduction in the positive charge density of polyarginine upon incorporation of neutral PNIPAM chains. Transfection studies in COS-1 cells showed that temporary cooling below the LCST of P(LArg)-*g*-PNIPAM was favorable for gene expression and that via this method, at an appropriate complexation ratio, the transfection efficiency of P(LArg)-*g*-PNIPAM was equivalent to that of Lipofectamine 2000.

PLL Derivatives

Derivatives of PLL containing endosomal escape moieties such as imidazole or histidine are presented in this section. Copolymers of PLL-*g*-Im (Fig. 9a) with various content of imidazole (>73.5%) were all capable of condensing DNA but at higher ratios and bigger size of polyplexes than PLL alone [150]. Nevertheless, they all had a very low cytotoxicity in various cell lines (CRL1476 smooth muscle cells, P388D1 macrophages, HepG2 hepatoblastoma) compared to PLL, which cannot be explained by big discrepancies in the zeta potentials. At pH 7.2, approximately 5% of the imidazole groups on the polymer are protonated and are potentially available to assist the PLL moieties in the condensation of DNA. Interestingly, with a 9%

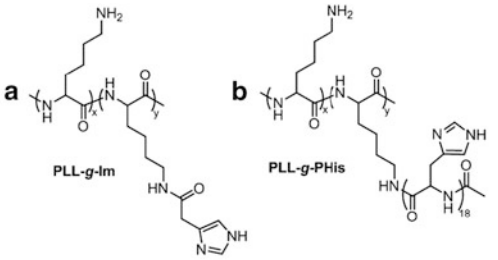

Name of the polymer	Abbreviation	Description of the polymer	DNA used	Ref
Poly(L-lysine)-*g*-imidazole	PLL-*g*-Im	PLL: M_t = 34.3kDa, mol.% imidazole grafting: 73.5. 82.5, 86.5%	pCMV-Luc	[150]
Poly(L-lysine)-*g*-imidazole	PLL-*g*-Im	PLL: M_w = 9.4kDa, mol.% imidazole grafting: 0, 16, 53, 80, 92%	pDNA: pCMV-Luc (5.5kb), pEGFP-N1 (4.7kb)	[151]
		PLL: M_w = 34.3kDa, mol.% imidazole grafting: 0, 58, 95%		
		PLL: M_w = 52.7kDa, mol.% imidazole grafting: 0, 23, 57, 90, 96%		
Poly(L-lysine)-*g*-polyhistidine	PLL-*g*-PHis	PLL: 8.0kDa, pHis: 18 His, 25% substitution	pDNA: pSV-*β*-gal	[153]

Fig. 9 (**a**, **b**) Weak polycations without steric stabilizer: PLL derivatives

increase in imidazole content (from 73.5 to 82.5 mol%), the level of luciferase expression approximately doubles at each DNA:polymer ratio. However, with a further 4% increase in imidazole content (from 82.5 to 86.5 mol%), luciferase expression levels approximately double again. These results suggest a nonlinear relationship between polymer imidazole content and protein expression. Later studies of PLL-*g*-Im with other M_w and percentage of grafting (Fig. 9a) gave more insights into this phenomenon [151]. The studies showed that the polymer cytotoxicity was reduced when the polymer was complexed with pDNA and decreased with increasing imidazole content and decreasing molecular weight. As in the previous study [150], the polymers with the highest IC_{50} (i.e., lowest toxicity and highest imidazole content) also mediated the highest level of protein expression in NIH-3T3 cells, probably due to the endosomal escape capacity of imidazole groups. But, increased protein expression in a culture population did not always correlate with an increased number of transfected cells. As the imidazole content increases, the polymer becomes less cationic and is therefore less able to electrostatically interact with DNA and quench EtBr fluorescence (condensation); at the same time, the relative binding affinity for DNA increases with increasing imidazole content for polymers of various molecular weights, which suggests that other intermolecular forces play a role [152].

Similar results concerning the cytotoxicity were found for PLL-*g*-PHis (Fig. 9b) [153], which are in line with the transfection efficiency. Once more, the decrease in cationic charges due to the substitution of PLL backbone led to a lowering of the cytotoxicity, and the introduction of histidine (imidazole ring) led to better transfection efficiency due to its buffering capacity, i.e., endosomal escape properties.

Other Amino Acid-Based Polymers

Generally, polymers modified with histidine or other moieties containing an imidazole group have shown significant enhancement of gene expression without

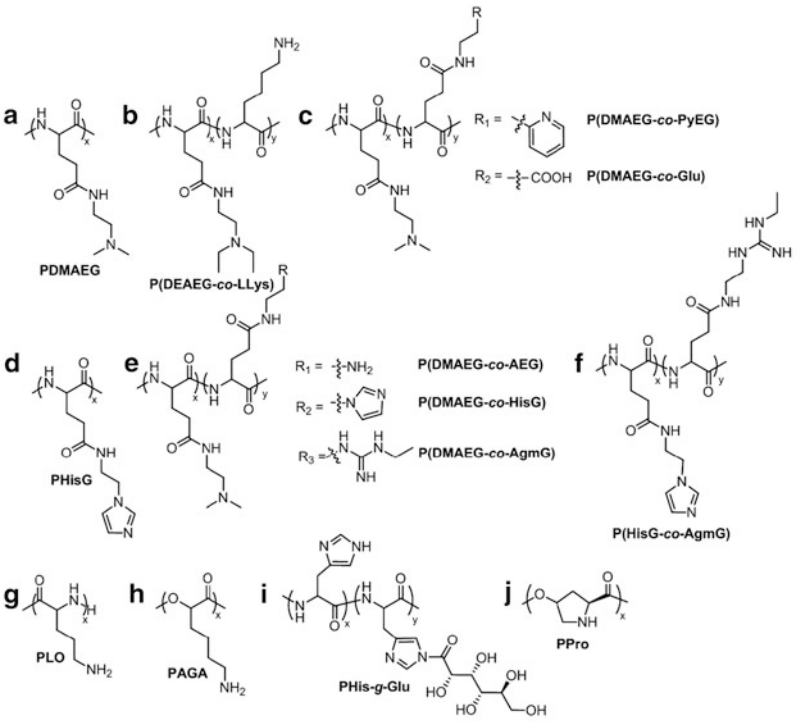

Name of the polymer	Abbreviation	Description of the polymer	DNA used	Ref
Poly(dimethylaminoethyl-L-glutamine)	PDMAEG	M_w[a] = 59kDa	DNA not specified	[161]
Poly[(dimethylaminoethyl-L-glutamine)$_{89\%}$-*co*-(pyridinoethyl-L-glutamine)$_{11\%}$]	P(DMAEG-*co*-PyEG)	M_w[a] = 60kDa		
Poly[(dimethylaminoethyl-L-glutamine)$_{92\%}$-*co*-(L-glutamic acid)$_{8\%}$]	P(DMAEG-*co*-Glu)	M_w[a] = 84kDa		
Poly[(diethylaminoethyl-L-glutamine)$_{67\%}$-*co*-(L-lysine)$_{33\%}$]	P(DEAEG-*co*-LLys)	M_w[a] = 77kDa		
Poly[(dimethylaminoethyl-L-glutamine)$_{85\%}$-*co*-(aminoethyl-L-glutamine)$_{15\%}$]	P(DMAEG-*co*-AEG)	M_w[a] = 77kDa	ctDNA not specified	[162]
Poly[(dimethylaminoethyl-L-glutamine)-*co*-(histamino-L-glutamine)]	P(DMAEG-*co*-HisG)	M_w = 23-32kDa %HisG substitution: 18, 36, 55, 76, 88%		
Poly(histamino-L-glutamine)	PHisG	M_n[b] = 22kDa		
Poly[(dimethylaminoethyl-L-glutamine)$_{83\%}$-*co*-(agmatino-L-glutamine)$_{17\%}$]	P(DMAEG-*co*-AgmG)	M_n[b] = 24kDa		
Poly[(histamino-L-glutamine)$_{73\%}$-*co*-(agmatino-L-glutamine)$_{27\%}$]	P(HisG-*co*-AgmG)	M_n[b] = 24kDa		
Poly(L-histidine)-*g*-gluconic acid	PHis-*g*-Glu	PHis: M_w = 11kDa, DP = 81, PHis-*g*-Glu: ~4 sugars / polymer chain (x:y = 1:23)	pDNA: pCMV-β-gal	[164]
Poly(L-ornithine)	PLO	M_w[c] = 50.7kDa, M_w/M_n = 1.24	pDNA: pCMVβ (7.2kb)	[165]
		M_w = 30-70kDa,	pDNA: pUC19	[169]
Poly[α-(4-aminobutyl)-L-glycolic acid]	PAGA	M_n[d] = 3.3kDa	pDNA: pSV-β-gal	[170]
Poly(4-hydroxy-L-proline ester)	PPro	M_n = 1.2kDa, M_w = 1.3kDa	pDNA: pCMV-β-gal	[171]

[a] determined by MALLS; [b] determined by ^{1}H NMR spectroscopy; [c] determined by LALLS; [d] determined by MALDI.

Fig. 10 (**a**–**j**) Weak polycations without steric stabilizer: other amino acid-based polymers such as polyglutamic acid, polyornithine, polyhistidine, etc.

increased cytotoxicity, compared with non-modified polymers, but can present solubility problems [154–160].

Schacht and colleagues. studied (co)polymers of dimethylaminoethyl-L-glutamine (PDMAEG, Fig. 10a) and L-glutamic acid [P(DMAEG-*co*-Glu); Fig. 10c-R_2], partially grafted with various moieties such as pyridine in P(DMAEG$_{89\%}$-*co*-

PyEG$_{11\%}$) (Fig. 10c-R$_1$) [161], primary amine in P(DMAEG$_{85\%}$-*co*-AEG$_{15\%}$ (Fig. 10e-R$_1$), imidazole in P(DMAEG-*co*-HisG) (Fig. 10e-R$_2$), and ethylguanidine in P(DMAEG$_{83\%}$-*co*-AgmG$_{17\%}$) (Fig. 10e-R$_3$) [162] and compared them with PDMAEG and P(DEAEG$_{67\%}$-*co*-LLys$_{33\%}$) (Fig. 10b) [161] as well as with PHisG (Fig. 10d) and poly[(histamino-L-glutamine)$_{73\%}$-*co*-(agmatino-L-glutamine)$_{27\%}$] (P(HisG-*co*-AgmG); Fig. 10f) [162]. The mass per charge for all the copolymers was in the range 222–290 Da. The highest condensations (EtBr) were obtained for PDMAEG and P(DEAEG-*co*-LLys) compared to P(DMAEG-*co*-PyEG) and P(DMAEG-*co*-Glu) (but all gave <50% EtBr fluorescence), respectively, because of the highest percentage of tertiary amines among the PDMAEG derivatives and the presence of the primary amines of PLL [161]. All the copolymers were degradable under biologically relevant conditions in a time frame varying from hours to days, and formed polyplexes with DNA with a diameter <100 nm. The most potent polymers in transfection studies in HEK293 cells were the polymers containing pyridine and acid groups (by a factor of ten) and not PDMAEG or P(DEAEG-*co*-LLys) [162]. The explanation for the better performances of the pyridine derivatives was not clear, given that the pyridine moiety did not provide extra buffering capacity. The potency of the polymers containing a carboxylic acid group could be because it eventually destabilized the cell membranes in its carboxylate form.

Polymers containing more than 70% imidazole were not able to condense DNA (>50% EtBr fluorescence), i.e., PHisG, P(HisG$_{73\%}$-*co*-Agm$_{27\%}$), or the copolymers from the P(DMAEG-*co*-HisG) series [162]. PDMAEG, P(DMAEG$_{85\%}$-*co*-AEG$_{15\%}$), P(DMAEG$_{82\%}$-*co*-HisG$_{18\%}$), and P(DMAEG$_{64\%}$-*co*-HisG$_{36\%}$) all possessed a similar charge ratio, causing 50% reduction of EtBr fluorescence (+/− around 0.8), and this value increased with increasing imidazole content; P(DMAEG$_{84\%}$-*co*-AgmG$_{16\%}$) showed a higher value than P(DMAEG$_{85\%}$-*co*-AEG$_{15\%}$). According to the authors, this might be due to the longer distance between the charged guanidine group and the main polymer chain in comparison with the polymers containing tertiary and primary amines, resulting in a weaker electrostatic interaction between the polymer and the DNA. On the same line, the smallest complexes were formed with P(DMAEG$_{85\%}$-*co*-AEG$_{15\%}$), probably because of the primary amines that allow a better interaction with the DNA in comparison with the tertiary amines (less steric hindrance, higher protonation degree). PHisG and P(His$_{73\%}$-*co*-AgmG$_{27\%}$) formed the largest complexes. In the case of pHisG, the large size could be due to the weak interaction between the polycation and the DNA (few imidazole functions are protonated). The large complexes formed with P(His$_{73\%}$-*co*-AgmG$_{27\%}$) could be explained by the fact that the zeta potential of the complexes was close to neutrality, leading to aggregation of the complexes. All the polyplexes, except those based on P(HisG$_{73\%}$-*co*-AgmG$_{27\%}$), had low transfection efficiency in COS-1 cells, which could be due to their poor ability to interact with the membrane of the cells and thus the polyplexes were not taken up by the cells [163]. On the other hand, polyplexes based on PHisG$_{73\%}$-*co*-PAgmG$_{27\%}$ (more cytotoxic) at a ratio of 8:1 were more efficient than PEI-DNA at a ratio of 2:1, which may be due to the presence of the guanidine functions (more pronounced

positive charge of the guanidine functions, $pK_a = 12.5$, in comparison with tertiary amines, $pK_a = 10$).

Other imidazole derivatives based on poly(L-histidine) partially grafted with gluconic acid (PHis-*g*-Glu, Fig. 10i) to impart solubility at physiological pH (polyhistidine is insoluble in aqueous solutions at pH >6.0) were reported by Pack et al. [164]. Approximately one carbohydrate–imidazole substitution out of every 23 imidazole groups was enough to confer solubility of at least 100 mg mL^{-1} at pH 7. Migration of DNA was completely retarded at a pHis-*g*-Glu:DNA weight ratio of 3:1, which was consistent with the charge ratio causing 50% reduction of EtBr fluorescence; the size of the polyplexes at this ratio was >500 nm. The DNA seemed to be fully condensed at a pHis-*g*-Glu:DNA weight ratio of 5:1, given that the size of the polyplexes was 240 nm at pH 7. Unfortunately, these polyplexes were unable to transfect COS-7 cells, maybe because of their large size, despite their negligible cytotoxicity.

Poly(L-ornithine) (PLO, Fig. 10g) has a structure similar to polylysine, except that it possesses one CH_2 less in the side chain. In a publication by the group of Gumbleton, polyplexes based on PLO, PLL and poly(D-lysine) (PDL) possessed roughly similar physico-chemical characteristics; nevertheless, the polyplexes based on PLO showed better transfection capacity in A459cells and COS-7 cells [165]. It should be noted that condensation of pDNA occurred at the following charge ratios (<10% EtBr fluorescence): 0.8:1 for PLO, 1.2:1 for PLL, and 1.5:1 for PDL, and that PLO polyplexes also showed greater resistance to polyanion-induced disruption. As explained by the authors, Blauer and Alfassi had previously suggested that the additional CH_2 group contained within the lysine may make the α-helix conformation in PLL more stable than in PLO [166]. Given the comparable pK_a values of the primary amine groups for lysine and ornithine ($pK_a = 10.5–10.7$) [167], it is probable that conformational differences rather than protonation per se provides a basis for the differential behavior of PLO-mediated pDNA condensation. The least effective condensing polycation was PDL. Given that the L-isomer is the natural orientation of nuclear enzymes and proteins, it is possible that DNA interactions with other macromolecules are biased towards L-isomer conformations [168].

In order to determine the size of the polyplexes, most of the studies use light scattering, which gives the R_h as well as other information, but is not able to give the exact structure of the polyplexes. Therefore, AFM is a complementary method to light scattering and allows imaging matter at the nanoscale (possible interactions with the surface of the wafers should nevertheless be taken into account). An AFM study of the complexation of DNA by PLO was conducted by the group of Ganguli and could provide insights into the mechanism of DNA condensation [169]. Based on AFM images, the mechanism seemed to be different at low (<7 μg mL^{-1}) and high DNA concentrations (>13 μg mL^{-1}), i.e., monomolecular and multimolecular condensations, respectively (Scheme 16). It should nevertheless be noted that in contrast to most of the studies where the polycation is added to DNA solution, in this study DNA was added to the polymer solution, which could influence the mechanism pathway.

Scheme 16 Proposed mechanism of condensation of plasmid DNA with poly-L-ornithine at high (13–20 μg mL^{-1}) and low DNA (3–7 μg mL^{-1}) concentrations. Monomolecular condensation is seen at low DNA concentration whereas both monomolecular and multimolecular condensation are seen at high DNA concentrations. Reprinted with permission from [169]. Copyright 2007 Elsevier

A low molecular weight PAGA (Fig. 10h) has also been tested [170]. The structure of PAGA is similar to PLL except for the backbone linkages, which are ester bonds for PAGA and peptide bonds (amide) for PLL. PAGA strongly condensed DNA at a charge ratio of less than 2 (<10% EtBr fluorescence), with a charge ratio of around 1 causing 50% reduction in EtBr fluorescence (results in the same order as PLL). The fast degradation of PAGA compared to PLL was suggested to be a way to reduce toxicity and lead to a faster release of DNA from the polyplexes after internalization by the cells, and was confirmed in 293 cells. The transfection efficiency of PAGA was indeed three times higher than PLL under optimized conditions (PLL, charge ratio 6; PAGA, charge ratio 60). According to the authors, the tenfold charge ratio required for PAGA compared to that for PLL was the result of the premature degradation of PAGA.

Poly(4-hydroxy-L-proline ester) (Fig. 10j) of low molecular weight, another polyester based on amino acids, was also hypothesized as a good candidate due

to its degradability, and indeed achieved low cytotoxicity in COS-7 cells [171]. Complete DNA retardation occurred at weight ratio of 1:1 where the polyplexes were neutral and therefore aggregated (size >1,300 nm) but efficient condensation was observed at polymer:DNA ratio of 2:1 (size of the polyplex <200 nm). Unfortunately the transfection efficiency of these polyplexes was not reported.

Peptoids (poly-*N*-substituted glycines) are a class of peptidomimetics whose side chains are appended to the nitrogen atom of the peptide backbone, rather than to the α-carbons [172]. Despite their relatively tedious synthesis, there are prospective applications in the biomedical field, for instance in gene therapy [173, 174]. The most efficient peptoid from a vast series as DNA condensing agent was based on the repetition of *N*-(2-aminoethyl)glycine (Nae) and *N*-(2-phenylethyl) glycine (Npe), $(NpeNpeNae)_{12}$, showing the importance of the presence of primary amines and hydrophobic motifs [175]. The authors could show that the spacing of charged residues on the peptoid chain as well as the degree of hydrophobicity of the side chains had much influence on the ability to form homogeneous complexes with DNA. Moreover, the authors found that the transfection efficiency was highly dependent on the primary sequence of the peptoid and, to a lesser degree, on the length of the peptoid. Zuckermann and colleagues studied another series of peptoids based on the alternance of primary amine and hydrophobic groups, either phenyl or isopropyl, and lipitoids (peptoid–phospholipid conjugates) starting from these peptoids [176]. At charge ratios above unity, only $(NpeNpeNae)_{12}$ and $(NaeNpeNpe)_{12}$ and both lipitoids were efficient in inducing transfection, which was correlated with significant cytotoxicity. Unfortunately, it was not possible in this study to correlate the physical properties of peptoid/lipitoid:DNA complexes with their transfection capabilities.

PMMA and Methacrylamide Derivatives

For a series of PAEM homopolymers (Fig. 11a) with various molecular weights [177], the ability to condense DNA and resistance against heparin destabilization increased with increasing molecular weight (retardation of DNA in gel electrophoresis at a ratio N:P of 1:1 for $PAEM_{75}$ and $PAEM_{150}$, and at a ratio 2:1 for $PAEM_{45}$). Regardless of PAEM chain length, the size of the polyplexes were <200 nm for a wide range of N:P ratio, their zeta potentials at N:P ratio of 8:1 were roughly similar, as was their cytotoxicity. On one hand, longer PAEM chains enhanced cellular uptake and nuclear localization of the polyplexes (probably linked to the greater stability of the polyplexes that might interact more strongly with membranes, according to the authors), while on the other hand shorter PAEM chains facilitated intracellular dissociation (more easily displaced from the polyplex). Nevertheless, even if the ideal carrier should posses both properties, the polymer with the longest chains also showed the highest transfection efficiencies in dendritic cells.

PHisA (Fig. 11a) is a water-soluble polymer possessing buffering capacity in the endosomal pH range [178]. All PHisA polymers with M_n in the range of

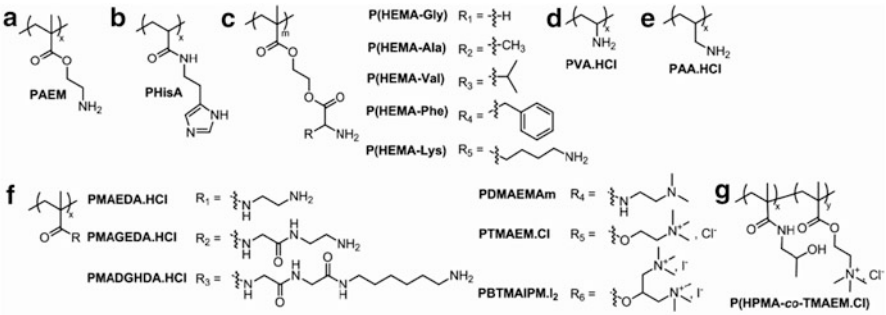

Name of the polymer	Abbreviation	Description of the polymer	DNA used	Ref
Poly(2-aminoethyl methacrylate)	PAEM	$PAEM_{45}$: DP = 45, M_n = 9.8kDa, M_w/M_n = 1.19 $PAEM_{75}$: DP = 75, M_n = 16.6kDa, M_w/M_n = 1.20 $PAEM_{150}$: DP = 150, M_n = 33.7kDa, M_w/M_n = 1.16	pDNA: pEGFP-N1, pCMV-Luc, pCMV-OVA	[177]
Poly(histamine acrylamide)	PHisA	$pHisA_{120}$: M_n = 9.2kDa, M_w/M_n = 1.82 $pHisA_{180}$: M_n = 12.7kDa, M_w/M_n = 1.46 $pHisA_{300}$: M_n = 17.5kDa, M_w/M_n = 1.91 $pHisA_{600}$: M_n = 28.7kDa, M_w/M_n = 1.72	pDNA: pEGFP-C1, pCMV-Luc	[178]
Poly(hydroxyethylmethacrylate) coupled with glycine	P(HEMA-Gly)	P(HEMA-Gly-Boc): M_n = 30.8kDa, M_w/M_n = 1.77	DNA not specified	[179]
Poly(hydroxyethylmethacrylate) coupled with alanine	P(HEMA-Ala)	P(HEMA-Ala-Boc): M_n = 13.8kDa, M_w/M_n = 1.71 P(HEMA-Ala-Boc): M_n = 28.8kDa, M_w/M_n = 2.10		
Poly(hydroxyethylmethacrylate) coupled with valine	P(HEMA-Val)	P(HEMA-Val-Boc): M_n = 29.2kDa, M_w/M_n = 1.41 P(HEMA-Val-Boc): M_n = 38.8kDa, M_w/M_n = 2.08		
Poly(hydroxyethylmethacrylate) coupled with phenylalanine	P(HEMA-Phe)	P(HEMA-Phe-Boc): M_n = 22.1kDa, M_w/M_n = 1.40		
Poly(hydroxyethylmethacrylate coupled with lysine)	P(HEMA-Lys)	P(HEMA-Lys-Boc): M_n = 12.4kDa, M_w/M_n = 1.64		
Poly(vinylamine) hydrochloride	PVA.HCl	Mass per primary amino group: 43Da, M_n = 3, 8, 60kDa	Circular 6 kb expression vector containing a CMV promoter-driven β-glactosidase reporter and ampicillin resistance	[180]
Poly(allylamine) hydrochloride	PAA.HCl	Mass per primary amino group: 57Da, M_w = 54.7kDa		
Poly[methacryloyl-NH-$(CH_2)_2$-NH_2] hydrochloride	PMAEDA.HCl	Mass per primary amino group: 164.5Da, M_w = 18.6, 41.9kDa		
Poly[methacryloyl-Gly-NH-$(CH_2)_2$-NH_2] hydrochloride	PMAGEDA.HCl	Mass per primary amino group: 221.6Da, M_w = 29.4, 82.0, 322.8kDa		
Poly[methacryloyl-Gly-Gly-NH-$(CH_2)_6$-NH_2] hydrochloride	PMADGHDA.HCl	Mass per primary amino group: 334.6Da, M_w = 38.4, 73.7, 333.5kDa		
Poly(2-dimethylaminoethyl methacrylamide)	PDMAEMAm	Mass per primary amino group: 157Da, M_w = 54.7kDa		
Poly[2-(trimethylammonio) ethyl methacrylate chloride]	PTMAEM.Cl	Mass per charge: 208 Da, M_n = 5 kDa or M_w = 8.5, 21.2, 34.1, 413.0kDa		
Poly[(2-hydroxypropyl)methacrylamide-*co*-(2-(trimethylammonio) ethyl methacrylate chloride)]	P(HPMA-*co*-TMAEM.Cl)	Mass per charge: 5% TMAEM.Cl: 2925 Da, M_w = 35kDa; 15% TMAEM.Cl: 351 Da, M_w = 41kDa; 50% TMAEM.Cl: 255 Da, M_w = 13kDa; 75% TMAEM.Cl: 208 Da, M_w = 16kDa		
Poly[1,3-bis-(trimethylammonio) isopropyl methacrylate iodide]	PBTMAIPM.I_2	Mass per charge: 249Da, M_w = 93.1kDa		

Fig. 11 (**a**–**g**) Weak polycations without steric stabilizer: PMMA and methacrylamide derivatives

9.2–28.7 kDa were able to completely inhibit DNA migration at a N:P ratio of 5:1 (higher ratios than for PAEM, containing primary amines [177]). At N:P ratios <15:1, the size of PHisA polyplexes decreased with increasing molecular weights from 9.2 to 17.5 kDa, whereas 17.5 and 28.7 kDa PHisA condensed DNA into comparable particle sizes at the same N:P ratios, as well as with increasing N:P ratio. For PAEM (M_n = 9.8–33.7 kDa)-based polyplexes, the size was nearly independent of chain length or charge ratio. At an N:P ratio of 15:1 and above, all PHisA polymers were able to condense DNA into nanosized particles (<220 nm), and the sizes as well as zeta potentials reached a plateau (moderate positive surface charges of 13–19 mV). Although less toxic than PEI25K, by comparing the transfection efficiency of $pHisA_{180}$ and $pHisA_{300}$ in COS-7 cells to that of PEI25K at N:P ratio of 10, it was shown that their efficiency was slightly higher than for PEI, which could be attributed to their higher buffering capacity.

Preliminary results were reported on PHEMA substituted with amino acids such as glycine [P(HEMA-Gly), Fig. 11c-R_1], alanine [P(HEMA-Ala), Fig. 11c-R_2], valine [P(HEMA-Val), Fig. 11c-R_3], phenylalanine [P(HEMA-Phe), Fig. 11c-R_4], and lysine [P(HEMA-Lys, Fig. 11c-R_5] [179]. These polymers were able to condense DNA, while having very little toxicity (up to 250 μg mL^{-1} tested on COS-7 and SPCA-1 cell lines); unfortunately, only preliminary results were reported and there was no comparison between these amino acid-substituted PHEMAs, despite their interesting structures.

Several poly(methacrylate)- and poly(methacrylamide)-based homopolymers with various side chains bearing primary, tertiary, and quaternary ammonio groups were designed by the group of Seymour in order to study the influence of (1) length of side chains bearing cationic residues; (2) the nature of the amine, i.e., primary, secondary, or tertiary amines and quaternary ammonio groups; (3) charge spacing along the polymer backbone; and (4) molecular weight or degree of polymerization [180]. These polymers are presented Fig. 11d–g: PVA.HCl (Fig. 11d), PAA.HCl (Fig. 11e), PMAEDA.HCl (Fig. 11f-R_1), PMAGEDA.HCl (Fig. 11f-R_2), PMADGHDA.HCl (Fig. 11f-R_3), PDMAEMAm (Fig. 11f-R_4), PTMAEM.Cl (Fig. 11f-R_5), P(HPMA-*co*-TMAEM.Cl (Fig. 11g), and PBTMAIPM.I_2 (Fig. 11f-R_6). At an N:P ratio of 2, considering first the influence of side-chain length, polymers with long side chains such as PMADGHDA.HCl were incapable of efficient complex formation with DNA (considerable residual EtBr fluorescence) but did show considerable transfection activity (positively charged complexes, thus their uptake by cells may be facilitated), despite their poor gene expression via direct intranuclear injection. At the other extreme, complexes formed using polymers with very short side chains, such as PVA.HCl and PAA.HCl, were efficient at complex formation (little residual EtBr fluorescence) and were remarkably stable to polyanion-mediated disruption. Efficient charge neutralization may explain their lack of surface charge, which probably underlies their tendency to aggregate. Their low transfection activity could be a consequence of their low surface charge (not uptaken by cells to a great extent), but their ability to undergo efficient intranuclear transcription was surprising in light of their stability to polyanions, as mentioned by the authors. The influence of cationic charge strength, using primary or tertiary amines or ammonio groups, on the properties of complexes formed with DNA was investigated. Polymers containing ammonio groups such as PTMAEM.Cl complexed DNA relatively efficiently, reflecting a stronger bond than with primary amino groups. The transfection activity of their complexes was 10- to 100-fold less than complexes based on most other cationic polymers. This poor transfection activity may be the result of poor access to the cytoplasm/nucleus, due to either cytotoxicity or poor endosomal release due to the absence of pH responsiveness (no proton sponge effect). By contrast, PDMAEMam containing tertiary amines was less effective at DNA condensation but showed good transfection activity in HEK 293 cells in vitro, probably because of the pK_a of its amines in the endosomal range. In the next step, the influence of the density of positive charge along the cationic polymer on the properties of complexes formed with DNA was investigated. Comparing PTMAEM.Cl with IBTMAIPM.I_2, which

bears two ammonio groups per monomer instead of one, it was found that the properties of the polyplexes were remarkably similar, suggesting that after reaching a certain density of positive charges, the effects (DNA condensation, cytotoxicity, etc.) might plateau. The effect of charge dilution was addressed using random copolymers containing TMAEM.Cl and HPMA as monomers. All these copolymers (TMAEM.Cl, 5–75%) were capable of binding DNA, although copolymers with greater than 50% TMAEM.Cl content were not capable of forming particulate complexes (as shown by AFM). According to the authors, it seems likely that these copolymers could not drive hydrophobic self-assembly of polymer/DNA complexes (because of the presence of hydrophilic HPMA). Moreover, the complexes based on these random copolymers showed low levels of transfection similar to the parent PTMAEM.Cl, but also poor ability to undergo transcription following intranuclear injection, which may be due to the steric protection of the DNA from polymerases by the presence of HPMA. Finally, the influence of cationic polymer molecular weight on the properties of complexes formed with DNA was examined and there were some indications of the effects of molecular weight on transfection activity against HEK 293 cells for many of the polymers examined in this study. PVA.HCl, PMAEDA.HCl, PMAGEDA.HCl, and PTMAEM.Cl:DNA complexes formed with higher molecular weight cationic polymer often showed greater expression of reporter genes, which was usually also linked to an increased cytotoxicity.

With Steric Stabilizer

Most of the publications on polycations for DNA condensation possessing a steric stabilizer deal with the influence of the polymer architecture on the properties of the polyplexes (physico-chemical characteristics and transfection efficiency). Two types of architectures are mainly studied: linear copolymers with block and/or graft (eventually brush) architectures (Scheme 17). The steric stabilizers most commonly used are based on ethylene glycol or contain hydroxyl groups such as hydroxyethyl methacrylate or sugars (only a few examples are presented here because sugar-based polycations are out of the scope of this review).

PDMAEMA Derivatives

For PDMAEMA-*b*-PEG (Fig. 12a), PDMAEMA-*b*-POEGMA, and P(DMAEMA-*stat*-PEGMA) (Fig. 12b) of relatively low M_n (7.8–21 kDa), the introduction of PEG did not significantly reduce the buffering capacity of PDMAEMA-based copolymers (for equivalent contents of DMAEMA units), but logically the buffering capacity is dependent on the DMAEMA content [182]. Of these polymers, the comb-type PDMAEMA-*stat*-PEGMA had the best complexing properties because charge neutrality was reached at a lower monomer:nucleotide molar ratio, which could be explained by its higher content of DMAEMA units compared to the other polymers (66% versus 30–37%). The steric effect of PEG chains

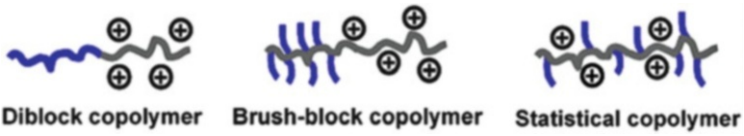

Scheme 17 Model cationic polymers containing different architectures of equivalent steric stabilizer components (represented by *blue line*) and comparable cationic components (represented by *gray lines* with positive charges). Reprinted with permission from [181]. Copyright 2011 Elsevier

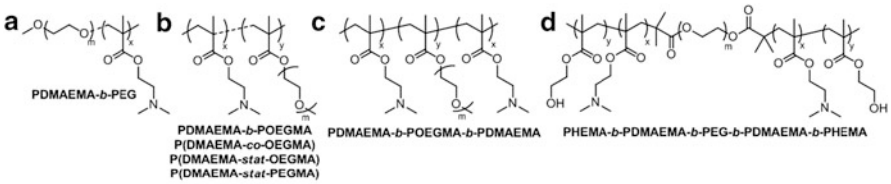

Name/Abbreviation of the polymer	Description of the polymer	DNA used	Ref
PDMAEMA	x = 32, M_n = 5.1kDa, M_w/M_n = 1.18	ctDNA, pCT0129LDNA (4.6kb), PRSVlucDNA (6kb)	[182] [186]
PDMAEMA-*b*-PEG	x = 37, m = 45, M_n = 7.8kDa, M_w/M_n = 1.25		
PDMAEMA-*b*-POEGMA	x = 37, y = 6-7, m = 7-8, M_n = 8.6kDa, M_w/M_n = 1.12		
	x = 30, y = 15, m = 7-8, M_n = 11.0kDa, M_w/M_n = 1.09		
P(DMAEMA-*stat*-PEGMA)	x = 66, y = 5, m = 45, M_n = 21.0kDa, M_w/M_n = 1.11		
PDMAEMA-*b*-PEG	x = 49, m = 47 (PEG: 2kDa), M_n = 10.1kDa, M_w/M_n = 1.18	pCMVLuc	[181]
PDMAEMA-*b*-POEGMA	x = 53, y = 7, m = 8.5, M_n = 11.8kDa, M_w/M_n = 1.25		
P(DMAEMA-*stat*-OEGMA)	x = 46, y = 7, m = 8.5, M_n = 10.7kDa, M_w/M_n = 1.23		
	x = 67, y = 9, m = 8.5, M_n = 15.0kDa, M_w/M_n = 1.15		
	x = 90, y = 12, m = 8.5, M_n = 19.6kDa, M_w/M_n = 1.13		
PDMAEMA-*b*-PEG	x = 64, m = 113 (PEG: 5kDa)	pDNA: pGL3-Luc	[189]
PDMAEMA-*b*-PEG	x = 70, m = 113 (PEG: 5kDa), M_n = 18kDa, M_w/M_n = 1.3	pDNA: phrGFP driven by CMV promoter (3.7kb)	[191]
P(DMAEMA-*co*-OEGMA)	f_{OEGMA} = 77%, m = 9, M_n = 40kDa, M_w/M_n = 1.96	pDNA: pCMVLuc, pCpGLuc	[193]
	f_{OEGMA} = 28%, m = 9, M_n = 25.5kDa, M_w/M_n = 1.51		
	f_{OEGMA} = 25%, m = 45, M_n = 54.5kDa, M_w/M_n = 1.35		
PDMAEMA-*b*-POEGMA	x = 100, y = 66, m = 6-8, M_n = 46.7kDa, M_w/M_n = 1.40	pDNA: pEGFP-C2 (4.7kb)	[195]
PDMAEMA-*b*-POEGMA-*b*-PDMAEMA	x = 50, y = 66, m = 6-8, M_n = 47kDa, M_w/M_n = 1.36		
PDMAEMA-*b*-PEG-*b*-PDMAEMA	m = 113, x = 33[a]; M_n = 13.8kDa, M_w/M_n = 1.13	pDNA: pRL-CMV	[196]
	m = 113, x = 48[a]; M_n = 18.6kDa, M_w/M_n = 1.17		
	m = 113, x = 61[a]; M_n = 25.2kDa, M_w/M_n = 1.28		
PHEMA-*b*-PDMAEMA-*b*-PEG-*b*-PDMAEMA-*b*-PHEMA	m = 113, x = 33[a], y = 12[a]; M_n = 16.9kDa, M_w/M_n = 1.18		
	m = 113, x = 48[a], y = 15[a]; M_n = 23.1kDa, M_w/M_n = 1.20		
	m = 113, x = 61[a], y = 18[a]; M_n = 30.4kDa, M_w/M_n = 1.31		

[a] determined by ^{1}H NMR spectroscopy.

Fig. 12 (**a**–**d**) Weak polycations with steric stabilizer: PDMAEMA derivatives

prevented the addition of excess polymer to the polyplexes but did not seem to hinder the complexation/condensation with DNA and even seemed to have a beneficial effect. The performances of these PEG-containing copolymers were better than for the PDMAEMA homopolymer at monomer:nucleotide ratio above that needed for neutralization as regards complexation in the EtBr displacement assay as well as the condensation properties (as illustrated by the nanoparticle size). As pointed out by the authors, the presence of a highly hydrophilic and non-condensing PEG block in the copolymer may be expected to decrease the affinity for binding DNA due to an unfavorable entropy change [183]. However, enhanced binding may be connected to a local crowding effect of the PEG chain

[184], or a decrease in the polarity of the polyion environment due to the presence of the PEG chains [185]. Moreover, the presence of PEG prevented the aggregation of polyplexes (as found in PDMAEMA polymer) and colloidally stable stoichiometric polyplexes were obtained. The capacity of a polymer to condense DNA is dependent on the DMAEMA content, but where the DMAEMA units are placed in the copolymers and the length of the PEG chains seem to play a role. Increasing DMAEMA content led to better condensing properties, i.e., smaller complexes. Despite, the propensity of these PEG-based copolymers to form small sterically stabilized complexes, their transfection ability in A549 cells at a monomer:nucleotide ratio inferior or equal to 5 was inferior to that of PDMAEMA homopolymer, maybe due to the presence of PEG, which provides a steric barrier around the polyplexes that inhibits contact with cells. In a subsequent publication [186], Stolnik and colleagues studied the cellular association and uptake and transfection efficiency of these copolymers at a fixed monomer:nucleotide molar ratio on three cell lines (A459, hepG2 and COS-7 cells) because transfection efficiency can be cell type-dependent. The transfection efficiencies were similar in the three cell lines for a given polymer but the rate of uptake of the complexes depended on the cell line used. Comb polymer P(DMAEMA-*stat*-PEGMA) consistently showed lower transfection efficiency than the linear PDMAEMA-*b*-PEG and bottle-brush PDMAEMA-*b*-POEGMA; the latter two giving similar transfection levels with all three cell lines. Indeed, P(DMAEMA-*stat*-PEGMA) showed less interaction with the cells (in flow cytometry studies) as well as less cell uptake (as shown by confocal microscopy) than the two other polymers. The authors explained this as being due to the different structures of the particles formed in the presence of DNA. Indeed, linear PDMAEMA-*b*-PEG and bottle-brush PDMAEMA-*b*-POEGMA have both diblock architectures, with the main difference being the spatial distribution of the EG units (linear PEG chain versus branched with OEG chains) but both polymers can form a micelle-like polyion complex with DNA. P(DMAEMA-*stat*-PEGMA) on the other hand, has several long pendant PEG chains (45 units) randomly distributed along the DMAEMA-based backbone; this statistical structure leads to rather soluble complexes (as shown by light scattering).

Given that a fraction of EG units much more than 20% in polymers seemed to hinder complexation in previous studies, Yang and colleagues conducted a systematic study [181] using a fixed fraction of EG units (~20%). This allowed comparison of various structures of PDMAEMA-PEG copolymers of the same molecular weight (M_n ~ 11 kDa): block with linear PEG (PDMAEMA-*b*-PEG, Fig. 12a), brush block copolymer (PDMAEMA-*b*-POEGMA, Fig. 12b), and statistical copolymer P(DMAEMA-*stat*-OEGMA); for this last structure, the effect of molecular weight was also tested. All these polymers were found to complex well with DNA and completely retarded DNA migration at an N:P ratio of 2, showing that in this case (low fraction of EG), the structure of the PEG block did not affect the gene binding capacity of the polymers (nevertheless surprising for stat and brush copolymers). Similar results were obtained for polyanion exchange, but the difference can be seen in the capacity of DNA compaction, where the hydrodynamic

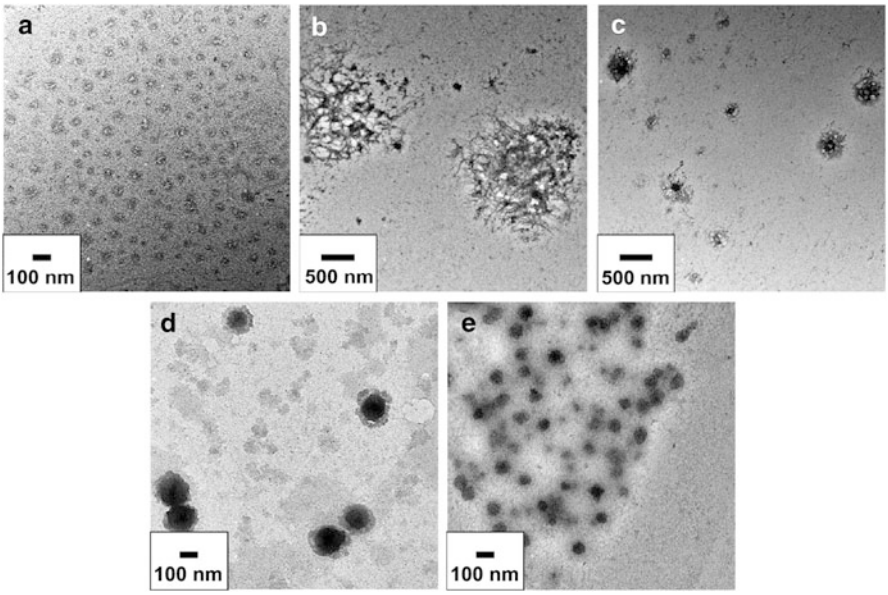

Fig. 13 TEM images of polymer/DNA complexes prepared in phosphate buffer (20 mM; pH = 6.5) at N:P 20 for (**a**) diblock copolymer PDMAEMA-*b*-PEG ($x = 49, m = 47$), (**b**) statistical copolymer P(DMAEMA-*stat*-OEGMA) ($x = 46, y = 7$), (**c**) statistical copolymer P(DMAEMA-*stat*-OEGMA) ($x = 67, y = 9$), (**d**) statistical copolymer P(DMAEMA-*stat*-OEGMA) ($x = 90, y = 12$) and (**e**) brush-block copolymer PDMAEMA-*b*-POEGMA ($x = 53, y = 7, m = 8.5$). Reprinted with permission from [181]. Copyright 2011 Elsevier

diameter of the polyplexes was dependent both on molecular weight and structure of the copolymers but in general decreased with increasing N:P ratio for all polymers. Of the polymers with similar molecular weight but with different nature of PEGylation, the statistical copolymer was not effective at compacting DNA (micron-sized particles), whereas the two block-like polymers gave polyplexes of 100–200 nm in size (Fig. 13). The oligo-brush-like architecture led to smaller sized complexes than the simple diblock sequence, which might be due to the more compact structure of the shell (nevertheless not more resistant to heparin displacement) but their zeta potentials were similar. For the statistical copolymer series, the hydrodynamic sizes of the polyplexes dramatically decreased with increasing molecular weight at N:P ratio in the range 2–20, while the zeta potential stayed constant. The authors pointed out that molecular modeling studies on cationic polymer with neutral polymer grafts predicted that polymers of higher molecular weight were required to form smaller complexes [187]. Similar observations on the influence of short PEG grafts were also reported with PEI [188]. For cationic polymers with similar cationic charge but different nature of PEGylation, the diblock copolymer generally showed better transfection activity in HEK293 and HepG2 cells than the brush block copolymer or statistical copolymer with OEG chains.

A study by Kataoka and colleagues of PDMAEMA-*b*-PEG (Fig. 12a), which had around the same ratio of DMAEMA:PEG as in the previous study but was twice as long [189], also showed the formation of micellar structures. There was a steep decrease in the size of these micelles with increasing N:P ratio, with a leveling off to approximately 95 nm in diameter at a N:P ratio of about 3, which was not only ascribed to DNA condensation (according to EtBr quenching, a fully condensed state occurred at N:P = 1.2) but also to a reduction in the association number to form non-stoichiometric micellar structures similarly to polyplexes based on PLL-*b*-PEG [190]. The presence of PEG in the polyplexes both increased the stability of pDNA against DNAse I and the affinity of the PDMAEMA segment for pDNA (exchange reaction with polyanions). Indeed, PEG provides a protecting layer by decreasing the permittivity of the microenvironment. The authors studied the transfection efficiency of this copolymer compared to PDMAEMA on HEK293 cells. In contrast to Stolnik and colleagues [182], they found a slightly better transfection efficiency of PDMAEMA-*b*-PEG compared to PDMAEMA, even at N:P ratio of 5 (and higher), possibly due to the longer chain length of the copolymer (or to the cell line). The authors also reported an unusual association of excess block copolymers on the micelles above the charge stoichiometric point, leading to an increase in zeta potential that finally leveled off at N:P = 15 (zeta potential of 17 mV), which could also be an explanation for the better transfection efficiency. Indeed, positively charged micellar polyplexes may benefit from a facilitated association with the cellular surface but, unfortunately, the comparison is difficult because the zeta potential was not reported in the studies of Stolnik and colleagues [182, 186]. Unfortunately, this improved performance was also associated with an increased toxicity compared to PDMAEMA.

For a similar PDMAEMA-*b*-PEG (Fig. 12a), Tam et al. took into consideration the critical micelle concentration (CMC; determined previously to be in the range 2 μg mL^{-1}) of the polymer to explain the changes in the size and shape of the polyplexes (Fig. 14) [191]. The results corresponded to those of Kataoka, with a maximum condensation at N:P = 1.2 (EtBr quenching and zeta potential). As the polymer solution was added to the naked DNA (R_h = 56 nm), at concentration below its CMC (shifted to higher values due to the presence of DNA), the polymer existed as a free cationic unimer that bound to the DNA to form complexes with a worm-like Gaussian structure. With the addition of more polymer, the polyplexes grew in size to around 90 nm (R_h) probably due to secondary aggregation of the neutral nanoparticles (zeta potential). Above a N:P ratio of 1, the size of the polyplexes decreased and excess unbound polymeric unimers started to appear in the solution (DNA + 0.02 mg mL^{-1} polymer, i.e., N:P ratio of 2). At a polymer concentration above 0.06 mg mL^{-1}, the polyplexes underwent significant structural rearrangements to form spherical aggregates of $R_h \approx 35$ nm, which was probably due to polymer aggregation above its CMC, accompanied by a coil–globule transition of the DNA molecules. The difference in the CMC with and without DNA can be attributed to two reasons. First, the DNA forms strong hydrogen bonds with water, which can "break" the water structure and consequently increase the CMC. Second, since binding between the polymer and DNA took place once the polymer

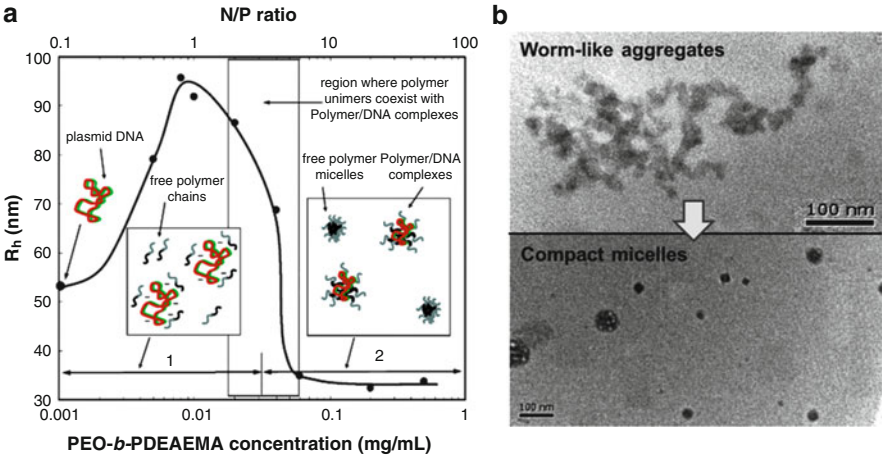

Fig. 14 (**a**) Proposed microstructure and R_h of the DNA/PEG-*b*-PDEAEMA complex at various polymer concentrations in PBS solution. (**b**) TEM micrographs of DNA/PEG-*b*-PDEAEMA copolymer complex in PBS solution: 0.02 mg mL^{-1} polymer solution (*upper part*) and 0.2 mg mL^{-1} polymer solution (*lower part*). Reprinted with permission from [191]. Copyright 2006 American Chemical Society

solution was added, there were insufficient unbound polymer chains in the solution to induce micellization at 2 μg mL^{-1}, shifting the CMC to a higher value [192].

A series of P(DMAEMA-*co*-OEGMA) (Fig. 12b) copolymers with constant chain length of 120 units but with various lengths of the OEG side chains and different comonomer compositions (variable DMAEMA/OEGMA composition, $M_n = 22.7–54.6$ kDa) were studied by Rudolph and colleagues [193]. Among these polymers, DNA complexation by P(DMAEMA-*co*-OEGMA) copolymers with low f_{OEGMA} (<50%) increased with increasing N:P ratios and decreased with increasing OEGMA molar ratio (f_{OEGMA}) and molecular weight. At high f_{OEGMA} (>50%), DNA complexation was abolished. Only at low f_{OEGMA} (~17%) and low OEGMA molecular weight (about nine EG units) was pDNA migration completely retarded (indicating complete DNA complexation), as observed for PDMAEMA. Verbaan and colleagues had already observed that copolymers with a high degree of PEG grafting (i.e., PEG < 22%) were not capable of binding to pDNA [194]. In general, the efficiency of the polyplexes regarding complexation of pDNA decreases with increasing f_{OEGMA} and OEGMA chain length, due to the reduction of the positive charge density of PDMAEMA and the introduction of sterically bulky OEGMA. This is consistent with the increasing particle size of the P(DMAEMA-*co*-OEGMA)-based polyplexes (condensation less efficient) and decreasing zeta potential (shielding effect of PEG) in a direct proportion to increasing f_{OEGMA} and OEG chain length. None of these copolymers were cytotoxic to BEAS-2B cells, even at 500 μg mL^{-1}. Following the same trend as for complexation, the transfection efficiency was dependent on the N:P ratio and decreased with increasing f_{OEGMA}, in BEAS-2B cells as well as in MLE 12 cells. The transfection efficiency of the most efficient P(DMAEMA-*co*-OEGMA)-based polyplex was still

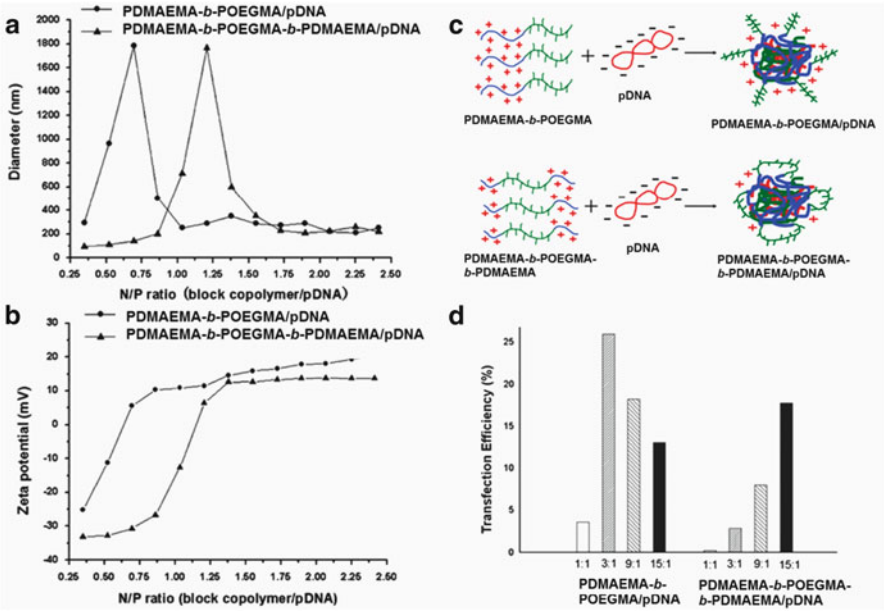

Fig. 15 Dynamic light scattering results indicating the particle sizes (**a**) and zeta potentials (**b**) of the complexes as a function of N:P ratios for PDMAEMA-*b*-POEGMA-*b*-PDMAEMA/pDNA (*triangles*) and PDMAEMA-*b*-POEGMA/pDNA (*dots*). Data were obtained after the interaction of polymers with pDNA at various N:P ratios in TE buffer at pH 8.0. (**c**) Models for the formation of the PDMAEMA-*b*-POEGMA/pDNA and PDMAEMA-*b*-POEGMA-*b*-PDMAEMA/pDNA complexes. (**d**) Transfection efficiency determined by flow cytometry analysis of the GFP gene expression of PDMAEMA-*b*-POEGMA/pDNA and PDMAEMA-*b*-POEGMA-*b*-PDMAEMA/pDNA complexes in 293T cells as a function of N:P ratio [195]. Copyright 2011 Royal Society of Chemistry

more than 10 times lower than that of branched PEI25K/DNA, which can be explained by the inefficient pDNA condensation but also by reduced cellular uptake and endosomal escape.

PDMAEMA-*b*-POEGMA (Fig. 12b), PDMAEMA-*b*-POEGMA-*b*-PDMAEMA (Fig. 12c) with the same number of DMAEMA units (100), and POEGMA (66) form different self-assembled structures in solution both in the absence and presence of DNA due to their different architectures (diblock A-B or triblock A-B-A, Fig. 15c) [195]. The diblock completely retarded DNA migration at N:P ratio of ~0.6:1, whereas the triblock retarded migration at ~1.2:1 (at these ratios, the zeta potential was neutral and the polyplexes formed aggregates of ~1.8 μm, Fig. 15a, b). A similar trend was observed for the EtBr displacement, reflecting the better ability of the diblock to interact with pDNA. When the N:P ratio was more than 1.75:1, the particle sizes of the two polyplexes were almost the same (diameter of 200 nm) but the zeta potential of the triblock-based polyplexes was slightly lower (12 versus 17 mV), which could be explained by the larger content of POEGMA blocks at the surface (higher shielding effect) according to the structure that the authors proposed for the polyplexes (Fig. 15c). The triblock copolymer

itself seemed to be far less toxic than the diblock to HEK293T cells (at 0.5 mg mL^{-1} there was nearly 100% cell viability versus 55% for the diblock). Following the trends of DNA complexation, the diblock copolymer was more efficient for transfection than the triblock at lower N:P ratio, with a bell-shaped dependence of the transfection efficiency as a function of the N:P ratio (Fig. 15d). For the range studied (N:P ratios of 1:1 to 15:), the maximum efficiency for PDMAEMA-*b*-POEGMA was reached at N:P = 3, while for PDMAEMA-*b*-POEGMA-*b*-PDMAEMA, the maximum seemed to be reached at N:P = 15, but it could also be a bell-shaped dependence shifted to higher ratios.

PDMAEMA-*b*-PEG-*b*-PDMAEMA and PHEMA-*b*-PDMAEMA-*b*-PEG-*b*-PDMAEMA-*b*-PHEMA with 113 EG units in the central block and on each side 33, 48, or 61 DMAEMA units (used to complex DNA) and eventually ~15 more HEMA units on each side (Fig. 12d) were studied by Kang and colleagues [196]. At a polymer:plasmid weight ratio above 5, all polymers condensed DNA into particles of less than 200 nm in size and more than 25 mV in zeta potential. The triblocks PDMAEMA-*b*-PEG-*b*-PDMAEMA showed increased DNA complexing ability as well as transfection efficiency with increasing number of DMAEMA units. Adding short PHEMA blocks to the triblocks (leading to the pentablocks PHEMA-*b*-PDMAEMA-*b*-PEG-*b*-PDMAEMA-*b*-PHEMA) did not significantly impede the complexation ability of the polymers compared to the triblock and led to higher transfection than PDMAEMA. By comparison, a random block copolymer of similar component composition could not condense DNA efficiently, showing the importance of the architecture of the polycation.

Linear PEI Derivatives

PEG_{45}-*b*-linear PEI_{600} (Fig. 16a) (M_w = 51 kDa) was obtained by complete hydrolysis of a block copolymer PEG-*b*-poly(ethyl oxazoline-*co*-methyl oxazoline) [197]. PEG_{45}-*b*-linear PEI_{600} inhibited DNA migration at a polymer:DNA weight ratio of 1 under physiological ionic strength, while linear PEI of 22 kDa achieved it at a ratio of 0.75. The levels of reporter gene expression obtained with the diblock copolymer were similar to those obtained for the linear PEI although at higher weight ratio, while the cytotoxicity as well as solubility were comparable, which was probably due to the relatively short length of the PEG block. Therefore, perhaps a longer PEG block should be introduced in order to see the benefits.

PHEMA-*g*-(linear PEI-*b*-PEG) (Fig. 16b) (M_w = 509 kDa) adopted a cylindrical brush topology at pH 5.0 [198] and completely retarded DNA migration at N:P ratio of 2, whereas efficient condensation started at an N:P ratio of 10, leading to small particles of 150 nm in diameter with a positive zeta potential of 20 mV. PHEMA-*g*-(linear PEI-*b*-PEG) was well tolerated by HEK293 cells up to a dose of 125 μg mL^{-1}, whereas exposure of the cells to PEI25K (branched) led to 50% viability at 16 μg mL^{-1}. PHEMA-*g*-(linear PEI-*b*-PEG)/pDNA complexes were internalized by BT474 cells to a greater extent than PEI25K/DNA complexes at the same ratio (N:P = 10) and led to a higher transfection efficiency in a variety of cell lines.

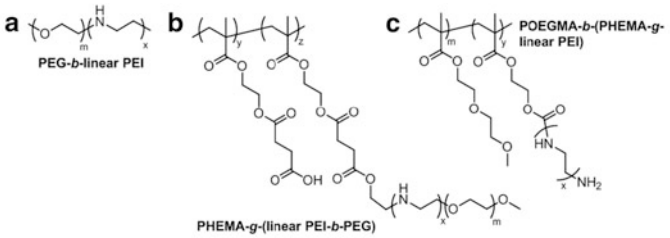

Name/Abbreviation of the polymer	Description of the polymer	DNA used	Ref
PEG-*b*-linear PEI	2kDa mPEG (m = 45), x = 600, M_n[a] = 51kDa ± 5kDa	SMD2-LucΔTR	[197]
PHEMA-*g*-(linear PEI-*b*-PEG)	2kDa mPEG (m = 45), x = 40, y = 40 and z = 112 (grafting efficiency 74%), M_w[b] = 509kDa	pGL3-Luc, pEGFP-N2, pcDNA3-p53	[198]
POEGMA-*b*-(PHEMA-*g*-linear PEI)	m/y = 89/3 (mol. ratio), x = 1.2kDa, M_n = 21kDa, LCST = 32.5°C	pGL3-control with SV40 promoter and enhancer sequences encoding luciferase	[199]
	m/y = 89/8 (mol. ratio), x = 1.2kDa, M_n = 27.6kDa, LCST = 38.7°C		

[a] determined by SANS; [b] determined by LS.

Fig. 16 (**a**–**c**) Weak polycations with steric stabilizer: linear PEI derivatives

POEGMA-*b*-(PHEMA-*g*-linear PEI) (Fig. 16c) is mainly composed of OEGMA units (89), which are thermoresponsive, and HEMA units grafted with linear PEI (3 or 8), which introduce more hydrophilicity and thus increase the LCST of the copolymer to close to body temperature [199]. Below their LCST, the polymer with most linear PEI grafts (8) retarded the movement of DNA at lower polymer:DNA ratio than the polymer with 3 grafts (3 versus 5). At 37°C, both polymers retarded DNA migration at a ratio of 3, given that the conformation of $POEGMA_{89}$-*b*-$(PHEMA\text{-}g\text{-linear PEI})_8$ was unchanged, while at 37°C, i.e., 5°C higher than the LCST of $POEGMA_{89}$-*b*-$(PHEMA\text{-}g\text{-linear PEI})_3$, the collapsed macromolecular chains covered more DNA and charges in the condensates, as confirmed by the zeta potential results. Moreover $POEGMA_{89}$-*b*-$(PHEMA\text{-}g\text{-linear PEI})_3$ compacted DNA more tightly at 37°C than at 20°C (EtBr displacement assay). At a polymer: DNA ratio of 15, the polyplexes based on this last polymer reached a size acceptable for gene delivery (<200 nm) and the transfection efficiency was found to increase with increasing charge ratio both in COS-7 and HEK293 cells. At charge ratios of 25:1, $POEGMA_{89}$-*b*-$(PHEMA\text{-}g\text{-linear PEI})_3$-based polyplexes achieved 100-fold higher transfection efficiency than PEI 1.2 kDa and levels comparable to that of PEI25K, while being far less toxic. As the incubation with DNA is usually done at 37°C, it is interesting to have non-viral gene delivery vectors that are more efficient at this temperature.

PLL Derivatives

At mixing charge ratio N:P of 1 [190], the polydispersity of the complexes of PEG_{272}-*b*-$PLL_{7,\ 19,\ 48}$ (Fig. 17a) with pDNA decreased dramatically before increasing again, whereas nearly complete condensation seemed to occur at N:P of 2:1 (EtBr exclusion assay), where the diameter of all the polyplexes was inferior to 100 nm. Note that condensation of a linearized pDNA by the same polymer was effective at lower N:P ratio. The explanation given by the authors is that native pDNA is in a super-coiled circular form, which certainly has a higher molecular

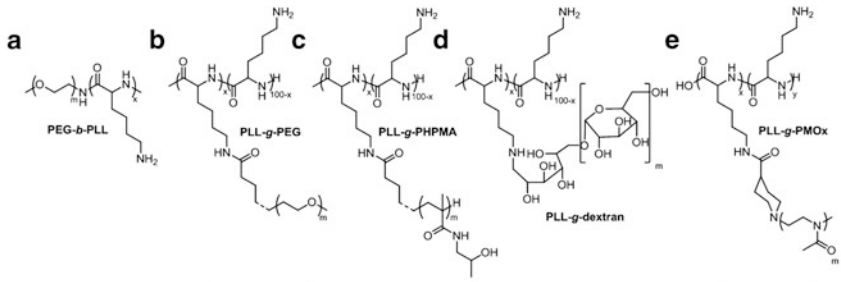

Name of the polymer	Abbreviation	Description of the polymer	DNA used	Ref
Poly(L-lysine)-*b*-poly(ethylene glycol)	PLL-*b*-PEG	M_nPEG = 12kDa (272 units), DP_{PLL} = 7, 19, 48	pGL3-Luc	[190]
Poly(L-lysine)	PLL	M_w = 9.6kDa and 22.4kDa, mass per charge: 209Da	Circular 6 kb expression vector containing a CMV promoter-driven β-galactosidase reporter	[185]
Poly(L-lysine)-*g*-poly(ethylene glycol)	PLL-*g*-PEG	M_nPEG grafts = 5kDa (113 units), PLL: M_w = 20kDa mol.% PEG: 5, 10%, mass per charge: 398 Da (5%), 698Da (10%)		
		M_nPEG grafts = 12kDa (272 units), PLL: M_w = 20kDa mol.% PEG: 5, 10%, mass per charge: 766Da (5%), 1476Da (10%)		
Poly(L-lysine)-*g*-dextran	PLL-*g*-dextran	$M_n$dextran grafts = 1kDa (7 units), PLL: M_w = 20kDa mol.% dextran: 5%, mass per charge: 187Da		
		$M_n$dextran grafts = 1kDa (7 units), PLL: M_w = 11.4kDa mol.% dextran: 7%, mass per charge: 212Da		
Poly(L-lysine)-*g*-poly[*N*-(2-hydroxypropyl)methacrylamide]	PLL-*g*-PHPMA	M_nPHPMA grafts = 4.4kDa (30 units), PLL: M_w = 19kDa mol.% PHPMA: 8%, mass per charge: 520Da		
Poly(L-lysine)-*g*-poly(2-methyl-2-oxazoline)	PLL-*g*-PMOx	M_nPLL = 20kDa (~150 units), M_nPMOx = 4kDa Grafting density (%) = 5, 7, 9, 14, 19, 32, 53, 77	pEGFP-N1	[200]
		M_nPLL = 20kDa (~150 units), M_nPMOx = 5kDa (~60 units) Grafting density (%) = 5		
		M_nPLL = 20kDa (~150 units), M_nPMOx = 8kDa (~100 units) Grafting density (%) = 11, 17, 20, 29, 50, 67		

Fig. 17 (**a**–**e**) Weak polycations with steric stabilizer: PLL derivatives

restraint than the linear-formed DNA; thus, it is likely that the differences in molecular topology may crucially affect the condensation process of the DNA molecules in the sense that condensation may not be complete at a stoichiometric charge ratio for pDNA due to steric reasons, requiring excess PLL strands to promote further condensation. They also hypothesized that such a significant decrease in the average diameter between ratios 1 and 2 (~120 nm to ~90 nm) could be also due to a concomitant decrease in the association number of these micelle-like polyplexes, which was confirmed in the case of PEG_{272}-*b*-PLL_{48} by LS. They could also show that a higher PEG content in the polymer resulted in micellar polyplexes with a decreased association number. The transfection efficiency in HEK293 cells was improved by increasing the length of the PLL segment and showed a bell-shaped dependency (as a function of the N:P ratio). The performance of PEG_{272}-*b*-PLL_{48} was comparable to that of Lipofectamine™ and was partly attributed to a more favorable cellular association than that of the derivatives with a shorter PLL segment.

PLL-*g*-PEG (Fig. 17b), PLL-*g*-PHPMA (Fig. 17c), and PLL-*g*-dextran (Fig. 17d) were compared to PLL as transfection agents [185]. All these polymers were slightly hampered in their ability to condense DNA as compared to PLL (as shown by EtBr quenching), probably due to steric hindrance and charge screening by the hydrophilic blocks. PLL-*g*-PHPMA was the most effective of these new polymers despite its intermediate value for mass per charge (between that of PEG and dextran derivatives), which was not further explained. All these grafted

copolymers with hydrophilic groups were capable of producing complexes with DNA that were more soluble than the PLL alone; as expected, the most efficient was the PEG-*b*-PLL with the longest PEG segment (12 kDa) at the highest grafting ratio (10%) and it was also the least toxic. PLL-*b*-dextran showed increased toxicity compared to low molecular weight PLL.

Polyoxazolines are thought to be an alternative to PEG as biocompatible blocks. In this frame, PLL-*b*-PMOx (Fig. 17e) and the polyplexes made thereof were synthesized and studied by the group of Lühmann [200]. As for PEG or other block copolymers comprising a cationic block and some hydrophilic modification, the complexation of DNA by PLL-*b*-PMOx was compromised at high grafting rates and/or long PMOx chains (as shown by gel electrophoresis). Condensates made of polymers with less than 7% grafting density showed aggregate formation at ratios supposedly above the neutral point (zeta potential not reported) and were over 500 nm in diameter. Above 7% grafting density, independent of the length of PMOx, the diameters of the polyplexes were less than 200 nm. These polymers were able to protect DNA from DNAse I digestion, but only PLL-*g*-PMOx with low molecular weight PMOx and low grafting densities of 7–14% showed significant gene expression in COS-7 cells (good transfection efficiency for this polymer was found at N:P ratio of 3.125), which correlated with their good cellular uptake.

Other Amino Acid-Based Polymers

PEG-*co*-(PLL-*g*-His) (Fig. 18a), a copolymer of PEG (1.45 kDa) and PLL modified with histidine at various grafting rates (5, 9, 16, and 22%) showed relatively poor EtBr displacement capacity [201]. EtBr displacement was only achieved at N:P ratio of 5 for the polymers with the two lowest grafting rates, and at ratios of 10 for the two others, which can be explained by a looser complexation due to the presence of PEG or the bulky imidazole groups or by the copolymer nature or by less cationic residues due to the grafting. Consistent with these high N:P ratios were the diameters of most of the complexes that remained between 150 and 200 nm for N:P ratios of 10 and above, whereas the complexes based on PLL were much smaller. The complexes of DNA based on PEG-*co*-(PLL-*g*-$His_{16\%}$) showed the highest transfection efficiency in the A7r5 cell line compared to the other polymers and the efficiency increased with the N:P ratio. Compared to polymers with lower degree of modification, this could be explained by the presence of more histidine residues, which are known to have endosomal buffering capacity (the buffering capacities increased with increasing His content), facilitating the escape of the polyplex into the cytoplasm. In addition, the decreased efficiency of PEG-*co*-(PLL-*g*-$His_{22\%}$) indicated the importance of having enough complexing units in the polymer. Probably because of the ester bonds, the polymer was totally degraded into its constituent PEG and PLL blocks after 24 h, which is an interesting approach to obtaining biodegradable polyplexes.

PEG has also been coupled to polyamino acids other than PLL in order to increase solubility (critical in the case of polyhistidine for instance) and design a polymer with great DNA complexation and transfection properties.

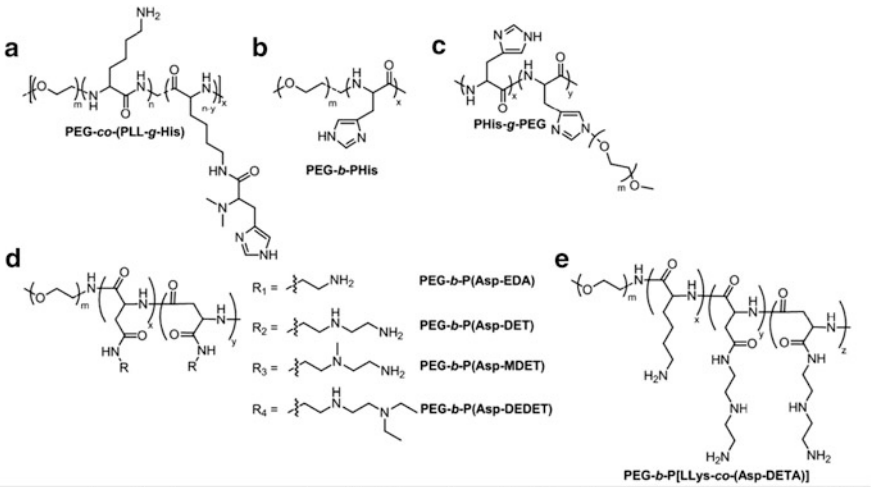

Name of the polymer	Abbreviation	Description of the polymer	DNA used	Ref
Poly(ethylene glycol)-*co*-[poly(L-lysine)-*g*-histidine]	PEG-*co*-(PLL-*g*-His)	M_nPEG = 1.45kDa (~33 units) M_nPEG-*co*-PLL = 27kDa, M_w/M_n = 3.12, x = 6 His Grafting density (%) = 5, 9, 16, 22	pSV-EGFP, pSV-Luc	[201]
Poly(ethylene glycol)-*b*-poly(L-histidine)	PEG-*b*-PHis	M_nPHis = 15-50kDa, M_nPEG = 5kDa (113 units), PEG:His mol. ratio ~ 1	pRL-CMV (~4 kbp)	[202]
Poly(L-histidine)-*g*-poly(ethylene glycol)	PHis-*g*-PEG	M_nPHis = 15-50kDa, M_nPEG = 5kDa (113 units), PEG:His mol. ratio = 2.4, 10, 20		
Poly(ethylene glycol)-*b*-polyaspartamide	PEG-*b*-PAsp (precursor)	M_nmPEG = 12 kDa (272 units), DP_{PAsp} = 68, M_w/M_n = 1.17	pDNA not specified	[203]
PEG-*b*-PAsp modified with ethylene diamine	PEG-*b*-P(Asp-EDA)	/		
PEG-*b*-PAsp modified with diethylenetriamine	PEG-*b*-P(Asp-DETA)			
PEG-*b*-PAsp modified with 4-methyldiethylenetriamine	PEG-*b*-P(Asp-MDETA)			
PEG-*b*-PAsp modified with *N,N*-diethyldiethylenetriamine	PEG-*b*-P(Asp-DEDETA)			
Poly(ethylene glycol)-*b*-poly[(L-lysine)-*co*-aspartamide modified with diethylenetriamine]	PEG-*b*-P[LLys-*co*-(Asp-DETA)]	M_nmPEG = 12kDa (272 units), $DP_{PAA(amino acid)}$ ~ 100, %Lys units: 24, 47, 71, 100	pDNA coding Luc with CAG promoter	[204]

Fig. 18 (**a**–**e**) Weak polycations with steric stabilizer: other amino acid-based polymers

PEG-*b*-PHis (Fig. 18b) and PHis-*g*-PEG (Fig. 18c) [202], would be presumably less able to complex and condense the genetic material into small polyplexes due to the relatively few protonated groups at pH 7 compared to the previous polymers, which had some free primary amine groups from the PLL segment [201]. In order to overcome this problem, the authors chose an approach where the complexation between the polymers and DNA was done at pH 5, at which the imidazole groups are protonated; then, the polyplexes were transferred into a neutral buffer, leading to partial deprotonation. The authors expected that DNA would remain in the partially protonated polyhistidine interior via hydrogen bonding and electrostatic interaction, while the partial deprotonation of polyhistidine would increase the hydrophobicity of the PHis segment, thus favoring the formation of micelles consisting of a DNA/PHis core surrounded by a PEG shell. The comb-shape polymer with 1 mol% ratio PEG complexed the DNA at a polymer:DNA weight ratio of 2, similarly to the block copolymer (PEG-*b*-PHis) and totally retained the DNA at a ratio of 3, while the other conjugates complexed DNA at a higher ratio and did not succeed in completely retaining DNA. This similarity between the comb-shape polymer and the block copolymer could eventually be explained by the low grafting rate, thus the effective structure of the polymers was rather

similar. But, the polymer with the block structure, despite the low content of PEG compared to some of the comb-shape polymers, protected DNA from enzymatic degradation to the greatest extent, giving an indication that the structure in solution might be different. Nevertheless, it should be mentioned that even at high polymer: DNA ratio (4 and above), the charge of the polyplexes remained negative for all the polymers, probably reflecting the low protonation degree of histidine at pH 7. At pH 5, the polyplexes had diameters between 100 and 300 nm and, most importantly, were stable for over a week at room temperature. It could be observed that increasing the PEG content also increased the diameter of the polyplexes. Once transferred to pH 7, their stability was limited and aggregation occurred after 24 h, showing a certain limitation of this approach. Moreover, the transfection efficiency of all these polymers was poor in COS-7 cells (comparable to the tested PLL, but three orders of magnitude lower than PEI).

In contrast to PLL, polyaspartamide modified with chosen oligoethyleneimine side chains of various lengths had the advantage of possessing both primary and secondary amines. PEG-*b*-PAsp derivatives modified with various amines (Fig. 18d) were synthesized by the group of Kataoka [203]: the PAsp segment was modified with ethylene diamine [PEG-*b*-P(Asp-EDA), Fig. 18d-R_1], diethylene triamine [PEG-*b*-P(Asp-DETA), Fig. 18d-R_2], 4-methyldiethylene triamine [PEG-*b*-P(Asp-MDETA), Fig. 18d-R_3], and *N*,*N*-diethyldiethylene triamine [PEG-*b*-P(Asp-DEDETA), Fig. 18d-R_4]. The focus was on PEG-*b*-P(Asp-DETA), which showed a two-step protonation process (pK_a 6.0 and 9.5) due to the presence of the ethylene diamine moiety, as illustrated in Fig. 19. At pH 7.4, this group is in the mono-protonated state (*gauche* form) and is capable of exerting a substantial buffering effect in the pH range down to 5. At pH 5, where 95% of the ethylene diamine unit is protonated (~diprotonated) the fluorescence in the EtBr dye-exclusion assay leveled off at N:P ratio of 1, while at pH 7.4 where the mono-protonated form is present, a N:P ratio of 2 is necessary to obtain substantial quenching.

It is interesting to note that the diameter of the polyplex micelles stayed constant at around 70–90 nm throughout the range of N:P ratios (1–20), even at neutral zeta potential, showing the efficiency of the hydrophilic shell to prevent aggregation. The transfection efficiency of this polymer was compared to the other PAsp derivatives [PEG-*b*-P(Asp-EDA), PEG-*b*-P(Asp-MDETA), PEG-*b*-P(Asp-DEDETA)], which all showed comparable sizes and zeta potential to PEG-*b*-P(Asp-DETA). The polyplex based on the polymer modified with the 2-aminoethyl group (pK_a 9.4), PEG-*b*-P(Asp-EDA), was far less efficient than PEG-*b*-P(Asp-DETA) (factor 10^3 at N:P ratio of 20), presumably because of the impaired buffering capacity of the polymer but also because of its marginal internalization by cells [203]. Concerning PEG-*b*-P(Asp-MDETA), which possesses a tertiary amine instead the secondary amine of PEG-*b*-P(Asp-DETA) (primary amine unchanged), and PEG-*b*-P(Asp-DEDETA), which possesses a tertiary amine instead of the primary amine of PEG-*b*-P(Asp-DETA) (secondary amine unchanged), they both showed lower transfection efficiency compared to PEG-*b*-P(Asp-DETA),

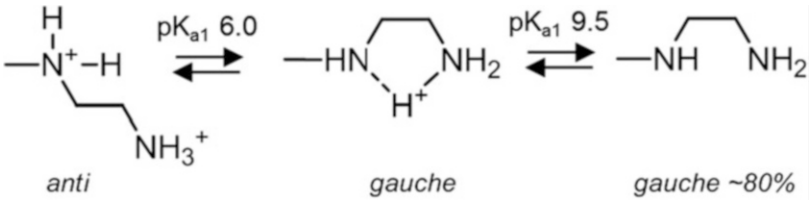

Fig. 19 Two-step protonation of the ethylene diamine unit with a distinctive *gauche-anti* conformational transition

especially at high N:P ratios, showing the importance of the presence of both primary and secondary amines in the polymers used for polyplex formation. Nevertheless, at comparable N:P ratio (10), this construct was less efficient by a factor of 5 than ExGen500™, but was also less cytotoxic. In order to improve the results of PEG-*b*-P(Asp-DETA) [203], Kataoka and colleagues introduced some lysine moieties, obtaining PEG-*b*-P[LLys-*co*-(Asp-DETA)] with various percentage of lysine units, i.e., 24, 47, 71, and 100% (Fig. 18e) [204]. As expected, the extent of fluorescence quenching in the EtBr dye-exclusion assay (i.e., tight complexation) was proportional to the amount of lysine units present in the polymer. Interestingly, the fluorescence, which was leveled off at a N:P ratio of 2 for PEG-*b*-P(Asp-DETA), showed a leveling off at N:P ratio of 1 for these PEG-*b*-P[LLys-*co*-(Asp-DETA)] (from ~25 to 100% lysine units), indicating the beneficial effect of the lysine units for complexation. This corresponded also to the zeta potential results, which were nearly neutral for all polymers at this N:P ratio. In view of the trend in the zeta potential, the authors suggested that at high concentration of polymer, the lysine units may preferentially bind to the pDNA, replacing the Asp-DETA units and resulting in the continuous binding of the block catiomers until the lysine units saturate the available binding sites. By replacing half or more of the Asp-DETA units by lysine units, the internalization of the polyplexes was increased tenfold and the transfection efficiency was 100 times that of PEG-*b*-P(Asp-DETA).

2.2 Amphiphilic Polycations

The cationic charges, which are needed for efficient DNA condensation, and hydrophobic domains, which promote membrane interaction, have been combined in hydrophobically modified polymers such as PEI, PLL, PAMAM, and poly(*N*-ethyl-4-vinylpyridinium) salts [205–208]. Moreover, the hydrophobic part contributes to the hydrophobically driven interaction of DNA with polycation [209]. This increases the hydrophobic component and therefore there is need of increased steric stabilization in order to obtain colloidally stable polyplexes. Some examples are presented in the next sections.

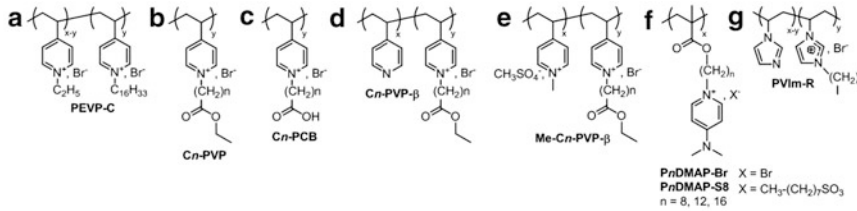

Name of the polymer	Abbreviation	Description of the polymer	DNA used	Ref
Poly[(*N*-ethyl-4-vinylpyridinium) bromide]	PEVP	DP = 18, 200; for 400: M_w ≈ 80kDa	pDNA (pBC16, pTZ19), contour length: M_w ≈ 3.10^7Da	[207]
Poly[[(*N*-ethyl-4-vinylpyridinium) bromide]-*co*-[*N*-cetyl-4-vinylpyridinium) bromide]]	PEVP-C	DP = 400, n:m = 97:3		
Poly(4-vinylpyridine) (precursor)	PVP	DP = 1600, M_w = 168kDa	ctDNA: pcDNA3-SEAP2 (10kb)	[210]
Quarternized poly(4-vinylpyridine) with *N*-alkyl ester substituents	C*n*-PVP	DP = 1600, n = 1-6		
Polycarboxybetaine with alkyl spacer	C*n*-PCB	DP = 1600, n = 4, 5		
Poly[(4-vinylpyridine)-*co*-(*N*-alkyl-4-vinylpyridinium)] with various quaternization degree β	C*n*-PVP-β	DP = 1600, β = 25-95%		
Poly[(*N*-methyl-4-vinylpyridine)-*co*-(*N*-alkyl-4-vinylpyridinium)] with various alkylation degree β	Me-C*n*-PVP-β	DP = 1600, β = 25-95%		
Dimethylaminopyridinium-alkyl polymethacrylate	PnDMAP-X	M > 10kDa	pDNA: pBudCE4.1/LacZ/CAT (~8.4kbp)	[211]
Poly[(1-vinylimidazole)-*co*-(*N*-alkyl-1-vinylimidazolium)] with various quaternization degree β	PVIm-R-β	M_w = 8.8kDa , n = 0, 1, 3, 7, β = ~20, 40%	Salmon testes DNA sodium salt	[212]

Fig. 20 (**a**–**g**) Amphiphilic polycations: strong polyelectrolytes with alkyl chains

2.2.1 Strong Polyelectrolytes with Alkyl Chains

A pioneering work of Kabanov et al. dealt with poly(*N*-ethyl-4-vinylpyridinium) bromide (PEVP) and its copolymer with *N*-4-vinylpyridinium modified with a longer alkyl chain, PEVP-C (Fig. 20a) [207]. For mole ratio [PEVP]/[DNA] between 0 and 0.5, where the polycation was in excess, soluble non-stoichiometric polyelectrolyte complexes were formed and the polycations were uniformly distributed along the DNA molecules. Further addition of PEVP led to the formation of an insoluble component composed of PEC with higher PEVP content (disproportionation). The addition even at 3% of a cetyl chain to the polymer ($DP_w = 400$) narrowed the mole ratio range where soluble PEC were formed to [PEVP-C]/[DNA] = 0–0.25, which did not go in the direction wanted for efficient polyplexes and gene delivery. Moreover, the cell membrane penetration properties of PEVP-C were less efficient than those of PEVP, thus showing that either these properties are not a simple function of hydrophobicity or, as suggested, the hydrophobic component was buried in the core of the polyplex.

Quaternized or partially quaternized derivatives of poly(4-vinylpyridine) (DP = 1,600, M_w = 168 kDa) were synthesized by the group of Izumrudov [210]. Among them, four different series were synthesized: quarternized poly(4-vinylpyridine) with *N*-alkyl ester substituents (C*n*-PVP, Fig. 20b), polycarboxybetaine with alkyl spacer (C*n*-PCB, Fig. 20c), poly[(4-vinylpyridine)-*co*-(*N*-alkyl-4-vinylpyridinium)] and poly[(*N*-methyl-4-vinylpyridine)-*co*-(*N*-alkyl-4-vinylpyridinium)] both with various alkylation degree β (respectively C*n*-PVP-β, Fig. 20d and Me-C*n*-PVP-β, Fig. 20e). Unfortunately, relatively few comparisons between these polymers were presented in this publication regarding the physico-chemical characteristics of their polyplexes. At a charge ratio of 5, C*n*-PVP-based polyplexes with short *N*-alkyl

substituents ($n = 1$–3) remained relatively inefficient regarding transfection, whereas more efficiency was noticeable for $n = 4$ and 5 (which could be due to the more pronounced destabilizing properties of cell membranes), then decreased again for $n = 6$, which might be due to a certain hindrance of its interaction with DNA itself by the presence of the long hydrophobic chain. The substitution of the ester moiety in the side chain of C*n*-PVP ($n = 4$ and 5) by a carboxylic group gave the corresponding polycarboxybetaines (C*n*-PCB). After complexation with DNA at a charge ratio of 5, they showed far less transfection activity compared to the parent polycations. The presence of the carboxylic group certainly weakened the interaction with DNA and possibly required a higher charge ratio for complexation. For the C*n*-PVP-β series with various quaternization degrees, at a charge ratio of 5 there was a bell-shaped dependency of the transfection efficiency as a function of the alkylation degree, with the maximum at $\beta = 65\%$ for $n = 5$ (1000% increase in efficiency compared to pDNA alone) ($\beta = 40\%$ for $n = 6$), despite the similar sizes and zeta potentials of the polyplexes over all the β range. The explanation of the authors regarding this increased transfection efficiency of the partially alkylated PVP, C*n*-PVP-β, was the presence of the pyridine groups, which could eventually be protonated in acidic media and thus could play a role in the proton sponge effect. Interestingly, the further methylation of these C*n*-PVP-β derivatives led to negligible transfection efficiencies.

More recently, amphiphilic dimethylaminopyridinium-containing polymethacrylates with tail-end geometries with octyl, dodecyl, and hexadecyl spacers ($n = 8$, 12, 16) neutralized by bromide (Br) and octylsulfonate (S8) counterions were studied (P*n*DMAP-X, Fig. 20f) [211]. This study allowed the comparison of pyridinium-based derivatives according to the length of the spacer, counterion, and geometry. These polymers possess two kinds of amino moieties: a tertiary amine tail linked directly to the heterocycle (not protonated under physiological conditions) and an ammonio group that forms part of the pyridinium heterocycle, which is involved in the electrostatic binding with DNA. The amphiphiles P*n*DMAP-X formed a mixture of worm-like and spherical micelles in water for concentrations above 0.5 mg mL^{-1}, with P_8DMAP-X forming the loosest structures. The weight ratios of P*n*DMAP-X:DNA needed to retard DNA in gel electrophoresis were about 1.5 for $n = 8$, 3–5 for $n = 12$, and 2.5–5 for P_{16}DMAP-X for X = Br and 5–7.5 for X = S8. Thus, the decrease in charge density for these derivatives with increasing spacer length could not only be accounted for by this trend in the minimum charge ratio needed. The counterion effect appeared for $n = 16$, where a higher weight ratio for S8 than for Br is needed to complex DNA, probably due to the reduced accessibility of the pyridinium group for DNA with this alkyl counterion (due to its size and/or hydrophobicity). Moreover, the transfection efficiency as a function of the spacer length followed the same trend in both series (X = Br and S8), with the highest transfection efficiency being obtained for $n = 12$, followed by $n = 8$ and finally $n = 16$. Also, a bell-shaped dependency of the transfection efficiency was observed as function of the length of the spacer. As in the previous example, it seems that a compromise between membrane destabilization (also reflected by increased cytotoxicity) and efficient DNA complexation has to be found for this type of derivative.

Poly(1-vinylimidazole)s alkylated with various chain lengths (R) and quaternization degree β (PVIm-R-β, Fig. 20g) were studied by the group of Asayama [212]. Due to the fact that imidazole groups are negligibly charged at physiological pH, quaternary nitrogen atoms as strong electrolytes were introduced in the structure. In order to still benefit from the pH buffering capacity of imidazole groups at endosomal pH, the quaternization was only partial. Taking PVIm-Bu as an example, complete DNA retardation occurred at a ratio of [butylated imidazole]/[phosphate] of around 1. Given that the pK_a of the unmodified imidazole groups is around 6, the efficiency of DNA complexation at pH 6 (retardation of DNA migration occurred at a ratio of [butylated imidazole]/[phosphate] of 0.5) was greater than at pH 7.4, benefiting from the protonation of these imidazole groups. Moreover, the polyplexes based on PVIm-Bu caused negligible hemolysis at pH 7.4 but had a membrane disruptive activity at endosomal pH, and their stability (against polyanion exchange) was between that of PVIm-NH_2 and PVIm-Oct. Concerning the cytotoxicity, PVIm-R with short alkyl chains (methyl, ethyl, butyl) were relatively non-cytotoxic, while PVIm-Oct caused significant cytotoxicity. Gene transfection of the luciferase gene to Hep2 cells was dependent on the length and density of the alkyl chains: for PVIm-Bu; the higher the density of butylated imidazole groups, the better was the transfection efficiency at low charge ratios (+/− < 12). For a middle density of alkylated imidazole groups (~20%), PVIm-Me and PVIm-Et mediated a higher gene expression than PVIm-Bu even at lower +/− charge ratio. This could be explained, as in the last case, by too much screening of the charges with the butyl chains.

2.2.2 Amphiphilic Polymers and Lipopolymers

Lipopolymers are polymers containing lipid moieties such as a fatty acid or a steroid such as cholesterol. At least some of the polymers presented in this section could eventually form micelles due to their amphiphilic structure, but either the concentration of their solution is under the CMC or the micelles are diluted and/or destabilized during their addition to the DNA solution.

Hydrophobicity can be introduced onto the side chains with hydrophobic moieties such as cholesterol and 1,2-dioleoyl-sn-glycero-3-phosphoethanolamine (DOPE) as will be presented in the next two examples. P(QuatDMAEMA-*co*-Chol) (Fig. 21a) is a copolymer containing quaternary ammonium units and cholesterol but no tertiary amines [213]. As previously seen, the range where the polyplexes are stable is diminished if the content of hydrophobic groups is too high. By slow addition of polycation to DNA, at N:P ratio close to 1, flocculation was observed for polyplexes based on the polymers with the highest cholesterol content (6.3 and 8.7 mol%) and only negatively charged polyplexes could be prepared. By fast addition of the polycation with highest cholesterol content to DNA, the M_w of the aggregates showed the inverse tendency and decreased with increasing N:P ratios, even close to unity as already observed in the studies by Kabanov and Kabanov [214] and Oupicky et al. [215], while staying relatively constant above N:P = 1 for the polyplexes based on

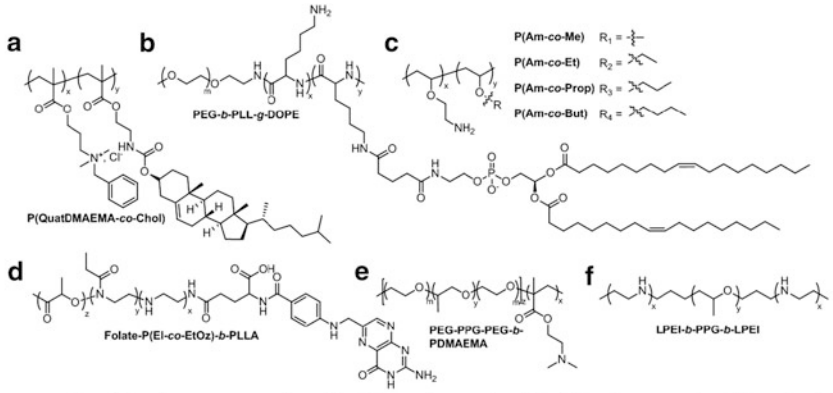

Name of the polymer	Abbreviation	Description of the polymer	DNA used	Ref
Poly[(2-{[(cholesteryloxy)carbonyl]amino}ethylmethylmethacrylate)-*co*-(benzyl-[2-(methacryloyloxy)ethyl]dimethylammonium chloride)]	P(QuatDMAEMA-*co*-Chol)	M_w = 10kDa, masse/charge = 290g.mol^{-1}, mol.% Chol = 1.4	DNA: M_w = 6.7.10^{6}Da	[213]
		M_w = 20kDa, masse/charge = 304g.mol^{-1}, mol.% Chol = 6.3		
		M_w = 20kDa, masse/charge = 338g.mol^{-1}, mol.% Chol = 8.7		
Poly(ethylene glycol)-*b*-polylysine	PEG-*b*-PLL (precursor)	M_w = 3-17kDa	pEGFP-N$_1$	[216]
Poly(ethylene glycol)-*b*-polylysine-*g*-(1,2-dioleoyl-sn-glycero-3-phosphoethanolamine)	PEG-*b*-PLL-*g*-DOPE	Degree of DOPE modification: 16, 30, 56%		
Poly[(2-aminoethyl vinyl ether)-*co*-(methyl vinyl ether)]	P(Am-*co*-Me)	M_w = 8.5kDa, masse/charge = 147g.mol^{-1}	pDNA: TMR-DNA	[217]
Poly[(2-aminoethyl vinyl ether)-*co*-(ethyl vinyl ether)	P(Am-*co*-Et)	M_w = 2.5kDa, masse/charge = 165g.mol		
Poly[(2-aminoethyl vinyl ether)-*co*-(propyl vinyl ether)]	P(Am-*co*-Prop)	M_w = 4.2kDa, masse/charge = 153g.mol		
Poly[(2-aminoethyl vinyl ether)-*co*-(butyl vinyl ether)]	P(Am-*co*-But)	M_w = 5.0kDa, masse/charge = 164g.mol		
Folate-poly[ethyleneimine-*co*-(2-ethyl-2-oxazoline)]-*b*-poly(L-lactide)	Folate-P(EI-*co*-EtOz)-*b*-PLLA	M_n = 5.6kDa, %hydrolysis = 75%, PEI/PLLA (mol) = 0.90, folic acid (μmol/g) = 110	pUHC 13-3	[218]
		M_n = 12.6kDa, %hydrolysis = 66%, PEI/PLLA (mol) = 0.93, folic acid (μmol/g) = 75		
		M_n = 3.6kDa, %hydrolysis = 85%, PEI/PLLA (mol) = 0.41, folic acid (μmol/g) = 42.1		
Pluronic-*b*-poly(2-*N*-(dimethylaminoethyl)methacrylate)	PEG-PPG-PEG-*b*-PDMAEMA	m = 8, y = 52, z= 1, x = 22.9	pDNA: pCMV-βGal	[219]
			DNA sodium salt from Salmon testes	[220]
Poly(ethyleneimine)-*b*-poly(propylene glycol)-*b*-poly(ethyleneimine)	LPEI-*b*-PPG-*b*-LPEI	x = 50, y = 36, M_n = 6.3kDa	SMD2-LucΔITR (7.6kb)	[221]
		x = 19, y = 36, M_n = 3.7kDa		
		x = 14, y = 68, M_n = 5.2kDa		

Fig. 21 (**a**–**f**) Amphiphilic polycations: amphiphilic polymers and lipopolymers not forming micelles after addition to DNA

the two other polycations (1.4 and 6.3 mol% cholesterol). Moreover, by fast addition of polycations to DNA, ζ-potential increased with increasing content of cholesterol, i.e., with the hydrophobicity of the polycations. This effect was explained by the authors as such: DNA and polycations were intermixed in the initially formed complex (electrostatic interactions) giving rise to hydrophobic particles. The particles started to attract hydrophobic polycations by hydrophobic interaction, forming core–shell structures with the strongly hydrophobic cholesterol moieties of polycations attached to the particle surface and the remaining positively charged parts of polycations forming the shell, increasing the ζ-potential of the particle surface. The particle growth was then stopped by repulsive interactions of positively charged PECs and polycations, and the colloid stability of PECs increased with increasing content of side chains bearing cholesterol moieties, which is related to the level of surface charge and hydrophobicity of polycations.

In the case of PEG-*b*-PLL-*g*-DOPE (Fig. 21b), the lengths of the PEG and PLL blocks were not given and the PEG-*b*-PLL precursor was relatively polydisperse [216]. The authors supposed that PEG-*b*-PLL-*g*-DOPE assembled into micelles,

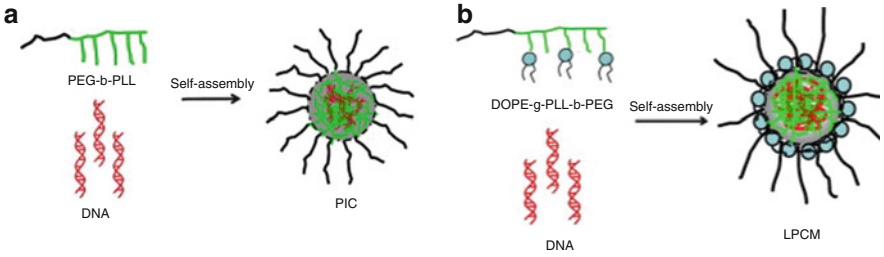

Scheme 18 Formation of (**a**) polyion complex micelles (PIC) for PEG-*b*-PLL and (**b**) lipid-modified polyion complex micelles (LPCM) for PEG-*b*-PLL-*g*-DOPE. Reprinted with permission from [216]. Copyright 2012 Elsevier

whose structure was then destroyed by addition of DNA (concentration before mixing not given). Unfortunately, the formation of micelles has not been proven (no TEM pictures of PEG-*b*-PLL-*g*-DOPE before complexation with DNA and no determination of CMC), but is extremely plausible given the concentration of DOPE in the copolymer. By addition of DNA, a structure composed of a PLL/DNA core with DOPE on the core surface and a hydrophilic PEG shell was proposed as model (Scheme 18b). With increasing the degree of modification with DOPE, the mass ratio of polycation to DNA needed to completely retard DNA migration increased: for the PEG-*b*-PLL precursor, the mass ratio was 6, and for PEG-*b*-PLL-*g*-DOPE polycations with degree of DOPE modification of 16, 30, and 56% it was 14, 20, and 25, respectively. The polyplexes based on these polymers showed improved transfection efficiency in HepG2 and HeLa cells compared to naked DNA and PEG-*b*-PLL/DNA and comparable results to PEI. The polymer with 30% modification with DOPE showed the best results, probably due to a good compromise between a lower degree of DOPE, which did not allow the complex to penetrate the membrane, and a too-high degree of DOPE, which reduced the ability of the polymer to complex DNA.

In the last examples of this section, interesting chemical structures will be presented but unfortunately relatively little information regarding their physico-chemical characteristics and/or transfection efficiency is available. Poly[(2-aminoethyl vinyl ether)-*co*-(alkyl vinyl ether)], with various alkyl chain lengths such as methyl, ethyl, propyl, and butyl [P(Am-*co*-Me), Fig. 21c-R_1; P(Am-*co*-Et), Fig. 21c-R_2; P(Am-*co*-Prop), Fig. 21c-R_3; and P(Am-*co*-But), Fig. 21c-R_4, respectively) is a good example [217]. The membrane lytic activity of these polymers was dependent on the length of the alkyl chains: the longer the better. Optimal transfections activities were obtained at an N:P ratio of 4, with P(Am-*co*-But) being the most efficient (ten times more efficient than PEI under these conditions), which correlated with the membrane lytic activity.

Hydrophobicity can also be introduced via a degradable hydrophobic block in a copolymer such as polylactide. For instance, folate-P(EI-*co*-EtOz)-*b*-PLLA (Fig. 21d) was synthesized via the partial hydrolysis of poly(2-ethyl-2-oxazoline) block at 66% and more, and the folic acid moiety also contributed to the hydrophobicity of the construct [218]. Folate-P(EI-*co*-EtOz)-*b*-PLLA began to form complexes with DNA

at a polymer:DNA ratio of 10, while linear PEI completely retarded DNA at a ratio of 6. Polymers containing a large amount of PLLA reduced toxicity on HeLa cells compared to linear PEI, but also mediated gene transfer less efficiently.

A non-degradable hydrophobic block in a copolymer can be used to introduce hydrophobicity. A good example is Pluronics and its hydrophobic segment poly (propylene glycol) (PPG), such as in PEG-PPG-PEG-*b*-PDMAEMA (Fig. 21e) [219]. The pK_a value of PEG-PPG-PEG-*b*-PDMAEMA was 7.1, lower than PEG-*b*-PDMAEMA and PDMAEMA, due to the effect of Pluronic™ lowering the dielectric constant of the amino groups. The polymer possessed a CMC of 5 g L^{-1}, which is relatively high. The polymer condensed DNA into polyplexes of 200 nm in diameter at polymer:DNA ratios of 6 and more and a slightly positive zeta potential. Compared to PEG-*b*-PDMAEMA, the condensation was less efficient but the transfection efficiency was much higher and at lower polymer:DNA ratio [220].

LPEI-*b*-PPG-*b*-LPEI (Fig. 21f) with various LPEI and PPG block lengths were studied [221]. Note that these polymers, at least the ones with the highest hydrophilic:hydrophobic ratio, may self-assemble into flower-like micelles. $LPEI_{50}$-*b*-PPG_{36}-*b*-$LPEI_{50}$ and $LPEI_{19}$-*b*-PPG_{36}-*b*-$LPEI_{19}$ were able to retard DNA migration at a polymer:DNA weight ratio of 3:4 and 1:1, respectively, while $LPEI_{14}$-*b*-PPG_{68}-*b*-$LPEI_{14}$ was not able to retard DNA even at a ratio of 15:1. These data, in correlation with AFM studies, suggest that $LPEI_{50}$-*b*-PPG_{36}-*b*-$LPEI_{50}$ forms micellar structures where the positive charges are still available for interactions with DNA, whereas in the case of $LPEI_{19}$-*b*-PPG_{36}-*b*-$LPEI_{19}$, the positive charges must be buried in the structure, hindering efficient electrostatic interactions with DNA.

2.2.3 Micelles of Amphiphilic Polymers and Lipopolymers

The polymers presented in this section can form micelles due to their amphiphilic structure. Moreover, there is the possibility to use these micelles as multicarriers, with hydrophobic drug loaded in the hydrophobic interior of the micelles and the genetic material complexed on the positively charged shell, if the micelles can structurally resist the addition of DNA.

P(MDS-*co*-CES) (Fig. 22a) is a biodegradable copolymer with a polyester main chain and containing potentially hydrolytically labile urethano groups to link the cholesterol moieties [222]. Moreover, this polymer contains both quaternary ammonium groups (DNA binding) and tertiary amine groups (endosomal buffering). This polymer formed micelles (CMC = 1.9 mg mL^{-1}), which were positively charged (72 mV) and had a diameter of 96 nm in sodium acetate buffer and these pre-formed micelles were used for complexation of pDNA. This approach is different from the approach previously seen, where the polymer was added to DNA and, consequently, micelle formation was hindered due to the stronger electrostatic interactions between DNA and the positively charged block of the copolymer. The obtained polyplexes exhibited decreased mobility in gel electrophoresis and complete retardation at N:P ratio of 2. By studying the changes in the microenvironment of pyrene entrapped in the micelles, the authors verified the integrity of the core–shell nanoparticles during the DNA binding process and that

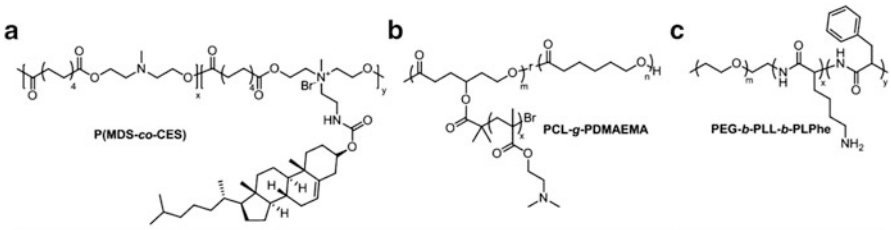

Name of the polymer	Abbreviation	Description of the polymer	CMC/CAC (mg.L^{-1})	DNA used	Ref
Poly{(*N*-methyldietheneamine sebacate)-*co*-[(cholesteryloxocarbonylamido ethyl) methyl bis(ethylene) ammonium bromide] sebacate}	P(MDS-*co*-CES)	M_w = 9.1kDa, M_w/M_n = 2.0 ~30-40% degree cholesterol grafting	1.9	pDNA: pCMV-luciferase VR1255_C (6.4kb), pEGFP-C1 driven by SV40 early promoter (4.7kb)	[222]
Poly(ε-caprolactone)-*g*-poly[2-(*N*,*N*-dimethylamino) ethyl methacrylate]	PCL-*g*-PDMAEMA	m+n = 83, m = 6, x = 56, M_n = 38.7kDa, M_w = 64.2kDa, M_w/M_n = 1.66	0.81	pDNA: pEGFP	[223]
Poly(ethylene glycol)-*b*-poly(L-lysine)-*b*-poly(L-phenylalanine)	PEG-*b*-PLL-*b*-PLPhe	M_n = 15kDa, mol.% EG = 45, mol.% LLys = 96, mol.% LPhe = 16	375	pDNA: pEGFP-C1	[224]
		M_n = 18kDa, mol.% EG = 45, mol.% LLys = 96, mol.% LPhe = 37	139		

Fig. 22 (**a–c**) Amphiphilic polycations: amphiphilic polymers and lipopolymers forming micelles even in the presence of DNA

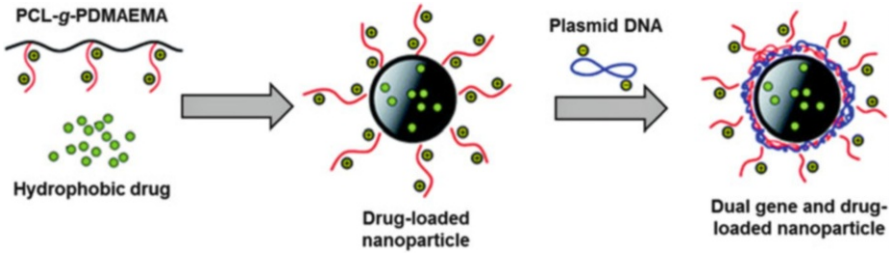

Scheme 19 Preparation of PCL-*g*-PDMAEMA NPs with payloads of hydrophobic drugs and plasmid DNA [223]. Copyright 2011 Royal Society of Chemistry

the DNA binding further increased the hydrophobicity of the pyrene's microenvironment. The transfection efficiency of this nanocarrier was tested on HEK293, HepG2, and 4T1 mouse breast cancer cell lines and depended strongly on the cell type and the N:P ratio. In HepG2 cells, the uptake of nanoparticle/DNA-based complexes was higher than for PEI/DNA, possibly due to their higher positive charge, which at the same time probably hindered the release of DNA intracellularly, leading to slightly lower overall gene expression. Importantly the amount of nanoparticles needed for optimal gene transfection was much lower than their IC_{50} values (around 150 μg mL^{-1} depending on the cell line).

The hydrophobic part in amphiphiles can be the backbone, for instance poly (ε-caprolactone) (PCL). Indeed, PCL-*g*-PDMAEMA (Fig. 22b) formed nanoparticles (CAC = 0.81 mg mL^{-1}) in water with diameters of several hundreds of nanometers (probably vesicles) and zeta potential of more than 40 mV (Scheme 19) [223]. These nanoparticles were pH- and thermoresponsive due to the presence of the PDMAEMA; the NPs were in a swollen state at an acidic pH range 6.0–6.9 at 37°C or higher but retracted at pH 7.4 and became even smaller when the temperature was above 37°C. Complete retardation was observed for N:P ratio of 2. In this case,

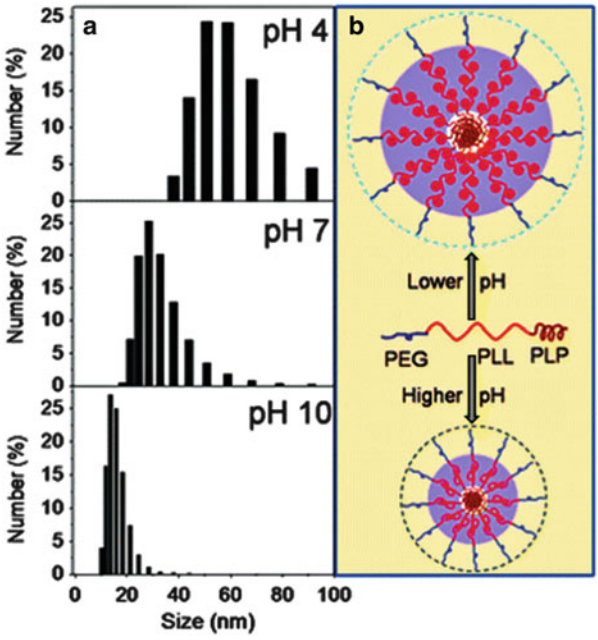

Scheme 20 (**a**) Size distribution of PEG-*b*-PLL-*b*-PLPhe micelles at different pH values. (**b**) Self-assembly of PEG-*b*-PLL-*b*-PLPhe copolymers at different pH values [224]. Copyright 2011 Royal Society of Chemistry

the environment of the pyrene did not become more hydrophobic during DNA binding. The polyplexes showed a bell-shaped dependency of the transfection efficiency as a function of N:P ratio in 293T cells, and comparable values to Lipofectamine™2000 at a N:P ratio of 10 and 15. The internalization of these polyplexes was relatively slow; adherence to the cell membrane arose after 6 h, and after 24 h internalization and release into the cytoplasm had taken place.

Hydrophobicity can be introduced via hydrophobic amino acids such as phenylalanine, as in PEG-*b*-PLL-*b*-PLPhe (Fig. 22c), which formed micelles (25–45 nm in diameter). The CMC of PEG-*b*-PLL-*b*-PLPhe decreased with increasing hydrophobic content (i.e., phenylalanine units) [224]. These CMC values (>100 mg mL^{-1}) are quite high compared to those of other polymers. The copolymers did not exhibit apparent toxicity until a concentration of 500 μg mL^{-1}. Due to the presence of PLL, the micelles self-assembled from PEG-*b*-PLL-*b*-PLPhe possessed pH-sensitive properties: from pH 4 to 10 their hydrodynamic diameter decreased from 60 nm to 15 nm (Scheme 20). The weight ratios at which the polymers can condense DNA were 2 and 15 for the PEG-*b*-PLL-*b*-PLP containing 16 and 37% phenylalanine, respectively, due to the higher density of amino groups of the first polymer. Moreover, at a ratio of 20, the size of the polyplexes were respectively 250 nm and 650 nm, while the zeta potentials were 25 and −10 mV, showing the incomplete condensation of DNA with the polymer containing the most phenylalanine units. Their transfection efficiency at a ratio of 20 and more was less efficient than PEI at a ratio of 10, despite their capacity to be internalized by cells. It was nevertheless not clear in this study if PEG-*b*-PLL-*b*-PLPhe were still self-assembled as micelles for DNA delivery.

3 Polyampholyte/DNA Complexes

Ampholytes are amphoteric molecules that contain both acidic and basic groups and exist mostly as zwitterions in a certain pH range. The pH at which the average charge is zero is known as the molecule's isoelectric point.

3.1 Polyzwitterions

A zwitterion is a neutral molecule with a positive charge introduced via a cationic functional group such as quaternary ammonium or phosphonium, which bears no hydrogen atom, and with a negative electrical charge introduced via a functional group such as carboxylate, which may not be adjacent to the cationic site. The overall neutrality of the molecule arises via a kind of intramolecular acid–base reaction between, for instance, an ammonium and a carboxylate group. Good examples of zwitterions are phosphorylcholine and betaines.

3.1.1 Polycarboxybetaines

The complexation of DNA with poly(pyridinio carboxylate)s with various lengths of additional alkyl chain at the α carbon and a carboxylate always in β position (Fig. 23a), also called polycarboxybetaines (PCB), was studied by Izumrudov et al. [225]. Given that these PCB possess quaternary ammoniums that are charged at any pH, these polymers indeed proved to be soluble in the pH range 2–11. For the pH range where DNA remains in the native state (4.0–10.0) these PCB were not able to bind DNA strongly enough to squeeze out EtBr (~15% reduction in fluorescence at N:P ratio of 2), which was explained by the authors by the amino group and the carboxylate group in β position forming a rather stable ionic pair. The influence of the length of additional alkyl chain at the α carbon was negligible.

More interesting are poly(pyridinio carboxylate)s with various lengths of alkyl chain (m) between charges (PCB_m, Fig. 23b) [226]. Even with increasing the length of the spacer between the quaternary ammonium and the carboxylate group ($m = 1$–8), a stable ion pair was formed in neutral and weakly acidic media, reflected by the hindered protonation of the carboxylate group (as shown by potentiometric titration), and could lead to a potential inhibition of their electrostatic interactions with DNA. Despite the similar potentiometric behavior of the PCB_m series, the length of the spacer in these polybetaines had an influence on their complexation with DNA. At N:P ratio of 5, PCB_5 showed a good propensity to exclude EtBr at pH 9 (reduction of 75% of fluorescence), followed by PCB_2 (reduction of 15% in fluorescence), while PCB_4 and PCB_8 showed similar behaviors (less than 5% reduction in fluorescence). The polyplexes followed the same trend in the dissociation of the complex in presence of salt (NaCl). The authors suggested that the propensity of PCB_m (for $m = 3$ and 4) to form betaine

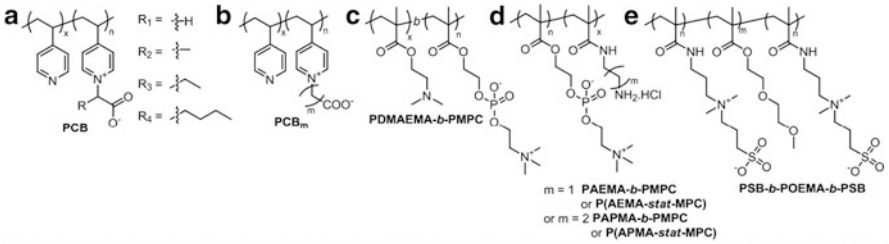

Name of the polymer	Abbreviation	Description of the polymer	DNA used	Ref
Poly(pyridinio carboxylate) with various lengths of additional alkyl chain at α carbon	PCB	Degree of substitution (n) > 79%, M_n = 21-23kDa	ctDNA (10kbp)	[225]
Poly(pyridinio carboxylate) with various lengths of alkyl chain (m) between charges	PCB$_m$	m = 1, 2, 3, 4, 5, 8 Degree of substitution (n) > 92%, M_n = 352-519kDa	ctDNA (10kbp)	[226]
Poly[2-(dimethylamino)ethyl methacrylate]-*b*-poly(2-methacryloyloxyethyl phosphorylcholine)	PDMAEMA-*b*-PMPC	PDMAEMA precursor: x = 40, M_n = 12.7kDa, M_w/M_n = 1.07; n = 10, 20, 40, 50, M_n = 9.0, 12.0, 18.0, 21.0kDa, M_w/M_n = 1.21-1.26, %MPC = 32, 48, 65, 70%	gWiz Luc pDNA (~ 6.7kbp)	[229]
		PMPC precursor: n = 30, M_n = 8.3kDa, M_w/M_n = 1.21; x = 10, 20, 40, 60, 100, M_n = 10.0, 12.0, 15.0, 18.0, 24.0kDa, M_w/M_n = 1.26-1.32, %MPC = 85, 74, 58, 48, 36%		
Poly[*N*-(2-aminoethyl) methacrylamide]-*b*-poly(2-methacryloxyethyl phosphorylcholine)	PAEMA-*b*-PMPC	x = 15-36, n = 17-40, M_n = 7.6-18.0kDa, M_w/M_n = 1.3, %MPC ~ 50%	Gwiz β-galactosidase pDNA	[231]
Poly{[*N*-(2-aminoethyl) methacrylamide]-*stat*-(2-methacryloxyethyl phosphorylcholine)}	P(AEMA-*stat*-MPC)	x = 10-40, n = 15-36, M_n = 6.0-17.0kDa, M_w/M_n = 1.2		
Poly[(3-aminopropyl) methacrylamide]-*b*-poly(2-methacryloxyethyl phosphorylcholine)	PAPMA-*b*-PMPC	x = 18-37, n = 16-40, M_n = 8.2-18.0kDa, M_w/M_n = 1.1-1.3		
Poly{[(3-aminopropyl)methacrylamide]-*stat*-(2-methacryloxyethyl phosphorylcholine)}	P(APMA-*stat*-MPC)	x = 7-32, n = 14-32, M_n = 5.4-15.0kDa, M_w/M_n = 1.2		
Poly{*N*-[3-(methacryloylamino)propyl]-*N*,*N*-dimethyl-*N*-(3-sulfopropyl) ammonium hydroxide}-*b*-poly[2-(2-methoxyethoxy)ethyl methacrylate]-*b*-poly{*N*-[3-(methacryloylamino)propyl]-*N*,*N*-dimethyl-*N*-(3-sulfopropyl) ammonium hydroxide}	PSB-*b*-POEMA-*b*-PSB	POEMA: m=200, n=0. M_n[a] = 24.5kDa, M_w/M_n = 1.28	ctDNA (5kbp) pDNA (~ 5.3kbp)	[232]

		PSB-*b*-POEMA-*b*-PSB:
		m = 160, n = 20, M_n = 34.6kDa, M_w/M_n = 1.31;
		m = 100, n = 50, M_n = 32.8kDa, M_w/M_n = 1.23;
		m = 40, n = 80, M_n = 15.9kDa, M_w/M_n = 1.28		

		PSB: m = 0, n = 200, M_n = 30.4kDa, M_w/M_n = 1.2		

[a] determined by ^{1}H NMR.

Fig. 23 (**a**–**e**) Polyampholytes based on betaines

rings spontaneously in aqueous solutions may be responsible for the first minimum, whereas the second minimum could be attributed to the ability of the relatively long spacer in PCB_8 for cross-binding intramolecular electrostatic interactions of the charges within neighboring repeat units.

From these results, it is clear that zwitterions can be used as steric stabilizer but that in order to complex DNA, positively charged moieties and a certain distance between the zwitterionic groups are needed. Other polybetaines with PDMAEMA or primary amines are presented in the next sections and constitute a further improvement of these systems.

3.1.2 Polyphosphobetaines

The zwitterionic 2-methacryloyloxyethyl phosphorylcholine (MPC) block is a highly hydrated structure, where each monomer associates with 12 water molecules [227, 228]. In a block copolymer, this block is thought to introduce steric stabilization for the polyplex after complexation of the polycationic block with DNA.

A series of PDMAEMA-*b*-PMPC (Fig. 23c) with various length of PMPC block starting from $PDMAEMA_{40}$ or various lengths of PDMAEMA blocks starting from $PMPC_{30}$ were studied by the group of Stolnik [229]. $PDMAEMA_{40}$-based

copolymers with shorter PMPC blocks (10 or 20) had DNA binding affinities comparable to PDMAEMA homopolymer and higher DNA binding affinities than copolymers with longer PMPC blocks. When the percentage of PMPC was 65% and higher, the copolymers exhibited decreased affinity for DNA, suggesting that the presence of a long PMPC block was deleterious to DNA complexation; moreover, above a 1:1 ratio, the presence of this steric stabilizer reduced the association of the excess polymer with the polyplexes formed, as already observed for PDMAEMA-*b*-PEG [182], and prevented aggregation, which was not the case for copolymers with shorter PMPC blocks (10 or 20). $PDMAEMA_{40}$-*b*-$PMPC_{30}$ and $PDMAEMA_{40}$-*b*-$PMPC_{40}$ formed well-defined polyplexes with hydrodynamic diameters of approximately 150 nm, while $PDMAEMA_{40}$-*b*-$PMPC_{50}$ formed larger polyplexes with DNA with higher polydispersity. In the $PMPC_{30}$-based copolymers series, increasing the size of the PDMAEMA block resulted in higher condensation ability as well as in smaller polyplexes in the sub-200 nm size range (except for $PDMAEMA_{10}$-*b*-$PMPC_{30}$), but also decreased the solubility of the polyplexes. As expected, the presence of PMPC block reduced the cellular association of these polyplexes, which correlated with their low transfection efficiencies (in the range of free DNA). A content ratio of the MPC unit to tertiary amine higher than 2 was required to produce spherical, well-condensed particles; MPC unit to amine ratios lower than 2 produced irregular structures ranging from toroids to rods [230].

Narain and coworkers studied copolymers of *N*-(2-aminoethyl) methacrylamide and 2-methacryloxyethyl phosphorylcholine as block or statistical copolymers [PAEMA-*b*-PMPC, P(AEMA-*stat*-MPC)] and (3-aminopropyl) methacrylamide and 2-methacryloxyethyl phosphorylcholine as block or statistical copolymers [PAPMA-*b*-PMPC, P(APMA-*stat*-MPC)] (see Fig. 23d) [231] in the same range of molecular weights as in the previous study [229] and around 50% modification in MPC. Unfortunately, little information is given about the physico-chemical characteristics of the polyplexes. Moreover, it was not clear which polymer:DNA ratios were used in order to obtain polyplexes with diameters ranging from 50 to 200 nm, but in general statistical polymers yielded polyplexes with larger diameters and irregular shapes compared to the corresponding diblock copolymers (which yielded spherical nanoparticles). Hence, not only the composition of MPC-based copolymers had an influence on the size and shape of the polyplexes but, as already seen for other systems, the architecture also played an important role. Copolymers with low molecular weights (6–7 kDa) showed lower gene expression as compared to polymers with higher molecular weights (10–12 kDa). A further increase in molecular weight led to a decrease in gene expression, probably due to their higher cytotoxicity. Moreover, the block copolymer architecture resulted in better transfection efficiency than the statistical copolymer, which was not due to an enhanced cellular uptake.

3.1.3 Polysulfobetaines

Polymers based on a sulfobetaine and the triblock thereof, PSB-*b*-POEMA-*b*-PSB (Fig. 23e) were found to be able to complex DNA [232]. The approach relied on OEMA as steric stabilizer, while the zwitterionic sulfobetaine itself was supposed to complex DNA, despite the presence at a short distance of the quaternary ammonium in the middle of the chain and the sulfonate as chain end (electrostatic repulsion with DNA). Nevertheless, its potential interest relied in the schizophrenic behavior of the polymer: the poly{*N*-[3-(methacryloylamino)propyl]-*N*,*N*-dimethyl-*N*-(3-sulfopropyl) ammonium hydroxide}block possessing an UCST (as heat energy is required to dissociate the crosslinking points stemming from ion pairings between ammonium cation and sulfo anion), whereas the poly [2-(2-methoxyethoxy)ethyl methacrylate] possessed an LCST. In the series obtained at 1 wt%, the polymers possessed an UCST in the range 14–18°C, followed by an LCST in the range 22–24°C (both transitions are dependent on the length of the blocks and concentration of the polymers in solution, in the range of DP considered for the PSB block and for the POEMA block with DP of 160 and less). The homopolymer PSB_{200} quenched 75% of EtBr fluorescence at polymer: DNA ratio of 5 and completely quenched it at N:P ratio of 20. The polymer condensed DNA into nanoparticles of less than 80 nm in diameter. PSB_{50}-*b*-$POEMA_{100}$-*b*-PSB_{50} and PSB_{80}-*b*-$POEMA_{40}$-*b*-PSB_{80} both quenched 40–45% of the fluorescence at ratio of 5, and reached a plateau of 55–60% at a ratio of 20. At a ratio of 10, they formed NPs with average size of 120 nm that were less compact and with irregular shape. This superior quenching of EtBr fluorescence cannot only be explained by the distance between opposite charges if we refer to the case of polycarboxybetaine. The capacity of the copolymers to bind DNA decreased with a decrease in the relative proportion of the PSB block (decrease in charge density) as well as an increase in the proportion of POEMA (steric hindrance).

3.2 Polyamphoters

An amphoteric species is a molecule or ion that can react as an acid as well as a base. One type of amphoteric species are amphiprotic molecules, which can either donate or accept a proton; examples are amino acids and proteins, which have amine and carboxylic groups. The competition between the acid–base equilibria of these groups leads to additional "complications" in their physical behavior but can also present some advantages due to the variation of their charge as a function of pH.

Poly(1,2-propylene H-phosphonate) modified with spermidine (PPA-*g*-SP, Fig. 24a with $m = 1$) had a LD_{50} of 85 μg mL^{-1} in HEK293 and COS-7 cells [233]. Efficient complexation with DNA was achieved for N:P ratios of 1.5 and

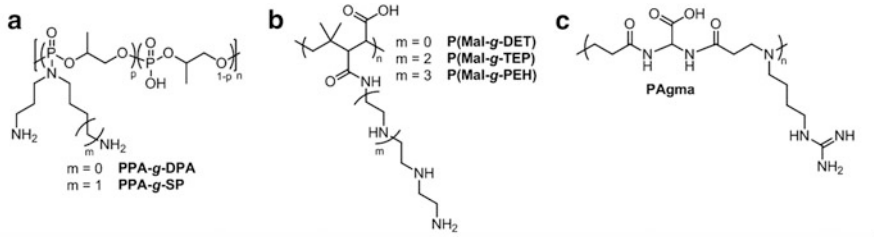

Name of the polymer	Abbreviation	Description of the polymer	DNA used	Ref
Poly(1,2-propylene H-phosphonate) modified with spermidine	PPA-*g*-SP	m = 1, p = 0.29, M_w = 34.4kDa, DP_n = 90, M_w/M_n = 1.43	pRE-Luciferase (11.9kbp) pcDNA3/Bcl-2	[233]

Poly(1,2-propylene H-phosphonate) modified with dipropyltriamine	PPA-*g*-DPA	m = 0 for all and:
		p = 0.49, M_w = 10.4kDa, DP_n = 54, M_w/M_n = 1.4;
		p = 0.50, M_w = 15.0kDa, DP_n = 77, M_w/M_n = 2.4;
		p = 0.50, M_w = 27.1kDa, DP_n = 139, M_w/M_n = 1.9;
		p = 0.51, M_w = 57.5kDa, DP_n = 344, M_w/M_n = 2.0:
		p = 0.56, M_w = 25.1kDa, DP_n = 124, M_w/M_n = 2.3;
		p = 0.65, M_w = 30.8kDa, DP_n = 146, M_w/M_n = 2.7
			VR1255C (6.4kb)	[234]

Poly(isobutylene-*alt*-maleic acid) grafted diethylenetriamine	P(Mal-*g*-DET)	93% grafting, M_w ~ 10kDa	pDNA: pCMV-luciferase VR1255C (6.4kb), pEGFP-C1 (4.7kb)	[235]
Poly(isobutylene-*alt*-maleic acid) grafted tetraethylenepentamine	P(Mal-*g*-TEP)	87% grafting, M_w ~ 12kDa		
Poly(isobutylene-*alt*-maleic acid) grafted pentaethylenehexamine	P(Mal-*g*-PEH)	77% grafting, M_w ~ 13kDa		
Poly{[2,2-bis(ethylamido)acetic acid]-*alt*-agmatine}	PAgma	M_n = 4.8kDa, M_w = 7.2kDa, M_w/M_n = 1.50	pDNA	[238]
		M_n = 3.3kDa, M_w = 4.5kDa, M_w/M_n = 1.38; M_n = 7.8kDa, M_w = 10.1kDa, M_w/M_n = 1.29; M_n = 16.4kDa, M_w = 20.5kDa, M_w/M_n = 1.25		[239]

Fig. 24 (**a**–**c**) Polyamphoters

higher (as shown by gel electrophoresis). According to zeta potential measurements, the polyplexes reached neutrality at N:P ratio of ~3, where aggregation took place (>1 μm); at N:P ratio of 5, the polyplexes had a size of 250 nm and zeta potential of 10 mV, which reached a plateau of 25 mV at N:P ratio of 25. The transfection efficiency increased with the N:P ratio, reaching maximal transfection efficiency at N:P ratio between 15 and 20, where the transfection was 30 times higher than PLL-mediated transfection, but still 40 times lower than TransFast™–DNA complexes. Interestingly, the transfection efficiency of the PPA-*g*-SP/DNA complexes was a function (but not linear) of DNA dose and transfection time, as previously seen in other examples. The conditions of preparation (ionic strength) were also important: a fourfold increase in the DNA dose resulted in a 50-fold increase in transfection efficiency, while extension of the incubation time from 30 min to 2 h resulted in a two orders of magnitude increase in the transfection efficiency, but further incubation time did not show further improvement. Preparation of the complexes in 1 M NaCl resulted in substantially larger particles (>1.3 μm), which showed a threefold increase in luciferase expression compared to complexes prepared in water (no explanation). With a similar polymer, poly(1,2-propylene H-phosphonate) modified with dipropyltriamine (PPA-*g*-DPA, Fig. 24a with $m = 0$) with either a similar grafting degree of 50% and different molecular weights or a similar backbone length but with different grafting degrees, the authors could study the influence of the molecular weight as well as grafting degree [234]. In the results presented by Ren et al., the ratio needed to complex DNA was not given but the studies started at N:P ratio of 10; which

makes it quite difficult to compare these results with those previously reported. For a grafting density of 50%, an increase in molecular weight of the polycation led to an increase in DNA compaction ability of the polymer and slight increase in the polyplex size (60–80 nm). An increase in the net positive charge density for a given chain length also led to an increase in compaction ability (EtBr quenching) and, correspondingly, in a decrease in size of the polyplex (from 67 to 32 nm for 0.49 and 0.94 net positive charge density, respectively). At similar N:P ratio (10 for instance), it was remarkable that these polyplexes were much smaller than poly (1,2-propylene H-phosphonate) modified with spermidine (which could be due to other conditions of preparation, as these are not mentioned). These polyplexes were relatively stable under physiological conditions as well as with time, except those based on the shortest polymer (10 kDa) with a net positive charge density of 0.49. The cellular uptake of these polyplexes was cell line-dependent. In HeLa cells, the polyplexes with the second highest zeta potential but by far the smallest size were preferentially taken up; in HEK293 cells, the difference in uptake was not significant when the M_w of the polymers was higher than 25 kDa; in HepG2 cells, there was no significant difference, showing that the zeta potential and size were not determining factors in these last two cell lines. Nevertheless, the transfection efficiency dramatically increased in all three cell lines with increasing molecular weight and grafting rate. As in the previous case, the influence of the partially negatively charged polymer backbone was not shown.

Poly(isobutylene-*alt*-maleic acid-*g*-oligoethyleneamine) grafted with diethylene triamine P(Mal-*g*-DET), tetraethylenepentamine P(Mal-*g*-TEP), and pentaethylenehexamine P(Mal-*g*-PEH) (Fig. 24b) were studied by Yang and coworkers [235]. Complete retardation was only observed for the polymers with the longest oligoethylene amine chains at N:P ratio of 10. The polyplexes based on P(Mal-*g*-TEP) and P(Mal-*g*-PEH) had a neutral zeta potential at N:P ratio of about 12 and were positively charged for higher N:P ratio, but their size stayed in the micrometer range until an N:P ratio of 16 for P(Mal-*g*-TEP) and 22 for P(Mal-*g*-PEH). This size was not adequate for gene delivery and could be explained by the difficulty in condensing the negatively charged DNA with the partially negatively charged backbone. Above these critical ratios, the nanoparticles obtained were in the range of 400–800 nm, P(Mal-*g*-TEP) being less efficient than P(Mal-*g*-PEH) for condensing DNA, which could be explained by a greater number of protonated amine groups in P(Mal-*g*-PEH). Due to the larger particle size and lower zeta potential of P(Mal-*g*-TEP) compared to P(Mal-*g*-PEH), the polyplexes based on the latter polymer were most efficient in transfecting cells, comparable to the performance of PEI in some cases. The transfection efficiency was dependent upon N:P ratio and also on the cell line but, most importantly, polyplexes based on P(Mal-*g*-PEH) were localized to a large extent in the nucleus after 8 h.

At pH 7.4, prevailing negatively charged amphoteric PAAs were found to be relatively cytotoxic [236], while positively charged PAAs were far less cytotoxic [237]. Among them, PAgma (Fig. 24c) possesses three ionizable groups: a strong acid ($pK_a = 2.3$), a medium-strength base ($pK_a = 7.4$) and a strong base ($pK_a > 12.1$) [238, 239]. At pH 7.4, PAgma has an excess average positive charge

of 0.55 per unit (not influenced by the molecular weight) and had negligible cytotoxicity and hemolytic properties (synonymous of membrane damage) up to concentrations of 7 and 15 mg mL^{-1}, respectively. But, as argued by the authors, the lack of membrane damaging properties did not necessarily imply lack of interactions with membranes, which is of importance for intracellular trafficking properties. At pH 7.4, complete retardation of DNA was achieved at N:P ratio of 15 for intermediate molecular weights ($M_n = 4.8$ kDa). The size of the polyplexes decreased with increasing molecular weight until $M_n = 10$ kDa, being less than 200 nm for this M_n and around 270 nm for a polymer with $M_n = 20$ kDa. At pH 5, compared to the values at pH 7.4, the size of the polyplexes decreased markedly and the zeta potential values became slightly more positive, which was due to an increase in average excess positive charge per polymer unit at this pH. The same rule as before seemed to apply: the smallest size and comparatively highest zeta potential helped the polyplexes based on polymers with molecular weight of 7–10 kDa to transfect cells more efficiently than polyplexes based on polymers with higher or lower molecular weights.

4 Conclusion

This review has shown that the design of polycations for gene delivery must take into account a balance between protection of DNA versus loss of efficiency for DNA condensation and efficient condensation versus hindering of DNA release, and that parameters leading to transfection efficiency in vivo still need to be optimized. Indeed, if the IPEC are not stable enough, premature dissociation will occur before delivery of the genetic material at the desired place, resulting in low transfection efficiency; on the other hand, a complex that is too stable will not release the DNA, also resulting in low gene expression. To determine these properties, gel electrophoresis to test the DNA/polymer complexation, EtBr or polyanion displacement to test the affinity of a polymer for DNA, and DLS to determine the extent of DNA condensation, are well-adapted techniques.

Polymers without steric stabilizer components were abandoned relatively early due to the inherent cytotoxicity of the permanent charges (even if these facilitate cellular entry of the polyplexes) and the propensity to be easily destabilized and precipitate. Strong complexation can also mean difficulty of release of the genetic material and, consequently, low transfection efficiency. The presence of steric stabilizers in the polyplexes results in an increased solubility under physiological conditions, but the problem of finding the right balance between steric stabilization and shielding of charges (that lowers the affinity of the polymer for DNA) is nevertheless present. On the other hand, this steric barrier and the shielding of the charges help the polymer to protect DNA from nuclease attacks, i.e., limit protein adsorption.

Unfortunately, until now, most of the polyplexes (if not all) presented in the studies reviewed here need to be prepared at high N:P ratio (higher than 10 and

often even much higher) in order to be comparable to the commercial polymeric gene delivery agents (usually prepared at N:P ratios of less than 10).

Unfortunately, in all these cases, there are nevertheless problems in defining clear structure–activity relationships and explaining the apparent discrepancies between the behavior of the polyplexes in vitro and their poor performance in vivo. It is highly probable that the actual morphology of the polyplexes deviates from the expected structure (core–shell, etc.).

Moreover, it should not be forgotten that, since gene therapy using oligonucleotides such as antisense oligodeoxynucleotides (ODN); short RNA molecules such as small interfering RNA (siRNA), micro-RNA (miRNA), and short hairpin RNA (shRNA); or a DNAzyme that leads to a reduction in target/protein activity [240] takes more and more importance, the study of the complexes of these oligomeric materials with polycations is of increasing interest. Moreover, the application of DNA–polymer complexes is not limited to gene therapy and they also find use as DNA vaccines and biosensors.

Some challenges remain concerning the synthesis and structure of these polymers; for instance, finding new biocompatible polymers other than PEG. Moreover, in order to define clear structure–function relationships, it is necessary to use new polymerization techniques to obtain well-defined materials rather than randomized polymers [241]. Similarly, more architecturally controlled macromolecules such as dendronized polymers appear to be promising prospects in the field of polycations for gene delivery [242].

References

1. Kundu PP, Sharma V (2008) Synthetic polymeric vectors in gene therapy. Curr Opin Solid State Mater Sci 12:89–102
2. Wong SY, Pelet JM, Putnam D (2007) Polymer systems for gene delivery–past, present, and future. Prog Polym Sci 32:799–837
3. Dubruel P, Schacht E (2006) Vinyl polymers as non-viral gene delivery carriers: current status and prospects. Macromol Biosci 6:789–810
4. Kabanov AV, Felgner PL, Seymour LW (eds) (1998) Self-assembling complexes for gene delivery. Wiley, New York
5. Shcharbin DG, Klajnert B, Bryszewska M (2009) Dendrimers in gene transfection. Biochemistry 74:1070–1079
6. Dufès C, Uchegbu IF, Schätzlein AG (2005) Dendrimers in gene delivery. Adv Drug Deliv Rev 57:2177–2202
7. Ainalem M-L, Nylander T (2011) DNA condensation using cationic dendrimers–morphology and supramolecular structure of formed aggregates. Soft Matter 7:4577–4594
8. Guillot-Nieckowski M, Eisler S, Diederich F (2007) Dendritic vectors for gene transfection. New J Chem 31:1111–1127
9. Paleos CM, Tsiourvas D, Sideratou Z (2007) Molecular engineering of dendritic polymers and their application as drug and gene delivery systems. Mol Pharm 4:169–188
10. Fischer W, Calderón M, Haag R (2010) Hyperbranched polyamines for transfection. Top Curr Chem 296:95–129

11. Zhou Y, Huang W, Liu J, Zhu X, Yan D (2010) Self-assembly of hyperbranched polymers and its biomedical applications. Adv Mater 22:4567–4590
12. Nakayama Y (2012) Hyperbranched polymeric "star vectors" for effective DNA or siRNA delivery. Acc Chem Res 45:994–1004
13. Mao S, Sun W, Kissel T (2010) Chitosan-based formulations for delivery of DNA and siRNA. Adv Drug Deliv Rev 62:12–27
14. Azzam T, Domb AJ (2005) Cationic polysaccharides for gene delivery. In: Amiji MM (ed) Polymeric gene delivery–principles and applications. CRC, Boca Raton, pp 279–299
15. Yudovin-Farber I, Eliyahu H, Domb AJ (2007) Cationic polysaccharides for DNA delivery. In: Friedmann T, Rossi J (eds) Gene transfer: delivery and expression of DNA and RNA, a laboratory manual. CSHL, Cold Spring Harbor, pp 507–513
16. Froehlich T, Wagner E (2010) Peptide- and polymer-based delivery of therapeutic RNA. Soft Matter 6:226–234
17. Osada K, Kataoka K (2006) Drug and gene delivery based on supramolecular assembly of PEG-polypeptide hybrid block copolymers. Adv Polym Sci 202:113–153
18. Kircheis R, Wightman L, Wagner E (2001) Design and gene delivery activity of modified polyethylenimines. Adv Drug Deliv Rev 53:341–358
19. Boussif O, Lezoualc'h F, Zanta MA, Mergny MD, Scherman D, Demeneix B, Behr JP (1995) A versatile vector for gene and oligonucleotide transfer into cells in culture and in vivo: Polyethylenimine. Proc Natl Acad Sci USA 92:7297–7301
20. Kim SW (2007) Polylysine copolymers for gene delivery. In: Friedmann T, Rossi J (eds) Gene transfer: delivery and expression of DNA and RNA, a laboratory manual. CSHL, Cold Spring Harbor, pp 461–471
21. Turrin C-O, Caminade A-M (2011) Dendrimers as transfection agents. In: Caminade A-M (ed) Dendrimers. Wiley, New York, pp 413–435
22. Kubasiak LA, Tomalia DA (2005) Cationic dendrimers as gene transfection vectors: dendri-poly(amidoamines) and dendri-poly(propylenimines). In: Amiji MM (ed) Polymeric gene delivery–principles and applications. CRC, Boca Raton, pp 133–157
23. Smedt SCD, Demeester J, Hennink WE (2000) Cationic polymer based gene delivery systems. Pharm Res 17:113–126
24. Bertin A, Hermes F, Schlaad H (2010) Biohybrid and peptide-based polymer vesicles. Adv Polym Sci 224:167–195
25. Iatrou H, Frielinghaus H, Hanski S, Ferderigos N, Ruokolainen J, Ikkala O, Richter D, Mays J, Hadjichristidis N (2007) Architecturally induced multiresponsive vesicles from well-defined polypeptides. Formation of gene vehicles. Biomacromolecules 8:2173–2181
26. Ho PS, Carter M (2011) DNA structure: alphabet soup for the cellular soul. In: Seligmann H (ed) DNA replication-current advances. InTech, New York
27. Calladine CR, Drew HR, Luisi BF, Travers AA (1992) Understanding DNA, 3rd edn. Elsevier Academic, Amsterdam
28. Ghosh A, Bansal M (2003) A glossary of DNA structures from A to Z. Acta Crystallogr Sect D Biol Crystallogr 59:620–626
29. Strick TR, Allemand J-F, Bensimon D, Bensimon A, Croquette V (1996) The elasticity of a single supercoiled DNA molecule. Science 271:1835–1837
30. Lu Y, Weers B, Stellwagen NC (2002) DNA persistence length revisited. Biopolymers 61:261–275
31. Chen H, Meisburger SP, Pabit SA, Sutton JL, Webb WW, Pollack L (2012) Ionic strength-dependent persistence lengths of single-stranded RNA and DNA. Proc Natl Acad Sci USA 109:799–804
32. Geggier S, Vologodskii A (2010) Sequence dependence of DNA bending rigidity. Proc Natl Acad Sci USA 107:15421–15426
33. Geggier S, Kotlyar A, Vologodskii A (2011) Temperature dependence of DNA persistence length. Nucleic Acids Res 39:1419–1426

34. Kypr J, Kejnovska I, Renciuk D, Vorlickova M (2009) Circular dichroism and conformational polymorphism of DNA. Nucleic Acids Res 37:1713–1725
35. Vorlíčkováa M, Kypra J, Sklenář V (2005) Nucleic acids: spectroscopic methods. In: Worsfold P, Townshend A, Poole C (eds) Encyclopedia of analytical science, 2nd edn. Elsevier, Amsterdam, pp 391–399
36. Mirkin SM (2001) DNA topology: fundamentals. In: Encyclopedia of life sciences. Wiley, New York, pp 1–11
37. Alfredsson V (2005) Cryo-TEM studies of DNA and DNA-lipid structures. Curr Opin Colloid Interface Sci 10:269–273
38. Lyubchenko YL (2004) DNA structure and dynamics–an atomic force microscopy study. Cell Biochem Biophys 41:75–98
39. Fransz P, Hd J (2011) From nucleosome to chromosome: a dynamic organization of genetic information. Plant J 66:4–17
40. Luger K, Mader AW, Richmond RK, Sargent DF, Richmond TJ (1997) Crystal structure of the nucleosome core particle at 2.8 Å resolution. Nature 389:251–260
41. Travers A (1993) DNA-protein interactions. Chapman and Hall, London
42. Dobrynina AV, Rubinstein M (2005) Theory of polyelectrolytes in solutions and at surfaces. Prog Polym Sci 30:1049–1118
43. Radeva T (2001) Physical chemistry of polyelectrolytes. Surfactant science. CRC, Boca Raton
44. Manning GS (1969) Limiting laws and counterion condensation in polyelectrolyte solutions I. Colligative properties. J Chem Phys 51:924–933
45. Rühe J, Ballauff M, Biesalski M, Dziezok P, Gröhn F, Johannsmann D, Houbenov N, Hugenberg N, Konradi R, Minko S, Motornov M, Netz RR, Schmidt M, Seidel C, Stamm M, Stephan T, Usov D, Zhang H (2004) Polyelectrolyte brushes. Adv Polym Sci 165:79–150
46. Israelachvili J (1985) Intermolecular and surface forces. Academic, London
47. Thünemann AF, Müller M, Dautzenberg H, Joanny J-F, Löwen H (2004) Polyelectrolyte complexes. Adv Polym Sci 166:19–33
48. Gohy JF, Varshney SK, Antoun S, Jerome R (2000) Water-soluble complexes formed by sodium poly(4-styrenesulfonate) and a poly(2-vinylpyridinium)-block-poly(ethyleneoxide) copolymer. Macromolecules 33:9298–9305
49. Kabanov AV, Bronich TK, Kabanov VA, Yu K, Eisenberg A (1996) Soluble stoichiometric complexes from poly(N-ethyl-4-vinylpyridinium) cations and poly(ethylene oxide)-block-polymethacrylate anions. Macromolecules 29:6797–6802
50. Harada A, Kataoka K (1995) Formation of polyion complex micelles in an aqueous milieu from a pair of oppositely-charged block copolymers with poly(ethylene glycol) segments. Macromolecules 28:5294–5299
51. Kakizawa Y, Kataoka K (2002) Block copolymer micelles for delivery of gene and related compounds. Adv Drug Deliv Rev 54:203–222
52. Voets IK, Keizer AD, Cohen Stuart MA (2009) Complex coacervate core micelles. Adv Colloid Interface Sci 147–148:300–318
53. Ilarduya CT, Sun Y, Düzgünes N (2010) Gene delivery by lipoplexes and polyplexes. Eur J Pharm Sci 40:159–170
54. Kabanov AV, Kabanov VA (1998) Interpolyelectrolyte and block ionomer complexes for gene delivery: physicochemical aspects. Adv Drug Deliv Rev 30:49–60
55. Davis KA, Matyjaszewski K (2002) Statistical, gradient, block, and graft copolymers by controlled/living radical polymerizations. Adv Polym Sci 159:1–13
56. Matyjaszewski K (ed) (2003) Advances in controlled/living radical polymerization. ACS symposium series, vol 854. American Chemical Society, Washington
57. Matyjaszewski K (ed) (2006) Controlled/living radical polymerization: from synthesis to materials. ACS symposium series, vol 944. American Chemical Society, Washington
58. Xu Y, Plamper F, Ballauff M, Müller AHE (2010) Polyelectrolyte stars and cylindrical brushes. Adv Polym Sci 228:1–38

59. Bakeev KN, Izumrudov VA, Kuchanov SI, Zezin AB, Kabanov VA (1992) Kinetics and mechanism of interpolyelectrolyte exchange and addition reactions. Macromolecules 25:4249–4254
60. Tang MX, Szoka FC Jr (1998) Structure of polycation-DNA complexes and theory of compaction. In: Kabanov AV, Felgner PL, Seymour LW (eds) Self-assembling complexes for gene delivery. Wiley, New York
61. Dias RS, Pais AACC, Miguel MG, Lindman B (2003) Modeling of DNA compaction by polycations. J Chem Phys 119:8150–8157
62. Sarraguça JMG, Dias RS, Pais AACC (2006) Coil-globule coexistence and compaction of DNA chains. J Biol Phys 32:421–434
63. Dragan ES, Mihai M, Schwarz S (2006) Polyelectrolyte complex dispersions with a high colloidal stability controlled by the polyion structure and titrant addition rate. Colloid Surf A 290:213–221
64. Gärdlund L, Wågberg L, Norgren M (2007) New insights into the structure of polyelectrolyte complexes. J Colloid Interface Sci 312:237–246
65. Hartig SM, Greene RR, Dikov MM, Prokop A, Davidson JM (2007) Multifunctional nanoparticulate polyelectrolyte complexes. Pharm Res 24:2353–2369
66. Philipp B, Dautzenberg H, Linow KJ, Koetz J, Dawydoff W (1989) Polyelectrolyte complexes - recent developments and open problems. Prog Polym Sci 14:91–172
67. Giorgetti L, Siggers T, Tiana G, Caprara G, Notarbartolo S, Corona T, Pasparakis M, Milani P, Bulyk ML, Natoli G (2010) Noncooperative interactions between transcription factors and clustered DNA binding sites enable graded transcriptional responses to environmental inputs. Mol Cell 37:418–428
68. Danielsen S, Varum KM, Stokke BT (2004) Structural analysis of chitosan mediated DNA condensation by AFM: influence of chitosan molecular parameters. Biomacromolecules 5:928–936
69. Bloomfield VA (1996) DNA condensation. Curr Opin Struct Biol 6:334–341
70. Ainalem M-L, Carnerup AM, Janiak J, Alfredsson V, Nylander T, Schillen K (2009) Condensing DNA with poly(amido amine) dendrimers of different generations: means of controlling aggregate morphology. Soft Matter 5:2310–2320
71. Carnerup AM, Ainalem M-L, Alfredsson V, Nylander T (2011) Condensation of DNA using poly(amido amine) dendrimers: effect of salt concentration on aggregate morphology. Soft Matter 7:760–768
72. Kabanov VA, Zezin AB (1984) Soluble interpolymeric complexes as a new class of synthetic polyelectrolytes. Pure Appl Chem 56:343–354
73. Kiriy A, Yu J, Stamm M (2006) Interpolyelectrolyte complexes: a single-molecule insight. Langmuir 22:1800–1803
74. Dautzenberg H, Rother G (2003) Response of polyelectrolyte complexes to subsequent addition of sodium chloride: time-dependent static light scattering studies. Macromol Chem Phys 205:114–121
75. Discher DE, Eisenberg A (2002) Polymer vesicles. Science 297(5583):967–973. doi:10.1126/science.1074972
76. Lo C-L, Lin S-J, Tsai H-C, Chan W-H, Tsai C-H, Cheng C-HD, Hsiue G-H (2009) Mixed micelle systems formed from critical micelle concentration and temperature-sensitive diblock copolymers for doxorubicin delivery. Biomaterials 30(23–24):3961–3970. doi:10.1016/j.biomaterials.2009.04.002
77. Dautzenberg H (1997) Polyelectrolyte complex formation in highly aggregating systems. 1. Effect of salt: polyelectrolyte complex formation in the presence of NaCl. Macromolecules 30:7810–7815
78. Michaels AS, Mir L, Schneider NS (1965) A conductometric study of polycation-polyanion reactions in dilute aqueous solution. J Phys Chem 69:1447–1455
79. Sukhishvili SA, Kharlampieva E, Izumrudov V (2006) Where polyelectrolyte multilayers and polyelectrolyte complexes meet. Macromolecules 39:8873–8881

80. Maskos M, Stauber RH (2011) Characterization of nanoparticles in biological environments. In: Comprehensive biomaterials, vol 3: Methods of analysis. Elsevier, Amsterdam, pp 329–339
81. Lebovka NI (2012) Aggregation of charged colloidal particles. In: Müller M (ed) Advances in polymer science. Springer, Berlin, doi: 10.1007/12_2012_171
82. Patchornik A, Berger A, Katchalski E (1957) Poly-L-histidine. J Am Chem Soc 79:5227–5230
83. Palchaudhuri R, Hergenrother PJ (2007) DNA as a target for anticancer compounds: methods to determine the mode of binding and the mechanism of action. Curr Opin Biotechnol 18:497–503
84. Hannon MJ (2007) Supramolecular DNA recognition. Chem Soc Rev 36:280–295
85. Mulligan RC (1993) The basic science of gene therapy. Science 260:926–932
86. Verma IM, Somia N (1997) Gene therapy – promises, problems and prospects. Nature 389:239–242
87. Edelstein ML, Abedi MR, Wixon J, Edelstein RM (2004) Gene therapy clinical trials worldwide 1989–2004 – an overview. J Gene Med 6:597–602
88. Edelstein ML, Abedi MR, Wixon J (2007) Gene therapy clinical trials worldwide to 2007 – an update. J Gene Med 9:833–842
89. Palmer DH, Young LS, Mautner V (2006) Cancer gene-therapy: clinical trials. Trends Biotechnol 24:76–82
90. Yeung ML, Bennasser Y, Le SY, Jeang KT (2005) siRNA, miRNA and HIV: promises and challenges. Cell Res 15:935–946
91. Kay MA, Glorioso JC, Naldini L (2001) Viral vectors for gene therapy: the art of turning infectious agents into vehicles of therapeutics. Nat Med 7:33–40
92. Behr J-P (1993) Synthetic gene-transfer vectors. Acc Chem Res 26:274–278
93. Glover DJ, Lipps HJ, Jans DA (2005) Towards safe, non-viral therapeutic gene expression in humans. Nat Rev 6:299–310
94. Kawakami S, Higuchi Y, Hashida M (2008) Nonviral approaches for targeted delivery of plasmid DNA and oligonucleotide. J Pharm Sci 97:726–745
95. Scholz C, Wagner E (2012) Therapeutic plasmid DNA versus siRNA delivery: Common and different tasks for synthetic carriers. J Control Release 161:554–565
96. Zamore PD, Tuschl T, Sharp PA, Bartel DP (2000) RNAi. Cell Res 101:25–33
97. Bonetta L (2004) RNAi: silencing never sounded better. Nat Methods 1:79–86
98. Pecot CV, Calin GA, Coleman RL, Lopez-Berestein G, Sood AK (2011) RNA interference in the clinic: challenges and future directions. Nat Rev Cancer 11:59–67
99. Wilson RW, Bloomfield VA (1979) Counterion-induced condensation of deoxyribonucleic acid. A light-scattering study. Biochemistry 18:2192–2196
100. Agarwal S, Zhang Y, Maji S, Greiner A (2012) PDMAEMA based gene delivery materials. Mater Today 15:388–393
101. Brissault B, Kichler A, Guis C, Leborgne C, Danos O, Cheradame H (2003) Synthesis of linear polyethylenimine derivatives for DNA transfection. Bioconjug Chem 14:581–587
102. Rungsardthong U, Ehtezazi T, Bailey L, Armes SP, Garnett MC, Stolnik S (2003) Effect of polymer ionization on the interaction with DNA in nonviral gene delivery systems. Biomacromolecules 4:683–690
103. Nimesh S, Aggarwal A, Kumar P, Singh Y, Gupta KC, Chandra R (2007) Influence of acyl chain length on transfection mediated by acylated PEI nanoparticles. Int J Pharm 337:265–274
104. Gabrielson NP, Pack DW (2006) Acetylation of polyethylenimine enhances gene delivery via weakened polymer/DNA interactions. Biomacromolecules 7:2427–2435
105. Tang GP, Zeng JM, Gao SJ, Ma YX, Shi L, Li Y, Too H-P, Wang S (2003) Polyethylene glycol modified polyethylenimine for improved CNS gene transfer: effects of PEGylation extent. Biomaterials 24:2351–2362

106. Brumbach JH, Lin C, Yockman J, Kim WJ, Blevins KS, Engbersen JFJ, Feijen J, Kim SW (2010) Mixtures of poly(triethylenetetramine/cystamine bisacrylamide) and poly(triethylenetetramine/cystamine bisacrylamide)-*g*-poly(ethylene glycol) for improved gene delivery. Bioconjug Chem 21:1753–1761
107. Allen MHJ, Green MD, Getaneh HK, Miller KM, Long TE (2011) Tailoring charge density and hydrogen bonding of imidazolium copolymers for efficient gene delivery. Biomacromolecules 12:2243–2250
108. Prevette LE, Kodger TE, Reineke TM, Lynch ML (2007) Deciphering the role of hydrogen bonding in enhancing pDNA-polycation interactions. Langmuir 23:9773–9784
109. Georgiou TK, Vamvakaki M, Patrickios CS (2004) Nanoscopic cationic methacrylate star homopolymers: synthesis by group transfer polymerization, characterization and evaluation as transfection reagents. Biomacromolecules 5:2221–2229
110. Deshpande MC, Garnett MC, Vamvakaki M, Bailey L, Armes SP, Stolnik S (2002) Influence of polymer architecture on the structure of complexes formed by PEG-tertiary amine methacrylate copolymers and phosphorothioate oligonucleotide. J Control Release 81:185–199
111. Luten J, van Nostrum CF, Smedt SCD, Hennink WE (2008) Biodegradable polymers as non-viral carriers for plasmid DNA delivery. J Control Release 126:97–110
112. Laga R, Carlisle R, Tangney M, Ulbrich K, Seymour LW (2012) Polymer coatings for delivery of nucleic acid therapeutics. J Control Release 161:537–553
113. Chan P, Kurisawa M, Chung JE, Yang Y-Y (2007) Synthesis and characterization of chitosan-*g*-poly(ethylene glycol)-folate as a non-viral carrier for tumor-targeted gene delivery. Biomaterials 28:540–549
114. Blessing T, Kursa M, Holzhauser R, Kircheis R, Wagner E (2001) Different strategies for formation of PEGylated EGF-conjugated PEI/DNA complexes for targeted gene delivery. Bioconjug Chem 12:529–537
115. Kursa M, Walker GF, Roessler V, Ogris M, Roedl W, Kircheis R, Wagner E (2003) Novel shielded transferrin-polyethylene glycol-polyethylenimine/DNA complexes for systemic tumor-targeted gene transfer. Bioconjug Chem 14:222–231
116. Nishikawa M, Huang L (2001) Non viral vectors in the new millennium: delivery barriers in gene transfer. Hum Gene Ther 12:861–870
117. Grigsby CL, Leong KW (2010) Balancing protection and release of DNA: tools to address a bottleneck of non-viral gene delivery. J R Soc Interface 7:S67–S82
118. Soliman M, Allen S, Davies MC, Alexander C (2010) Responsive polyelectrolyte complexes for triggered release of nucleic acid therapeutics. Chem Commun 46:5421–5433
119. Spain SG, Yasayan G, Soliman M, Heath F, Saeed AO, Alexander C (2011) Nanoparticles for nucleic acid delivery. In: Ducheyne P (ed) Comprehensive biomaterials, vol 4. Elsevier, Amsterdam, pp 389–410
120. Sonawane ND, Szoka FC Jr, Verkman A (2003) Chloride accumulation and swelling in endosomes enhances DNA transfer by polyamine DNA polyplexes. J Biol Chem 278:44826–44831
121. Hunter AC, Moghimi SM (2010) Cationic carriers of genetic material and cell death: a mitochondrial tale. Biochim Biophys Acta 1797:1203–1209
122. Izumrudov VA, Zhiryakova MV (1999) Stability of DNA-containing interpolyelectrolyte complexes in water-salt solutions. Macromol Chem Phys 200:2533–2540
123. Xu FJ, Chai MY, Li WB, Ping Y, Tang GP, Yang WT, Ma J, Liu FS (2010) Well-defined poly (2-hydroxyl-3-(2-hydroxyethylamino)propyl methacrylate) vectors with low toxicity and high gene transfection efficiency. Biomacromolecules 11:1437–1442
124. Ma M, Li F, Yuan Z-F, Zhuo R-X (2010) Influence of hydroxyl groups on the biological properties of cationic polymethacrylates as gene vectors. Acta Biomater 6:2658–2665
125. Hemp ST, Allen J, Green MD, Long TE (2012) Phosphonium-containing polyelectrolytes for nonviral gene delivery. Biomacromolecules 13:231–238

126. Zelikin AN, Putnam D, Shastri P, Langer R, Izumrudov VA (2002) Aliphatic ionenes as gene delivery agents: elucidation of structure-function relationship through modification of charge density and polymer length. Bioconjug Chem 13:548–553
127. Izumrudov VA, Wahlund P-O, Gustavsson P-E, Larsson P-O, Galaev IY (2003) Factors controlling phase separation in water-salt solutions of DNA and polycations. Langmuir 19:4733–4739
128. Andersson T, Aseyev V, Tenhu H (2004) Complexation of DNA with poly(methacryl oxyethyl trimethylammonium chloride) and its poly(oxyethylene) grafted analogue. Biomacromolecules 5:1853–1861
129. Nisha CK, Manorama SV, Ganguli M, Maiti S, Kizhakkedathu JN (2004) Complexes of poly (ethylene glycol)-based cationic random copolymer and calf thymus DNA: a complete biophysical characterization. Langmuir 20:2386–2396
130. Howard KA, Dash PR, Read ML, Ward K, Tomkins LM, Nazarova O, Ulbrich K, Seymour LW (2000) Influence of hydrophilicity of cationic polymers on the biophysical properties of polyelectrolyte complexes formed by self-assembly with DNA. Biochim Biophys Acta 1475:245–255
131. Kimura T, Yamaoka T, Iwase R, Murakami A (2002) Effect of physicochemical properties of polyplexes composed of chemically modified PL derivatives on transfection efficiency in vitro. Macromol Biosci 2:437–446
132. Licciardi M, Campisi M, Cavallaro G, Carlisi B, Giammona G (2006) Novel cationic polyaspartamide with covalently linked carboxypropyl-trimethyl ammonium chloride as a candidate vector for gene delivery. Eur Polym J 42:823–834
133. Caputo A, Betti M, Altavilla G, Bonaccorsi A, Boarini C, Marchisio M, Buttò S, Sparnacci K, Laus M, Tondelli L, Ensoli B (2002) Micellar-type complexes of tailor-made synthetic block copolymers containing the HIV-1 tat DNA for vaccine application. Vaccine 20:2303–2317
134. Itaka K, Ishii T, Hasegawa Y, Kataoka K (2010) Biodegradable polyamino acid-based polycations as safe and effective gene carrier minimizing cumulative toxicity. Biomaterials 31:3707–3714
135. Zhang M, Liu M, Xue Y-N, Huang S-W, Zhuo R-X (2009) Polyaspartamide-based oligo-ethylenimine brushes with high buffer capacity and low cytotoxicity for highly efficient gene delivery. Bioconjug Chem 20:440–446
136. Cavallaro G, Scirè S, Licciardi M, Ogris M, Wagner E, Giammona G (2008) Polyhydroxyethylaspartamide-spermine copolymers: efficient vectors for gene delivery. J Control Release 131:54–63
137. Liu M, Chen J, Cheng Y-P, Xue Y-N, Zhuo R-X, Huang S-W (2010) Novel poly (amidoamine)s with pendant primary amines as highly efficient gene delivery vectors. Macromol Biosci 10:384–392
138. Kim T-I, Kim SW (2011) Bioreducible polymers for gene delivery. React Funct Polym 71:344–349
139. Lin C, Blaauboer C-J, Timoneda MM, Lok MC, van Steenbergen M, Hennink WE, Zhong Z, Feijen J, Engbersen JFJ (2008) Bioreducible poly(amido amine)s with oligoamine side chains: synthesis, characterization, and structural effects on gene delivery. J Control Release 126:166–174
140. Du F-S, Wang Y, Zhang R, Li Z-C (2010) Intelligent nucleic acid delivery systems based on stimuli-responsive polymers. Soft Matter 6:835–848
141. Verbaan FJ, Crommelin DJA, Hennink WE, Storm G (2005) Poly(2-(dimethylamino)ethyl methacrylate)-based polymers for the delivery of genes in vitro and in vivo. In: Amiji MM (ed) Polymeric gene delivery-principles and applications. CRC, Boca Raton
142. van de Wetering P, Cherng J-Y, Talsma H, Crommelin DJA, Hennink WE (1998) 2-(dimethylamino)ethyl methacrylate based (co)polymers as gene transfer agents. J Control Release 53:145–153

143. van de Wetering P, Moret EE, Schuurmans-Nieuwenbroek NME, van Steenbergen MJ, Hennink WE (1999) Structure-activity relationships of water-soluble cationic methacrylate/methacrylamide polymers for nonviral gene delivery. Bioconjug Chem 10:589–597
144. Asayama S, Maruyama A, Cho C-S, Akaike T (1997) Design of comb-type polyamine copolymers for a novel pH-sensitive DNA carrier. Bioconjug Chem 8:833–838
145. Jiang X, Lok MC, Hennink WE (2007) Degradable-brushed pHEMA-pDMAEMA synthesized via ATRP and click chemistry for gene delivery. Bioconjug Chem 18:2077–2084
146. Dubruel P, Strycker JD, Westbroek P, Bracke K, Temmerman E, Vandervoort J, Ludwig A, Schacht E (2002) Synthetic polyamines as vectors for gene delivery. Polym Int 51:948–957
147. Hinrichs WLJ, Schuurmans-Nieuwenbroek NME, van de Wetering P, Hennink WE (1999) Thermosensitive polymers as carriers for DNA delivery. J Control Release 60:249–259
148. Oupicky D, Reschel T, Konak C, Oupicka L (2003) Temperature-controlled behavior of self-assembly gene delivery vectors based on complexes of DNA with poly(L-lysine)-graft-poly(N-isopropylacrylamide). Macromolecules 36:6863–6872
149. Cheng N, Liu W, Cao Z, Ji W, Liang D, Guo G, Zhang J (2006) A study of thermoresponsive poly(N-isopropylacrylamide)/polyarginine bioconjugate non-viral transgene vectors. Biomaterials 27:4984–4992
150. Putnam D, Gentry CA, Pack DW, Langer R (2001) Polymer-based gene delivery with low cytotoxicity by a unique balance of side-chain termini. Proc Natl Acad Sci USA 98:1200–1205
151. Chen DJ, Majors BS, Zelikin A, Putnam D (2005) Structure-function relationships of gene delivery vectors in a limited polycation library. J Control Release 103:273–283
152. Burckhardt G, Zimmer C, Luck G (1976) Conformation and reactivity of DNA in the complex with protein: IV. Circular dichroism of poly-l-histidine model complexes with DNA polymers and specificity of the interaction. Nucleic Acids Res 3:561–580
153. Benns JM, Choi J-S, Mahato RI, Park J-S, Kim SW (2000) pH-sensitive cationic polymer gene delivery vehicle: N-Ac-poly(L-histidine)-graft-poly(L-lysine) comb shaped polymer. Bioconjug Chem 11:637–645
154. Roufai MB, Midoux P (2001) Histidylated polylysine as DNA vector: elevation of the imidazole protonation and reduced cellular uptake without change in the polyfection efficiency of serum stabilized negative polyplexes. Bioconjug Chem 12:92–99
155. Kim TH, Ihm JE, Choi YJ, Nah JW, Cho CS (2003) Efficient gene delivery by urocanic acid-modified chitosan. J Control Release 93:389–402
156. Park JS, Han TH, Lee KY, Han SS, Hwang JJ, Moon D, Kim SY, Cho YW (2006) N-acetyl histidine-conjugated glycol chitosan self-assembled nanoparticles for intracytoplasmic delivery of drugs: endocytosis, exocytosis and drug release. J Control Release 115:37–45
157. Mishra S, Heidel JD, Webster P, Davis ME (2006) Imidazole groups on a linear, cyclodextrin-containing polycation produce enhanced gene delivery via multiple processes. J Control Release 116:179–191
158. Swami A, Aggarwal A, Pathak A, Patnaik S, Kumar P, Singh Y, Gupta KC (2007) Imidazolyl-PEI modified nanoparticles for enhanced gene delivery. Int J Pharm 335:180–192
159. Pichon C, Goncalves C, Midoux P (2001) Histidine-rich peptides and polymers for nucleic acids delivery. Adv Drug Deliv Rev 53:75–94
160. Midoux P, Pichon C, Yaouanc J-J, Jaffrès P-A (2009) Chemical vectors for gene delivery: a current review on polymers, peptides and lipids containing histidine or imidazole as nucleic acids carriers. Br J Pharmacol 157:166–178
161. Dekie L, Toncheva V, Dubruel P, Schacht EH, Barrett L, Seymour LW (2000) Poly-L-glutamic acid derivatives as vectors for gene therapy. J Control Release 65:187–202
162. Dubruel P, Dekie L, Schacht E (2003) Poly-L-glutamic acid derivatives as multifunctional vectors for gene delivery. Part A. Synthesis and physicochemical evaluation. Biomacromolecules 4:1168–1176

163. Dubruel P, Dekie L, Christiaens B, Vanloo B, Rosseneu M, Vandekerckhove J, Mannisto M, Urtti A, Schacht E (2003) Poly-L-glutamic acid derivatives as multifunctional vectors for gene delivery. Part B. Biological evaluation. Biomacromolecules 4:1177–1183
164. Pack DW, Putnam D, Langer R (2000) Design of imidazole-containing endosomolytic biopolymers for gene delivery. Biotechnol Bioeng 67:217–223
165. Ramsay E, Hadgraft J, Birchall J, Gumbleton M (2000) Examination of the biophysical interaction between plasmid DNA and the polycations, polylysine and polyornithine, as a basis for their differential gene transfection in-vitro. Int J Pharm 210:97–107
166. Blauer G, Alfassi ZB (1967) A comparison between poly-α, L-ornithine and poly-α, L-lysine in solution: the effect of a CH_2 group on the side-chain on the conformation of the poly-α-amino acids. Biochim Biophys Acta 133:206–218
167. Morgan DML, Larvin VL, Pearson JD (1989) Biochemical characterisation of polycation-induced cytotoxity to human vascular endothelial cells. J Cell Sci 94:553–559
168. Reich Z, Ittah Y, Weinberger S, Minsky A (1990) Chiral and structural discrimination in binding of polypeptides with condensed nucleic acid structures. J Biol Chem 265:5590–5594
169. Mann A, Khan MA, Shukla V, Ganguli M (2007) Atomic force microscopy reveals the assembly of potential DNA "nanocarriers" by poly-L-ornithine. Biophys Chem 129:126–136
170. Lim Y-B, Kim C-H, Kim K, Kim SW, Park J-S (2000) Development of a safe gene delivery system using biodegradable polymer, poly[α-(4-aminobutyl)-L-glycolic acid]. J Am Chem Soc 122:6524–6525
171. Putnam D, Langer R (1999) Poly(4-hydroxy-L-proline ester): low-temperature polycondensation and plasmid DNA complexation. Macromolecules 32:3658–3662
172. Simon RJ, Kania RS, Zuckermann RN, Huebner VD, Jewell DA, Banville S, Ng S, Wang L, Rosenberg S, Marlowe CK, Spellmeyer DC, Tan R, Frankel AD, Santi DV, Cohen FE, Bartlett PA (1992) Peptoids: a modular approach to drug discovery. Proc Natl Acad Sci USA 89:9367–9371
173. Fowler SA, Blackwell HE (2009) Structure-function relationships in peptoids: recent advances toward deciphering the structural requirements for biological function. Org Biomol Chem 7:1508–1524
174. Zuckermann RN, Kodadek T (2009) Peptoids as potential therapeutics. Curr Opin Mol Ther 11:299–307
175. Murphy JE, Uno T, Hamer JD, Cohen FE, Dwarki V, Zuckermann RN (1998) A combinatorial approach to the discovery of efficient cationic peptoid reagents for gene delivery. Proc Natl Acad Sci USA 95:1517–1522
176. Lobo BA, Vetro JA, Suich DM, Zuckermann RN, Middaugh CR (2003) Structure/function analysis of peptoid/lipitoid: DNA complexes. J Pharm Sci 92:1905–1918
177. Ji W, Panus D, Palumbo RN, Tang R, Wang C (2011) Poly(2-aminoethyl methacrylate) with well-defined chain length for DNA vaccine delivery to dendritic cells. Biomacromolecules 12:4373–4385
178. Luo S, Cheng R, Meng F, Park TG, Zhong Z (2011) Water soluble poly(histamine acrylamide) with superior buffer capacity mediates efficient and nontoxic in vitro gene transfection. J Polym Sci A Polym Chem 49:3366–3373
179. Sun H, Gao C (2010) Facile synthesis of multiamino vinyl poly(amino acid)s for promising bioapplications. Biomacromolecules 11:3609–3616
180. Wolfert MA, Dash PR, Nazarova O, Oupicky D, Seymour LW, Smart S, Strohalm J, Ulbrich K (1999) Polyelectrolyte vectors for gene delivery: influence of cationic polymer on biophysical properties of complexes formed with DNA. Bioconjug Chem 10:993–1004
181. Venkataraman S, Ong WL, Ong ZY, Loo SCJ, Ee PLR, Yang YY (2011) The role of PEG architecture and molecular weight in the gene transfection performance of PEGylated poly (dimethylaminoethyl methacrylate) based cationic polymers. Biomaterials 32:2369–2378
182. Rungsardthong U, Deshpande M, Bailey L, Vamvakaki M, Armes SP, Garnett MC, Stolnik S (2001) Copolymers of amine methacrylate with poly(ethylene glycol) as vectors for gene therapy. J Control Release 73:359–380

183. Stolnik S, Illum L, Davis SS (1995) Long circulating microparticulate drug carriers. Adv Drug Deliv Rev 16:195–214
184. Kleideiter G, Nordmeier E (1999) Poly(ethylene glycol)-induced DNA condensation in aqueous/methanol containing low-molecular-weight electrolyte solutions. Part II. Comparison between experiment and theory. Polymer 40:4025–4033
185. Toncheva V, Wolfert MA, Dash PR, Oupicky D, Ulbrich K, Seymour LW, Schacht EH (1998) Novel vectors for gene delivery formed by self-assembly of DNA with poly(L-lysine) grafted with hydrophilic polymers. Biochim Biophys Acta 1380:354–368
186. Deshpande MC, Davies MC, Garnett MC, Williams PM, Armitage D, Bailey L, Vamvakaki M, Armes SP, Stolnik S (2004) The effect of poly(ethylene glycol) molecular architecture on cellular interaction and uptake of DNA complexes. J Control Release 97:143–156
187. Ziebarth J, Wang Y (2010) Coarse-grained molecular dynamics simulations of DNA condensation by block copolymer and formation of core-corona structures. J Phys Chem B 114:6225–6232
188. Petersen H, Fechner PM, Martin AL, Kunath K, Stolnik S, Roberts CJ, Fischer D, Davies MC, Kissel T (2002) Polyethylenimine-graft-poly(ethylene glycol) copolymers: influence of copolymer block structure on DNA complexation and biological activities as gene delivery system. Bioconjug Chem 13:845–854
189. Wakebayashi D, Nishiyama N, Itaka K, Miyata K, Yamasaki Y, Harada A, Koyama H, Nagasaki Y, Kataoka K, Harada A (2004) Polyion complex micelles of pDNA with acetal-poly(ethylene glycol)-poly(2-(dimethylamino)ethyl methacrylate) block copolymer as the gene carrier system: physicochemical properties of micelles relevant to gene transfection efficacy. Biomacromolecules 5:2128–2136
190. Itaka K, Yamauchi K, Harada A, Nakamura K, Kawaguchi H, Kataoka K (2003) Polyion complex micelles from plasmid DNA and poly(ethylene glycol)-poly(l-lysine) block copolymer as serum-tolerable polyplex system: physicochemical properties of micelles relevant to gene transfection efficiency. Biomaterials 24:4495–4506
191. Tan JF, Too HP, Hatton TA, Tam KC (2006) Aggregation behavior and thermodynamics of binding between poly(ethylene oxide)-block-poly(2-(diethylamino)ethyl methacrylate) and plasmid DNA. Langmuir 22:3744–3750
192. Wang C, Tam KC (2002) New insights on the interaction mechanism within oppositely charged polymer/surfactant systems. Langmuir 18:6484–6490
193. Uzgun S, Akdemir O, Hasenpusch G, Maucksch C, Golas MM, Sander B, Stark H, Imker R, Lutz J-F, Rudolph C (2010) Characterization of tailor-made copolymers of oligo(ethylene glycol) methyl ether methacrylate and N, N-dimethylaminoethyl methacrylate as nonviral gene transfer agents: influence of macromolecular structure on gene vector particle properties and transfection efficiency. Biomacromolecules 11:39–50
194. Verbaan FJ, Oussoren C, Snel CJ, Crommelin DJA, Hennink WE, Storm G (2004) Steric stabilization of poly(2-(dimethylamino)ethyl methacrylate)-based polyplexes mediates prolonged circulation and tumor targeting in mice. J Gene Med 6:64–75
195. Yao Y, Feng D-F, Wu Y-P, Ye Q-J, Liu L, Li X-X, Hou S, Yang Y-L, Wang C, Li L, Feng X-Z (2011) Influence of block sequences in polymer vectors for gene transfection in vitro and toxicity assessment of zebrafish embryos in vivo. J Mater Chem 21:4538–4545
196. Xu F-J, Li H, Li J, Zhang Z, Kang E-T, Neoh K-G (2008) Pentablock copolymers of poly (ethylene glycol), poly((2-dimethyl amino) ethyl methacrylate) and poly(2-hydroxyethyl methacrylate) from consecutive atom transfer radical polymerizations for non-viral gene delivery. Biomaterials 29:3023–3033
197. Brissault B, Kichler A, Leborgne C, Danos O, Cheradame H, Gau J, Auvray L, Guis C (2006) Synthesis, characterization, and gene transfer application of poly(ethylene glycol-b-ethylenimine) with high molar mass polyamine block. Biomacromolecules 7:2863–2870
198. Liu X-Q, Du J-Z, Zhang C-P, Zhao F, Yang X-Z, Wang J (2010) Brush-shaped polycation with poly(ethylenimine)-b-poly(ethylene glycol) side chains as highly efficient gene delivery vector. Int J Pharm 392:118–126

199. Yang J, Zhang P, Tang L, Sun P, Liu W, Sun P, Zuo A, Liang D (2010) Temperature-tuned DNA condensation and gene transfection by PEI-*g*-(PMEO$_2$MA-*b*-PHEMA) copolymer-based nonviral vectors. Biomaterials 31:144–155
200. Tv E, Zwicker S, Pidhatika B, Konradi R, Textor M, Hall H, Lühmann T (2011) Formation and characterization of DNA-polymer-condensates based on poly(2-methyl-2-oxazoline) grafted poly(L-lysine) for non-viral delivery of therapeutic DNA. Biomaterials 32:5291–5303
201. Bikram M, Ahn C-H, Chae SY, Lee M, Yockman JW, Kim SW (2004) Biodegradable poly (ethylene glycol)-co-poly(L-lysine)-*g*-histidine multiblock copolymers for nonviral gene delivery. Macromolecules 37:1903–1916
202. Putnam D, Zelikin AN, Izumrudov VA, Langer R (2003) Polyhistidine-PEG: DNA nanocomposites for gene delivery. Biomaterials 24:4425–4433
203. Kanayama N, Fukushima S, Nishiyama N, Itaka K, Jang W-D, Miyata K, Yamasaki Y, Chung U-I, Kataoka K (2006) A PEG-based biocompatible block catiomer with high buffering capacity for the construction of polyplex micelles showing efficient gene transfer toward primary cells. ChemMedChem 1:439–444
204. Miyata K, Fukushima S, Nishiyama N, Yamasaki Y, Kataoka K (2007) PEG-based block catiomers possessing DNA anchoring and endosomal escaping functions to form polyplex micelles with improved stability and high transfection efficacy. J Control Release 122:252–260
205. Vuillaume PY, Brunelle M, Calsteren M-RV, Laurent-Lewandowski S, Begin A, Lewandowski R, Talbot BG, ElAzhary Y (2005) Synthesis and characterization of new permanently charged poly(amidoammonium) salts and evaluation of their DNA complexes for gene transport. Biomacromolecules 6:1769–1781
206. Thomas M, Klibanov AM (2002) Enhancing polyethylenimine's delivery of plasmid DNA into mammalian cells. Proc Natl Acad Sci USA 99:14640–14645
207. Kabanov AV, Astafyeva IV, Chikindas ML, Rosenblat CF, Kiselev VI, Severin ES, Kabanov VA (1991) DNA interpolyelectrolyte complexes as a tool for efficient cell transformation. Biopolymers 31:1437–1443
208. Doody AM, Korley JN, Dang KP, Zawaneh PN, Putnam D (2006) Characterizing the structure/function parameter space of hydrocarbon-conjugated branched polyethylenimine for DNA delivery in vitro. J Control Release 116:227–237
209. Liu Z, Zhang Z, Zhou C, Jiao Y (2010) Hydrophobic modifications of cationic polymers for gene delivery. Prog Polym Sci 35:1144–1162
210. Juan AS, Letourneur D, Izumrudov VA (2007) Quaternized poly(4-vinylpyridine)s as model gene delivery polycations: structure-function study by modification of side chain hydrophobicity and degree of alkylation. Bioconjug Chem 18:922–928
211. Vuillaume PY, Brunelle M, Bazuin CG, Talbot BG, Begin A, Calsteren M-RV, Laurent-Lewandowski S (2009) Tail-end amphiphilic dimethylaminopyridinium-containing polymethacrylates for gene delivery. New J Chem 33:1941–1950
212. Asayama S, Hakamatani T, Kawakami H (2010) Synthesis and characterization of alkylated poly(1-vinylimidazole) to control the stability of its DNA polyion complexes for gene delivery. Bioconjug Chem 21:646–652
213. Filippov SK, Konak C, Kopeckov P, Starovoytova L, Spirkova M, Stepanek P (2010) Effect of hydrophobic interactions on properties and stability of DNA-Polyelectrolyte complexes. Langmuir 26:4999–5006
214. Kabanov AV, Kabanov VA (1995) DNA complexes with polycations for the delivery of genetic material into cells. Bioconjug Chem 6:7–20
215. Oupicky D, Konak C, Ulbrich K, Wolfert MA, Seymour LW (2000) DNA delivery systems based on complexes of DNA with synthetic polycations and their copolymers. J Control Release 65:149–171
216. Sun X, Liu C, Liu D, Li P, Zhang N (2012) Novel biomimetic vectors with endosomal-escape agent enhancing gene transfection efficiency. Int J Pharm 425:62–72

217. Wakefield DH, Klein JJ, Wolff JA, Rozema DB (2005) Membrane activity and transfection ability of amphipathic polycations as a function of alkyl group size. Bioconjug Chem 16:1204–1208
218. Wang C-H, Hsiue G-H (2005) Polymer-DNA hybrid nanoparticles based on folate-polyethylenimine-block-poly(L-lactide). Bioconjug Chem 16:391–396
219. Bromberg L, Deshmukh S, Temchenko M, Iourtchenko L, Alakhov V, Alvarez-Lorenzo C, Barreiro-Iglesias R, Concheiro A, Hatton TA (2005) Polycationic block copolymers of poly (ethylene oxide) and poly(propylene oxide) for cell transfection. Bioconjug Chem 16:626–633
220. Alvarez-Lorenzo C, Barreiro-Iglesias R, Concheiro A (2005) Biophysical characterization of complexation of DNA with block copolymers of poly(2-dimethylaminoethyl) methacrylate, poly(ethylene oxide), and poly(propylene oxide). Langmuir 21:5142–5148
221. Lidgi-Guigui N, Guis C, Brissault B, Kichler A, Leborgne C, Scherman D, Labdi S, Curmi PA (2010) Investigation of DNA condensing properties of amphiphilic triblock cationic polymers by atomic force microscopy. Langmuir 26:17552–17557
222. Wang Y, Gao S, Ye W-H, Yoon HS, Yang Y-Y (2006) Co-delivery of drugs and DNA from cationic core-shell nanoparticles self-assembled from a biodegradable copolymer. Nat Mater 5:791–796
223. Guo S, Qiao Y, Wang W, He H, Deng L, Xing J, Xu J, Liang X-J, Dong A (2010) Poly (ε-caprolactone)-graft-poly(2-(N, N-dimethylamino) ethyl methacrylate) nanoparticles: pH dependent thermo-sensitive multifunctional carriers for gene and drug delivery. J Mater Chem 20:6935–6941
224. Li Y-Y, Hua S-H, Xiao W, Wang H-Y, Luo X-H, Li C, Cheng S-X, Zhang X-Z, Zhuo R-X (2011) Dual-vectors of anti-cancer drugs and genes based on pH-sensitive micelles self-assembled from hybrid polypeptide copolymers. J Mater Chem 21:3100–3106
225. Izumrudov VA, Zelikin AN, Zhiryakova MV, Jaeger W, Bohrisch J (2003) Interpolyelectrolyte reactions in solutions of polycarboxybetaines. J Phys Chem B 107:7982–7986
226. Izumrudov VA, Domashenko NI, Zhiryakova MV, Davydova OV (2005) Interpolyelectrolyte reactions in solutions of polycarboxybetaines, 2: Influence of alkyl spacer in the betaine moieties on complexing with polyanions. J Phys Chem B 109:17391–17399
227. Ishihara K, Nomura H, Mihara T, Kurita K, Iwasaki Y, Nakabayashi N (1998) Why do phospholipid polymers reduce protein adsorption? J Biomed Mater Res A 39:323–330
228. Konno T, Kurita K, Iwasaki Y, Nakabayashi N, Ishihara K (2001) Preparation of nanoparticles composed with bioinspired 2-methacryloyloxyethyl phosphorylcholine polymer. Biomaterials 22:1883–1889
229. Lam JKW, Ma Y, Armes SP, Lewis AL, Baldwin T, Stolnik S (2004) Phosphorylcholine-polycation diblock copolymers as synthetic vectors for gene delivery. J Control Release 100:293–312
230. Chim YTA, Lam JKW, Ma Y, Armes SP, Lewis AL, Roberts CJ, Stolnik S, Tendler SJB, Davies MC (2005) Structural study of DNA condensation induced by novel phosphorylcholine-based copolymers for gene delivery and relevance to DNA protection. Langmuir 21:3591–3598
231. Ahmed M, Bhuchar N, Ishihara K, Narain R (2011) Well-controlled cationic water-soluble phospholipid polymer-DNA nanocomplexes for gene delivery. Bioconjug Chem 22:1228–1238
232. Dai F, Wang P, Wang Y, Tang L, Yang J, Liu W, Li H, Wang G (2008) Double thermoresponsive polybetaine-based ABA triblock copolymers with capability to condense DNA. Polymer 49:5322–5328
233. Wang J, Zhang P-C, Lu H-F, Ma N, Wang S, Mao H-Q, Leong KW (2002) New polyphosphoramidate with a spermidine side chain as a gene carrier. J Control Release 83:157–168

234. Ren Y, Jiang X, Pan D, Mao H-Q (2010) Charge density and molecular weight of polyphosphoramidate gene carrier: are key parameters influencing its DNA compaction ability and transfection efficiency. Biomacromolecules 11:3432–3439
235. Khan M, Beniah G, Wiradharma N, Guo XD, Yang YY (2010) Brush-like amphoteric poly [isobutylene-alt-(maleic acid)-graft-oligoethyleneamine)]/DNA complexes for efficient gene transfection. Macromol Rapid Commun 31:1142–1147
236. Ferruti P, Manzoni S, Richardson SCW, Duncan R, Pattrick NG, Mendichi R, Casolaro M (2000) Amphoteric linear poly(amido-amine)s as endosomolytic polymers: correlation between physicochemical and biological properties. Macromolecules 33:7793–7800
237. Franchini J, Ranucci E, Ferruti P, Rossi M, Cavalli R (2006) Synthesis, physicochemical properties, and preliminary biological characterizations of a novel amphoteric agmatine-based poly(amidoamine) with RGD-like repeating units. Biomacromolecules 7:1215–1222
238. Ferruti P, Franchini J, Bencini M, Ranucci E, Zara GP, Serpe L, Primo L, Cavalli R (2007) Prevailingly cationic agmatine-based amphoteric polyamidoamine as a nontoxic, nonhemolytic, and "stealthlike" DNA complexing agent and transfection promoter. Biomacromolecules 8:1498–1504
239. Cavalli R, Bisazza A, Sessa R, Primo L, Fenili F, Manfredi A, Ranucci E, Ferruti P (2010) Amphoteric agmatine containing polyamidoamines as carriers for plasmid DNA in vitro and in vivo delivery. Biomacromolecules 11:2667–2674
240. Strachan T, Read AP (1999) Human molecular genetics, 2nd edn. Wiley-Liss, New York, Chap 22
241. Gössl I, Shu L, Schlüter D, Rabe JP (2002) Molecular structure of single DNA complexes with positively charged dendronized polymers. J Am Chem Soc 124:6860–6865
242. Laschewsky A (2012) Recent trends in the synthesis of polyelectrolytes. Curr Opin Colloid Interface Sci 17:56–63
243. Schlick T, Hayes J, Grigoryev S (2012) Toward convergence of experimental studies and theoretical modeling of the chromatin fiber. J Biol Chem 287:5183–5191

Adv Polym Sci (2014) 256: 197–260
DOI: 10.1007/12_2012_170

Published online: 21 July 2013

Sizing, Shaping and Pharmaceutical Applications of Polyelectrolyte Complex Nanoparticles

M. Müller

Abstract This contribution reviews polyelectrolyte (PEL) complex (PEC) nanoparticles prepared by mixing solutions of oppositely charged PELs, with special focus on the regulation of their size and shape by PEL structural and media parameters and on their pharmaceutical applications. Experimental and simulation evidence indicates that salt and PEL concentration, pH, mixing ratio and order, PEL molecular weight and topology are useful parameters for regulation of the size and internal structure of spherical PEC nanoparticles. Experimental and theoretical data are presented to show that PEL flexibility and stiffness are able to influence and even control PEC nanoparticle shape. Finally, the options, advantages, and challenges of dispersed PEC particles for pharmaceutical applications are outlined, emphasizing the uptake and release properties towards proteins and drugs and the interaction of these nanoparticles with cells.

Keywords Coacervate · Nanoparticles · Polyelectrolyte cell interaction · Polyelectrolyte complexes · Polyelectrolyte drug interaction

Contents

M. Müller (✉)
Department of Polyelectrolytes and Dispersions, Leibniz-Institut für Polymerforschung (IPF) Dresden e.V., Hohe Strasse 6, 01069 Dresden, Germany

Fachrichtung Chemie und Lebensmittelchemie, Technische Universität Dresden (TUD), 01062 Dresden, Germany
e-mail: mamuller@ipfdd.de

1 Introduction

Polymer-based nanoparticles are increasingly used for the immobilization, storage, carriage, and release of drugs and proteins. In this context, the nanodimension offers a high surface-to-volume ratio and allows interaction with biological systems at their structural size level. Examples of widely known polymeric nanoparticular systems for biomedical and pharmaceutical applications are polymer liposomes [1, 2], block copolymer micelles [3, 4], solid polymer nanoparticles [5, 6], polymer capsules [7, 8], and spherical PEL brushes [9]. Related to both systems and applications, the aim of our work is to prepare nanoparticles on the basis of PEL complexes (PEC) in aqueous media. Generally, PEC are the product of the volume reaction between a polycation (PC^+) and its counter anions (CA^-) and a polyanion (PA^-) and its counter cations (CC^+) according to:

$$PC^{+}\cdots CA^{-} + PA^{-}\cdots CC^{+} \rightarrow PC{-}PA + CA^{-} + CC^{+}$$

Three different product types resulting from PEL complexation in the volume phase are shown in Fig. 1.

Molecular complexes containing few PEL ($N \ll 10$) are formed (clear solutions) by mixing highly dilute polycation and polyanion solutions. Colloidal aggregated structures (coacervate phase) containing nanoparticles of many PEL ($N \gg 100$) are obtained (turbid dispersions) at increased PEL concentrations. Microscopic to macroscopic precipitate structures are formed by mixing highly concentrated polycation and polyanion solutions.

Our work is mainly focused on colloidal PEC particles, which are prepared by mixing polycation and polyanion solutions in nonstoichiometric ratios [10–15], and on exploring their potential to interact in a useful manner with pharmaceutically and biomedically relevant compounds. The main issues of our research are reproducibility in the preparation protocol, uniformity of size and shape, conservation of colloidal stability after binding of compounds and the interaction with surfaces. In typical PEC systems, standard cationic and anionic PELs and PELs of natural origin (e.g., polypeptides, polysaccharides, and their modified analogues) are combined.

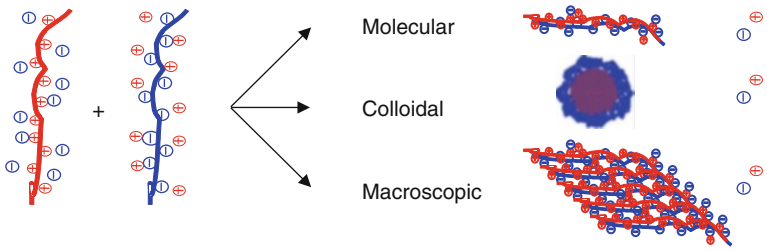

Fig. 1 Structural product types resulting from PEL complexation

As well as PEL structural parameters, important parameters were found to be the molar mixing ratio of charged units (n^-/n^+), concentration, pH, and ionic strength. These parameters can regulate particle size [16], distribution, and shape [17] and the interaction with surfaces [18–21]. Dynamic light scattering (DLS) and colloid titration were applied to study the dispersions as well as scanning force microscopy (SFM) and attenuated total reflection (ATR) Fourier transform infrared (FTIR) spectroscopy for particle layers. Recently, the monomodality of PEC dispersions was significantly improved by applying consecutive centrifugation, separation, and redispersion steps of the coacervate phase. The improvement was explained by "accelerated ripening" due to Ostwald ripening of the raw dispersion [16]. This experimental finding was confirmed by recent simulation studies [22], which will be commented on in Sect. 3.2.3 and in an article by Lebovka in this volume [23].

This contribution reviews the sizing and shaping of PEC particles and showcases applications for pharmacy and biomedicine. Additional topics emerging at several places in this contribution are the hierarchical aspect of PECs as aggregates of primary particles (particles of particles), aspects related to the stoichiometric core and nonstoichiometric shell, the softness and rather emulsive appearance, and the compartmentation and porosity of the PEC internal structure (which opens applications for loading and release of functional life science cargo such as proteins or drugs). Although individually these single aspects seem to be understood, together they are not completely consistent and even contradictory. Hence, this review, phenomenologically rather than theoretically oriented, illustrating some principles of manageable preparation and controllable properties and outlining some usable life science applications of PEC nanoparticles, might be of value for those sharing an interest in this field.

2 PEC Characterization and Preparation: Critical Experimental Aspects

Mixing two oppositely charged PELs usually results in the separation of a milky polymer-rich phase from a clear polymer-depleted phase. Given the task of preparing a PEL complex from standard PELs like poly(diallyldimethylammonium chloride) (PDADMAC) and poly(styrenesulfonate) (PSS), one would expect a similar

outcome from three different laboratories. However, the three laboratories will probably prepare the PEC sample by three different protocols and, of course, will measure three different particle radii and distributions, probably using different analytical methods and expertise. Hence, this section will not describe or propose unified protocols for the reproducible analytical characterization and preparation of PEC dispersions, but will give some experimental hints from selected experimentally oriented reports for consideration and critical discussion.

2.1 Characterization

Dynamic and static light scattering (DLS, SLS), scanning force microscopy (SFM), scanning electron microscopy (SEM), and transmission electron microscopy (TEM) are still the main methods for determining the size and shape of PEC particles in solution or turbid dispersions. Therefore, a short summary on the history of size and shape analysis of PEC nanoparticles, with a focus on light scattering and microscopy, will be given.

2.1.1 Static Light Scattering

General experimental and theoretical principles and modalities on the SLS characterization of polydisperse particle systems can be found in the literature [24, 25]. To the best of our knowledge, the group of Philipp and Dautzenberg were the first to perform SLS studies on PEC dispersions. Comprehensive reviews on the approach and modalities of applying SLS to PEC dispersions have been published [26, 27]. In a related early article [28], Dautzenberg et al. reported SLS and viscosimetry results on the influence of charge density and mixing ratio of PEC dispersions containing a cationic copolymer of acrylamide and *N*-methyl-*N*,*N*-diethyl-*N*-ethylacrylate and an anionic copolymer of acrylamide and acrylate (see Fig. 2).

2.1.2 Dynamic Light Scattering

General experimental and theoretical principles and modalities of DLS applied to polydisperse particle systems can be found in the literature [24, 29]. The first DLS work on PEC particles came to our knowledge from Dubin and Davis [30] and Kabanov and Zezin [11]. Dubin and Murrell reported early DLS studies on PEL/micelle complexes, including characterization of protein/PEL complexes such as the BSA/PDADMAC system and its pH dependence by DLS [3] (see Fig. 3). Kabanov and Zezin reported DLS studies on the complexation between synthetic poly(*N*-dimethylaminoethylmethacrylate hydrochloride) (PDMAEMA) and sodium polyphosphate and its dependence on the mixing ratio [11].

Recently, Lindhoud reported DLS titration studies on the reversibility and relaxation behavior of PEC micelles composed of PDMAEMA, poly(acrylic

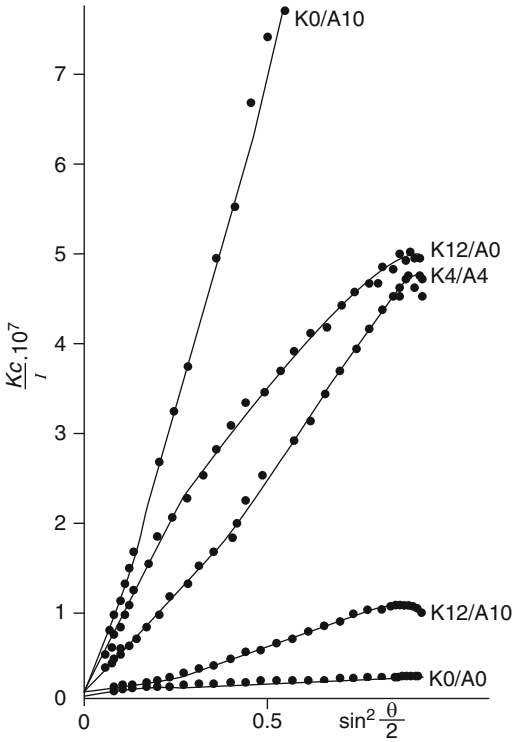

Fig. 2 First SLS data (Zimm plot) on PEC particle dispersions consisting of cationic and anionic copolymers of acrylamide. (From [28] with kind permission of Wiley-VCH)

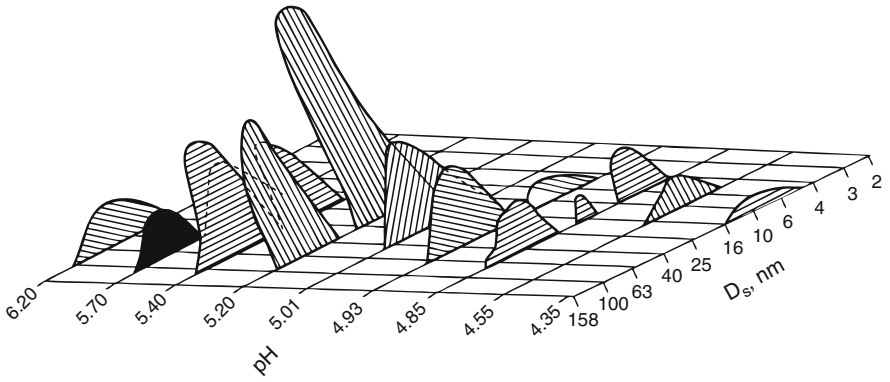

Fig. 3 First DLS data on PEC particle dispersions prepared by mixing PDADMAC (1 mg/mL) and BSA (6.7 mg/mL) solutions. The distributions of hydrodynamic diameters at various pH values are shown. (From [31] with kind permission of ACS)

acid-block-acrylamide) and lysozyme, in which the light scattering intensity is measured as a function of the composition [32] (see Sect. 3.2.1). Principles of this novel DLS approach addressing kinetic structural equilibration processes on PEC systems were reported earlier by van der Burgh [33] and will be also reviewed in a dedicated article by Lindhoud and Cohen Stuart [34].

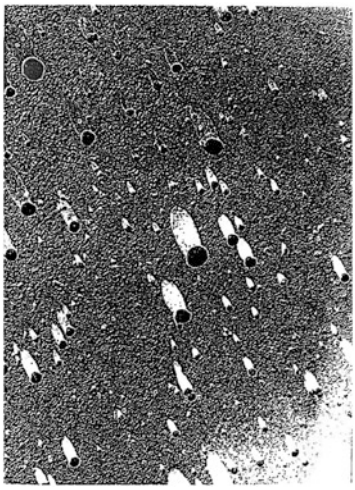

Fig. 4 Cryo-TEM images of PDADMAC (0.2 mg/mL)/PSS (0.4 mg/mL) particles (magnification: 90,000×). (From [36] with kind permission of Deutsche Bunsen-Gesellschaft)

2.1.3 Transmission Electron Microscopy

The first low resolution TEM images of PEC phases can be found in the review article of Philipp et al. [12] and a research article of Tiersch et al. [35]. Therein, TEM images of cast pure carboxymethylcellulose (CMC) featuring fibrillar network structures are compared with those of a CMC/PDADMAC PEC sample featuring domain-like structures. Later, Dautzenberg et al. [36] showed the first cryo-TEM images of PEC particles of PDADMAC/PSS, which are given in Fig. 4. Therein, singularized PEC particles featuring spherical shapes and a considerable amount of polydispersity, which was supported by light scattering data, can be observed.

2.1.4 Scanning Electron Microscopy

Early SEM images on the PEC system consisting of an integral type polycation and poly(methacrylic acid) (PMAA) were reported by Tsuchida and colleagues [37, 38]. The PEL solutions in the 0.01 M concentration range were mixed at a ratio of $n^-/n^+ = 0.5$. At first, no turbidity was registered, but after several hours the solution became hazy. From this state on, SEM was performed on PEC samples cast on a thin carbon layer and shadowed by gold, as shown in Fig. 5. Fibrous extended and network structures with diameters below 1,000 nm were obtained in this case, which were explained by a growth process along the rather stiff main chains of the PELs due to hydrophobic interactions between neutralized PEC regions.

In contrast to such morphologies, SEM images on adsorbed spherical PEC particles were shown by Reihs et al. [20, 21], one of which is given in the Fig. 6. PEC particles of PDADMAC/poly(maleic acid-*alt*-α-methylstyrene) (PMA-MS) were adsorbed from 0.002 M PEC solutions onto silicon substrates, which had been pretreated with a thin precursor multilayer of poly(ethyleneimine)/poly(acrylic

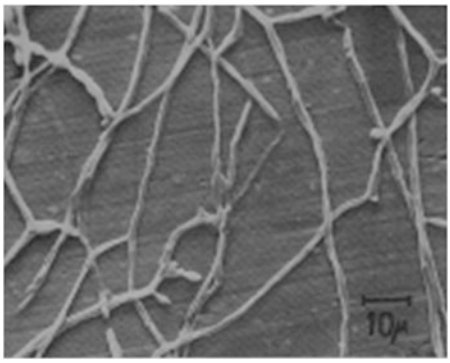

Fig. 5 SEM images of the PEC system consisting of an integral type polycation and polymethycrylic acid. (From [38] with kind permission of ACS)

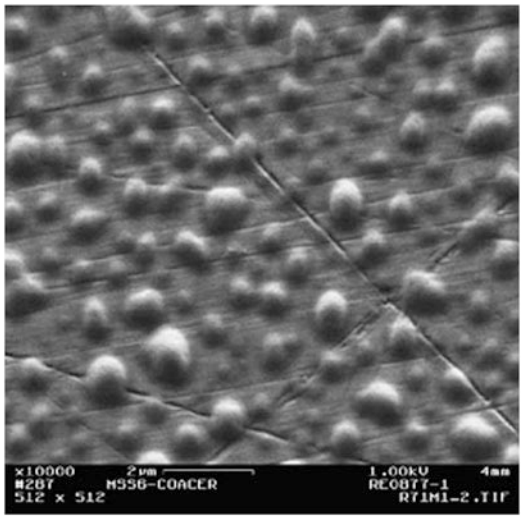

Fig. 6 SEM images of adsorbed PEC particles at a silicon support modified by PEM-6 of PEI/PAC. (From [21] with kind permission of Elsevier)

acid) (PEI/PAC). Half-sphere morphologies were obtained due to flattening of the soft PEC particles. The PEC particles appeared to form more of an emulsion than a suspension.

2.1.5 Scanning Force Microscopy

One of the first SFM studies on PEC particles was reported by Wolfert and Seymour [39], whereby complexes of poly(L-lysine) (PLL) and DNA were deposited and their size determined. Early SFM studies on spherical PEC particles consisting of synthetic PEI and poly(maleic acid-*co*-propylene) adsorbed onto mica came also from Kramer et al. [40]. Singularized particles were obtained, whose size could be related to that measured with DLS (166 nm). Similar adsorbed singularized spherical particles of PDADMAC/PMA-MS were reported [16, 17], showing an improvement with respect to monomodal size distribution.

2.2 Preparation

2.2.1 Determination of True Charge

Before mixing oppositely charged PEL in defined stoichiometric ratios, the molar concentration related to the charged monomer groups of polycation and polyanion must be determined because the molar concentration of all repeating units is definitely not identical to the molar concentration of the charges. This mismatch is predominantly the case for weak PEL because their charge density (fraction charged/all repeating units) is pH-dependent. This step is mandatory, even for strong PEL, because highly charged PEL show counterion binding.

Colloid titration [41] is a powerful analytical technique for determining the number or molar concentration of charges in a sample. Commonly, this can be realized by a particle charge detector (Mutek, Herrsching, Germany) and involves titrating a given PEL solution by a titrator solution of an oppositely charged low molecular weight PEL (PDADMAC or poly(vinylsulfate) (PVS)) until a zeta-potential of zero is reached. Zeta-potential is related to the voltage [mV] needed to compensate the sheared ion cloud when a PTFE piston is periodically moved within a PTFE tube filled with the sample PEL solution. Usually, a volume of 1 mL of a 0.001 M sample PEL solution is further diluted to 10 mL and the titrator solution is dosed in. From the volume of the consumed titrator solution, the factor F of the PEL solution is determined using $F =$ consumed volume/probe volume. Repeating units bearing one potential charged group (e.g., monobasic acid) can ideally have a factor of $F = 1$; those bearing two to three charges can ideally have values of $F = 2$–3. To control the stoichiometry of the complexation of polyanion/polycation mixtures, which is an often-used parameter for PEC dispersions, the mixing ratio n^-/n^+ has to be directly related to these obtained factors of the used PEL solutions. Unfortunately, in the literature the reported n^-/n^+ values are based on different concentration expressions so that no consistent picture prevails when parameters like turbidity, size or polydispersity are plotted versus n^-/n^+.

In this review, we use the abbreviation e.g. "PEC-0.66" for PEC systems with a mixing ratio $n^-/n^+ = 0.66$, (i.e., a cationic PEC system) and e.g. "PEC-1.50" for those with $n^-/n^+ = 1.50$ (i.e., an anionic PEC system).

Different modes of realizing nonstoichiometric mixing ratios are possible. Some authors always use equally concentrated solutions with respect to charge or monomer concentration and control the mixing ratio by the volumes of the PC and PA solutions (e.g., PEC-0.66 indicates 0.66 mL PA in 1 mL PC) [21, 42]. Others use differently concentrated PC and PA solutions and use equal volumes or even different volumes.

2.2.2 Mixing Procedure

Mixing polycation and polyanion solutions to form PEL complexes is expected to be dependent on the mixing type, protocol, and device because the irreversible process is said to be kinetically controlled and local effects may play a role [12].

However, the mixing protocol for polycation and polyanion solutions is not extensively described in the reports on PEL complexation. Often, PEL solutions are mixed (for the order of addition see Sect. 2.2.3) using magnetic stirrers at a fixed velocity. Only a few systematic studies can be found describing this important aspect.

Recently, Wågberg and coworkers reported the influence of mixing procedure on the complexation of poly(allylamine) (PAH) and poly(acrylic acid) (PAC) by comparing jet mixing [43] with the frequently used mode termed "colloid titration" [44], which should not be confused with the analytical technique mentioned above. They obtained small PECs for both low molecular weight PELs at short mixing times, whereas for high molecular weight PELs PEC size first decreased with decreasing mixing time until a minimum and then increased again. This behavior was explained by diffusion-controlled formation of "precomplexes" occurring sufficiently quickly so that stable complexes were formed. However, for larger PELs non-equilibrium precomplexes prone to aggregation were formed. Comparing the two mixing procedures, jet mixing gave smaller PECs, allowing mixing time to control PEC size, whereas PEL titration gave larger PECs. Furthermore, higher PEL concentration gave larger jet-mixed PECs.

Qualitatively similar results were obtained by Saether et al., who reported the influence of mixing speed on the particle size of chitosan/alginate (CHT/ALG) PEC particles [45] using an Ultraturrax procedure. With increasing mixing speed, smaller CHT/ALG particles were obtained.

Schatz and coworkers reported another mixing procedure dependence, comparing ordinary dropwise mixing with one-shot mixing [46] for the chitosan/dextran sulfate (CHT/DS) system. They found that the rapid one-shot mixing process gave PEC colloids with higher stability and lower diameters compared with the dropwise mixing process.

2.2.3 Order of Addition

A very sensitive experimental parameter was found by several authors to be the order of PEL addition when the PEL solutions are mixed slowly with one another [47, 48]. In principle, nonstoichiometric mixing ratios $n^-/n^+ < 1$ or $n^-/n^+ > 1$ can be experimentally achieved by dosing the minority component into the majority component or vice versa. For example, a PEC-0.66 can be prepared by dosing the minority PA solution into the majority PC solution ("minor-to-major") or by dosing the majority PC into the minority PA solution ("major-to-minor"). For the PEC system of PEI/PAC we found smaller particle sizes for minor-to-major dosing and larger ones for major-to-minor (see Fig. 7) [48]. Obviously, there is a dramatic difference between minor-to-major dosing, which is related to the interval $n^-/n^+ = 0.1$–0.7 for addition of PEI to PAC (1. PEI 2. PAC) or $n^-/n^+ = 1.0$–1.6 for addition of PAC to PEI (1. PAC 2. PEI), and major-to-minor dosing, which is related to the interval $n^-/n^+ = 0.9$–1.6 for 1. PEI 2. PAC or $n^-/n^+ = 0.1$–0.8 for 1. PAC 2. PEI. For the former case (minor-to-major), we suggest a more

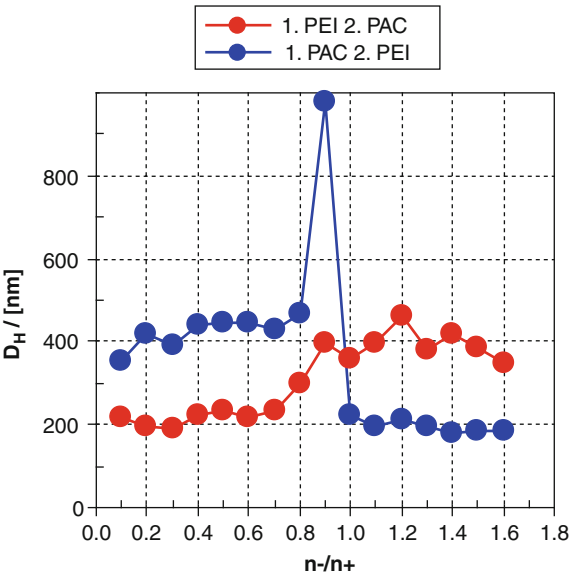

Fig. 7 Size of PEI/PAC particles versus n^-/n^+, at $c_{PEL} = 0.001$ M, pH = 10/4 for the order of addition PEI-to-PAC (*1. PEI 2. PAC*) and PAC-to-PEI (*1. PAC 2. PEI*). (From [48] with kind permission of MDPI)

equilibrated consumption of the "dosed-in PEL" because the point of 1:1 stoichiometry (not necessarily exactly at $n^-/n^+ = 1$) must not be exceeded. For the latter case (major-to-minor), consumption of the dosed-in PEL is in a nonequilibrium state because the 1:1 point must be exceeded. Similar trends have also been found by Schatz et al. [46, 49] and by Delair and coworkers [50] for the CHT/DS system. Interestingly, rapid mixing ("one-shot," see above) was reported to give the same results [47]. This step-like behavior of the particle size in dependence on n^-/n^+, which is diametrically different for 1. PEI 2. PAC compared with 1. PAC 2. PEI, was also obtained for the count rate.

Dosing the minority component into the majority component solution causes the count rate to increase continuously up to 250–300 kHz at the more or less defined range of 1:1 stoichiometry ($n^-/n^+ = 0.8$–1.0), which holds for both 1. PEI 2. PAC and 1. PAC 2. PEI scenarios. Exceeding this point (range) of 1:1 stoichiometry, i.e., starting to dose major-to-minor, the count rate falls stepwise to around 50–100 kHz and maintains this level. Obviously, the stepwise increase in particle size is paralleled by a corresponding drop in the count rate. This could be explained by either a decreasing concentration or structural density of the particles. This lower density of the particles obviously correlates with larger particle sizes.

On the basis of these findings, we suggest a more compact structure for PEI/PAC particles mixed in the minor-to-major scenario than in the major-to-minor scenario. An explanation is still speculative. However, based on the PEC formation scheme given in Sect. 3.2.3, according to which the observed secondary PEC particles are aggregates of primary particles, one could rationalize the two scenarios. For the minor-to-major scenario, either cationic (1. PEI 2. PAC) or anionic (1. PAC 2. PEI) secondary PEC particles are "electrosterically" stabilized by the excess like-charged

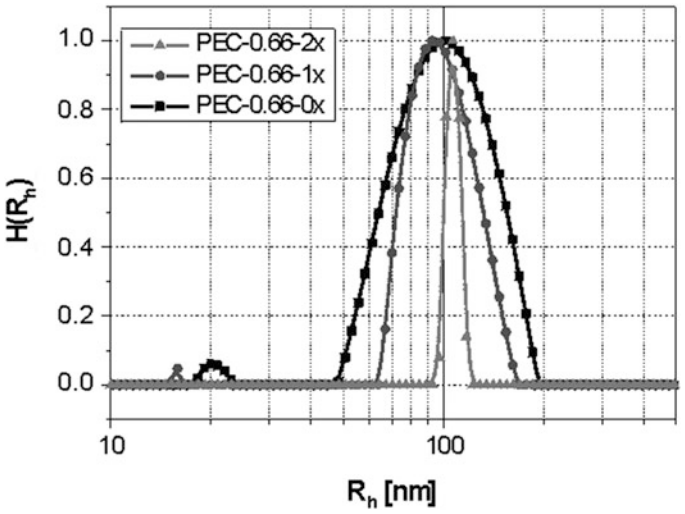

Fig. 8 Size (hydrodynamic radius R_H) distributions of PEC dispersions of PDADMAC/PMA-MS (300 kg/mol/23 kg/mol, $n^-/n^+ = 0.66$) with different numbers of centrifugation steps: *PEC-0x* no centrifugation, *PEC-1x* one centrifugation, and *PEC-2x* two centrifugations. (From [16] with kind permission of ACS)

PEI or PAC component. This is not the case for the major-to-minor scenario, where immediately after exceeding the critical 1:1 stoichiometry the excess oppositely charged PAC or PEI component can "crosslink" the secondary particles to form colloidal networks with lower structural density. We emphasize that for both scenarios the suggested PEC structures are not in equilibrium and that local and kinetic factors play a substantial role. The minor-to-major scenario might result in more "equilibrated" PEC structures because the charge sign is never reversed, whereas the major-to-minor scenario might result in "unequilibrated" and looser PEC structures.

2.2.4 Refinement

Another influence on PEC parameters can be achieved by post treatment of the PEC dispersion. Among other treatments, freshly prepared raw dispersions can be refined by consecutive centrifugation steps [16]. Thereby, the initial raw dispersion was centrifuged, the supernatant discarded and the formed coacervate phase of the serum dissolved again to the original volume. Figure 8 shows the effect of consecutive centrifugation on PEC dispersions prepared by mixing 0.002 M PMA-MS into 0.002 M PDADMAC at a mixing ratio $n^-/n^+ = 0.66$. The black curve represents the initial raw dispersion (PEC-0x), while dark gray and light gray curves represent the dispersion after one (PEC-1x) or two (PEC-2x) centrifugations (11,000 revolutions/min for 20 min), discarding the supernatant and redispersion of the coacervate phase with an equal volume. While the polydispersity index (PDI) could be significantly lowered from PEC-0x to PEC-1x to PEC-2x, the intensity maximum of the size

distribution measured by DLS kept approximately constant at around 100 nm. However, the solid content was reduced to a certain extent because there was considerable precipitation during the two centrifugation steps during the two centrifugation steps. Furthermore, in PEC-0x and PEC-1x dispersions DLS signals at $\leq$20 nm were present, while in PEC-2x ones they were absent, which can be explained by the removal of primary PEC particles upon centrifugation in the sense of an accelerated Ostwald ripening (see Sects. 3.2.3 and 3.3.2).

Other authors, e.g., Dautzenberg and Jaeger [51] and Pergushov et al. [52], filtered the raw dispersions before SLS or DLS, respectively. Membrane syringe filters with cutoff pores up to 450 nm were used, allowing removal of larger aggregate particles and collection of smaller particles at a lower PDI.

3 Sizing of PEC Particles

PEC particle size can be influenced by various parameters related to preparation, PEL structure, and the medium (pH and concentration of PEL and salt). Preparative parameters have already been mentioned in Sect. 2.2. In this section, PEL structural parameters (Sect. 3.1) and then media parameters (Sect. 3.2) influencing PEC particle size will be discussed. Finally, sizing the internal structural density of PEC systems by structural and media parameters will be outlined (Sect. 3.3). In that frame, the pore size and the degree of compartmentation are important observables. This is of high relevance for PEC-based pharmaceutical carrier systems because pore size and compartmentation control the retention potential of PEC systems towards low and high molecular weight drugs.

3.1 PEL Structural Parameters

The influence of PEL structural parameters such as weakness/strength, charge density, molecular weight, linear or branched topology, and monomer properties of charged copolymers on PEC particle size are reviewed.

3.1.1 Charge Density

The influence of charge density was addressed in early work of Dautzenberg and colleagues [28] using a system of cationic and anionic copolymers of acrylamide. They showed that for equal charge density of the PEL components, the "symplex" particles adopt a compact structure, whereas in systems with strongly deviating charge density of the PEL components a loose "fluctuating" structure prevails. This finding was in line with later work of Dautzenberg and Jaeger [51] on cationic copolymers of DADMAC and *N*-methylvinyl acetamide (NMVA) and anionic PSS. The work of Mende et al. [53] on PDADMAC and degraded anionic copolymers of acrylamide and acrylate (PAMAC) with varying charge density confirmed this

finding, showing that the smallest and most stable PEC particles were found for the PAMAC with charge density closest to that of PDADMAC, while the PAMAC with low charge density had an opposite effect.

However, seemingly in contrast to the latter findings are recent studies of Claesson and coworkers [54] based on a cationic copolymer of methacryloxyethyl trimethylammonium (METAC) with varying portions of the nonionic poly(ethylene oxide) ether methacrylate (PEO45MEMA) and anionic PSS. They showed that with decreasing charge density it was possible to obtain soluble PEC particles with decreasing hydrodynamic radii to around 20 nm and increasing stability, even for 1:1 stoichiometry. This finding was explained by steric stabilization via the hydrophilic PEO-decorated shell, which prevented secondary aggregation.

3.1.2 Molecular Weight

In a classical paper by Dautzenberg [26] on the standard PDADMAC(250 kg/mol)/PSS system, no systematic change in the size and structural density with change in M_W (8–1,000 kg/mol) of PSS was found. This finding was interpreted as a large kinetic effect in the complexation process that suppressed the influence of molecular weight, but conflicts with the findings of several other authors.

The size of spherical PLL/DNA complexes deposited and dried on mica substrates was studied by Wolfert and Seymour [39] by SFM using PLL M_w ranging from 4 to 225 kg/mol. From the height and radius of the flattened particles, the volumes were determined and showed an increase with increasing PLL M_w. Figure 9 shows a plot of the PLL/DNA particle dimension versus PLL M_w. SFM images for DNA complexed with PLL of M_w 4,000 or 225,000 g/mol are given in the insets of Fig. 9.

Recently, Hu and coworkers [55] reported on the influence of CHT M_W on the particle size of carboxymethylpachyman (CMP)/CHT nanoparticles. Increasing CHT M_W from 12,000 to 46,000 g/mol resulted in an increase of PEC particle size from 135 to 279 nm. As an explanation, they emphasized that longer chains of positively charged CHT molecules can complex with a larger number of negatively charged CMP molecules.

Figure 10 shows our own results on the influence of molecular weight of PEI and PAC on the size of PEC-0.6 and PEC-1.5 particles mixed at pH = 7/7 (i.e., PEC solution at pH 7 and PAC solution at pH 7) [48]. In the case of PEC-0.6 particles, only the M_w of PEI was varied and for PEC-1.5 particles only the M_w of PAC was varied, because we assume that the excess PEL dominates the shell region and therefore is more effective for particle size changes. Only for the pH combination of pH = 7/7 and only in the case of PEI was there a significant particle size enlargement of D_H = 120 nm to D_H = 380 nm upon increasing the M_W of PEI from 1,300 to 750,000 g/mol (Fig. 10) for PEC-0.6 particles. For pH = 10/4 PEC-0.6 particles showed no significant dependence on the M_w of PEI, for which we have no straightforward explanation. Presumably, in the more compact state of PEI at pH = 10/4 the formed PEI/PAC particles are not so sensitive to M_w variation. Furthermore, neither for pH = 10/4 nor for pH = 7/7 was there a significant enlargement of particle size with increasing M_w of PAC. Even for pH = 10/4

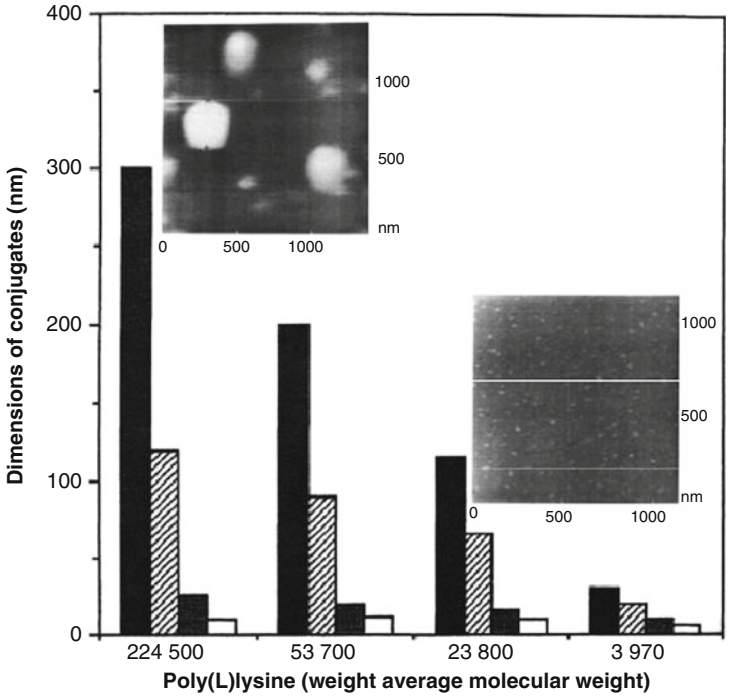

Fig. 9 Influence of poly(L-lysine) (PLL) molecular weight on the dimensions of PLL/DNA particles obtained by SFM (see *insets*). (From [39] with kind permission of Nature Publishing Group)

there was a decrease of particle size with increasing M_W of PAC. Furthermore, it should be noted that in our studies on PEI/PAC particle size parameters, the smallest particle size of $D_H = 80$ nm was obtained for PEC-1.5, mixed at pH = 7/7 at PAC M_w of 2,000 g/mol, which is evident from Fig. 10 (first open square data point in bottom series).

3.1.3 PEL Topology: Linear Versus Branched

Imae and Miura reported complexation between fourth generation PAMAM dendrimers (DEN) and poly(L-glutamic acid) (PLG) in 0.25 M NaCl [56]. They observed a constant course for molecular DEN/PLG ratios $X \ll 300$ but a steep increases of the PEC particles from around $R_G = 100$ nm up to $R_G > 300$ nm for $X > 300$ (DEN and PLG concentration was 0.1% w/w) (see Fig. 11). This means that DEN spheres bind to PLG chains like a loading process up to a certain threshold value, but thereupon may act as crosslinkers for PLG chains, resulting in larger aggregate-like PEC particles.

In principle, a similar behavior was found for cationic aromatic dendrimers (excess component) complexed with DNA in studies by Shifrina and coworkers aiming at positively charged DNA vectors [57].

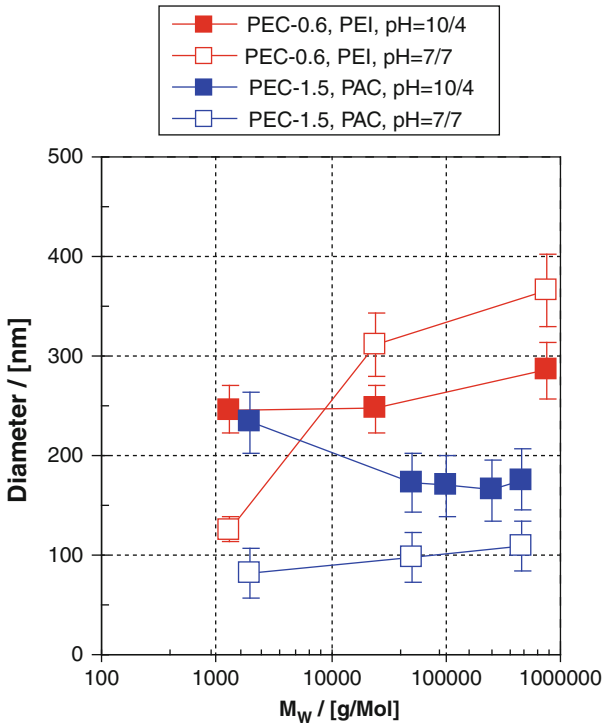

Fig. 10 Plot of D_H versus the M_W of PEI or PAC within PEC dispersions of PEI/PAC at $c_{PEL} = 0.001$ M (all) and $n^-/n^+ = 0.6$ or 1.5. (From [48] with kind permission of MDPI)

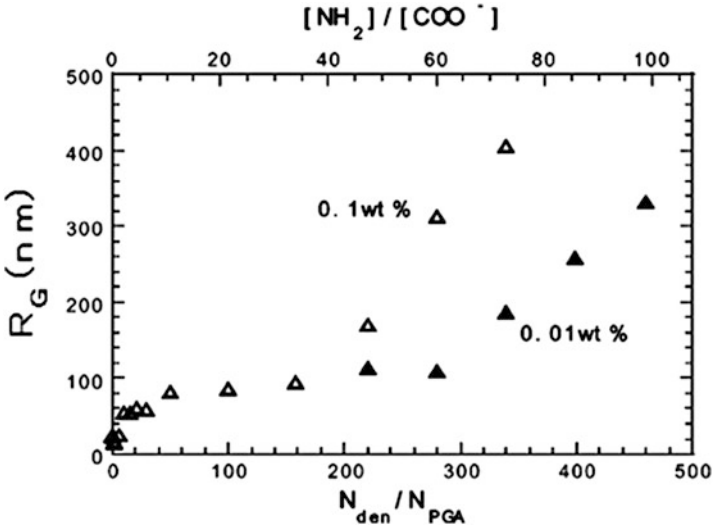

Fig. 11 Evolution of R_G in dependence of dendrimer/poly(L-glutamic acid) ratio (N_{den}/N_{PGA}). (From [56] with kind permission of ACS)

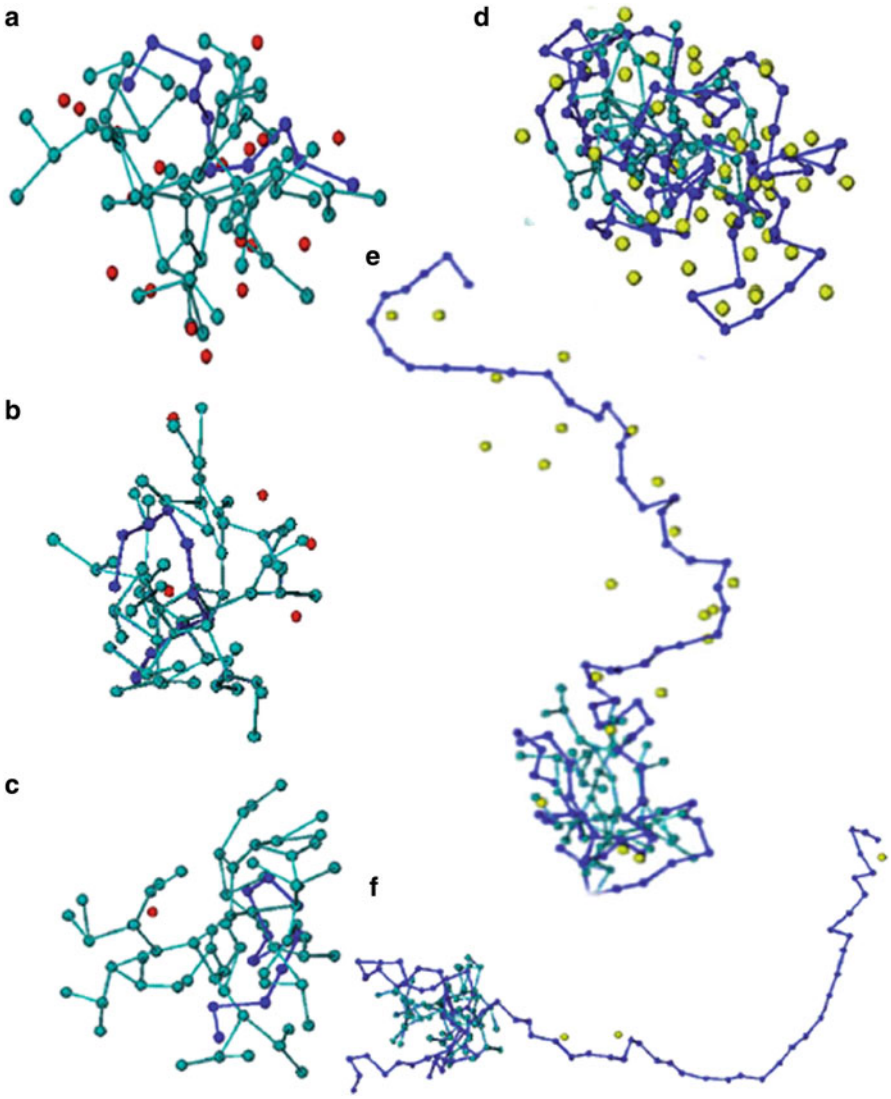

Fig. 12 Dendrimer/linear PEL/counterions conformations at the reduced temperatures $\tau = 0.05$ (**a**, **d**), $\tau = 0.2$ (**b**, **e**), and $\tau = 0.4$ (**c**, **f**) for chain lengths of 10 (**a**–**c**) and 80 (**d**–**f**) beads, respectively. The *lines* represent the dendrimer or linear polyelectrolyte; *spheres* represent the counterions. (From [58] with kind permission of AIP)

Simulations on such charged dendrimer/linear PEL systems were made by Klos and Sommer [58] based on one dendrimer binding at one charged chain, including counterions, with temperature as the main simulation parameter. The results are shown in Fig. 12. They found that the distribution of tail lengths of the adsorbed chain depends on both temperature and length of the chain. Although for short

Table 1 Combination matrix of linear and branched polycations and polyanions with respect to count rate (scattering intensity) from DLS measurements

	Polyanion/polycation-0.9 count rate [kHz]	
	Linear polyanion (PSS, CS, ALG, HEP)	Branched polyanion (DS)
Linear polycation (PDADMAC, PLL)	149 ± 32	249 ± 34
Branched polycation (PEI, DEAE)	250 ± 47	108 ± 6

Errors relate to the standard deviation among all measured polycation/polyanion combinations

chains, the tails are of nearly the same length, different scenarios were observed for long chains. At very low temperatures two tails of equal length are preferred, whereas at intermediate temperatures a long and a short tail are formed, and at higher temperatures random fluctuations of tail length prevail. Tails of longer chains in the complex are stretched at certain temperatures due to repulsion between their beads and shrink further as temperature decreases due to multipole attraction between the tails caused by chain counterion condensation.

Recently, we studied the effect of polycation and polyanion topology on the size and count rate of PEC particles. Various combinations of branched and linear polycations and polyanions were considered. The polycation/polyanion combinations and preliminary results on the averaged count rates of the various PEC-0.9 particles mixed at 0.002 M are given in Table 1 (unpublished data).

Interestingly, all PEC-0.9 samples showed roughly the same size of $R_H = 82 \pm 9$ nm within the error range of the DLS measurements, while significant differences were seen in the count rate, although partly the error values were quite high. The linear/branched combinations like e.g. PEI/CS and e.g. PDADMAC/DS showed very high count rates (250 ± 47 kHz), whereas the linear/linear (149 ± 32 kHz) and especially the branched/branched combinations (108 ± 6 kHz) showed significantly lower count rates. For equal particle sizes and distributions, and under the assumption of equal particle concentrations and neglectance of particle chemistry variations, the count rate (scattering intensity) roughly scales with the internal particle density. Hence, qualitatively it can be concluded that for branched/linear combinations higher internal structural densities prevail compared to the other combinations. One reasonable argument for these results might be the higher interpenetration between branched and linear PELs in contrast to the lower interpenetration between two branched PELs.

3.1.4 Selected Copolymers of Charged and Uncharged Functional Comonomers

Ethylene Oxide Comonomers

Kabanov et al. [59] reported nonstoichiometric complexes between cationic poly (*N*-ethyl-4-vinylpyridinium) and anionic block copolymer poly(ethyleneoxide-*co*-methacrylate). This system revealed highly soluble stoichiometric PEC particles,

which were stable in a much broader pH range than PEC particles containing the anionic homopolymer. These PEC particles were claimed to feature a neutral core of complexed PELs decorated by a PEO shell, which can be denoted as block copolymer micelles.

N-Isopropylacrylamide Comonomers

It is well known that poly(*N*-isopropylacrylamide) (PNIPAAM) systems undergo thermotropic phase transitions, resulting in polymer segment density increases at temperatures higher than the lower critical solution temperature (LCST) [60]. This phase transition is associated with a loss of external hydrogen bonds of the amide units to water and a gain of internal hydrogen bonds between amide units expelling water from the aggregated phase. Copolymers of NIPAAM with charged monomer units can result in a loss of this thermotropic behavior. Dautzenberg and coworkers checked whether the complexation of a cationic copolymer of NIPAAM [poly (methacryloyl-oxyethyldimethyl benzylammonium chloride)] with an anionic copolymer of NIPAAM [poly(2-acrylamido-2-methylpropanesulfonate)] can regain the known thermotropic properties of the homo PNIPAAM [61]. Indeed, they could show significant decreases of the particle size of a PEC-0.6 at a NaCl concentration of 0.01 M from R_H = 200–240 nm at temperatures below LCST to around R_H = 100–140 nm at temperatures above the LCST. Furthermore, this process was reversible and accompanied by a respective increase and decrease in structural density of the PEC system. Such a thermoswitchable change in structural density may have interesting consequences for applications like the controlled uptake and release of drugs or enzymes.

Kleinen and Richtering [62] complexed microgels of weakly crosslinked P(NIPAAM-*co*-methacrylic acid) P(NIPAAM-*co*-MAA) with PDADMAC and the resulting submicron particles showed thermosensitive behavior (see Fig. 13). A significant drop in the hydrodynamic radius of PEC from around R_H = 300–350 nm (X = 1:0.2–1:1.25) at 20°C to around R_H = 120–170 nm at 45°C took place. The lower the PDADMAC content in the PEC, the higher was the particle size in the swollen state and the higher was the size difference between swollen and compact state.

Nolan, Serpe, and coworkers showed that thermoresponsive PEL complex films containing poly(*N*-isopropylacrylamide-*co*-acrylic acid) and PAH fabricated by the layer-by-layer (LbL) technique could load and release doxorubicin [63] or insulin [64] under temperature control. No such behavior was shown to our knowledge for PEC particle systems of equivalent oppositely charged PNIPAAM-derived PEL components.

Amphoteric Terpolymers of Oppositely Charged and Neutral Blocks

Recently, water-soluble micellar PEC particles formed by the self-complexation of polyampholytic amphiphilic polybutadiene-*block*-quaternized poly(2-vinylpyridine)-*block*-poly(methacrylic acid) (PB-*b*-P2VPQ-*b*-PMAA) triblock terpolymers were

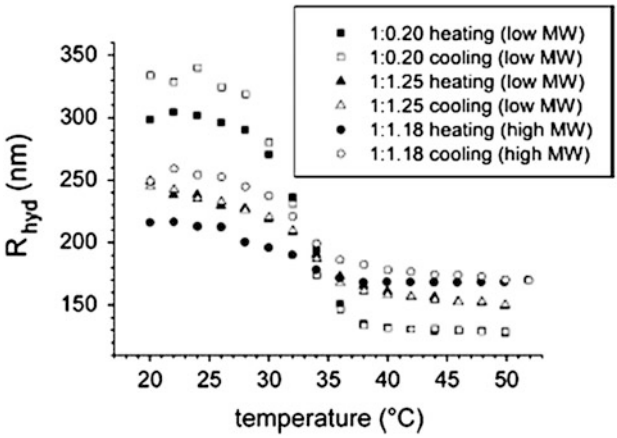

Fig. 13 Hydrodynamic radii of complexes of P(NIPAAM-*co*-MAA)/PDADMAC. *Squares* show complexes of low M_W PDADMAC with ratios of 0.2 and *triangles* those with ratios of 1.25. *Circles* show a complex consisting of microgel and an excess of 1.18 of high M_W PDADMAC. *Filled symbols* represent heating curves and *open symbols* cooling curves. (From [62] with kind permission of ACS)

reported by the groups of Schacher and Pergushov [65, 66]. These PEC systems self-assemble to multicompartment micelles in aqueous media featuring a hydrophobic PB core and complexed PMAA(−)/P2VPQ(+) domains on the PB core formed by electrostatic interaction. In the corona of these micelles, excess portions of the respective PEL block (PMAA or P2VPQ) with the higher polymerization degree are located and provide their solubility and colloidal stability in water. Formation of the multicompartment structure of these PEC micelles is highly dynamic, so that the authors claim applications as temporal carriers for various compounds. More details on these dynamic micellar PEC systems can be found in a dedicated article by Pergushov [67].

3.2 Media Parameters

The influence of mixing ratio $X = n^-/n^+$, PEL concentration (c_{PEL}), and salt concentration (c_S) on PEC particle size will be reviewed in this section.

3.2.1 Mixing Ratio

Mixing ratio is the parameter that is by far the most used and varied in experimental studies on PEC particles, wherein the most frequent observable is turbidity. Mixing ratio is also used to influence PEC particle size.

In a classical report by Kabanov and Zezin [11], the radius of gyration (R_G) as well as the average number of polymers of PEC particles of PDMAEMA/

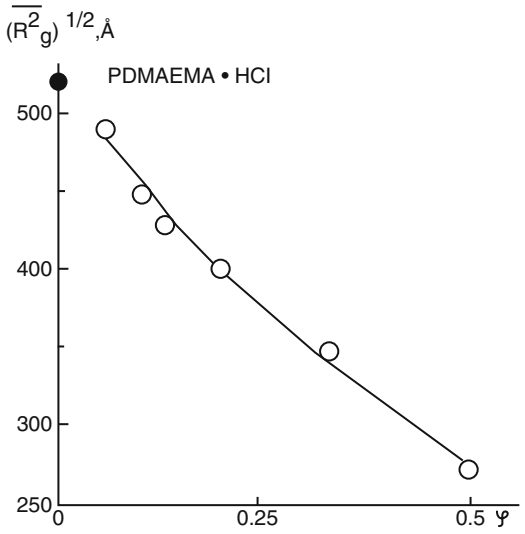

Fig. 14 Dependence of PEC particle size (Å) of PDMAEMA/polyphosphate on the composition (mixing ratio). (From [11] with kind permission of ACS)

polyphosphate was determined by SLS. A drastic drop of R_G from 49 nm at $X = 0.067$ down to 27 nm at $X = 0.5$ and a respective rise of average polymer number from 1.4 up to 10 was found (Fig. 14). They interpreted these effects by the original coil dimension of PDMAEMA at $X = 0.067$ and the existence of a ladder-like structure at $X = 0.5$.

In a further classical report by Dautzenberg [68], the molecular weight and size of PDADMAC/PSS particles were studied in dependence of the mixing ratio. A slight decrease in molecular weight and a strong decrease in the size from around 400 nm ($X = 0.1$) to 200 nm ($X = 1.0$) was found with increasing mixing ratio in the saltless system, which was qualitatively interpreted as an increase in structural density when X approaches 1:1 stoichiometry because mutual charge-compensated chains might be more compactly coiled. However, it is argued that polydispersity effects might overestimate this structural density effect. In the presence of ionic strength ($c_S = 0.01$ M), the particle size and molecular weight were generally much smaller and the size increased slightly with X from around 50 nm ($X = 0.1$) to about 120 nm ($X = 1.0$). This was interpreted by a lower aggregation number of the salted system ($N \approx 30$ chains per PEC particle) compared to the salt-free system ($N = 1{,}000$ chains per PEC particle). Possibly, these already compact smaller PEC particles increase size by additional aggregation upon loosing excess charge.

Although in these studies the mixing ratio did not exceed $X = 1$, Buchhammer et al. [69] reported the influence of the mixing ratio on the PEC particle size for PDADMAC and a copolymer of acrylamide and acrylic acid (Praestol). When the minority component was dosed to the majority component (see Sect. 2.2.3), the PEC size decreased very slightly from $X = 1.6$ to $X = 1.0$, which might support the classical findings above. However, exceeding this quasi-stoichiometric (1:1) point by dosing the majority to the minority component, a significant abrupt size increase from 130 nm to around 330 nm at $X = 0.8$ was obtained. This was paralleled by a significant drop in the PDI. The authors explain this effect by the

early formation of (loose) larger PEC particles, which are stabilized by the further addition of excess PEL so that no secondary aggregates are formed (low PDI). By contrast, when the minority component is added to the majority component an early formation of small compact particles takes place, which can readily aggregate to different aggregate sizes (high PDI).

Schatz and coworkers [49] reported similar trends for CHT/DS particles, where CHT had a low charge density. Under these conditions, PEC size also dropped from about 1,000 nm at values of $X = 20$ down to about 400 nm at $X = 1$; however, PDI values were 0.2 and higher, with no significant X dependence.

Also related to mixing ratio variations van der Burgh [33] at first reported and discussed DLS titration experiments on complexes between homopolyelectrolytes (HP, e.g. PDMAEMA) and oppositely charged diblock copolymers (CP, e.g. poly (acrylic acid-block-acrylamide)) under variation of the cationic fraction F^+ = HP/(HP + CP) related to the chargeable monomer units, which were later reviewed and extended by Lindhoud [32]. Based on plots of light scattering intensity as function of the composition $I(F^+)$ these authors claimed a symmetrical pattern consisting of four regions (I–IV). Starting at F^+=0, $I(F^+)$ increases slightly upon titrant (HP) addition, which has been argued to be due to the formation of small soluble complexes having a negative charge (I). Thereupon at a certain F^+ value the slope (dI/dF^+) becomes steeper and PEC micelles start to form (II) until at $F^+ \approx 0.5$ the system is neutral and maximum intensity (micelle number) is found. Further increase of F^+ results in the disintegration of PEC micelles, leading to a decrease of $I(F^+)$ similar to the formation of micelles (III) but with negative slope. Finally, the slope becomes less pronounced, and the solution contains again soluble complexes (disintegrated micelles) but with positive charge (IV).

3.2.2 PEL Concentration

At first glance, PEL concentration seems to be an easily and frequently applied parameter that can influence PEC particle size. However, only a few related reports are available in the open literature.

Among them, Dautzenberg et al. reported early work on the influence of PEL concentration on the mass (M_w, not to be confused with the molecular weight of the PEL components) and size (herein: $R_G = a_m$) of PEC particles, based on SLS measurements of the PDADMAC/PSS system [27] (see Fig. 15). The plot of R_G versus c_{PEL} could be fitted by a simple power law of the type $R_G \sim {c_{PEL}}^{0.58}$ and that of M_W versus c_{PEL} by $M_W \sim {c_{PEL}}^{1.70}$. Moreover, the direct dependence between R_G and M_W reads $R_G \sim {M_W}^{0.58/1.70} = {M_W}^{0.34}$, from which an exponent close to 1/3 could be obtained, which is in line with the expected classical relation for homogeneous spheres or polymer globules ($R_G \sim {M_W}^{0.33}$). In this work, the structural density of PEC particles was found to be invariant of concentration and was $\rho = 0.43$ g/mL.

Furthermore, Schatz et al. [49] reported the influence of c_{PEL} on the size of biopolyelectrolyte complex particles of CHT/DS. Increasing particle sizes were obtained with increasing DS concentration, but only at high mixing ratios n^+/n^-.

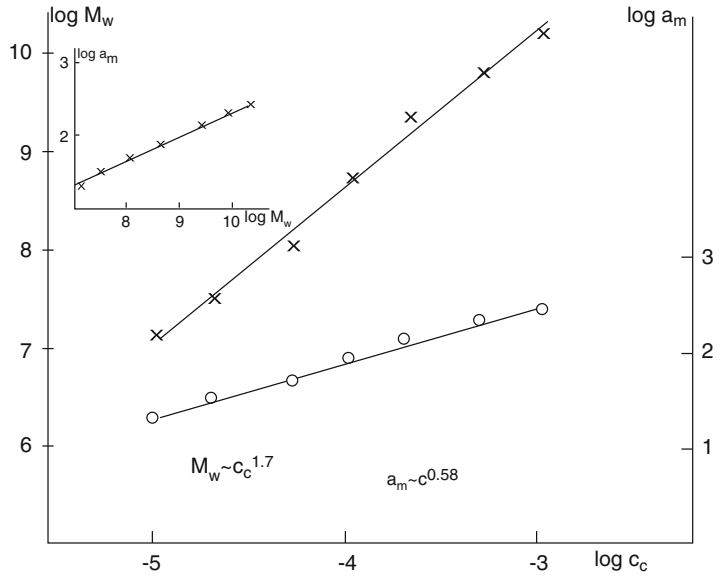

Fig. 15 Dependence of PEL concentration on the M_W of PDADMAC/PSS PEC particles. (From [27] with kind permission of ACS)

Reihs and coworkers [17] reported nanoparticular complexes between PDADMAC or PLL and copolymers of maleic acid at $n^-/n^+ = 0.6$, which increased in size from around 60 to 120 nm by increasing c_{PEL}. This was explained by subsequent exceeding of the overlap concentration of either of the PEL components, which increased the complexation and aggregation probability.

Recently, the dependence of PEC particle size on PEL concentration (c_{PEL}) was reported by our group [48]. PEC-0.6 particles of PEI/PAC were prepared in dependence of c_{PEL}, whereby PEI with $M_w = 750{,}000$ g/mol and PAC with $M_w = 50{,}000$ g/mol were used in these series. The plot of particle size and count rate versus c_{PEL} is given in Fig. 16. Generally, by varying c_{PEL} it is possible to generate PEC-0.6 particles of PEI/PAC with defined diameters D_H of 200–1,000 nm. Generally, the PEC particle size increased with c_{PEL}. However, for $c_{PEL} > 0.01$ M, the PEC dispersions tend to instability, as can be seen from the drop in count rate. As an explanation for the increasing PEC particle size with increasing c_{PEL} we assume an influence of the Debye length, which is a measure of electrostatic reach. As pointed out by Wandrey [70], not only increasing salt but also PEL concentration decreases the Debye length of a PEL system. Hence, based on the model of aggregation of primary PEC to secondary PEC particles due to short range dispersive interactions, we suggest that increasing c_{PEL} results in reduced electrostatic repulsion between like-charged primary PEC particles and thus in their elevated dispersive attraction. Furthermore, an increase in c_{PEL} might also result in a larger number of primary PEC particles per volume. Both could lead to larger secondary PEC particle sizes, but exceeding certain c_{PEL} values can also lead to precipitation.

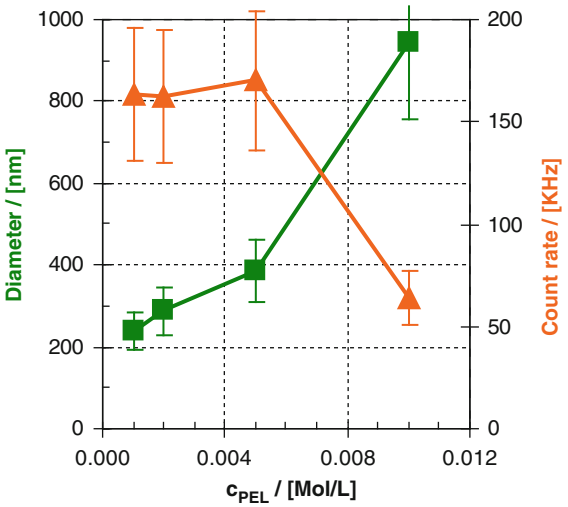

Fig. 16 Dependence of hydrodynamic diameter D_H and count rate of PEC-0.6 dispersions of PEI/PAC on PEL concentration (c_{PEL}). (From [48] with kind permission of MDPI)

3.2.3 Salt Concentration

The influence of salt on colloidal PEC parameters like size (and structural density) can be divided into two scenarios: (1) salt addition during complexation, being already present in the PEL solutions, and (2) salt addition after complexation to already-formed PEC dispersions.

Salt Addition During Complexation

A classical paper on the effect of salt on PEL complexation has been given by Dautzenberg [68]. PEC particles of the standard PDADMAC/PSS system were prepared at a PEL concentration of $c_{PEL} = 0.00025$ M (PSS) and $c_{PEL} = 0.0005$ M (PDADMAC) in the presence of no, 0.01 M and 0.1 M NaCl.

For no salt, the PEC particle size (R_G) dropped from around 300 nm at mixing ratio $X = 0.1$ to about 130 nm at $X = 0.95$. For 0.01 M NaCl, R_G kept constant at about 40 nm at $X = 0.1$–0.9. For 0.1 M NaCl, at $X = 0.1$ $R_G = 50$ nm, which was slightly higher than for 0.01 M, and increased to about 120 nm at $X = 0.95$. For $X = 0.5$, the PDADMAC/PSS system was studied at a higher resolution of NaCl concentration, resulting in a pronounced minimum at around 0.005 M, which is shown in Fig. 17. This was explained by a double influence of ionic strength and thus the charge screening on PEC particles, which is based on the hypothetical PEL complexation scenario of rapidly formed primary molecular complexes prone to secondary aggregation. In this picture, on the one hand increasing salt concentration favors coagulation of PEC (primary) particles to larger (secondary) particles, while on the other hand the PEL shells of the finally formed PEC aggregates shrink.

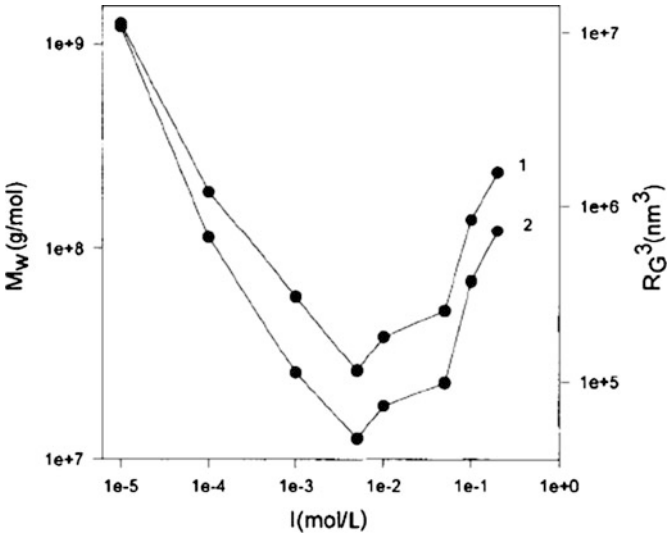

Fig. 17 Dependence of size parameters (Mw and R_G) of PEC particles of PDADMAC/PSS at $X = 0.5$ on ionic strength ($I \sim c_S$) in the mixing PEL solutions. (From [68] with kind permission of ACS)

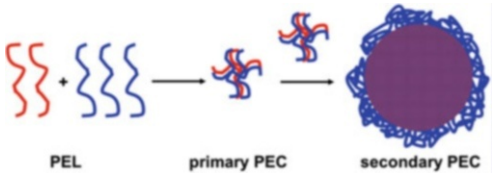

Fig. 18 Scheme of the PEC formation process, as supported by experiment and simulation [22]. (From [48] with kind permission of MDPI)

In comparable experiments using PDADMAC/poly(maleic acid-*co*-propylene) at $c_{PEL} = 0.001$–0.004 M, Pergushov and Buchhammer found an increase in the hydrodynamic radius R_H from100 nm with no NaCl to 300 nm at 0.23 M NaCl [71]. In these experiments, the resolution of the salt concentrations was lower. Presumably, at $c_{NaCl} \approx 0.005$ M a minimum of R_H for PDADMAC/PSS would also have been found.

The influence of salt on biopolyelectrolyte complexes was also shown by Schatz and coauthors [46]. These authors observed a decrease of particle size from around 450 nm to 250 nm by increasing salt concentration from 0.005 to 0.1 M. However, they used rather high mixing ratios of $n^+/n^- = 5$.

These experimental findings were confirmed by recent simulation studies of Starchenko et al. [22], supporting the idea that the PEC formation process can be subdivided into an initial rapid formation of molecular or primary complex particles ($R_H = 5$–20 nm) and a subsequent aggregation of these primary particles to secondary particles. This proposed scenario is shown in Fig. 18. Primary particles are

suggested to consist ideally of only one or a few polycation/polyanion pairs held together by long range electrostatic interactions. Since the whole PEC formation process is claimed to be athermal [10, 72], the driving force of the evidently occurring polycation/polyanion pairing is claimed to be the gain of entropy when the respective counterions are released ("escaping tendency of the counterions" [10]) from their parent PEL backbone. By contrast, secondary particles, the final particles found in a freshly prepared raw PEC dispersion, consist of some 100 primary PEC particles held together by short range dispersive interactions. It might be speculated that this second process is slightly enthalpic (i.e. exothermic) because no entropy gain is expected during this process. We see this aggregation process of primary to secondary PEC particles in the line of the classical concept of Ostwald ripening [73]. According to Voorhees [74], Ostwald ripening denotes "*a first-order transformation process resulting in a two-phase mixture composed of a dispersed second phase in a matrix. However, as a result of the large surface area present, the mixture is not initially in thermodynamic equilibrium. The total energy of the two-phase system can be decreased via an increase in the size scale of the second phase and thus a decrease in total interfacial area. Such a process is termed Ostwald ripening or coarsening*". Transferred to colloidal systems, this means that a dispersion of small primary colloid particles below a critical size tends to become unstable and thus aggregates to larger secondary particles until theoretically reaching one final macroparticle to decrease surface area. Since Ostwald assigned the final aggregated product state to a lower energy than the initial unaggregated educt state, it might be questioned whether the process should be of enthalpic nature. However, this dynamic (see Sect. 3.1.4) and occasionally long-term irreversible process is influenced by the two classic types of colloid interaction forces: the short range ($<$5 nm) dispersive attractive force and the long range ($\gg$5 nm) electrostatic repulsive force, which was summarized in classical DLVO theory [75, 76].

Salt Addition After Complexation

Examining the salt effect on already-formed PEC particles is a completely different task. The response or stability of the PEC system can be studied on the colloidal level as well as on the (molecular) ionic binding level. Generally, the salt tolerance of the PEC system concerning ionic binding is quite large. Dautzenberg [68] claimed such ionic binding stability up to $c_S = 4$ M. The salt tolerance concerning colloidal stability is lower because flocculation and aggregation sets in with increasing c_S, beginning at $c_S \approx 0.6$ M. This can be illustrated by the observation that the structural density remains constant, even for $c_S > 0.6$ M. However, the latter salt-mediated colloidal stability is also crucially dependent on the mixing ratio because the more nonstoichiometric the mixing ratio (i.e., the greater the deviation from neutrality: $n^-/n^+ \gg 1$ or $n^-/n^+ \ll 1$), the thicker is the surrounding excess PEL shell. In other words, PEC particles with thicker PEL shells have higher salt tolerance. The influence of ionic strength on size parameters of already-formed PEC particles was also shown in a narrower c_S range with higher resolution by

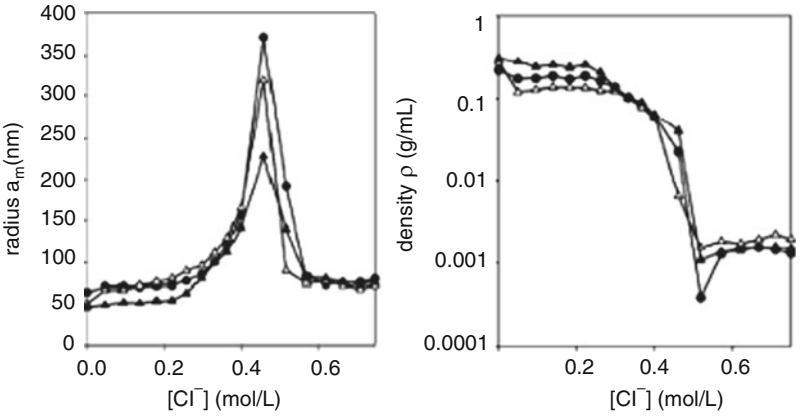

Fig. 19 Salt dependence of radius (a_m), and structural density (ρ) of PEC Cop47/NaPMA at $X = 0.6$ for different monovalent salts: *black circles* NaCl, *black triangles* LiCl, and *open triangles* KCl. (From [77] with kind permission of ACS)

Dautzenberg and Kriz [77] for a copolymer of PDADMAC and acrylamide complexed by polymethacrylate. A constant mixing ratio of $X = 0.6$ was used and LiCl, NaCl, and KCl were used as the salts. As shown in Fig. 19, using this salt addition mode, there was an increase from around 70 nm at $c_{NaCl} = 0$ up to a sharp peak of 370 nm at around $c_{NaC\ l} \approx 0.5$ M and a decrease to again around 80 nm at $c_{NaCl} > 0.5$ M.

The other salts showed a similar trend, which was interpreted in terms of salt-induced aggregation of small soluble complexes to larger aggregates at salt concentrations of 0–0.5 M, which was also supported by the decrease in PDI to a value suggesting monodisperse, large aggregate particles. To explain the sharp particle size drop for $c_S > 0.5$ M, dissolution of PEC aggregates to small soluble complexes or partly to the PEL components was proposed. The change in structural density ρ with c_S is in line with this finding because at low c_S PEC particles have a typical value of $\rho \approx 0.4$ g/mL, which drops down to 0.001 g/mL due to formation of loose larger aggregates (370 nm for NaCl) at $c_S \approx 0.5$ M. It is surprising that ρ stays approximately constant for $c_S > 0.5$ M, since the radii were again about the same as the initial ρ values at low c_S.

3.2.4 pH

In Fig. 20, the influence of pH combination on PEC particle size is shown for the PEC system consisting of the weak PELs PEI (M_w 750,000 g/mol) and PAC (M_w 50,000 g/mol) at the molar mixing ratio $n^-/n^+ = 1.50$. Significantly, a decrease in particle size from $D_H \approx 400$ to ≈ 160 nm was obtained with decreasing values of pH (10, 8.5, 7, and 4) of the PEI solution at a constant pH = 4 of the PAC solution. This trend can be explained at the intramolecular level by the graded charging up of the PEI, resulting in a rather stretched conformation. Moreover, for pH = 4/10 a

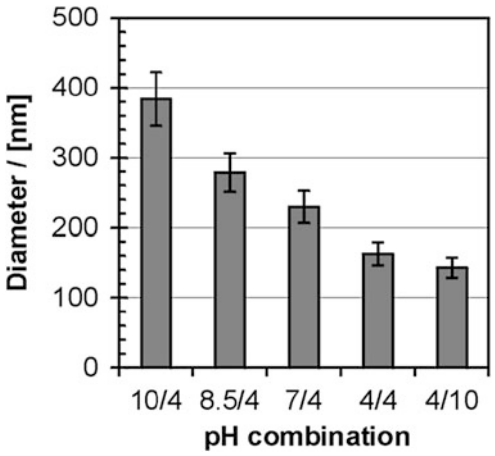

Fig. 20 Influence of pH combination (pH_{PEI}/pH_{PAC}) on the diameter D_H of PEC-1.5 particles of PEI/PAC ($n^-/n^+ = 1.5$, $c_{PEL} = 0.005$ M). (From [48] with kind permission of MDPI)

further size drop was seen, since both PEI and PAC were fully charged. At the colloidal level, the accepted model of aggregation of small primary PEC particles to larger secondary particles [22, 71] could be an explanation. For that model and that system, the lower charge screening at lower ionic strength led to the repulsion of primary PEC particles and therefore to lower coagulation tendency and lower particle size. Analogously, the highly charged primary particles of PEI/PAC at pH = 4/10 may have a lower coagulation tendency due to mutual electrostatic repulsion, compared to the lower charged primary particles formed at pH = 10/4 due to electrostatic attraction.

3.3 Sizing the Internal Structural Density of PECs

Sizing or tailoring the internal structure of PEC systems in terms of density, mesh size, porosity, hydration or even charge compensation types (PEL/PEL vs. PEL/ion) is of great relevance for PEC applications such as membranes [177, 178], ion-conductive materials [179, 180] and drug delivery (see Sect. 5.2). However, like many other materials, PEC material features various structural levels, which are partly given in Fig. 1. Herein, we focus on PEC nanoparticles, which can be singularized (Sect. 3.3.1) or secondarily aggregated (Sect. 3.3.2).

3.3.1 Internal Structure of Singularized Nanoparticles

Dautzenberg studied the influence of the mixing ratio on the structural density ρ of PEC-PDADMAC/PSS [26]. A slight linear increase from around 0.4 g/cm^3 at

$X < 0.5$ up to around 0.5 g/cm^3 at $X = 1$ was found, which was interpreted to mean that the formation of new particles rather than further growth dominates the density/mixing ratio profile. Furthermore, PDADMAC concentration had no significant influence on ρ, which stayed constant for c_{PDADMAC} of 10^{-5} to 10^{-3} M, and neither did ionic strength show any influence on ρ. The results implied that individual PEC particles may aggregate, but in principle their internal structure remains unaltered. However, based on the P(DADMAC-*co*-acrylamide)/PSS system [36] with decreasing DADMAC content, and thus charge density, PEC particles were found to decrease in ρ due to increasing charge mismatch. Therefore, charge density was claimed to be an important parameter for the swelling degree of PEC particles. Of course, in PEC systems of oppositely charged copolymers of PNIPAAM dramatic temperature-dependent increases from $\rho \approx 0.1$ g/cm^3 at 25°C to $\rho \approx 0.7$ g/cm^3 at 50°C can be found. Therefore, such thermotropic PEC systems are most interesting for applications such as triggerable drug delivery.

Related to this, Wagberg and colleagues [78] studied subtle molecular effects on the internal structure of PECs. These authors found that replacing PAC by poly (methacrylic acid) (PMAA) in PECs containing PAH revealed a significant increase in the water content and particle size.

3.3.2 Internal Structure of PEC Aggregates

In the previous section, considerations on the internal structure of PEC systems were raised on the singular particle level. This section discusses aggregated systems. Secondary PEC aggregation, where primary PEC particles aggregate to larger clusters [16, 22] in some analogy to Ostwald ripening, is of relevance. Such aggregate particles may adopt "raspberry" structures, where large spherical particles form the envelope of many smaller particles. However, only few experimental proofs (such as microscopy) for such structures have been reported up to now. This could be explained by the soft and water-rich nature of such raspberry-like PEC particles, where the soft primary particles might show no sufficient distinction due to fusing (PEC dispersions might be better described as emulsions). Nevertheless, raspberry structures were obtained in some selected examples, where hydrophobic PELs were used for complexation (unpublished results).

Recent contributions on the internal structure of macroscopic PEC systems circle around the term "saloplasticity" raised by Schlenoff and coworkers [79–81]. Saloplasticity denotes and makes use of the phenomenon that upon addition of salt the PEC material becomes more fluid-like and hence formable. This property is seen as analogous to thermoplasticity, which denotes changes in polymer material properties with increasing temperature. Earlier results on PEC-related PEL multilayer (PEM) saloplasticity (denoted therein as "salt softening") were reported by Fery and coworkers [82], who studied the effect of salt concentration on the mechanical elasticity and compressibility of hollow PEM capsules.

4 Shaping of PEC Particles

Shaping aspects of PEC particles, especially on the nanolevel, is a relatively new field, although early interesting experimental work addressing other aspects has been carried out. For example, the groups of Gelman [83] and Shinoda [84] performed early experiments on a molecular level, focusing on what one would nowadays call the template effects of the semiflexible host PEL molecules on the conformation of the oppositely charged guest PEL molecules (see Sect. 4.2.2). These authors used combinations of charged homopolypeptides and oppositely charged polysaccharides in low concentration ranges, but to our knowledge did not observe or study colloidal aspects such as phase separation and nanoparticle formation. Hence, neither particle size nor shape aspects were addressed. However, due to the potential applications, these early original experiments together with more recent results (including colloidal aspects) will be discussed further.

4.1 Spherical PEC Particles

PEC particles with a spherical shape are the most prominent and the possibility to influence their overall particle size has been extensively described in Sect. 3. Additional internal shaping aspects within spherical PECs can be seen in the ratio between the more flexible hydrophilic nonstoichiometric shell and the more compact hydrophobic stoichiometric core part of PEC particles, according to a widely claimed PEC model [85]. Such internal shaping presumably could also be influenced by structural and media parameters. However, analytical access to the internal structure of water-rich and therefore emulsion-like rather than suspension-like PEC particles is limited with the present analytical techniques. More information can be obtained on the overall external shape of PEC particles.

4.2 Rod-like PECs

4.2.1 PECs of Synthetic Polyelectrolytes

In contrast to spherical PECs, studies on rod-like PECs are less known and to date there are few reports on the influence of the PEL conformation (globular, flexible, or stiff) on the shape (spheres, rods, disks) of the final PEC particles, which could be used for structuring or scaffolding purposes on the nano- or microlevel of e.g. biomaterials. An initial nice example on templating elongated nanoscopic structures of PEC by inherently stiff PEL was given by Rabe and coworkers [86]. Complexes between stiff dendronized poly(styrene) bearing protonated peripherical amine groups (PG4) and DNA are reported. In Fig. 21, high resolution SFM images of PG4/DNA complexes deposited onto mica are shown.

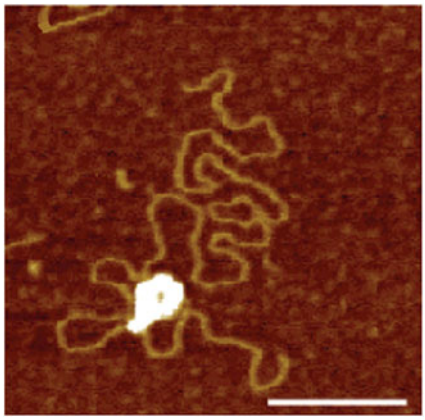

Fig. 21 High-resolution SFM image of DNA/PG4 complexes of charge ratio 1:0.7 precipitated onto poly-L-ornithine-coated mica. The *scale bars* represent 250 nm. (From [86] with kind permission of ACS)

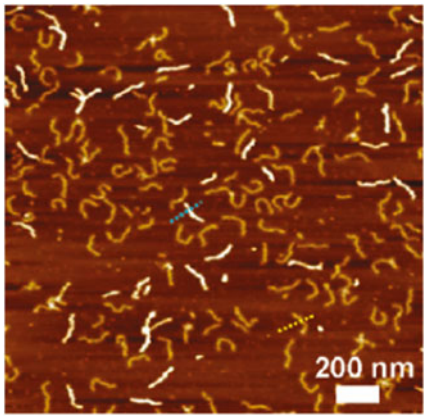

Fig. 22 AFM height image (z range: 10 nm) of spin-coated IPECs of CPB/PSS (13,000 kDa) ($c_{PEC} = 0.02$ mg/mL, $n^-/n^+ = 0.1$) on mica. (From [87] with kind permission of ACS)

Stiff chain structures are visible. At even higher resolution, evidence was found that the DNA wraps periodically around the dendronized polymer core of PG4, so that a defined regular pitch of 2 nm could be determined.

Recently, Ballauff and coworkers [87] reported complexes consisting of cationic cylindrical PEL brushes (CPB) and anionic PSS. The CPB consisted of a long polyvinyl-based backbone (1,500 repeating units) to which poly[2-(methacryloyloxy) ethyl]tri-methylammonium iodide (PMETAI) with 84 repeating units were grafted. An AFM image of spin-coated dilute solutions of complexes of CPB and a short chain PSS (13 kDa) is shown in Fig. 22 for a low ratio $n^-/n^+ = 0.1$. Wormlike structures were obtained, which changed to pearl-necklace and finally to spherical structures ($n^-/n^+ = 1.0$) upon increasing the n^-/n^+ ratio. Using long chain PSS (22,000 kDa), only a transition from worm-like extended to spherical structures was observed.

Moreover, Maskos and coworkers [88] reported topologically controlled interpolyelectrolyte complexes involving high- and low-charged cationic cylindrical CPB based on PEI macromonomers (PMMPEI) and anionic PSS

macromonomer (PMMPSS) precomplexed with dodecyltrimethylammonium bromide (C_{12}) in DMF. Applying SLS, DLS, and AFM, elongated shapes were observed only for the PEC of the low-charged PMMPEI and PMMPSS-C_{12}, whereas the PEC consisting of highly charged PMMPEI resulted in spherical particle shapes. The authors claim that the first type (low charge) corresponds to thermodynamically controlled PEC particle structures allowing topological control, while the second type (high charge) corresponds to kinetically controlled structures with no topological control. No dependence on the order of addition was only observed for the first type, which supports the assumed equilibrium state of this PEC type.

In the line of these studies, we investigated rod-like PEC particles using stiff cationic α-helical PLL as the templating PEL component to be complexed by a flexible polyanion [16]. On the one hand, the α-helix of PLL might be induced by media parameters like pH or certain salt ions, as used for the fabrication of anisotropic related PEM. On the other hand, early work by Shinoda et al. [89] based on circular dichroism (CD) spectroscopy reported induction of the α-helical conformation of PLL by certain polyanions. PAC was used, which was claimed to form a stoichiometric left-handed superhelix around the right-handed α-helix of PLL. However, this polyanion/PLL templating effect on the intermacromolecular order was not studied further on the supramolecular, nanoscopic, or even colloid level.

4.2.2 Biorelated PEC of Charged Homopolypeptides

Influence of the Complexing PEL

We started this area of research with systems based predominantly on PLL and copolyanions of maleic acid (PMA-X) and olefins (X) [17]. Using CD spectroscopy, we could show that the copolyanion of maleic acid with α-methylstyrene (PMA-MS) induced the random coil conformation, whereas the same copolyanion with propylene (PMA-P) resulted in the α-helical conformation, respectively [17] (see Fig. 23).

In both cases, the PLL and copolyanion solutions were kept at pH = 6, at which it is known that PLL adopts exclusively the random coil conformation. Hence, the induction of the α-helical conformation by PMA-P, which does not occur for PMA-MS, is assumed to be a macromolecular templating effect. As an explanation, we suggest that preaggregated globular structures of PMA-MS in accordance with Garnier et al. [90] prevent α-helix formation of PLL within PLL/PMA-MS complex particles. The unaggregated and more extended structures of PMA-P in solution before complexation with PLL are assumed to favor the α-helical conformation of PLL within PLL/PMA-P complex particles. The influence of other complexing polyanions on the PLL conformation were also studied at pH = 6/6 (PLL/polyanion) [19]. Analogously to PMA-P and PMA-MS, polyanionic α-helix formers and α-helix breakers could be identified. This macromolecular templating effect also showed

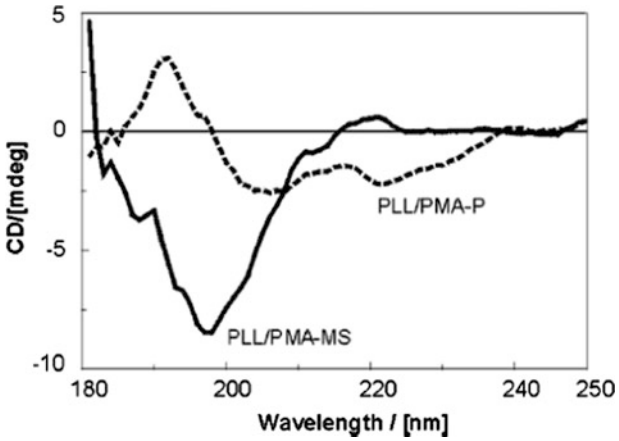

Fig. 23 CD spectra of dispersions of the PECs PLL/PMA-MS (*solid line*) and PLL/PMA-P (*dashed line*) in the range between 180 and 250 nm. (From [17] with kind permission of ACS)

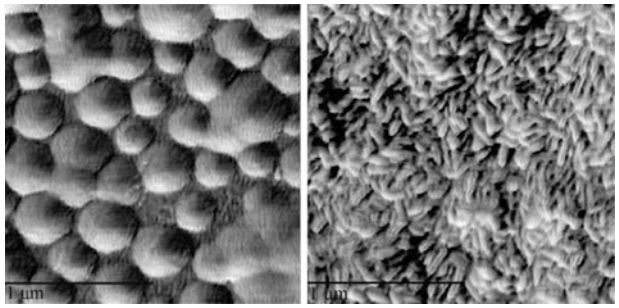

Fig. 24 SFM images of solution-cast nanoparticles of the PECs PLL/PMA-MS and PEC PLL/PMA-P at Si supports ($c_{PEL} = 0.002$ mol/L, $n^-/n^+ = 0.6$). (From [17] with kind permission of ACS)

morphological consequences on the nanoscopic or colloidal level, which are shown in Fig. 24. PLL/PMA-MS revealed half-spherical singularized particles with diameters of around 300 nm, whereas PLL/PMA-P featured needle-like particles.

The specific intermolecular interaction of polyanions with PLL has been a challenging topic. To our knowledge, the groups of Gelman [83, 91], Shinoda [84, 89], and Stone [92] initiated studies based on CD spectroscopy on the induction of PLL conformations by synthetic and biorelated polyanions. Factors like the conformation and configuration (even tacticity) as well as the number, type, and position of anionic groups (especially those in anionic polysaccharides) were shown to have a decisive influence on the conformation of PLL in the PLL/polyanion complex. Later Bystricky and coworkers [93, 94] contributed to this topic with CD measurements on stoichiometric pectate and ALG complexes with PLL or poly(D-lysine) (PDL). They emphasized the influence of the stereochemistry and thus the spatial arrangement of charges of a pectate rich in α-D-galacturonan

and of an alginate rich in α-L-guluronate units. These authors concluded that the conformation of this ALG form is too stiff (twofold helix) and can interact neither with PLL nor with PDL effectively due to a lack of charge matching. Whereas this pectate form exhibits more conformational freedom, both twofold and threefold helices are possible and thus it allows better charge matching. However, this was only found for pectate/PLL and not for pectate/PDL. Therefore, the handedness of the polysaccharide was claimed to also have an influence and the authors finally concluded that PLL shows both α-helical induction and complexation with right handed anionic polysaccharides, whereas PDL shows α-helical induction and complexation with left-handed polysaccharides.

Such model interaction studies will find a certain "renaissance" in the framework of the interaction between anionic polysaccharides constituting the extracellular matrix (ECM) and proteinogenic growth factors (cytokines), which is highly relevant for research on angiogenesis (vascularization) and tissue engineering. Recently, Petitou and coworkers [95] reported molecular modeling work on the specific interaction between heparan sulfate and cellular growth factors, emphasizing the plasticity of their interaction at a molecular scale. Also related to this topic is a report by Pisabarro and coworkers [96], who used fluorescence and computational methods to study the interaction between interleukin-8 (IL-8) and glycosaminoglycans of the ECM and their derivatives with defined sulfation degrees. They found that the sulfation pattern determines the binding strength, so that generally increasing the sulfation degree resulted in enhanced binding. Furthermore, in the case of equal sulfation degree, the sulfate substitution position is also important. The analysis revealed a tetrasaccharide as the minimum glycosaminoglycan unit necessary to obtain specific binding to IL-8.

Influence of pH

It is well known that uncomplexed PLL at pH = 10 is nearly uncharged ($pK_a \approx 10$) and adopts the α-helical conformation [97] without any polyanion complexation. Hence, PEC particles of PLL and sodium polymethacrylate (PMAC) were prepared at pH = 6/6 (PLL/PAC) and at pH = 10/10 to study the influence of pH on the conformation of PLL in the complexed state. It was found that even for complexes of PLL with α-helix-breaking polyanions, the PLL conformation was always α-helical when the complex was formed at pH = 10/10. In Fig. 25, typical CD spectra for PEC particles consisting of PLL and PMAC formed at pH = 6/6 and at pH = 10/10 are shown [98].

The typical negative peak at around 195 nm of the randomly coiled/extended chain was observed for pH = 6/6 (PLL/PMAC), whereas the diagnostic doublet at 208 and 225 nm of the α-helix was observed for pH = 10/10. Obviously, at pH = 10/10 the PLL in PLL/PMAC complex particles shows the α-helical conformation. Two arguments can be raised: first, PLL at pH = 10 adopts an α-helical conformation, which does not change upon complexation with PMAC; and second, PMAC at pH = 10 is fully ionized and is expected to adopt an extended

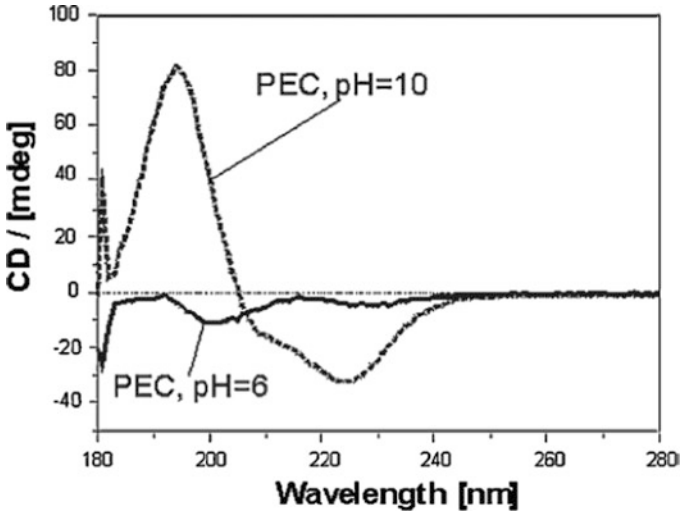

Fig. 25 CD spectra of PEC-1.5 particles containing PLL/PMAC mixed from 0.002 M solutions at pH = 6/6 (*solid line*) and pH = 10/10 (*dashed line*). (From [98] with kind permission of Wiley-VCH)

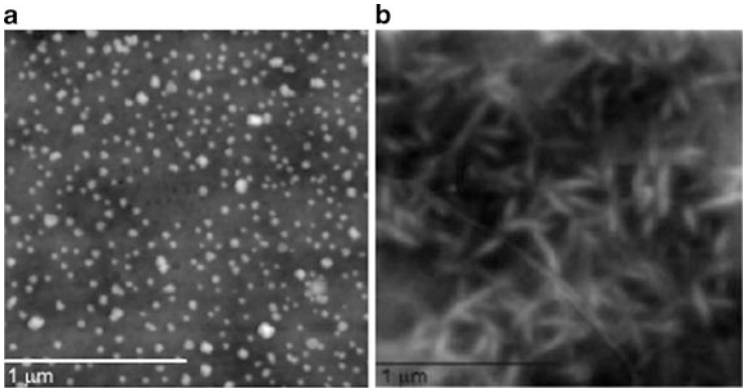

Fig. 26 AFM images (2 × 2 µm) of (**a**) PEC-1.5 of PLL/PMAC (pH = 6), and (**b**) PEC-1.5 of PLL/PMAC (pH = 10) at Si supports. (From [98] with kind permission of Wiley-VCH)

conformation. This extended conformation in addition to the pH effect is thought to act as a macromolecular template for both the α-helical conformation of complexed PLL and the final elongated needle-like particle shape, which could be seen as an analogous result to the PLL/PMA-P complexes described above. By contrast, at pH = 6/6, the PLL in PLL/PMAC complexes adopts the random coil conformation as is evident from Fig. 26. At this pH setting, uncomplexed PLL is known to adopt a random coil conformation [97] and PMAC is expected to be in a less charged and thus more coiled conformation. Therefore, the observed random coil conformation

of complexed PLL should prevent an elongated particle shape and result in a final spherical particle shape at pH = 6/6, which is analogous to the behavior of the PLL/PMA-MS complexes described above.

PDADMAC/PLG: Influence of Salt Type

Analogous experiments to those on PECs of PLL/polyanion were performed on PECs of poly(L-glutamic acid) (PLG)/polycation. Similar to PLL, the conformation of PLG can be switched by both pH and salt type [98]. It is known that uncomplexed PLG at pH < 4 adopts the α-helical conformation, whereas at pH > 7 it adopts the random coil conformation. Moreover, PLG conformation in PLG/PDADMAC complexes can also be influenced by divalent cations like Mg^{2+} and Cu^{2+} at neutral pH, such that Mg^{2+} caused the random coil and the Cu^{2+} the α-helical conformation, as demonstrated by CD spectroscopy. Up to now, we could not find elongated PEC particle shapes for PLG/polycation. This result is in line with Zhengzhan et al. [99], who also found only spherical shapes for PLG/CHT complexes, as shown by TEM.

Analogy to PEM Films

Analogously to these PEC particle systems, PEC-derived PEM film systems were generated by consecutively adsorbing from solutions of oppositely charged similar or equal PELs using the layer-by-layer concept [100]. The obtained PEM structures were compared to the PEC structures in a recent conceptual report [98]. It was shown that polypeptides can controllably template PEC/PEM nanostructures via their secondary structure (stiffness) and molecular weight. Polypeptide conformation can be controlled by certain oppositely charged non-peptidic PELs, pH value, or salt type. The α-helical conformation of high molecular weight PLL induced needle-like PEC particles shapes or oriented quasi-nematic PEM film morphologies, whereas the random coiled conformation of PLL induced spherical PEC particles or granular PEM film morphologies (see Fig. 27). Low molecular weight PLL and PLG did not induce anisotropic PEC particle shapes or PEM film morphologies. Anisotropic PEL/polypeptide complex structures are forecast to be suitable substrates or templates for unidirectional cell growth, polymer/cell scaffolds, and non-spherical nanocarriers.

4.2.3 Simulation Work on Rod-Like PEC Particles

Such templating effects of stiff PEL onto the complex with the oppositely charged PEL have been theoretically treated by Narambuena and coworkers [101] using Monte Carlo simulation studies. A coarse grain model was applied to analyze the structure and morphology of complexes formed between fully flexible polycations and polyanions with varied chain stiffness. Different morphologies such as globules, toroids, and rods were obtained depending on the chain stiffness. Longer

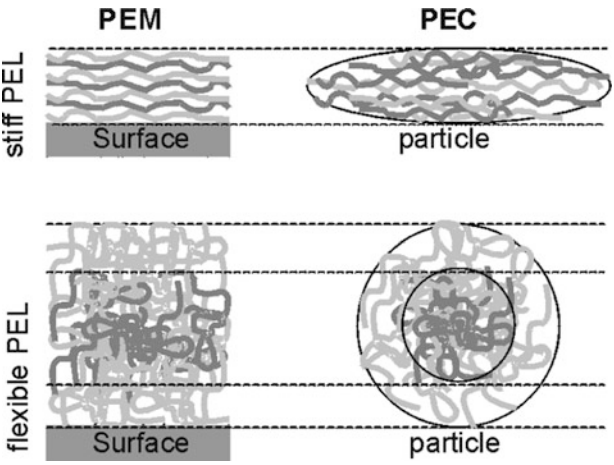

Fig. 27 Concept of templating PEC particle shape or PEM film morphology using flexible (randomly coiled) or stiff (α-helical) PELs (charged polypeptides). (From [98] with kind permission of Wiley-VCH)

chains yielded toroids more frequently than rods, as compared with shorter chains, but the size of toroids did not depend entirely on the chain length. The authors concluded that the final structure of the toroids was highly dependent on the intrinsic chain rigidity rather than on the electrostatic contributions.

Also in this line, Kunze and Netz [102] treated complexation between a stiff charged cylinder and an oppositely charged semiflexible PEL using linear Debye–Hückel theory, which is valid for weak electrostatic interactions mediated by high salt concentration or weakly charged PEL. The phase diagram in dependence of salt concentration featured helical wrapping morphologies of the PEL around the oppositely charged cylinder for lower PEL stiffness. Whereas higher stiffness of the wrapping PEL resulted in straight wrapping morphologies, i.e., PEL are adsorbed onto the cylinder and unidirectionally oriented with respect to the cylinder axis. Moreover, the wrapping/binding process is thought to be associated with counterion release effects.

4.3 Toroid PEC

As mentioned in the preceding section, PEC particles may also tend to adopt toroid shapes. Interesting work in this sense was reported by Maurstadt and coworkers [103]. They investigated morphologies of PEC particles (cast from very diluted dispersions) consisting of CHT and the semiflexible biopolyanions ALG, acetan (ACN), circular plasmid DNA, and xanthan (XAN), using AFM and quantitative image analysis to classify various morphologies due to form factors. For persistence

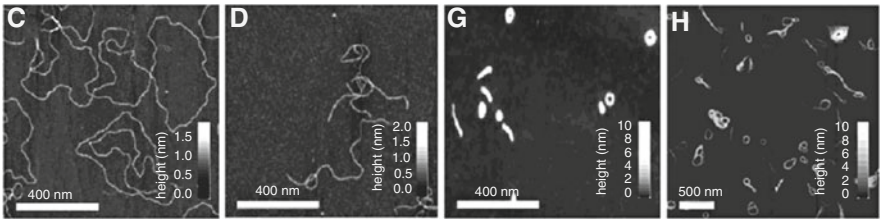

Fig. 28 Tapping mode AFM images (topography) of DNA pBR332 (*C*), xanthan (*D*), and the corresponding PEL complexes with CHT (*G*, *H*). CHT with a degree of acetylation of 0.1 and $M_W = 33$ kDa was used to obtain the complexes shown in topograph *H*, while CHT with a degree of acetylation of 0.15 and $M_W = 196$ kDa was used for the complexes shown in topograph *G*. Experimental conditions were as follows: DNA/CHT complex at 150 mM, pH 7.4, and $c_{DNA} = 4$ μg/mL; XAN/CHT complex at 5 mM, pH 5.5 and $c_{XAN} = 2.5$ μg/mL. (From [103] with kind permission of ACS)

lengths $L_P \leq 25$ nm (ACN), only small amounts of torus morphology were reached, whereas for DNA ($L_P = 50$ nm) and XAN ($L_P = 120$ nm) a substantial fraction of toroid morphology was found (see Fig. 28).

In Fig. 28, the uncomplexed polyanions (DNA and XAN) are shown on the left (C, D) and the CHT complexed polyanions on the right (G, H). Although rod-like PECs were additionally observed within CHT/DNA complexes, none were found for high M_W CHT/XAN ($M_W = 5{,}000$ kDa). Low M_W CHT/XAN ($M_W = 400$ kDa) revealed smaller fractions of toroids. An average height of 2 nm for CHT/XAN toroids and of 5 nm for CHT/DNA was found. Additionally, metastable states featuring interconnected loops (racquets) were found for CHT/XAN, which could be supported by simulations [104]. The authors concluded that toroid PEC formation was not affected by specific interactions but by electrostatics and chain stiffness.

5 Pharmaceutical Applications of PEC Nanoparticles

As described in the previous sections, PEC particles represent liquid–liquid phase-separated, soft core–shell-like and hydrogel-like nanoparticles, whose size, internal structure, and shape can be influenced or even controlled by media or molecular structure parameters. Like others, our group uses PEL complexation for the entrapment, delivery, and local and retarded release of drugs because it is a simple and versatile technique, is based on aqueous media, uses mild conditions, and allows the involvement of biorelated components, which might enhance biocompatibility. This section is organized as follows: First, some general aspects on drug delivery from nanoparticles are given (Sect. 5.1). We restrict the discussion to low molecular weight drugs and neglect or only mention the huge body of work on nanoparticular protein or polynucleotide carriers. Second, pharmaceutical applications of PEC

systems are outlined, among which PEC hydrogels, PEM films, and PEC nanoparticles are treated (Sect. 5.2).

5.1 General Aspects on Drug Delivery from Nanoparticles

Before reviewing the pharmacodynamic aspects of drug delivery by PEC particles, some general aspects on the particle–cell or particle–biofluid interactions will be addressed. There are numerous reviews on drug-loaded nanoparticle systems in general and on factors that influence their delivery modalities and performance. The review of Duncan and Gaspar [105] presents the current state on systems, classes, scientific research areas, players and opponents, definitions, and terminology in the field of nanomedicine, whose individual notations and citations would burst the extent of this chapter. Their review describes a topological and size classification that includes liposomes (80–200 nm), (gold) nanoparticles (5–50 nm), nanocapsules (20–1,000 nm), DNA/drug complexes, polymer/drug conjugates and therapeutics (5–25 nm), polymer/protein conjugates, antibody/drug conjugates, albumin/drug conjugates, nanosized drug crystals (100–1,000 nm), and block copolymer micelles (50–200 nm). On the one hand, it is widely accepted that drug/nanoparticle formulations offer advantages over pure drug formulations, e.g., prolonged drug circulation time (in blood), biodistribution, specific and selective local targeting (modification with antibodies, folate), controlled cell uptake (endocytosis), resistance to phagocytosis, passage through tissue interstices, controlled pharmacodynamics (improved drug availability/release), and chemical and physical drug protection. On the other hand, drug/nanoparticles can have disadvantages with respect to toxicology, especially when they are administered systemically in direct contact with blood. Warning examples in this respect are poly(L-lactic acid) (PLLA) or poly(lactide-glycolide) (PLGA) nanoparticle formulations using toxic solvents like methylene chloride [5], or nanoparticular poly(alkylcyanoacrylate) systems bearing toxic degradation products [106].

Recently, the influence of size, shape, and surface chemistry of nanoparticle systems on drug delivery performance and modalities like blood circulation time, biodistribution, pharmacokinetics, toxicology, targeting ability, and internalization have been comprehensively reviewed and outlined by Petros and DeSimone [107]. Nanoparticle uptake by, e.g., internalization in the target cells, is still treated as the key factor in this and other earlier articles. Important properties and requirements in this respect were identified and can be summarized by the following four points:

1. Rigid spherical particles of 100–200 nm diameter have the highest potential for prolonged blood circulation time, biodistribution, and cellular uptake by endocytosis because they are large enough to avoid uptake in the liver, but small enough to avoid filtration in the spleen and removal by phagocytes, blockage of blood capillaries, and inflammatory tissue responses [108, 109]. This may also hold in principle for nonspherical particles by engineering deformability into

particles >300 nm or by keeping at least one dimension of the particle on a length scale of >100 nm to prevent accumulation in the liver and maintaining at least two dimensions at <200 nm to allow the particles to navigate the sinusoids of the spleen. Also, a low polydispersity index has been discussed as a requirement for cellular uptake [110, 111].

2. Nanoparticle geometry (shape) plays a key role in particle internalization, but optimum parameters for engineered nanoparticles have yet to be determined [112]. Spherical morphology and a low polydispersity index are generally claimed to be advantageous for cellular uptake. To name only one example, spherical and nonspherical polystyrene microparticles were incubated with macrophages (phagocytosis) by Champion and Mitragotri [113]. These authors demonstrated that spherical particles were readily internalized due to their symmetry, whereas elliptical disk-shaped particles were only internalized when their first contact was along the major and not the minor axis.
3. Surface chemistry has three vital roles in the function of engineered nanoparticles, i.e., control of opsonization, which ultimately dictates the reticulo-endothelial-system (RES) response; cellular targeting; and organellae targeting via ligands known to bind cell or organellae surface receptors [112]. Favorable in that respect are nanoparticles bearing a surface charge magnitude larger than 30 mV (+/−) [114, 115]. Furthermore, Harada and Kataoka point out that particles bearing a hydrophilic corona are advantageous for prolonged circulation time, low uptake by RES, low nonspecific protein adsorption, and solubilization of hydrophobic drugs in the micellar core [116].
4. In the line of Petros and DeSimone [107], it has to be emphasized that the "*tailored release of therapeutics still represents a key barrier in the field of engineered nanoparticles*," which in our understanding of DDS is a very important remark. We see (without criticism) a certain preference in the nanomedicine and drug/nanoparticle literature for phenomena like tailored drug uptake, toxicology, and cell interaction, whereas tailored drug release related to molecular understanding of pharmacodynamics is of minor interest ("drug release will take place anyway"). In that framework, predominant strategies so far incorporate materials that are enzymatically degradable, pH-sensitive or reductively labile, which facilitate breaking or destabilizing bonds between drug and carrier on reaching the intended site of action. Further efforts should be directed to molecular structures and mechanisms allowing tailored release (not only uptake) kinetics of one or multiple drugs according to the specific requirements of clinicians.

5.2 Drug Delivery from PEC Systems

Interestingly, PEC nanoparticles do not fall directly into one of the nanomedicine classes denoted or defined in classical review papers like that of Duncan and Gaspar [105], although their controllable sizes (20–500 nm), shapes (spheres, rods), and surface chemistries match well those of nanomedicine. However, although size,

shape, and surface chemistries are also expected to influence the drug delivery performance of PEC nanoparticles, detailed reports on these influencing factors are rare. More reports are available on drug delivery systems based on other non-nanoparticle PEC systems like hydrogels or layered films (PEM), from which nanoparticle PEC systems can also be prepared or from which interesting analogies can be drawn, as in a recent article by Ball and coworkers [117]. Therefore, we think it useful to review some reports on nanoparticle and non-nanoparticle macroscopic PEC systems (see Sect. 5.2.1) before we discuss drug-loaded PEC particles (see Sect. 5.2.2).

5.2.1 Drug-Loaded Macroscopic PEC Systems

In the past, concepts have been developed on loading not only of nanoscopic PEC particles but also of macroscopic PEC systems like microcapsules, hydrogels, or membranes with drugs aiming at a local or systemic release of the drug in the human body or in vitro systems. For such purposes, PEC material is prepared from biorelated PELs like polysaccharides, polypeptides or polynucleotides, for which a biocompatibility exceeding that of synthetic PEL might be expected. Examples of reports on the ability of PEC systems to load and release drugs in a retarded manner are numerous.

Early studies on drug release from non-particular PEC systems have been reported by Siegel et al. [118]. The model drug caffeine was incorporated and released from a PEC hydrogel consisting of anionic poly(methylmethacrylate) and cationic poly(dimethylaminoethylmethacrylate) crosslinked by divinylbenzene. Caffeine was released at rates varying sharply with pH. At pH = 7.3 no caffeine was released, whereas at pH = 5 (moderate) and pH = 3 (highest) caffeine was released with near-zero-order kinetics. Furthermore, the release of caffeine was found to be associated with water uptake at pH = 3 and pH = 5, and based on this finding the authors claimed evidence for a moving front mechanism for sorption and release. Also, Shiraishi et al. [112] reported release of indomethacin from PEC hydrogel beads consisting of CHT and tripolyphosphate (TPP), focusing on molecular weight effects of CHT in the range of 7,600–83,000 g/mol. The authors found decreasing release rates with increasing CHT molecular weight in both in vitro and in vivo systems and found that a medium molecular weight of 25,000 g/mol was best suited for their application. The authors claimed that decreasing porosity and increasing tortuosity of the PEC matrix with increasing molecular weight were crucial molecular properties. They stated that low molecular weight CHT was able to complex with TPP to form loose and easy hydratable structures, so that hydrophobic indomethacin can be better dissolved. By contrast, PEC of high molecular weight CHT and TPP had a rather compact structure with smaller porosity and worse accessibility for water. Further reports on this issue are those of Akbuga and coworkers [119, 120], who loaded CHT/polyphosphate beads with piroxicam and calcitonin.

For the description of kinetic drug release data from hydrogel-like materials, the Ritger–Peppas equation [121] is frequently used according to $C_{\mathrm{DRUG}}(t) = at^{\mathrm{b}}$,

where $C_{DRUG}(t)$ is the actual concentration of a drug at a given time t, a is an empirical prefactor, and b the exponent diagnostic for the release type. This model accounts for porous structure in a releasing (hydrogel) matrix. If the pores are large in comparison to the drug size, drug release is dominated by free diffusion and the exponent b should be close to 0.5. If the pores are small with respect to the drug size, drug release is hindered and b should be closer to 1, defining zero-order kinetics. In a more recent report of de la Torre et al. [122], such an analysis is described. These authors loaded PEC gels of CHT/PAC with either the charged or the uncharged form of the antibiotic amoxicillin (trihydrate versus sodium salt). The release of the charged form was slower than that of the neutral form due to ionic binding.

5.2.2 Drug-Loaded PEC Particles

The literature on PEC/drug particles is overwhelming and PEC/protein (e.g., growth factors) and PEC/polynucleotide (e.g., small interfering RNA (siRNA)) systems dominate over systems of PEC loaded by low molecular weight drugs. Generally, we will focus on nanoscopic PEC particles loaded by low molecular weight drugs (Sect. 5.2.2) rather than proteins or polynucleotides and will discuss factors like size, shape, internal core, and surface shell structure. However, a few comments on PEC/protein and PEC/polynucleotide carriers will be given.

PEC/Protein Carriers

The first results on protein entrapment came from Calvo et al. [123], who demonstrated the loading and controlled release of several proteins for complexes of CHT and copolymers of ethylene oxide and propylene oxide (Pluronics). In these classical studies, PECs were generally introduced as therapeutic delivery vehicles. Loading of the model proteins human serum albumin (HSA), myoglobin (MYO), and lysozyme (LYZ) has also been shown by Ouyang and Müller [124]. These proteins were bound to PEC particles of PDADMAC/PSS and PDADMAC/PMA-MS under mild electrostatically repulsive conditions. However, protein release was not studied. Furthermore, Tyaboonchai et al. investigated insulin loading and release from PEC nanoparticles (ca. 250 nm) of PEI and DS [125]. Entrapment efficiencies ($EE = m_0 - m_R/m_0 \times 100\%$, where m_0 and m_R are total and released drug mass, respectively) of up to 90% were found. However, rather rapid release kinetics of insulin in phosphate buffer were found, featuring saturation even after some minutes. A successful encapsulation of vascular endothelial growth factor (VEGF), relevant for tissue engineering applications, within PEC particles of DS and various polycations was shown by Berkland and coworkers [126]. Thereby, the known high affinity of VEGF for heparin was also valid for DS. Encapsulation efficiencies between 50–85% and a retarded release of up to several days were found.

PEC/Polynucleotide Carriers

In the early work of Kabanov et al., PEC particles of DNA and poly(*N*-ethyl-4-vinylpyridinium) were shown to effectively transfect mammalian cells, especially when administered with poly(ethylene oxide)-*block*-poly(propylene oxide)-*block*-poly(ethylene oxide) copolymer (Pluronic P85) [127]. Later nanoparticular systems of crosslinked nanogels of PEI and poly(ethylene oxide) (PEO) were developed for the delivery of oligonucleotides by these authors [128]. Also, Kataoka et al. contributed to PEC-mediated delivery of antisense oligonucleotides complexed with a copolymer of ethylene glycol and lysine (PEG-*co*-Lys) under physiological conditions [129]. Note that in these systems the drug (oligo/polynucleotide) is also one of the complexing components. The triggerable release of nucleic acids was recently reviewed by Soliman et al. [130], who discussed temperature, redox potential, and light triggers in PEC systems.

Small Drug-Loaded PEC Particles

Numerous reports are available on binary drug/PEL complex (nano)particles, where a charged drug is complexed by an oppositely charged PEL. For example, Kim and Nujoma complexed cationic oxprenolol with a copolymer of methylmethacrylate and sodium methacrylate (PMMA/MANa), forming gel beads from which the drug was released in a retarded manner in dependence of pH by a combined swelling/erosion mechanism [131]. More recently, Jimenez-Kairuz et al. [132] reported high loading of swellable complexes of model drugs (atenolol, lidocain hydrochloride) and anionic carbomers and their release. Very recently, Cheow and Hadinoto [133] reported nanoparticular ciprofloxacin/DS complexes (200–400 nm, 80% drug loading), which showed a dissolution rate twice that of the poorly soluble free drug crystals.

However, exclusively ternary PEC nanoparticles consisting of complexed polycation and polyanion and loaded by low molecular weight organic drug compounds (PC/PA/drug) with a size range of 10–500 nm shall be reviewed herein.

One of the first reports on the usage of ternary drug/PEC nanoparticles for small pharmaceutical drug delivery applications was from Tiyaboonchai et al. [134]. The authors described how the fungicide drug amphotericin B (AMB) can be uploaded and released from PEC coacervate particles consisting of PEI and DS in the presence of zinc sulfate as ionic crosslinker and manitol as redispersing agent. As colloid parameters, PEI/DS particles featured a zeta potential of around 30 mV, spherical particle shape with diameters in the range 100–600 nm (PDI = 0.2), which could be controlled by pH, mixing ratio, and concentration. A fast release of AMB was found, which could be modulated by pH and the presence of surfactant in the release medium (HEPES) (Fig. 29). AMB/PEC particles showed no toxicity against HeLa cells and were able to kill *Candida albicans* (human fungal test strain).

At the same time, Alonso and coworkers [135] reported doxorubicin (DOX)-loaded PEC particles of CHT and DS. DOX loadings of up to 4% could be achieved

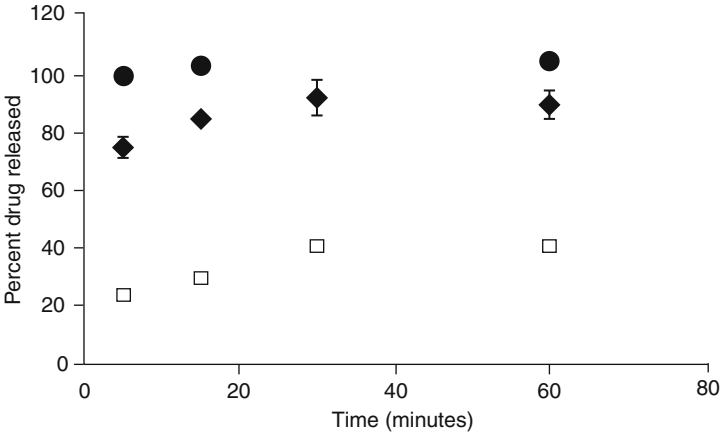

Fig. 29 In vitro release of AmB-loaded PEI/DS nanoparticles: *circles* pH = 8, SDS in HEPES buffer; *diamonds* pH = 8, Tween 80 in HEPES buffer; and *squares* pH = 7.4, in HEPES buffer without surfactant. (From [134] with kind permission of Wiley-VCH)

and an initial rapid release followed by a slow release phase was obtained. DOX-loaded CHT/DS nanoparticles maintained cytostatic activity relative to free DOX, whereas DOX/CHT complexes showed reduced activity. Confocal laser scanning microscopy (CLSM) studies showed that DOX entered the cells while remaining associated to the nanoparticles and was not released before into the medium. Recently, a similar PEC/DOX system was reported for osteosarcoma therapy [136].

The same PEC system but loaded with streptomycin, gentamicin, or tobramycin was recently reported by Popescu and coworkers [137] and tested against mycobacterium tuberculosis in a mouse model. Particle sizes in the nanometer range were obtained, and release studies showed residual drug amounts of $> 60\%$ in the nanoparticle interior at low acidic pH after 6 h. Oral administration of streptomycin-loaded particles reduced bacilli growth by a factor of 10, similarly effective to subcutaneously injected aqueous streptomycin solution at a concentration of 0.1 mg/mL.

Escobar and coworkers reported studies on diltiazem release from CHT/ALG and CHT/carrageenan complex particles and found that CHT/ALG provided a prolonged drug release compared to CHT/carrageenan [138]. They argued that the latter system allowed a higher amount of water to enter the PEC matrix, so that no regular swelling but disintegration takes place, which liberates the drug more quickly.

Also related to small drug-loaded PEC particles are the studies of Bohidar et al. [139] on the entrapment of salbutamol (a bronchodilator) in PEC coacervate particles (> 400 nm) prepared by mixing anionic and cationic gelatin in the presence of the drug. They claim that salbutamol release from the coacervate phase could not be described by known release models because too many factors prevail, e.g., dissolution, permeation of solvent into the matrix, and non-Fickian drug diffusion in a crowded environment.

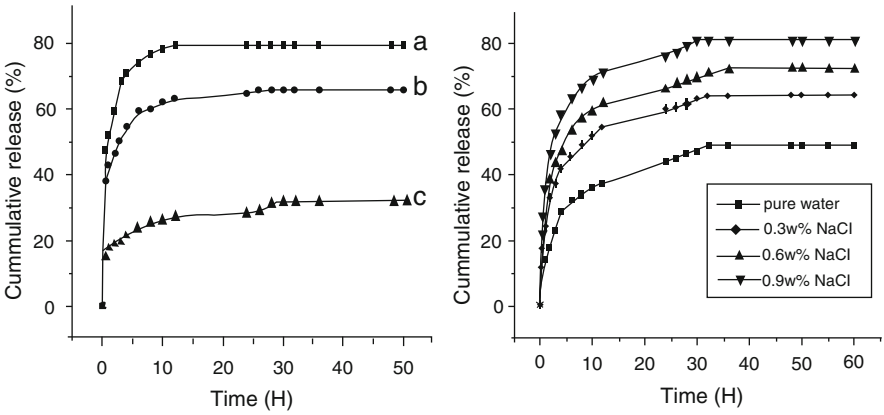

Fig. 30 Release of doxorubicin from PDMAEMA/ALG PEC particles in phosphate-buffered saline solutions. *Left*: Release at pH = 5.8 (*a*), pH = 7.4 (*b*), and pH = 8.0 (*c*). *Right*: Release at 0, 0.3. 0.6, 0.9% NaCl concentration. (From [140] with kind permission of Elsevier)

Recently, various drug/PEC particle systems have been reported using synthetic PEL, with favorable toxicological and biotolerable properties. A combination of synthetic cationic PDMAEMA and alginic acid (ALG) was used to form monodispersed DOX-loaded PEC nanoparticles [140]. The authors found a strong pH influence on the particle size, resulting in diameters of around 850 nm at pH = 5 and 150 nm at pH = 7.2. The internal PEC structure was affected significantly by ionic strength (0–0.9% NaCl), so that part dissolution (decomplexation) and thus formation of channels was claimed. Hence, the cumulative DOX release could be minimized by pH elevation and by decreased ionic strength, which is shown in Fig. 30. The effects of pH on drug release were also investigated in a related system. Lee and coworkers [141] studied the release of guaifenesin from PEC microparticles of CHT and ALG for different pH values used during preparation of the loaded microcapsules. They observed a minimum release rate for pH = 4.8, and the release rate increased for increasing pH values. They argued that at pH around 5 both PEL are highly charged, leading to stiff conformations and almost ideal charge matching. However, at pH = 2.8 or pH = 8.8, either the ALG or the CHT, respectively, has a low charge or is even uncharged, which results in the formation of loops due to a mismatch of charges. Such loops are claimed to make the PEC phase less dense and more porous and thus the guaifenesin could be better released. Additionally, the authors varied the kind of N-acyl groups introduced to the CHT and found a higher release for longer (i.e., bulkier) N-acyl groups, which were claimed to perturbate the PEC structure more effectively. Recently, Coppi and Iannuccelli [142] reported tamoxifen release from the same system and pointed out that the drug loading and release was strongly affected by the mannuronic/guluronic ratio of the alginate component.

A completely different PEC system for the loading and release of hydrophobic drugs like dihydroxyanthraquinone (DHA) was introduced by Wenz and coworkers [143]. They prepared PEC nanoparticles ($D_H > 130$ nm) of anionic starch and

cationically modified cyclodextrins, emphasizing colloidal stability, narrow size distribution of the formed nanoplexes, and satisfactory DHA uptake.

Furthermore, Yuan et al. [144] introduced spherical PEC particles obtained by complexation of the cationic graft copolymer PEI-*graft*-poly(*N*-vinylpyrrolidone) (PEI-*g*-PVP) with anionic block copolymer of PVP-*block*-poly(2-acrylamido-2-methyl-1-propanesulfonic acid) (PVP-*b*-PAMPS); the particle size was around 140 nm. Folic acid was entrapped in the micelle core by electrostatic attraction and the release rate was strongly dependent on the pH of the release medium.

Another complexation technique was reported by Chuang et al. [145], who prepared PEC particles by templating polymerization of acrylic acid in the presence of CHT at various monomolar ratios (0.2/1.1 to 1.0/1.1). Hollow CHT/PAC particles were formed with sizes of around 200 nm, which varied with the pH of the medium, and zeta-potentials of around 25 mV. The release of doxycycline (DOC) incorporated by various feeding processes was found to last for up to 8 days.

Recently, thermosensitive PEC particles were prepared by Guiying et al. [146], who complexed the block copolymer poly(*t*-butyl acrylate-*co*-acrylic acid)-*block*-poly(*N*-isopropylacrylamide) [P(tBA-*co*-AA)-*b*-PNIPAM] with the graft copolymer chitosan-*graft*-poly(*N*-isopropylacrylamide) (CHT-*g*-PNIPAM) and entrapped DOX. Like the complexes between terpolymer systems described by Schacher et al. [65], these PEC particles had a multishell structure with hydrophobic PtBA in the core, anionic PAC and cationic CHT in the middle, and PNIPAM in the outer shell (Fig. 31a). DOX release was suppressed at neutral pH and elevated at low pH due to electrostatic repulsion between cationic DOX and the polycation component or reduced ion pairing between polycation and polyanion, resulting in channels enabling DOX passage (Fig. 31b). At temperatures above the LCST, DOX release was promoted and the authors claim that PEC/PEC aggregation was responsible. Although such thermoinducable drug release by PEC nanoparticles had been initiated by these authors, Lyon and coworkers [63] previously reported the uptake and release of DOX from a related PEM. This PEM consisted of cationic PAH and an anionic copolymer of NIPAAM and acrylic acid. A significant dependence of porosity and thus drug retention/release on both temperature and pH was found.

5.2.3 Adhesive Films of PEC Nanoparticles for Local Drug Administration

In the previous section, release from such drug-loaded PECs was shown for PEC particles in the volume phase and the drug delivery was intended to act systemically, i.e., the whole body should be reached by PEC particles through blood circulation.

Recently, initial work was described by us regarding drug release from an adhesive layer of cast PEC particles [147]. Such interfacial drug-loaded PEC systems are closely related to drug-loaded PEM systems, which were initiated by Chung and Rubner [148] based on dye/PEM. Both approaches, PEM and adhesive PEC, are highly relevant for the generation of locally acting drug-eluting modification layers on biomedical devices such as stents, implants, bone substituting

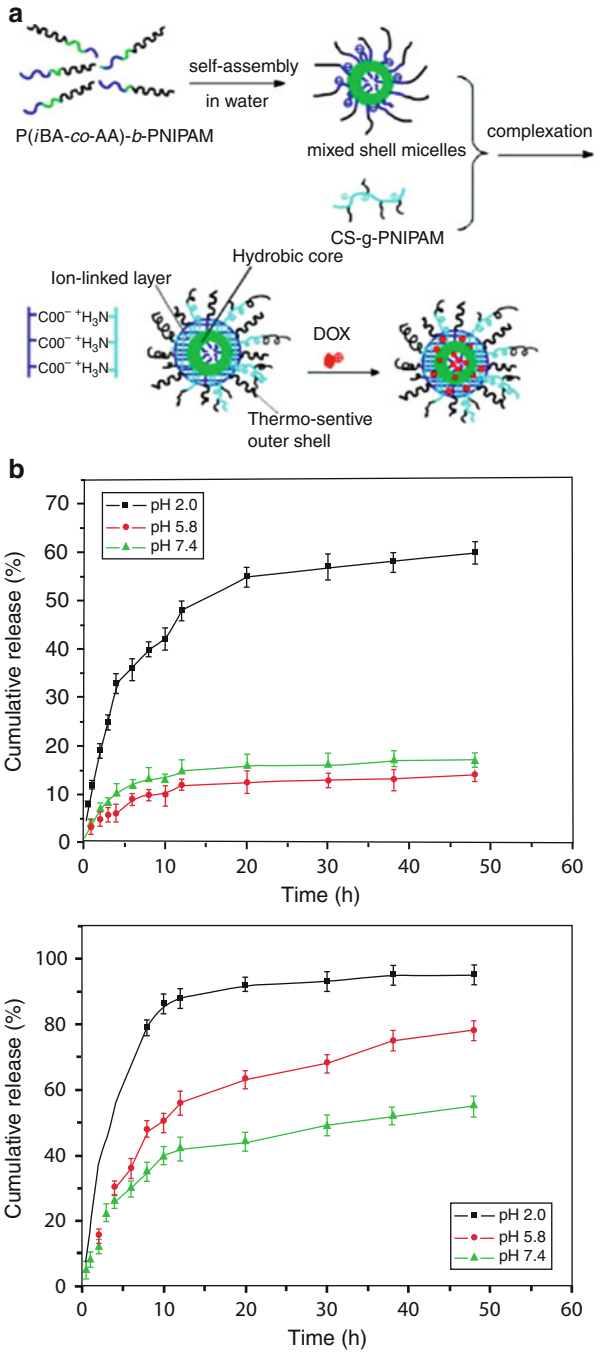

Fig. 31 (**a**) Assembly of thermosensitive PEC particles of chitosan-*g*-PNIPAM/P(tBA-*co*-AA)-*b*-PNIPAM. (**b**) Release of DOX from the PEC particles shown in (**a**) for different pH values at 25°C (*top*) and 40°C (*bottom*). (From [146] with kind permission of Elsevier)

materials (BSM) or tissue engineering scaffolds (TES). Recently, we reported on PEC nanoparticles that were loaded by the bisphosphonate pamidronate (PAM) and deposited as adhesive films onto planar Ge model substrates [149]. Bisphosphonates like PAM are known to inhibit osteoclastic activity via the farnesyl pathway [150], favoring osteoblastic bone formation, and are widely used as therapeutics for systemic bone diseases like osteoporosis [151]. A retarded release of PAM under conservation and adhesive stability of the bare PEC particle film was shown by in situ ATR-FTIR spectroscopy, monitoring the depletion of PAM in the cast PEC film matrix. Up to now, this surface-sensitive method has been widely applied by us to analyze the sorption and conformation processes of PEC layers [152, 153], melanin-like films [154], chiral model drug compounds [155], lipids [156], peptides [157], and proteins [158]. Various factors of PAM release were studied. The influence of PAM/PEC ratio and PEC concentration were of prime interest. A PEC system based on PEI and cellulose sulfate (CS) was used because these compounds are easily available and according to section 3.1.3 and Table 1 especially branched/linear PEL combinations might feature high structural densities enabling better drug entrapment. Although CS is a biorelated PEL and might be expected to be biocompatible, there has been some debate on the biocompatibility of PEI. PEI/DNA complexes in solution to be used as gene vectors are reported to be cytotoxic [159], whereas layers of PEI/heparin complexes are claimed to have positive effects on cell adhesion and viability in dependence of the PEI/heparin composition [160]. Some detailed results on factors influencing PAM release can be found in Fig. 32a, where the relative PAM content with respect to the initial dry state is plotted versus time in contact with the release medium. The

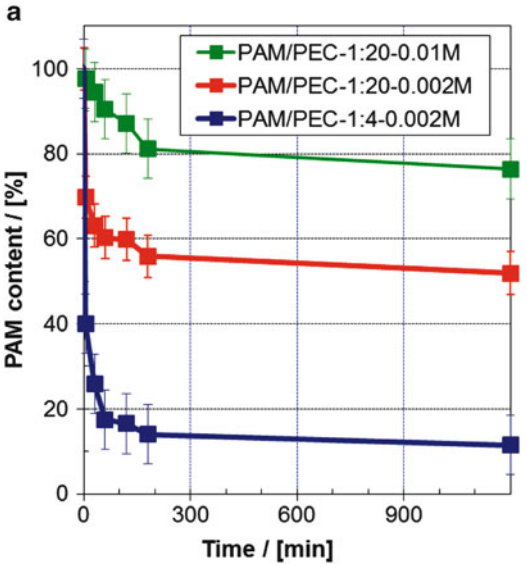

Fig. 32 (continued)

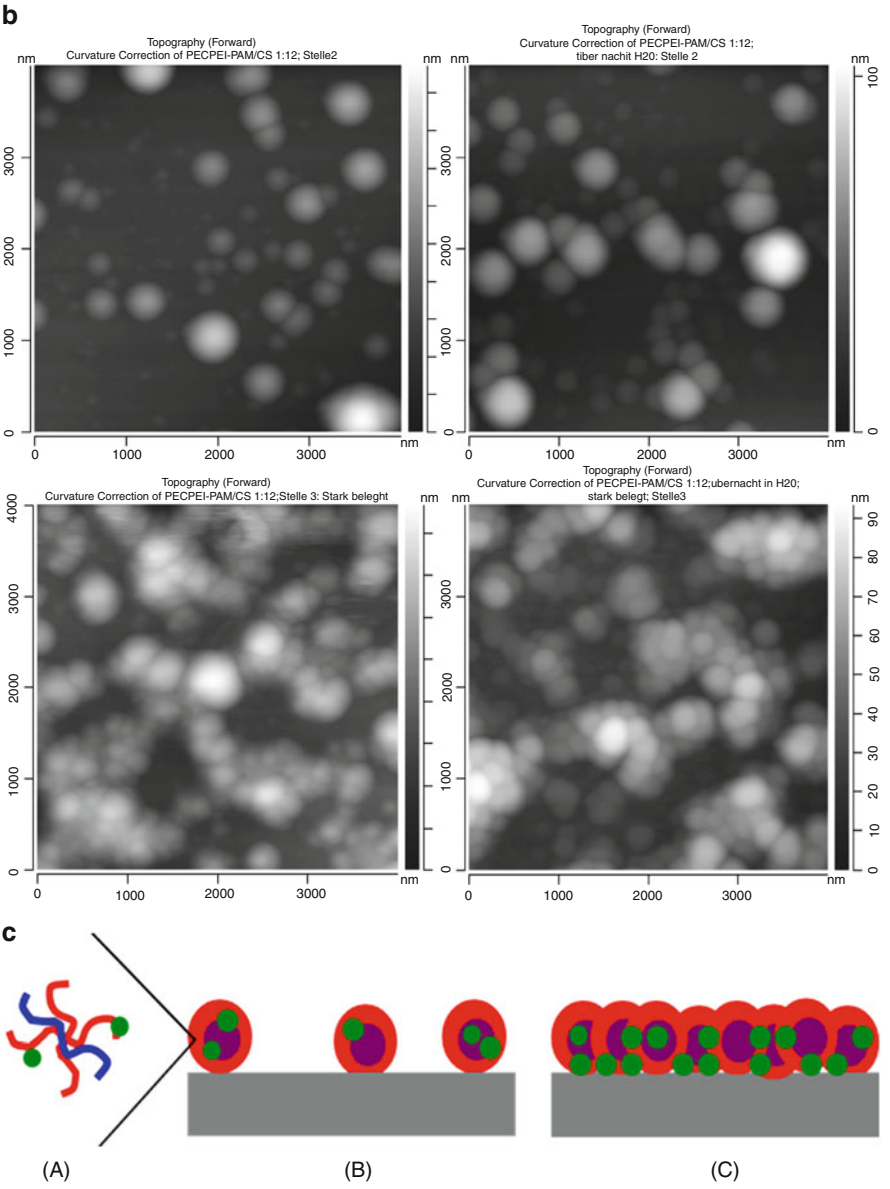

Fig. 32 (**a**) Release profiles of PAM from solution-cast PAM-loaded PEC-0.9 particle films for various samples. From *bottom* to *top*: Single cast PAM/PEC-1:4 (relative PAM/PEC content is 1:4) at 0.01 M; single cast PAM/PEC-1:20 at 0.002 M; and single cast PAM/PEC-1:20 at 0.01 M. (From [149] with kind permission of Elsevier). (**b**) SFM images of a PAM/PEI-1:12 particle film cast from 0.002 M PEC dispersions onto the Ge support before (*left*) and after (24 h in H_2O, pH = 6) (*right*) PAM release. Weakly covered (*top*) and highly (*bottom*) covered regions are shown. (**c**) Proposed model for the binding locations of PAM (*green*) at PEC particles consisting of PEI (*red*) and cellulose sulfate (*blue*): (*A*) at cationic sites of primary PEC particles, (*B*) within secondary PEC particles, and (*C*) within a surface aggregated PEC phase. (From [149] with kind permission of Elsevier).

lowest initial burst behavior and slowest release kinetics were obtained for the highest PEC concentration (0.01 M) and lowest PAM/PEC ratio (1:20). SFM images of PAM-loaded (left) and PAM-depleted (right) PEI/CS-0.9 particles are shown in Fig. 32b (unpublished data). From DLS we obtained hydrodynamic radii of around 60–90 nm for PAM-loaded PEC nanoparticles and the bare unloaded PEC particles showed smaller radii.

Furthermore, kinetic analysis based on the Ritger–Peppas model revealed values of $b \ll 0.5$ (see Sect. 5.2.1) for PAM/PEC samples cast from 0.002 M dispersions, suggesting dissolution of dried PAM in the PEC matrix. However, PAM/PEC samples cast from 0.01 M dispersions revealed values of b close to 0.5, suggesting hindered dissolution or diffusion due to a more dense PEC matrix and lower drug/surface area ratio. A model describing three levels of retention of PAM in PEC particle films is suggested and shown in Fig. 32c. On the molecular level, the negatively charged PAM is bound or condensed at free uncomplexed cationic PEI sites within small primary PEC particles. On an intraparticular nanoscopic level, PAM is physically entrapped within single secondary PEC particles of aggregated primary PEC particles. On an interparticular mesoscopic level, PAM is entrapped within the zone formed by the surface-aggregated secondary PEC particles upon solution casting.

5.3 Interaction of PEC Particles with Cells and Biofluids

PEC particles designed for use in the human body must be critically studied for their cell toxicity, immunoresponse, and cellular interactive properties. Thereby, the related requirements of PEC particles in systemic pharmaceutical applications are expected to be even more strict compared to the locally confined particles introduced in Sect. 5.2.3, since the exposed surface areas recognized by in vitro or in vivo systems are different. While cast PEC particles films offer less surface area to cells cultured on top, dispersed PEC particles expose more surface area to cells in the volume phase. Many reports can be obtained in the open literature on the toxicology and biocompatibility of DNA/polycation complexes [128, 161], but only a few are available on other biorelated PEL systems. The development and potential applications of nontoxic multifunctional PEC particles with respect to targeted tissue delivery, organelle trafficking, and imaging was reviewed comprehensively by Hartig et al. [162]. Colloidal stability, hydrodynamic diameter of less than 200 nm, spherical morphology, low polydispersity, and surface charge magnitude > 30 mV are outlined as key physicochemical parameters for a successful delivery vehicle or for imaging purposes in the human body. Furthermore, Delair has reviewed PEC particles of CHT and DS [163] useful in nanomedicine. Some application examples are small drug delivery [135], growth factor delivery [126, 164], and magnetic resonance imaging using gadolinium-loaded CHT/DS PEC particles [165]. In the following sections we give examples, modalities, and requirements of PEC nanoparticle systems related to toxicity, immuneresponse, and cell

interaction, arranged with respect to relevant cell types (in vitro) (Sect. 5.3.1) and blood (in vivo) (Sect. 5.3.2).

5.3.1 In Vitro Interaction of PEC Particles with Cells

Studies on PEC–cell interaction have different aspects and motivation. Very generally, on the one hand an inert influence of PEC particles on cell growth and differentiation partly under release of drugs is desired, while on the other hand an active influence like apoptosis of cancer cells is aimed at. Regardless of the specific scope, cellular and subcellular binding and endocytosis are key events in the PEC–cell interaction, as for all other nanoparticle systems [162]. This results in the internalization of the cell plasma membrane with the formation of vesicles that can capture PEC particles in the extracellular environment and, after a complicated fusion scenario, direct them to a given intracellular compartment. According to Courtoy and coworkers [166], three types of endocytosis can be distinguished: fluid-phase, adsorptive, and receptor-mediated, whereby the first implies unspecific uptake directly related to the extracellular concentration and the other two imply more effective specific binding and accumulation at the cell surface (via glycosylated aminoglycans and sulfated proteoglycans) followed by internalization.

Interaction of PEC Particles with Cancer Cells

In an early report by Janes et al. [135], the interaction between DOX-loaded PEC nanoparticles (consisting of CHT and polyanions) and human melanoma cells was investigated with reference to the polyanion type and preparation protocol. Evidence was found that DOX-loaded PEC particles consisting of DS maintained the cytostatic activity with respect to free DOX, whereas DOX precomplexed with CHT before complexation with the polyanion showed slightly decreased activity (according to the MTT assay). Furthermore, CLSM studies revealed that DOX release did not take place in the cell culture medium, but that DOX was taken up into the melanoma cells by endocytosis while still bound to PEC particles and finally released intracellularly.

Related studies on the cytotoxicity of a CHT/gelatin hydrogel PEC system were reported by Mao et al. [167]. Fibroblast cell adhesion, proliferation, and apoptosis were investigated at CHT and CHT/gelatin membranes having different degrees of deacetylation. This study confirmed that CHT/gelatin induced fibroblasts to enter the cell cycle and proliferate and decreased their apoptosis, in contrast to pure CHT membranes, for which the deacetylation degree modulates the undesired cell adhesion.

In a recent report by Tsai et al. [168], the cytotoxicity of DOX-loaded chitosan/chondroitin (CHT/CHO) PEC particles to human oral carcinoma and lung carcinoma cells was studied with methacrylate modification and/or crosslinking as

synthetic parameters. It was found that the cell killing ability of DOX released from any of the PEC types was higher than that of free DOX (as measured by flow cytometry and CLSM). In oral carcinoma cells, a higher internalization of PEC particles was found compared with lung carcinoma cells. The highest internalized DOX amount was found for the crosslinked PEC particles (by capillary electrokinetic analysis). Among the various PEC formulations, the best was PEC with a crosslinked shell. The authors emphasized the use of natural polysaccharides because of safety concerns about empty PEC particles after drug release.

Interaction of PEC Particles with Endothelial Cells

A very concise study on the interaction between PEC particles and human microvascular endothelial cells (HMVEC) was reported by Hartig et al. [169]. A PEC system with PEL components known from successful microencapsulation protocols [170] was used. Cationic PEC particles were generated in highly nonstoichiometric ratios from dosing a mixture of ALG and CHO as the molar minority component into a mixture of fluorescein isothiocyanate (FITC)-modified poly(methylene-*co*-guanidinium chloride) (PMCG) and spermine hydrochloride (SPM) as the molar majority component. All PELs had rather low molecular weights, and $CaCl_2$ and a Pluronic-type dispergator were additionally included. Consecutive centrifugation was applied, resulting in particle diameters of around 160 nm and cationic surface charge of around +35 mV. These PEC particles were incubated in cell culture medium, resulting in slightly larger particle diameters and negative surface charge (−10 mV). Cell proliferation studies and propidium iodide staining revealed nontoxicity. Moreover, both the binding and internalization kinetics (2 h) of fluorescent PEC (PMCG-FITC/SPM/ALG/CHO) particles were compared with those of the free fluorescent FITC-PMCG at HMVEC (see Fig. 33a).

Anionic FITC-PEC particles showed saturation features with large amounts, whereas free cationic FITC-PMCG showed linear behavior with small amounts in both binding and internalization. CLSM imaging demonstrated perinuclear accumulation (Fig. 33b), and related Z-sectioning revealed that PEC particles were in the same plane as the cytoplasm. The authors argued that although the surface charge of PEC particles was negative, positive patches of PMCG may bind to polyanionic sites (proteoglycans) of the ECM of HMVEC, followed by macropinocytosis as the internalization mechanism [169].

Huang et al. [126] reported studies on human umbilical vein endothelial cells (HUVEC) cultures incubated with PEC particles of the systems CHT/DS, PEI/DS, and PLL/DS, the charge signs of which were not reported in detail. Both VEGF-loaded and VEGF-unloaded PEC particles (250 nm) were studied for their effects on cell proliferation (mitogenic activity) by MTS (tetrazolium salt) assays. Irrespective of the PEC composition, similar proliferation values were obtained at the 4th day after incubation for all empty control PEC particle systems, for the free VEGF, and for the controls. Only in the case of PEC-bound VEGF for all polycation/polyanion systems was an enhanced HUVEC proliferation found.

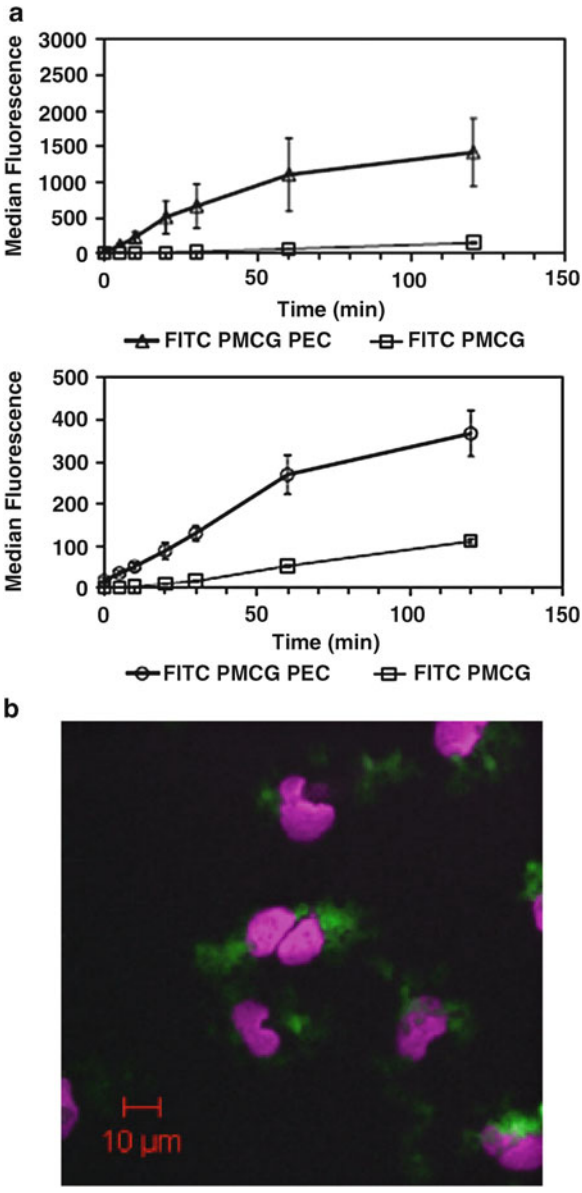

Fig. 33 (**a**) Flow cytometric results on the binding (*top*) and internalization (*bottom*) of either PEC (PMCG-FITC/SPM/CHO/ALG) particles or free PMCG-FITC (0.075 mg/mL) at HMVEC. (**b**) CLSM image of FITC-labeled PEC particles (*green*) incubated with HMVEC (2 h). Cell nuclei were stained with TOPRO-3 (*violet*). (From [169] with kind permission Elsevier)

Apart from these two references, we could not find further open literature reports on the interaction between PEC nanoparticles and endothelial cells.

However, the fact that PEC material positively interacts with HUVECs was noticed earlier by Boura et al. using the related PEM of PAH/PSS or PLL/PLG [171]. It was shown that these PEM enhanced initial cell adhesion compared with single PEL layers and are neither cytotoxic nor change the HUVEC phenotype. Recently, related collagen/heparin multilayers were shown to have similar positive

effects on the adhesion and proliferation of embryonal carcinoma (EC) cells on stent material [172].

Similar studies on angiogenesis in the frame of a joint project between material scientists, cell biologists, and clinicians have been made by us with HUVECs and concerned their interaction with PEC particle systems. Preliminary results on the influence of PEC particle charge revealed that the charge sign of the PEC particles had a crucial influence on the viability of HUVECs (unpublished results).

Interaction of PEC Particles with Osteoblast Cells

As well as the engineering of vascular tissue based on endothelial cells, there is huge interest in the engineering of bone tissue, osseous scaffolds, or BSM based on, e.g., osteoblasts (OB). In this framework, Nagahata reported on the development of new scaffolds for bone regeneration based on precipitated and washed biomimetic PEC particle films on culture dishes [173]. Analogously to endothelial cells, the mimicking of the ECM of OB by PELs such as CHT, anionically modified (carboxyl, phosphate, sulfate) chitin or hyaluronic acid, was aimed at. PEC films with variable PEL compositions were prepared, and their effects on OB functions like attachment, morphology, growth, and differentiation (as measured by alkaline phosphatase assay) were evaluated. Use of PEL bearing carboxyl and phosphate groups resulted in decreased OB attachment, occurrence of cell aggregation, and suppressed differentiation and proliferation. By contrast, PEC films bearing sulfated polysaccharides showed an adhesion and proliferation performance almost similar to collagen-coated dishes, which enables their use as scaffolds for bone regeneration (see Fig. 34a).

Additionally, these authors [173] addressed an additional effect of PEC films on cell function, which is gap junctional intercellular communication (GJIC) allowing OB cells to maintain homeostasis. Figure 34b shows the results of GJIC measurement by fluorescence recovery after photobleaching (FRAP) on an extracellularly binding dye at cells in contact with at least two other cells. There was no significant difference between PEC films and the collagen-coated dish. By contrast, OB on pure CHT-coated dishes showed suppression of GJIC after 1 week. This suggests that CHT disturbs homeostasis maintenance of OB, but that this effect can be avoided by complexation with, e.g., anionic polysaccharides.

Related to this, the Abe group reported earlier on the interaction between PEC precipitate systems consisting of anionic phosphated and carboxymethylated chitin (PCHN and CCHN) and cationic CHT and rat OB cells in cell culture dishes [174]. OB aggregates were observed on both CHT/PCHN (4th day) and CHT/CCHN (2nd day) to exhibit inhibited growth as compared with controls. However, OB differentiation (as shown by alkaline phosphatase assay) increased and osteocalcin mRNA was expressed for both PEC systems, indicating the importance of OB aggregation for bone mineralization capability.

Recently, a joint project between material scientists, cell biologists, and clinicians was installed aiming at local and time-controlled delivery of osteoporotic drugs from implant or bone-substituting materials. Before drug-loaded PEC particles were studied,

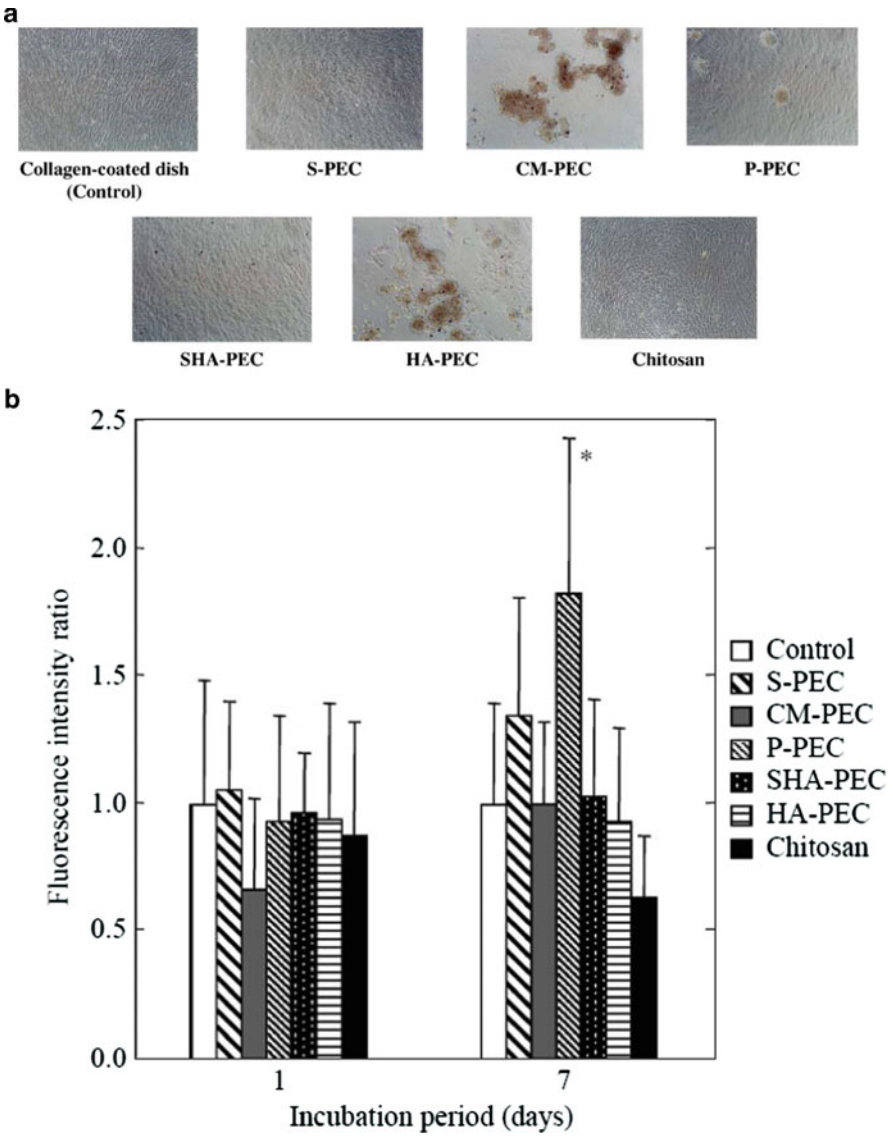

Fig. 34 (**a**) Micrographs of human OB cells on various PEC films after 24 h of incubation (magnification: 100×). (**b**) Gap junctional intercellular communication activity of OB cells on various PEC films as determined by the FRAP technique. (From [173] with kind permission of Elsevier)

the metabolic activity of OB differentiated human mesenchymal stem cells (hMSC) grown onto cast empty PEC particles was investigated. Preliminary results showed that the metabolic activity of hMSC on various PEC particle systems was critically dependent on the PEL composition and the surface coverage (unpublished results).

A novel approach based on composites of nanoparticular hydroxyapatite (HA) and PEC of CHT/phosphorylated CHT, which were co-cultured with rat OB in vitro, was reported by Li et al. [175]. After implantation of this PEC/HA material into rabbit femur marrow cavities, a promoted OB adhesion, proliferation, and differentiation in vitro was obtained (bioactive). Because PEC/HA is also biodegradable, it is claimed to be a promising bone-repair material.

5.3.2 In Vivo Interaction of PEC Particles with Blood

The multicomponent biofluid blood consists, among other components, of proteins and cells and still represents a challenge for interaction studies with PEC particles. A comprehensive study on the interaction of complexes of PDMAEMA and either a crosslinked CHT or poly(2-acrylamido-2-methylpropanesulfonic acid) (PAMPSNa) with human blood from healthy volunteers was reported by Yancheva et al. [176]. Thereby, PDMAEMA complexed with CHT no longer caused inherent cytotoxicity compared with the uncomplexed state, but haemostatic activity was still present. However, PEC of PDMAEMA/PAMPSNa featured both low cytotoxicity and low haemostatic activity. The degree of PDMAEMA quaternization had an additional influence on both blood compatibility parameters. In particular, the authors claimed a higher interaction of samples containing higher quaternized PDMAEMA with the cell walls of blood cells (both red and white) because of electrostatic attraction to the anionic compounds of their cell membranes.

6 Summary and Outlook

PEC nanoparticles can be easily prepared by controlled mixing of diluted polycation and polyanion solutions, which may consist of natural polyelectrolytes. Their size typically ranges between 20 and 500 nm, and they can have spherical, rod-like, or toroid shapes and can have a loose gel-like up to compact internal structure.

PEC particles have strong aggregation tendencies, but the formed aggregates may have sufficient colloidal stability.

The colloidal parameters of size, shape, internal structure, and stability of PEC nanoparticles can be modulated by PEL concentration, ionic strength, pH, PEL structure, and molecular weight.

PEC particles already serve as drug, protein, and polynucleotide carriers for pharmaceutical applications.

Knowledge on the interaction between PEC particles and cells of different natures is in its beginning. Various examples report nontoxic effects and the binding or internalization of PEC particles at various types of human cells.

The reviewed sizing, shaping, and compartmentalization capabilities of PEC particles can be applied to tailor drug delivery and cell uptake properties in response to clinical requirements.

Acknowledgements Concepts and experimental work outlined and shown in this review are partly related to the Special Research Area/Transregional 79 (TRR 79, part project M7) entitled "Materials for Tissue Regeneration in Systemically Diseased Bones" by Deutsche Forschungsgemeinschaft (DFG) involving universities and research institutes in Giessen, Heidelberg and Dresden, Germany.

DRESDEN concept linking research activities of IPF Dresden and TU Dresden is gratefully acknowledged.

References

1. Lasic DD (1994) Sterically stabilized vesicles. Angew Chem Int Ed 33(17):1685–1698
2. Antonietti M, Förster S (2003) Vesicles and liposomes: a self-assembly principle beyond lipids. Adv Mat 15(16):1323–1333
3. Gros L, Ringsdorf H, Schupp H (1981) Polymeric antitumour agents on a molecular and cellular level. Angew Chem Int Ed 20:301–323
4. Slepnev VI, Kuznetsova LE, Gubin AN, Batrakova EV, Alakhov V, Kabanov AV (1992) Micelles of poly(oxyethylene)-poly-(oxypropylene) block copolymer (pluronic) as a tool for low-molecular compound delivery into a cell: phosphorylation of intracellular proteins with micelle incorporated [gamma-32P]ATP. Biochem Int 26:587–595
5. Krause HJ, Schwarz A, Rohdewald P (1985) Polylactic acid nanoparticles: a colloidal drug delivery system for lipophilic drugs. Int J Pharm 27(2–3):145–155
6. Chawla JS, Amiji MM (2002) Biodegradable poly(epsilon-caprolactone) nanoparticles for tumor-targeted delivery of tamoxifen. Int J Pharm 249(1–2):127–138
7. Speiser PP (1978) Non-liposomal nanocapsules, methodology and application. Front Biol 48:653–668
8. Couvreur P, Tulkens P, Roland M, Trouet A, Speiser P (1977) Nanocapsules: a new type of lysosomotropic carrier. FEBS Lett 84(2):323–326
9. Guo X, Weiss A, Ballauff M (1999) Synthesis of spherical polyelectrolyte brushes by photoemulsion polymerization. Macromolecules 32:6043–6046
10. Michaels AS (1965) Polyelectrolyte complexes. Ind Eng Chem 57:32–40
11. Kabanov VA, Zezin AB (1984) Soluble interpolymeric complexes as a new class of synthetic polyelectrolytes. Pur Appl Chem 56:343–354
12. Philipp B, Dautzenberg H, Linow KJ, Kötz J, Dawydoff W (1989) Polyelectrolyte complexes: recent developments and open problems. Prog Polym Sci 14:91–172
13. Dubin P, Bock J, Davies RM, Schulz DN, Thies C (1994) Macromolecular complexes in chemistry and biology. Springer, Berlin
14. Harada A, Kataoka K (1995) Formation of polyion complex micelles in an aqueous milieu from a pair of oppositely charged block-copolymers with poly(ethylene glycol) segments. Macromolecules 28(15):5294–5299
15. Harada-Shiba M, Yamauchi K, Harada A, Takamisawa I, Shimokado K, Kataoka K (2002) Polyion complex micelles as vectors in gene therapy - pharmacokinetics and in vivo gene transfer. Gene Ther 9(6):407–414
16. Müller M, Kessler B, Richter S (2005) Preparation of monomodal polyelectrolyte complex nanoparticles of PDADMAC/poly(maleic acid-*alt*-α-methylstyrene) by consecutive centrifugation. Langmuir 21(15):7044–7051
17. Müller M, Reihs T, Ouyang W (2005) Needlelike and spherical polyelectrolyte complex nanoparticles of poly(L-lysine) and copolymers of maleic acid. Langmuir 21(1):465–469
18. Oertel U, Buchhammer HM, Müller M et al (1999) Surface modification by polyelectrolytes: studies on model systems. Macromol Symp 145:39–47

19. Thünemann AF, Müller M, Dautzenberg H, Joanny JF, Löwen H (2004) Polyelectrolyte complexes. Adv Polym Sci 166:113–171
20. Reihs T, Müller M, Lunkwitz K (2003) Deposition of polylelectrolyte complex nano-particles at silica surfaces characterized by ATR-FTIR and SEM. Coll Surf A 212(1):79–95
21. Reihs T, Müller M, Lunkwitz K (2004) Preparation and adsorption of refined polyelectrolyte complex nanoparticles. J Colloid Interface Sci 271(1):69–79
22. Starchenko V, Müller M, Lebovka N (2008) Growth of polyelectrolyte complex nanoparticles: computer simulations and experiments. J Phys Chem C 112(24):8863–8869
23. Lebovka NI (2012) Aggregation of charged colloidal particles. Adv Polym Sci
24. Burchard W (1983) Static and dynamic light scattering from branched polymers and biopolymers. Adv Polym Sci 48:1–124
25. Schnablegger H, Glatter O (1993) Simultaneous determination of size distribution and refractive index of colloidal particles from static light-scattering experiments. J Colloid Interface Sci 158(1):228–242
26. Dautzenberg H (2001) Polyelectrolyte complex formation in highly aggregating systems: methodical aspects and general tendencies. In: Radeeva I (ed) Physical chemistry of polyelectrolytes (surfactant science series 99). ACS symposium series, Washington
27. Dautzenberg H, Rother G, Hartmann J (1994) Light scattering studies of polyelectrolyte complex formation: effect of polymer concentration. In: Schmitz KS (ed) Macro-ion characterization: from dilute solution to complex fluids. ACS Symposium Series, Washington
28. Dautzenberg H, Linow KJ, Philipp B (1982) Zur Bildung wasserlöslicher Polysalze (Symplexe) aus anionischen und kationischen Copolymeren des Acrylamids. Acta Polymerica 33(11):619–623
29. Schmitz KS (1990) Dynamic light scattering by macromolecules. Academic, San Diego
30. Dubin PL, Davis DD (1984) Quasi elastic light scattering of polyelectrolyte micelle complexes. Macromoleculaes 17(6):1294–1296
31. Dubin PL, Murrell JM (1988) Size distribution of complexes formed between PDADMAC and BSA. Macromolecules 21(7):2291–2293
32. Lindhoud S, Norde W, Cohen Stuart MA (2009) Reversibility and relaxation behavior of polyelectrolyte complex micelle formation. J Phys Chem B 113:5431–5439
33. van der Burgh S, de Keizer A, Cohen Stuart MA (2004) Complex coacervation core micelles. Colloidal stability and aggregation mechanism. Langmuir 20:1073–1084
34. Lindhoud S, Cohen Stuart MA (2012) Relaxation phenomena during polyelectrolyte complex formation. Adv Polym Sci DOI 10.1007/12_2012_178
35. Tiersch B, Hartmann H, Dautzenberg H et al (1986) Elektronenmikroskopische Untersuchungen an Fällungen von Polyanion-Polykation-Komplexen. Acta Polymerica 37(1):47–51
36. Dautzenberg H, Hartmann J, Grunewald S et al (1996) Stoichiometry and structure of polyelectyroltye complex particles in diluted solutions. Ber Bunsenges PhysChem 100:1024–1032
37. Tsuchida E (1974) The formation of higher structure through hydrophobic interaction of interpolymer complexes. Die Makromolekulare Chernie 175:603–611
38. Tsuchida E, Abe K, Honma M (1976) Aggregation of polyion complexes between synthetic polyelectrolytes. Macromolecules 9:112–120
39. Wolfert MA, Seymour LW (1996) AFM analysis of the influence of the molecular weight of poly(L-lysine) on the size of the polyelectrolyte complex with DNA. Gene Ther 3:269–273
40. Kramer G, Buchhammer HM, Lunkwitz K (1997) Surface modification by polyelectrolyte complexes: influence of different polyelectrolyte components and substrates. Coll Surf A 122:1–12
41. Bernhardt H, Schell H (1993) Control of flocculants by use of a streaming current detector. J Water SRT-Aqua 42:239–251
42. Buchhammer HM, Petzold G, Lunkwitz K (1999) Salt effect on formation and properties of interpolyelectrolyte complexes and their interactions with silica particles. Langmuir 15:4306–4310

43. Johnson BK, Prud'homme RK (2003) Chemical processing and micromixing in confined impinging jets. AIChE J 49:2264–2282
44. Ankerfors C, Ondaral S, Wågberg L et al (2010) Using jet mixing to prepare polyelectrolyte complexes: complex properties and their interaction with silicon oxide surfaces. J Coll Interf Sci 351:88–95
45. Saether HV, Holme HK, Maurstad G et al (2008) Polyelectrolyte complex formation using alginate and chitosan. Carbohydr Polym 74:813–821
46. Schatz C, Domard A, Viton C, Pichot C, Delair T (2004) Versatile and efficient formation of colloids of biopolymer-based polyelectrolyte complexes. Biomacromolecules 5:1882–1892
47. Mende M, Buchhammer HM, Schwarz S (2004) The stability of polyelectrolyte complex systems of PDADMAC with different polyanions. Macromol Symp 211:121–133
48. Müller M, Keßler B, Fröhlich J et al (2011) Polyelctrolyte complex nanoparticles of poly (ethyleneimine) and poly(acrylic acid): preparation and applications. Polymers 3:762–778
49. Schatz C, Lucas JM, Viton C et al (2004) Formation and properties of positively charged colloids based on polyelectrolyte complexes of biopolymers. Langmuir 20(18):7766–7778
50. Drogoz A, David L, Rochas C et al (2007) Polyelectrolyte complexes from polysaccharides: formation and stoichiometry monitoring. Langmuir 23(22):10950–10958
51. Dautzenberg H, Jaeger W (2002) Effect of charge density on the formation and salt stability of polyelectrolyte complexes. Macromol Chem Phys 203:2095–2102
52. Pergushov DV, Babin IA, Plamper FA et al (2008) Water-soluble complexes of star-shaped poly(acrylic acid) with quaternized poly(4-vinylpyridine). Langmuir 24:6414–6419
53. Mende M, Petzold G, Buchhhammer HM (2002) Polyelectrolyte complex formation between poly(diallyldimethylammonium chloride) and copolymers of acrylamide and sodium-acrylate. Colloid Polym Sci 280:342–351
54. Shovsky A, Varga I, Makuska R, Claesson PM (2009) Formation and stability of water-soluble, molecular polyelectrolyte complexes: effects of charge density, mixing ratio, and polyelectrolyte concentration. Langmuir 25(11):6113–6121
55. Hu Y, Yang T, Hu X (2012) Novel polysaccharides-based nanoparticle carriers prepared by polyelectrolyte complexation for protein drug delivery. Polym Bull 68:1183–1199
56. Imae T, Miura A (2003) Binding of poly(amido amine) dendrimer on sodium poly-L-glutamate in aqueous NaCl solution. J Phys Chem B 107:8088–8092
57. Shifrina ZB, Kuchkina NV, Rutkevich PN et al (2009) Water-soluble cationic aromatic dendrimers and their complexation with DNA. Macromolecules 42:9548–9560
58. Kłos JS, Sommer JU (2011) Monte Carlo simulations of charged dendrimer-linear polyelectrolyte complexes and explicit counterions. J Chem Phys 134:204902
59. Kabanov AV, Bronich TK, Kabanov VA et al (1996) Soluble stoichiometric complexes from poly(*N*-ethyl-4-vinylpyridinium) cations and poly(ethylene oxide)-block-polymethacrylate anions. Macromolecules 29(21):6797–6802
60. Schild HG (1992) Poly(*N*-isopropylacrylamide) – experiment, theory and applications. Prog Polym Sci 17(2):163–249
61. Dautzenberg H, Gao Y, Hahn M (2000) Formation, structure, and temperature behavior of polyelectrolyte complexes between ionically modified thermosensitive polymers. Langmuir 16:9070–9081
62. Kleinen J, Richtering W (2008) Defined complexes of negatively charged multisensitive poly (*N*-isopropylacrylamide-co-methacrylic acid) microgels and poly(diallydimethylammonium chloride). Macromolecules 41:1785–1790
63. Serpe MJ, Yarmey KA, Nolan CM, Lyon LA (2005) Doxorubicin uptake and release from microgel thin films. Biomacromolecules 6:408–413
64. Nolan CM, Serpe MJ, Lyon LA (2004) Thermally modulated insulin release from microgel thin films. Biomacromolecules 5:1940–1946
65. Schacher F, Betthausen E, Walther A et al (2009) Interpolyelectrolyte complexes of dynamic multicompartment micelles. ACS Nano 3(8):2095–2102

66. Pergushov DV, Borisov OV, Zezin AB et al (2011) Interpolyelectrolyte complexes based on polyionic species of branched topology. Adv Polym Sci 241:131–161
67. Pergushov DV et al. (2012) Advanced functional structures based on interpolyelectrolyte complexes. Adv Polym Sci
68. Dautzenberg H (1997) Polyelectrolyte complex formation in highly aggregating systems. 1. Effect of salt: polyelectrolyte complex formation in the presence of NaCl. Macromolecules 30:7810–7815
69. Buchhammer HM, Mende M, Oelmann M (2003) Formation of mono-sized polyelectrolyte complex dispersions: effects of polymer structure, concentration and mixing conditions. Coll Surf A 218:151–159
70. Wandrey C, Hunkeler D, Wendler U et al (2000) Counterion activity of highly charged strong polyelectrolytes. Macromolecules 33:7136–7143
71. Pergushov DV, Buchhammer HM (1999) Effect of a low-molecular-weight salt on colloidal dispersions of interpolyelectrolyte complexes. Colloid Polym Sci 277:101–107
72. Feng X, Leduc M, Pelton RH (2008) Polyelectrolyte complex characterization with isothermal titration calorimetry and colloid titration. Coll Surf A 317:535–542
73. Ostwald WZ (1897) Phys Chem 22:289
74. Voorhees PM (1985) The theory of Ostwald ripening. J Stat Phys 38(1/2):231–252
75. Derjaguin BV, Landau L (1941) Acta Physicochim USSR 14:633
76. Verwey EJW, Overbeek JTG (1948) Theory of stability of lyophobic colloids. Elsevier, New York
77. Dautzenberg H, Kriz J (2003) Response of polyelectrolyte complexes to subsequent addition of salts with different cations. Langmuir 19:5204–5211
78. Gardlund L, Wagberg L, Norgren M (2007) New insights into the structure of polyelectrolyte complexes. J Colloid Interface Sci 312(2):237–246
79. Porcel CH, Schlenoff JB (2009) Compact polyelectrolyte complexes: "saloplastic" candidates for biomaterials. Biomacromolecules 10:2968–2975
80. Hariri HH, Schlenoff JB (2010) Saloplastic macroporous polyelectrolyte complexes: cartilage mimics. Macromolecules 43:8656–8663
81. Markarian MZ, Hariri HH, Reisch A et al (2012) A small-angle neutron scattering study of the equilibrium conformation of polyelectrolytes in stoichiometric saloplastic polyelectrolyte complexes. Macromolecules 45:1016–1024
82. Heuvingh J, Zappa M, Fery A (2005) Salt softening of polyelectrolyte multilayer capsules. Langmuir 21:3165–3171
83. Gelman RA, Blackwell J (1973) Heparin-polypeptide interactions in aqueous solution. Arch Biochem Biophys 169:427–433
84. Nakajima A, Shinoda K, Hayashi T, Sato H (1975) Interactions between oppositely charged polypeptides. Polymer J 7:550–557
85. Dautzenberg H (2000) Light scattering studies on polyelectrolyte complexes. Macromol Symp 162:1–21
86. Goessl I, Shu L, Schlüter AD, Rabe JP (2002) Molecular structure of single DNA complexes with positively charged dendronized polymers. J Am Chem Soc 124:6860–6865
87. Xu Y, Borisov OV, Ballauff M, Müller AHE (2010) Manipulating the morphologies of cylindrical polyelectrolyte brushes by forming interpolyelectrolyte complexes with oppositely charged linear polyelectrolytes: an AFM study. Langmuir 26(10):6919–6926
88. Duschner S, Störkle D, Schmidt M, Maskos M (2008) Topologicallly controlled interpolyelectrolyte complexes. Macromolecules 41:9067–9071
89. Shinoda K, Hayashi T, Yoshida T et al (1976) Complex formation of poly(L-lysine) with poly (acrylic acid). Polymer J 8(2):202–207
90. Garnier G, Duskova-Smrckova M, Vyhnalkova R et al (2000) Association in solution and adsorption at an air-water interface of alternating copolymers of maleic anhydride and styrene. Langmuir 16:3757–3763

91. Gelman RA, Rippon WB, Blackwell J (1973) Interactions between chondroitin-6-sulfate and poly-L-lysine in aqueous solution: circular dichroism studies. Biopolymers 12:541–558
92. Stone AL, Epstein P (1977) The aggregation of basic polypeptide residues bound to heparin. Biochim Biophys Acta 497:298–306
93. Bystricky S, Malovlikova A, Sticzay T (1991) Interaction of acidic polysaccharides with polylysine enantiomers. Conformation probe in solution. Carbohyd Polym 15:299–308
94. Bystricky S, Malovlikova A, Sticzay T (1990) Interaction of alginates and pectins with cationic polypeptides. Carbohydr Polym 13:283–294
95. Sapay N, Cabannes E, Petitou M, Imberty A (2011) Molecular modeling of the interaction between heparin sulfate and cellular growth factors: bringing pieces together. Glycobiology 21(9):1181–1193
96. Pichert A, Samsonov SA, Theisgen S et al (2012) Characterization of the interaction of interleukin-8 with hyaluronan, chondroitin sulfate, dermatan sulfate and their sulfated derivatives by spectroscopy and molecular modelling. Glycobiology 22(1):134–145
97. Greenfield N, Fasman GD (1969) Computed circular dichroism spectra for the evaluation of protein conformation. Biochemistry 8(10):4108–4116
98. Müller M, Ouyang W, Bohata K et al (2010) Nanostructured complexes of polyelectrolytes and charged polypeptides. Adv Biomaterials 12(9):519–528
99. Zhengzhan D, Jingbo Y, Shifeng Y et al (2007) Polyelectrolyte complexes based on chitosan and poly(L-glutamic acid). Polymer Int 56(9):1122–1127
100. Decher G (1997) Fuzzy nanoassemblies: toward layered polymeric multicomposites. Science 277(5330):1232–1237
101. Narambuena CF, Leiva EPM, Chávez-Páez M et al (2010) Effect of chain stiffness on the morphology of polyelectrolyte complexes. A Monte Carlo simulation study. Polymer 51:3293–3302
102. Kunze KK, Netz RR (2002) Morphologies of semiflexible polyelectrolyte complexes. Europhys Lett 58(2):299–305
103. Maurstad G, Danielsen S, Stokke BT (2003) Analysis of compacted semiflexible polyanions visualized by atomic force microscopy: influence of chain stiffness on the morphologies of polyelectrolyte complexes. J Phys Chem B 107:8172–8180
104. Schnurr B, Gittes F, MacKintosh FC (2002) Metastable intermediates in the condensation of semiflexible polymers. Phys Rev E 65:061904
105. Duncan R, Gaspar R (2011) Nanomedicine(s) under the microscope. Mol Pharm 8:2101–2141
106. Cruz T, Gaspar R, Donato A, Lopes C (1997) Interaction between polyalkylcyanoacrylate nanoparticles and peritoneal macrophages: MTT metabolism, NBT reduction, and NO production. Pharm Res 14(1):73–79
107. Petros RA, DeSimone JM (2010) Strategies in the design of nanoparticles for therapeutic applications. Nat Rev Drug Discov 9:615–627
108. Panyam P, Labhasetwar V (2003) Biodegradable nanoparticles for drug and gene delivery to cells and tissue. Adv Drug Deliv Rev 55:329–347
109. Debuigne F, Cuisenaire J, Jeunieau L et al (2001) Synthesis of nimesulide nanoparticles in the microemulsion epikuron/isopropyl myristate/water/n-butanol (or isopropanol). J Colloid Interface Sci 243:90–101
110. Chern CS, Lee CK, Chang CJ (2004) Electrostatic interactions between amphoteric latex particles and proteins. Colloid Polym Sci 283:257–264
111. Fatouros DG, Piperoudi S, Gortzi O et al (2005) Physical stability of sonicated arsonoliposomes: effect of calcium ions. J Pharm Sci 94:46–55
112. Shiraishi S, Imai T, Otagiri M (1993) Controlled release of indomethacin by chitosan-polyelectrolyte complex: optimization and in viva/in vitro evaluation. J Control Release 25:217–225
113. Champion JA, Mitragotri S (2006) Role of target geometry in phagocytosis. Proc Natl Acad Sci USA 103:4930–4934

114. Desai MP, Labhasetwar V, Walter E et al (1997) The mechanism of uptake of biodegradable microparticles in caco-2 cells is size dependent. Pharm Res 14:1568–1573
115. Chithrani BD, Ghazani AA, Chan CW (2006) Determining the size and shape dependence of gold nanoparticle uptake into mammalian cells. Nano Lett 6:662–668
116. Harada A, Kataoka K (2006) Supramolecular assemblies of block copolymers in aqueous media as nanocontainers relevant to biological applications. Prog Polym Sci 31:949–982
117. Mjahed H, Voegel JC, Chassepot A (2010) Turbidty diagrams of polycation/polyanion complexes in solution as a potential tool to predict the occurrence of polyelectrolyte multilayer deposition. J Colloid Interface Sci 346:163–171
118. Siegel RA, Falamarzian M, Firestone BA et al (1988) pH-controlled release from hydrophobic polyelectrolyte copolymer hydrogels. J Control Release 8:179–182
119. Sezer AD, Akbuga J (1995) Controlled release of piroxicam from chitosan beads. Int J Pharm 121:113–116
120. Aydin Z, Akbuga J (1996) Chitosan beads for the delivery of salmon calcitonin:preparation and release characteristics. Int J Pharm 131:101–103
121. Ritger PL, Peppas NA (1987) A simple equation for description of solute release I. Fickian and non fickian release from non swellable devices in the form of slabs, spheres, cylinders or discs. J Control Release 5:23–36
122. de la Torre PM, Enobakhare Y, Torrado G, Torrado S (2003) Release of amoxicillin from polyionic complexes of chitosan and poly(acrylic acid): study of polymer/polymer and polymer/drug interactions within the network structure. Biomaterials 24:1499–1506
123. Calvo P, Remunan Lopez C, Vila Jato JL, Alonso MJ (1997) Chitosan and chitosan ethylene oxide propylene oxide block copolymer nanoparticles as novel carriers for proteins and vaccines. Pharm Res 14(10):1431–1436
124. Ouyang W, Müller M (2006) Monomodal polyelectrolyte complex nanoparticles of PDADMAC/poly(sty-renesulfonate): preparation and protein interaction. Macromol Biosci 6:929–941
125. Tiyaboonchai W, Woiszwillo J, Sims RC, Middaugh CR (2003) Insulin containing polyethylenimine–dextran sulfate nanoparticles. Int J Pharm 255:139–151
126. Huang M, Vitharana SN, Peek LJ et al (2007) Polyelectrolyte complexes stabilize and controllably release vascular endothelial growth factor. Biomacromolecules 8(5):1607–1614
127. Kabanov AV, Astafieva IV, Maksimova IV (1993) Efficient transformation of mammalian cells using DNA interpolyelectrolyte complexes with carbon chain polycations. Bioconjugate Chem 4:448–454
128. Vinogradov SV, Bronich TK, Kabanov AV (2002) Nanosized cationic hydrogels for drug delivery: preparation, properties and interactions with cells. Adv Drug Deliv Rev 54 (1):135–147
129. Kataoka K, Togawa H, Harada A et al (1996) Spontaneous formation of polyion complex micelles with narrow distribution from antisense oligonucleotide and cationic block copolymer in physiological saline. Macromolecules 29:8556–8557
130. Soliman M, Allen S, Davies MC et al (2010) Responsive polyelectrolyte complexes for triggered release of nucleic acid therapeutics. Chem Commun 46(30):5421–5433
131. Kim CJ, Nujoma YN (1995) Drug release from an erodible drug/polyelectrolyte complex. Eur Polym J 31(10):937–940
132. Jimenez-Kairuz AF, Llabot JM, Allemandi DA et al (2005) Swellable drug-polyelectrolyte matrices (SDPM) - characterization and delivery properties. Int J Pharm 288(1):87–99
133. Cheow WS, Hadinoto K (2012) Self-assembled amorphous drug-polyelectrolyte nanoparticle complex with enhanced dissolution rate and saturation solubility. J Colloid Interface Sci 367:518–526
134. Tiyaboonchai W, Woiszwillo J, Middaugh CR (2001) Formulation and characterization of amphotericin B-polyethylenimine-dextran sulfate nanoparticles. J Pharm Sci 90(7):902–914
135. Janes KA, Fresneau MP, Marazuela A et al (2001) Chitosan nanoparticles as delivery systems for doxorubicin. J Control Release 73(2–3):255–267

136. Tan ML, Friedhuber AM, Dunstan E et al (2010) The performance of doxorubicin encapsulated in chitosan–dextran sulphate microparticles in an osteosarcoma model. Biomaterials 31(3):541–551
137. Lu E, Franzblau S, Onyuksel H et al (2009) Preparation of aminoglycosideloaded chitosan nanoparticles using dextran sulphate as a counterion. J Microencaps 26(4):346–354
138. Costa E, Sapag-Hagar J, Valenzuela F et al (2004) Comparative studies on polyelectrolyte complexes and mixtures of chitosan–alginate and chitosan–carrageenan as prolonged diltiazem clorhydrate release systems. Eur J Pharm Biopharm 57:65–75
139. Tiwari A, Bindal S, Bohidar HB (2009) Kinetics of protein-protein complex coacervation and biphasic release of salbutamol sulfate from coacervate matrix. Biomacromolecules 10:184–189
140. Hong C, Caihua N, Liping Z (2012) Preparation of complex nano-particles based on alginic acid/poly[(2-dimethylamino) ethyl methacrylate] and a drug vehicle for doxorubicin release controlled by ionic strength. Eur J Pharm Sci 45(1–2):43–49
141. Lee KY, Park WH, Ha WS (1997) Polyelectrolyte complexes of sodium alginate with chitosan or its derivatives for microcapsules. J Appl Polymer Sci 63:425–432
142. Coppi G, Iannuccelli V (2009) Alginate/chitosan microparticles for tamoxifen delivery to the lymphatic system. Int J Pharm 367:127–132
143. Thiele C, Auerbach D, Jung G et al (2011) Nanoparticles of anionic starch and cationic cyclodextrin derivatives for the targeted delivery of drugs. Polym Chem 2:209–215
144. Yuan J, Luo Y, Gao Q (2011) Self-assembled polyion complex micelles for sustained release of hydrophilic drug. J Microencaps 28(2):93–98
145. Chuang CY, Chiu WY, Don TM (2011) Synthesis of chitosan-poly(acrylic acid) complex particles by dispersion polymerization and their applications in ph buffering and drug release. J Appl Polym Sci 120(3):1659–1670
146. Lei G, Yanfeng M, Guiying L et al (2011) Self-assembled nanoparticles from thermosensitive polyion complex micelles for controlled drug release. Chem Eng J 174(1):199–205
147. Müller M (2011) Method for producing a drug delivery system on the basis of polyelectrolyte complexes. Patent publication DE 10 2010 003 615 A1 and WO 2011/121019 A2
148. Chung AJ, Rubner MF (2002) Methods of loading and releasing low molecular weight cationic molecules in weak polyelectrolyte multilayer films. Langmuir 18:1176–1183
149. Müller M, Keßler B (2012) Release of pamidronate from poly(ethyleneimine)/cellulose sulphate complex nanoparticle films: An in-situ ATR-FTIR study. J Pharm Biomed Anal 66:183–190
150. Rogers MJ, Crockett JC, Coxon FP et al (2011) Biochemical and molecular mechanisms of action of bisphosphonates. Bone 49:34–41
151. Rachner TD, Khosla S, Hofbauer LC (2011) Osteoporosis: now and the future. Lancet 377:1276–1287
152. Müller M, Rieser T, Lunkwitz K et al (1998) An in-situ ATR-FTIR study on polyelectrolyte multilayer assemblies on solid surfaces and their susceptibility to fouling. Macromol Rapid Commun 19(7):333–336
153. Keller TF, Müller M, Ouyang W et al (2010) Templating alpha-helical poly(L-lysine)/polyanion complexes by nanostructured uniaxially oriented ultrathin polyethylene films. Langmuir 26(24):18893–18901
154. Müller M, Keßler B (2011) Deposition from dopamine solutions at Ge substrates: an in situ ATR-FTIR study. Langmuir 27(20):12499–12505
155. Ouyang W, Müller M, Appelhans D, Voit B (2009) In situ ATR-FTIR investigation on the preparation and enantiospecificity of chiral polyelectrolyte multilayers. ACS Appl Mater Interfaces 1(12):2878–2885
156. Müller M, Grosse I, Jacobasch HJ, Sams P (1998) Surfactant adsorption and water desorption on thin cellulose films monitored by in-situ ATR FTIR spectroscopy. Tenside Surfactants Detergents 35(5):354

157. Bauer HH, Müller M, Goette J et al (1994) Interfacial adsorption and aggregation associated changes in secondary structure of human calcitonin monitored by ATR-FTIR spectroscopy. Biochemistry 33:12276–12283
158. Müller M, Keßler B, Houbenov N et al (2006) pH dependence and protein selectivity of poly (ethyleneimine)/poly(acrylic acid) multilayers studied by in situ ATR-FTIR spectroscopy. Biomacromolecules 7(4):1285–1294
159. Alexis F, Lo SL, Wang S (2006) Covalent attachment of low molecular weight poly(ethylene imine) improves Tat peptide mediated gene delivery. Adv Mater 18:2174–2178
160. Niepel MS, Peschel D, Sisquella X et al (2009) pH-dependent modulation of fibroblast adhesion on multilayers composed of poly(ethylene imine) and heparin. Biomaterials 30:4939–4947
161. Carlesso G, Kozlov E, Prokop A, Unutmaz D, Davidson JM (2005) Nanoparticulate system for efficient gene transfer into refractory cell targets. Biomacromolecules 6:1185–1192
162. Hartig SM, Greene RR, Dikov MM et al (2007) Multifunctional nanoparticulate polyelectrolyte complexes. Pharm Res 24(12):2353–2369
163. Delair T (2011) Colloidal polyelectrolyte complexes of chitosan and dextran sulfate towards versatile nanocarriers of bioactive molecules. Eur J Pharm Biopharm 78:10–18
164. Min H, Cory B (2009) Controlled release of repifermin(R) from polyelectrolyte complexes stimulates endothelial cell proliferation. J Pharm Sci 98(1):268–280
165. Min H, Zhixin LH, Mehmet B et al (2008) Magnetic resonance imaging of contrast-enhanced polyelectrolyte complexes. Nanomedicine 4(1):30–40
166. Amyere M, Mettlen M, Van der Smissen P et al (2002) Origin, originality, functions, subversions and molecular signalling of macropinocytosis. Int J Med Microbiol 291 (6–7):487–494
167. Mao JS, Cui YL, Wang XH et al (2004) A preliminary study on chitosan and gelatin polyelectrolyte complex cytocompatibility by cell cycle and apoptosis analysis. Biomaterials 25:3973–3981
168. Tsai CC, Chiu PC, Lin SH et al (2011) Antitumor efficacy of doxorubicin released from crosslinked nanoparticulate chondroitin sulfate/chitosan polyelectrolyte complexes. Macromol Biosci 11:680–688
169. Hartig SM, Greene RR, Carlesso G et al (2007) Kinetic analysis of nanoparticulate polyelectrolyte complex interactions with endothelial cells. Biomaterials 28:3843–3855
170. Wang T, Lacźk I, Brissova M et al (1997) An encapsulation system for the immunoisolation of pancreatic islets. Nat Biotechnol 15:358–362
171. Boura C, Menu P, Payan E et al (2003) Endothelial cells grown on thin polyelectrolyte mutlilayered films:nan evaluation of a new versatile surface modification. Biomaterials 24:3521–3530
172. Lin Q, Yan J, Qiu F et al (2011) Heparin/collagen multilayer as a thromboresistant and endothelial favorable coating for intravascular stent. J Biomed Mater Res 96A (1):132–141
173. Nagahata M, Nakaoka R, Teramoto A et al (2005) The response of normal human osteoblasts to anionic polysaccharide polyelectrolyte complexes. Biomaterials 26(25):5138–5144
174. Hamano T, Chiba D, Nakatsuka K, Nagahata M, Teramoto A, Kondo Y, Hachimori A, Abe K. (2002) Evaluation of a polyelectrolyte complex(PEC) composed of chitin derivatives and chitosan, which promotes the rat calvarial osteoblast differentiation. Polym Adv Technol:13:46–53
175. Li QL, Wu MY, Tang LL et al (2008) Bioactivity of a novel nano-composite of hydroxyapatite and chitosan-phosphorylated chitosan polyelectrolyte complex. J Bioact Compat Polym 23(6):520–531
176. Yancheva E, Paneva D, Danchev D et al (2007) Polyelectrolyte complexes based on (quaternized) poly[(2-dimethylamino)ethylmethacrylate]: behavior in contact with blood. Macromol Biosci 7:940–954
177. Stanton BW, Harris JJ, Miller MD et al (2003) Ultrathin, multilayered polyelectrolyte films as nanofiltration membranes. Langmuir 19(17):7038–7042

178. Hong SU, Malaisamy R, Bruening ML (2007) Separation of fluoride from other monovalent anions using multilayer polyelectrolyte nanofiltration membranes. Langmuir 23(4):1716–1722
179. De S, Cramer C, Schönhoff M (2011) Humidity dependence of the ionic conductivity of polyelectrolyte complexes. Macromolecules 44(22):8936–8943
180. Bhide A, Schönhoff M, Cramer C (2012) Cation conductivity in dried poly(4-styrene sulfonate) poly(diallydimethylammonium chloride) based polyelectrolyte complexes. Solid State Ionics 214:13–18

Index